Factors that Affect the Immunogenicity of Lipid-PLGA Nanoparticle-Based Nanovaccines against Nicotine Addiction

Zongmin Zhao

Dissertation submitted to the faculty of Virginia Polytechnic Institute and State University in partial fulfillment of the requirements for the degree of

Doctor of Philosophy

In

Biological Systems Engineering

Chenming Zhang, Chair

Marion F. Ehrich

Tanya LeRoith

Xueyang Feng

August 9th, 2017

Blacksburg, VA

Keywords: nicotine addiction, nicotine vaccine, nanoparticle, anti-nicotine antibody, smoking cessation, poly(lactic-co-glycolic acid), liposome

Factors that Affect the Immunogenicity of Lipid-PLGA Nanoparticle-Based Nanovaccines against Nicotine Addiction

Zongmin Zhao

Abstract

Tobacco smoking has consistently been the leading cause of preventable diseases and premature deaths. Currently, pharmacological interventions have only shown limited smoking cessation efficacy and sometimes are associated with severe side effects. As an alternative, nicotine vaccines have emerged as a promising strategy to combating nicotine addiction. However, conventional conjugate nicotine vaccines have shown limited ability to induce a sufficiently strong immune response due to their intrinsic shortfalls.

In this study, a lipid-poly(lactic-co-glycolic acid) (PLGA) nanoparticle-based next-generation nicotine vaccine has been developed to overcome the drawbacks of conjugate nicotine vaccines. Also, the influence of multiple factors, including nanoparticle size, hapten density, hapten localization, carrier protein, and molecular adjuvants, on its immunogenicity has been investigated. Results indicated that all these studied factors significantly affected the immunological efficacy of the nicotine nanovaccine. First, 100 nm nanovaccine was found to elicit a significantly higher anti-nicotine antibody titer than the 500 nm nanovaccine. Secondly, the high-density nanovaccine exhibited a better immunological efficacy than the low- and medium-density counterparts. Thirdly, the nanovaccine with hapten localized on both carrier protein and nanoparticle surface induced a significantly higher anti-nicotine antibody titer and had a considerably better ability to block nicotine from entering the brain of mice than the nanovaccines with hapten localized only on carrier protein or nanoparticle surface. Fourthly, the nanovaccines carrying cross reactive materials 197 (CRM_{197}) or tetanus toxoid (TT) showed a better immunological efficacy than the

nanovaccines using keyhole limpet hemocyanin (KLH) or KLH subunit as carrier proteins. Finally, the co-delivery of monophosphoryl lipid A (MPLA) and Resiquimod (R848) achieved a considerably higher antibody titer and brain nicotine reduction than only using MPLA or R848 alone as adjuvants.

Collectively, the findings from this study may lead to a better understanding of the impact of multiple factors on the immunological efficacy of the hybrid nanoparticle-based nicotine nanovaccine. The findings may also provide significant guidance for the development of other drug abuse and nanoparticle-based vaccines. In addition, the optimized lipid-PLGA hybrid nanoparticle-based nicotine nanovaccine obtained by modulating the studied factors can be a promising candidate as the next-generation nicotine vaccine for treating nicotine addiction.

Factors that Affect the Immunogenicity of Lipid-PLGA Nanoparticle-Based Nanovaccines against Nicotine Addiction

Zongmin Zhao

General Audience Abstract

Tobacco smoking is prevalent and represents one of the largest public health concerns in the world. Tobacco use remains to be the leading cause of preventable diseases and premature deaths. Typically, smokers without medications experience huge difficulty in quitting smoking due to the addictiveness of nicotine. Although several pharmacological interventions are available to smokers, they have only shown limited smoking cessation efficacy. In recent years, nicotine vaccines that can induce the production of nicotine specific antibodies have been proposed as a promising strategy for smoking cessation. Currently, almost all the already-developed nicotine vaccines are conjugate nicotine vaccines in which nicotine haptens are attached to a carrier protein for presentation. However, conventional conjugate nicotine vaccines suffer from many innate shortcomings that largely limit their immunological efficacy.

This study aimed to develop a nanoparticle-based next-generation nicotine vaccine to overcome the drawbacks of conventional conjugate nicotine vaccines. Because many factors may potentially affect the immunological efficacy of a nicotine vaccine, this study focused on investigating the influence of multiple factors, including nanoparticle size, hapten density, hapten localization, carrier protein, and molecular adjuvants, on the immunological efficacy of the developed hybrid nanoparticle-based nicotine vaccine. Results from this study revealed that all these studied factors significantly influenced the immunological efficacy of the nicotine nanovaccine. By modulating

these factors, enhanced immune responses that can result in higher titers of anti-nicotine antibodies and better ability in blocking nicotine from entering the brain of mice could be achieved.

The findings from this study would lead to a better understanding of how multiple factors influence the immunological efficacy of a nanoparticle-based nicotine vaccine. In addition, the findings from this study can also provide significant guidance for the development of other drug abuse and nanoparticle-based vaccines. More importantly, the hybrid nanoparticle-based nicotine nanovaccine can be a promising candidate for smoking cessation.

Dedication

To my dear wife and parents

Acknowledgements

I am lucky enough to have Dr. Mike Zhang as my advisor. I would like to give my greatest thanks to him for the generous support on my research work and constant help in my life. He has been the most valuable and reliable source I have for guidance, inspiration, and advice. It is my fortune to have an advisor like him who is always optimistic, energetic, and backing me with understanding and patience.

I am grateful to my committee members, Dr. Ehrich Marion, Dr. Tanya LeRoith, and Dr. Xueyang Feng for their kind guidance and support.

I enjoyed all the days working with my colleges, Dr. Yun Hu, Dr. Song Lou, Frank Gillam, Yi Lu, Kyle Saylor, Reece Hoerle, Meaghan Devin, Kristen Powers, Niki Balani, and Brian Harris. I would like to express my thanks to all my colleges for their help in the past four years. I am grateful for the help provided by Dr. Mary Leigh Wolfe, Cora Chen, Teresa Cox, Barbara Wills, Denton Yoder, Ling Li, and Melody Clark.

I am grateful for all the assistance and help provided by Jie Zhu and David Ruth on FTIR, Kathy Lowe on transmission electron microscope, Melissa Makris on flow cytometer, and Dr. Kristi DeCourcy on confocal microscope.

I am so lucky to have Mengyao Luo as my wife. I would like to express my deepest thanks to my dear wife for the constant support behind me. I will remember all the times that you accompanied me to do experiments till midnight.

I am thankful for the generous funding support from National Institute on Drug Abuse (U01DA036850).

Attribution

I declare that the work in Chapter 3 was contributed equally by Zongmin Zhao and Dr. Yun Hu. Work in other chapters was primarily performed by Zongmin Zhao. Dr. Chenming (Mike) Zhang supervised all the work, participated in experimental design, coordinated the experiments, and conducted manuscript revisions. Dr. Marion Ehrich participated in experimental design and conducted manuscript revisions. Dr. Paul R. Pentel, Dr. Michael Raleigh, and Dr. Theresa Harmon from Minneapolis Medical Research Foundation tested brain and serum nicotine concentrations in Chapter 3, 4, 5, 6, and 7. In Chapters 3-7, undergraduate researchers (Reece Hoerle, Meaghan Devine, Kristen Powers, and Brian Harris) and Dr. Yun Hu participated in conduction of parts of experiments. Melissa Makris from College of Veterinary Medicine at Virginia Tech performed the flow cytometry analysis. Dr. Kristi DeCourcy from Fralin Life Science Institute at Virginia Tech provided assistance on confocal microscopy. Kathy Lowe from College of Veterinary Medicine at Virginia Tech provided assistance on TEM imaging. David Ruth from Biological Systems Engineering Department at Virginia Tech and Jie Zhu from Chemistry Department at Virginia Tech helped collect FT-IR data.

Table of Contents

List of Figures

Chapter 3

Chapter 4

Chapter 5

Chapter 7

List of Tables

Chapter 3

Chapter 4

Chapter 5

Chapter 6

Chapter 7

List of Abbreviations

3’-AmNic: 3’-aminomethylnicotine

AF350: Alexa Fluor 350

AF647: Alexa Fluor 647

APCs: antigen presenting cells

BCA: bicinchoninic acid

CDC: Centers for Disease Control and Prevention

CHOL: cholesterol

CLSM: confocal laser scanning microscopy

CM-6: coumarin-6

CNVs: conjugate nicotine vaccines

COPD: chronic obstructive pulmonary diseases

CpG ODN: CpG oligonucleotide

CRM_{197}: cross reactive material 197

DAPI: 4',6-diamidino-2-phenylindole

DCM: dichloromethane

DCs: dendritic cells

DMSO: dimethyl sulfoxide

DOTAP: 1,2-Dioleoyl-3-trimethylammonium-propane

DSPE-PEG2000-amine: 1,2-distearoyl-sn-glycero-3-phosphoethanolamine-N-[amino(polyethylene glycol)-2000]

DSPE-PEG2000-maleimide: 1,2-distearoyl-sn-glycero-3-phosphoethanolamine-N-[maleimide(polyethylene glycol)-2000]

EDC: 1-ethyl-3-[3-dimethylaminopropyl]carbodiimide hydrochloride

EDTA: ethylenediaminetetraacetic acid

ELISA: enzyme-linked immunosorbent assay

FCA: flow cytometry

FTIR: Fourier transform infrared

GC/MS: gas chromatography/mass spectrometry

GM-CSF: granulocyte-macrophage colony-stimulating factor

H&E: hematoxylin and eosin

HPLC: high performance liquid chromatography

IC_{50}: 50% inhibitory concentration

IgG: immunoglobulin G

KLH: keyhole limpet hemocyanin

KN: nicotine-keyhole limpet hemocyanin conjugate

KS: keyhole limpet hemocyanin subunit

LP: lipid-polymeric

LPKN: hybrid nanoparticle-based nicotine vaccine with hapten localized on only carrier protein

LPN: nicotine hapten-conjugated lipid-polymeric hybrid nanoparticle

LPNK: hybrid nanoparticle-based nicotine vaccine with hapten localized on only nanoparticle surface

LPNKN: hybrid nanoparticle-based nicotine vaccine with hapten localized on both carrier protein and nanoparticle surface

MES: 2-(N-morpholino)ethanesulfonic acid

M.F.I.: mean fluorescence intensity

MHC: major histocompatibility complex

MPLA: monophosphoryl lipid A

MSE: standard error of the mean

nAChRs: nicotinic acetylcholine receptors

Nano-CRM_{197}-Nic: nicotine nanovaccine with cross reactive material 197 as stimulating protein

Nano-KLH-Nic: nicotine nanovaccine with keyhole limpet hemocyanin as stimulating protein

Nano-KS-Nic: nicotine nanovaccine with keyhole limpet hemocyanin subunit as stimulating protein

NanoNicVac: lipid-polymeric hybrid nanoparticle-based nicotine nanovaccine

Nano-TT-Nic: nicotine nanovaccine with tetanus toxoid as stimulating protein

NBD: nitro-2-1,3-benzoxadiazol-4-yl

NBD-PE: 1,2-diphytanoyl-sn-glycero-3-phosphoethanolamine-N-(7-nitro-2-1,3-benzoxadiazol-4-yl)

Nic: O-Succinyl-3'-hydroxymethyl-(±)-nicotine

NicAb: nicotine-specific antibody

Nic-BSA: nicotine-bovine serum albumin

Nic-CRM_{197}: nicotine-cross reactive material 197

Nic-KLH: nicotine-keyhole limpet hemocyanin

Nic-KS: nicotine-keyhole limpet hemocyanin subunit

Nic-TT: nicotine-tetanus toxoid

NIH: National Institutes of Health

NPs: nanoparticles

NRT: nicotine replacement therapy

PBS: phosphate-buffered saline

PDI: polydispersity indexes

PEG: polyethylene glycol

PK: pharmacokinetic

PLGA: poly(lactic-co-glycolic acid)

R848: Resiquimod

rEPA: recombinant *Pseudomonas aeruginosa* exoprotein A

Sulfo-NHS: N-hydroxysulfosuccinimide

TEM: transmission electron microscopy

TLR: Toll-like receptor

TNBSA: 2,4,6-trinitrobenzenesulfonic acid

TT: tetanus toxoid

UV: ultraviolet

Chapter 1: Introduction

Tobacco is the most-widely abused substance, and tobacco smoking remains a leading cause of preventable diseases and premature deaths worldwide.[1] Tobacco use not only directly causes cardiovascular diseases, chronic obstructive pulmonary diseases, and cancers, but also is responsible for respiratory tract and other infections, osteoporosis, reproductive disorders, adverse postoperative events and delayed wound healing, duodenal and gastric ulcers, and diabetes.[2] There are currently more than 60 million smokers and 480,000 related deaths per year in U.S., and approximately 6 million tobacco-related deaths annually in the world.[3]

Nicotine is the major addictive substance in cigarettes. Nicotine addiction is responsible for the difficulty in quitting smoking. As a small molecule, nicotine can cross the blood-brain barrier to bind to nicotinic acetylcholine receptors. This binding can subsequently cause the release of dopamine that provides a euphoric feeling to smokers.[2] In fact, most smokers have strong desires to quit, but only less than 5% of them can finally succeed without the help of medications. Abstinence is known to reduce smoking related diseases significantly, but the powerful addiction has been proven to be a difficult hurdle to surpass.[4] Many withdrawal symptoms may be caused by the abstinence from smoking, such as craving for tobacco, distraction, anxiety, and restlessness, all of which enormously compromise a smoker's efforts to quit smoking.[5] Therefore, medications are required to alleviate these symptoms and to aid smokers in quitting smoking.

Currently, there are three major pharmacological medications available to smokers for quitting smoking, nicotine replacement therapy, bupropion, and varenicline.[6] They function via different mechanisms: nicotine replacement therapy works by substituting nicotine from cigarettes with artificial nicotine sources to reduce the craving and withdrawal symptoms after quitting[7]; bupropion is a nicotinic receptor antagonist that can inhibit re-uptake of dopamine and

noradrenaline in the central nervous system that occurs in nicotine withdrawn[8]; varenicline is a nicotinic receptor partial agonist and its competitive binding will reduce the ability of nicotine to bind and stimulate the mesolimbic dopamine system[7]. These pharmacological medications have shown some extents of effectiveness in smoking cessation. However, even with the help of these pharmacological medications, the smoking cessation rate is still disappointingly low (10-25%). In addition, they are sometimes associated with some serious side effects, such as skin irritation, headache, and depression with suicide behaviors.[6] Therefore, it is in urgent need to develop more effective and safe strategies for smoking cessation.

Nicotine vaccines have been proposed in recent decades as a promising strategy for smoking cessation. In principal, a nicotine vaccine can induce the production of nicotine specific antibodies that can bind with nicotine in serum and thus block nicotine from crossing the blood-brain barrier to stimulate the mesolimbic dopamine system.[9, 10] Compared to currently available pharmacological medications, nicotine vaccines have the superiorities of 1) distinguished safety, 2) specific interactions between antibodies and nicotine molecules, 3) limited number of administrations of vaccines for long-lasting effects and hence improved patient compliance, and 4) its complimentary mechanism to pharmacological therapies for potential combination therapies.[9, 11]

A number of conjugate nicotine vaccines have been reported to achieve promising immunological efficacy in preclinical trials, and several of them have reached various stages of clinical trials.[12, 13] However, despite the promising results in preclinical and early-stage clinical trials, no conjugate nicotine vaccines have achieved satisfactory smoking cessation rate, mainly due to the insufficient and highly-variable antibody titers.[9] The phase 2 clinical studies of NicVax® and NicQb® revealed that while the overall smoking cessation rate was not enhanced in the study group

in comparison to the placebo group, the quit rate improved in the top 30% of subjects that had the highest antibody titers.[14, 15] This suggests that the concept of using nicotine vaccines to promote smoking cessation is fundamentally sound, but there is an undoubtedly urgent need for improved vaccines that can elicit stronger immune response.

Theoretically, nicotine is too small to induce an immune response and it has to be attached to a large molecule to be recognized by the immune system.[9] Currently, almost all the already-developed nicotine vaccines are conjugate vaccines in which nicotine haptens are conjugated to a carrier protein for presentation. Although multiple strategies have been applied to improve their immunogenicity, conventional conjugate nicotine vaccines suffer from several innate shortfalls, such as poor recognition and internalization by immune cells, low bioavailability, low specificity, fast degradation, difficulty in integrating with molecular adjuvants, and short immune persistence, all of which lead to low immunological efficacy.[16-18]

In the recent decades, nanoparticles have been widely studied for the delivery of drugs, proteins, and vaccine.[19, 20] Having many advantages, such as high payload loading capacity, controlled payload release, tunable physicochemical properties, and many others, nanoparticles have the potential to overcome many of the abovementioned drawbacks of conjugate nicotine vaccines. In this study, a lipid-poly(lactic-co-glycolic acid) (PLGA) hybrid nanoparticle-based nicotine vaccine was developed, in which lipid-PLGA nanoparticles were used for the efficient delivery of nicotine vaccine components, as a next-generation vaccine candidate for treating nicotine addiction. Because many factors may potentially affect the immunogenicity of a nanoparticle-based nicotine vaccine, we focused on studying the effect of multiple factors, including nanoparticle size, hapten density, hapten localization, carrier protein, and molecular adjuvants, on the immunological efficacy of the hybrid nanoparticle-based nicotine vaccine. In Chapter 3, hybrid nanoparticle-based

nicotine nanovaccines with different particle sizes (100 and 500 nm) were fabricated by controlling the size of PLGA nanoparticles. The cellular uptake of different sized nanovaccine particles were studied in dendritic cells. The immunogenicity of nanovaccines with different particle sizes were investigated in mice. In Chapter 4, a series of hybrid nanoparticle-based nicotine nanovaccines with different hapten densities (high-, medium-, and low-density) were prepared to study the influence of hapten density on their immunological efficacy. The immunogenicity and pharmacokinetic efficacy of nanovaccines with different hapten densities were studied in mice. In Chapter 5, in order to investigate the impact of hapten localizations on the immunological efficacy of the nicotine nanovaccines, three hybrid nanoparticle-based nicotine nanovaccines, which had nicotine localized only on carrier protein, only on nanoparticle surface, or on both, were fabricated and characterized. Their immunogenicity and pharmacokinetic efficacy were studied and compared in mice. In Chapter 6, different carrier protein candidates (cross reactive material 197 (CRM_{197}), tetanus toxoid (TT), keyhole limpet hemocyanin (KLH), and KLH subunit) were conjugated to the nicotine nanovaccines to study the influence of carrier protein on their immunological efficacy. The uptake and processing of nanovaccines with different carrier proteins were studied in dendritic cells. The immunogenicity and pharmacokinetic efficacy of the nanovaccines were investigated in mice. In Chapter 7, multiple molecular adjuvants (monophosphoryl lipid A (MPLA), Resiquimod (R848), and CpG oligonucleotide (CpG OND)) or their combinations were incorporated to the nanovaccine nanoparticles. The influence of different adjuvants on improving the immunological efficacy of the hybrid nanoparticle-based nicotine nanovaccines were studied in mice. Chapter 8 is a general conclusion of this work.

References

[1] Polosa R, Benowitz NL. Treatment of nicotine addiction: present therapeutic options and pipeline developments. Trends Pharmacol Sci. 2011;32:281-9.

[2] Benowitz NL. Nicotine addiction. New Engl J Med. 2010;362:2295-303.

[3] Henley SJ, Thomas CC, Sharapova SR, Momin B, Massetti GM, Winn DM, et al. Vital signs: disparities in tobacco-related cancer incidence and mortality - United States, 2004-2013. Mmwr-Morbid Mortal W. 2016;65:1212-8.

[4] al'Absi M, Amunrud T, Wittmers LE. Psychophysiological effects of nicotine abstinence and behavioral challenges in habitual smokers. Pharmacol Biochem Be. 2002;72:707-16.

[5] Wetter DW, Carmack CL, Anderson CB, Moore CA, De Moor CA, Cinciripini PM, et al. Tobacco withdrawal signs and symptoms among women with and without a history of depression. Exp Clin Psychopharm. 2000;8:88-96.

[6] Cahill K, Stevens S, Perera R, Lancaster T. Pharmacological interventions for smoking cessation: an overview and network meta-analysis. Cochrane Db Syst Rev. 2013.

[7] Stapleton JA, Watson L, Spirling LI, Smith R, Milbrandt A, Ratcliffe M, et al. Varenicline in the routine treatment of tobacco dependence: a pre-post comparison with nicotine replacement therapy and an evaluation in those with mental illness. Addiction. 2008;103:146-54.

[8] Roddy E. ABC of smoking cessation - Bupropion and other non-nicotine pharmacotherapies. Brit Med J. 2004;328:509-11.

[9] Pentel PR, LeSage MG. New directions in nicotine vaccine design and use. Adv Pharmacol. 2014;69:553-80.

[10] Raupach T, Hoogsteder PH, Onno van Schayck CP. Nicotine vaccines to assist with smoking cessation: current status of research. Drugs. 2012;72:e1-16.

[11] Brimijoin S, Shen XY, Orson F, Kosten T. Prospects, promise and problems on the road to effective vaccines and related therapies for substance abuse. Expert Rev Vaccines. 2013;12:323-32.

[12] McCluskie MJ, Thorn J, Mehelic PR, Kolhe P, Bhattacharya K, Finneman JI, et al. Molecular attributes of conjugate antigen influence function of antibodies induced by anti-nicotine vaccine in mice and non-human primates. Int Immunopharmacol. 2015;25:518-27.

[13] Goniewicz ML, Delijewski M. Nicotine vaccines to treat tobacco dependence. Hum Vacc Immunother. 2013;9:13-25.

[14] Hatsukami DK, Jorenby DE, Gonzales D, Rigotti NA, Glover ED, Oncken CA, et al. Immunogenicity and smoking-cessation outcomes for a novel nicotine immunotherapeutic. Clin Pharmacol Ther. 2011;89:392-9.

[15] Cornuz J, Zwahlen S, Jungi WF, Osterwalder J, Klingler K, van Melle G, et al. A vaccine against nicotine for smoking cessation: A randomized controlled trial. Plos One. 2008;3.

[16] Pryde DC, Jones LH, Gervais DP, Stead DR, Blakemore DC, Selby MD, et al. Selection of a novel anti-nicotine vaccine: influence of antigen design on antibody function in mice. Plos One. 2013;8.

[17] de Villiers SHL, Lindblom N, Kalayanov G, Gordon S, Baraznenok I, Malmerfelt A, et al. Nicotine hapten structure, antibody selectivity and effect relationships: Results from a nicotine vaccine screening procedure. Vaccine. 2010;28:2161-8.

[18] Chen XY, Pravetoni M, Bhayana B, Pentel PR, Wu MX. High immunogenicity of nicotine vaccines obtained by intradermal delivery with safe adjuvants. Vaccine. 2012;31:159-64.

[19] Gregory AE, Titball R, Williamson D. Vaccine delivery using nanoparticles. Front Cell Infect Mi. 2013;3.

[20] Reverter J. The use of nanoparticles conjugates as vaccine adjuvant and antigen delivery vehicles. New Biotechnol. 2009;25:S29-S37.

Chapter 2: Literature Review: Nicotine Vaccines as a Promising Immunotherapeutic Strategy for Treating Nicotine Addiction

2.1 Current status and the health effects of tobacco smoking

Tobacco smoking is very prevalent in almost every country, regardless of the stage of economy development. It is estimated that there are currently more than 1.1 billion smokers in the world.[1, 2] According to the Centers for Disease Control and Prevention (CDC), for the year of 2015, approximately 36.5 million U.S adults (16.7% of males and 13.6% of females) were tobacco smokers.[3] In addition, it has been estimated that each day, over 3,200 U.S. people younger than 18 years of age try to smoke for the first time, and around 2,100 U.S. youths become daily smokers from occasional smokers.[4]

There has been sufficient evidence to show that tobacco smoking is correlated with increased health risks. Smoking harms almost every organ of the body and significantly influences the overall health of a person.[5, 6] Tobacco use not only directly causes cardiovascular diseases, chronic obstructive pulmonary diseases, and cancers, but also is responsible for respiratory tract and other infections, osteoporosis, reproductive disorders, adverse postoperative events and delayed wound healing, duodenal and gastric ulcers, and diabetes.[7, 8] It has been reported that, compared to non-smokers, smokers have 2 to 4 times higher risk of coronary heart disease, 2 to 4 times higher risk of stroke, and at least 25 times higher risk of lung cancer.[4]

Cardiovascular disease represents the leading cause of deaths in the United States that kills over 800,000 people every single year.[9] Smoking is one of the major causes of cardiovascular disease, and specifically, one of three people dying from cardiovascular disease has tobacco smoking as a

contributing factor.[10] The mechanism of tobacco smoking causing cardiovascular disease is that chemicals in cigarettes can lead the blood vessel cells to be swollen and inflamed, thus making blood vessels thicken and narrower.[11, 12] This change of blood vessels can cause many serious cardiovascular conditions, such as atherosclerosis, coronary heart disease, stroke, peripheral arterial disease, and abdominal aortic aneurysm.[13, 14] Any amount of smoking, no matter heavy or light or even occasional, may be a potential factor to cause cardiovascular diseases. Studies reveal that even people who smoke less than five cigarettes per day may develop early signs of cardiovascular diseases.[15] Even worse, secondhand smoking can also significantly increase the risk of cardiovascular diseases.[16] In fact, more than 33,000 nonsmokers died from secondhand smoking-induced cardiovascular diseases every year.[4]

Tobacco smoking can cause respiratory diseases by damaging the airways and small air sacs in the lungs.[17] Toxins in cigarettes can significantly harm the human body right from the moment mouths and noses are exposed. Chemicals in cigarettes can be absorbed in the lungs once they reach there. As a consequence, the absorbed chemicals may cause lung diseases like chronic obstructive pulmonary diseases (COPD), cause COPD to be more severe, and increase the risk of respiratory infections.[18] It has been reported that smokers have 12 to 13 times higher risk of dying from COPD in comparison to non-smokers.[19] In addition, chemicals in cigarettes can slow down the lung growth of young people if their lungs are still growing. This damage will cause the lungs of young people to fail to grow to the full size and never to perform at full capacity, increasing the risk of COPD throughout their entire life.[20, 21]

Smoking is the leading cause of cancers and cancer-related deaths. Smoking contributes to cancers almost everywhere in human body, including the bladder, blood, cervix, colon and rectum, esophagus, kidney and ureter, larynx, liver, oropharynx, pancreas, stomach, trachea, bronchus, and

lung.[22] Particularly, smoking is the leading cause of lung cancers, and more than 80% of lung cancers are attributed to tobacco smoking.[23] Besides lung cancer, tobacco smoking also accounts for 42% of oral and oropharynx cancer, 42% of esophageal cancer, 13% of stomach cancer, 14% of liver cancer, 22% of pancreatic cancer, 28% of bladder cancer, 9% of blood cancer, and 2% of cervical cancer.[24, 25] It has been estimated that if all U.S. people quit smoking, one of every three deaths caused by smoking would not happen.[4]

Overall, by harming every organ of human body and contributing to many diseases, tobacco smoking remains the leading cause of preventable deaths.[7] Tobacco use causes nearly 6 million deaths annually in the world, and it is estimated that the figure will increase to 8 million by the year of 2030. In U.S. alone, there are currently more than 480,000 people dying from tobacco smoking every single year, among whom over 41,000 people died from secondhand smoke exposure. Deaths caused by tobacco use account for nearly 1/5 of total deaths annually in the United States.[3] In addition, it has been reported that the lifespan of smokers is almost 10 years shorter than that of non-smokers on average. Also, it has been predicted that if current U.S. youths continue to smoke at the current rate, nearly 5.6 million of them (about one in every thirteen) are expected to die from smoking-related diseases in the future.[26]

2.2 The need of using medications to aid in smoking cessation

To stop tobacco smoking is very difficult as nicotine is addicting. Nicotine is a small molecule (MW=162.23) naturally existing in cigarettes and is the major component causing the addiction of tobacco smokers.[7] Research has suggested that nicotine may be as addictive as cocaine, heroin, and alcohol. The mechanism of nicotine addiction has been well described. Nicotine is such a small molecule that it can be transported across the blood-brain barrier to reach the brain of a subject. Around 1.5 mg of nicotine will be inhaled if a cigarette is smoked. The inhaled nicotine

can reach the brain in 10-20 s after a puff.[27, 28] After reaching the brain, nicotine initiates its action by binding to nicotinic acetylcholine receptors (nAChRs), which are ligand-gated ion channels.[29, 30] The binding of nicotine can enable the stimulation of nAChRs, which subsequently opens the ion-channels to allow the influx of sodium or calcium into nerve cells. The membrane of nerve cells is subsequently depolarized and thereby initiates the release of a variety of neurotransmitters, such as dopamine.[31] The release of dopamine results in positive psychological effects of pleasure, arousal, and mood modulation, and contributes to development of nicotine addiction.[7, 32-34]

If nicotine addiction has developed, more nicotine will be required to maintain euphoria because receptors can adapt. Meanwhile, smokers also need nicotine to maintain their normal brain functioning since their brain has become tolerant.[7] Thus, to combat smoking, a smoker needs to deal with both the altered neurotransmitter release and many severe withdrawal systems, including irritability, depressed mood, restlessness, anxiety, difficulty concentrating, hunger, and weight gain. Nicotine addiction is sustained both by the positive effects of pleasure and arousal and by the avoidance of the unpleasant effects of nicotine withdrawal.[35, 36] In fact, a substantial portion of smokers have strong desire to quit smoking. It has been shown that 68% of current adult smokers and 45.5% of current high school smokers in U.S. reported in 2015 that they wanted to quit smoking. However, most of them experienced relapse in one month and only less than 3% of them finally succeeded without medications.[37, 38] Due to the super-strong addictiveness of nicotine, medications are needed to aid smoking cessation.

2.3 Pharmacological medications for smoking cessation

Although abstinence has shown some extent of success in helping people quit smoking, its efficacy is generally very low and some severe adverse effects are associated with the abstinence process.

In order to aid smokers in quitting tobacco smoking, great efforts have been made to develop pharmacological medications. Currently, there are three major classes of pharmacological medications available to smokers, nicotine replacement therapy (NRT), bupropion, and varenicline.[39]

NRT is the first FDA-approved pharmacological medication for smoking cessation.[40] There are currently six forms of FDA-approved NRT therapies available to smokers in the market: nicotine patch, nicotine gum, nicotine lozenge, nicotine sublingual tablets, nicotine nasal spray, and nicotine vapor inhalers.[36, 41, 42] The mechanism of action of NRT is believed to rely on two aspects. First, nicotine delivered by NRT can stimulate nAChRs in the ventral tegmental area of the brain of smokers, thus inducing the release of dopamine in the nucleus accumbens. This action together with some other peripheral actions of nicotine can attenuate some of the withdrawal symptoms in regular smokers obtained from smoking.[43] Second, via a coping mechanism, NRT can make cigarettes less rewarding to smokers. Nicotine delivered by NRT enters the human body by systemic venous absorption rather than systemic arterial delivery that is with smoking, and thus NRT only slowly delivers nicotine and achieves a lower level of arterial nicotine. As a result, NRT can provide some effects for which the smokers previously relied on cigarettes, such as sustaining desirable mood and attention states.[39, 43, 44] Current evidence suggests that all NRTs, no matter what form, considerably increase the possibility of successfully quitting smoking. Specifically, NRTs increase the smoking cessation rate by 50%-70%.[44] However, although NRT is widely recommended as an aid for smoking cessation, it has several limitations that largely affect the patient compliance. First, NRT needs to be administered very frequently, causing high cost and inconvenience to smokers.[45] Second, some adverse effects are associated with NRT, such as skin irritation, depression, anxiety, dizziness, and headache.[46-50]

Bupropion, which was first developed as an antidepressant agent in 1989,[51] was found in 1997 to have smoking cessation properties.[52] After further evaluation as a smoking cessation agent, it was marketed as Zyban® and used as a first line smoking cessation pharmacological medication.[53-55] The mechanism of action of bupropion has not been fully determined. However, it has been proposed that bupropion may exert its main mechanism of action via inhibiting dopamine and noradrenalin reuptake.[56] The inhibition of dopamine reuptake by influencing the dopamine transporter system may reduce the dopamine deficiency experienced in nicotine withdrawal and may explain the attenuating effect of bupropion on nicotine withdrawal symptoms.[57, 58] In addition, some other mechanisms have also been suggested. Bupropion may antagonize the effect of nicotine at the postsynaptic nicotinic acetylcholine receptor.[59] Bupropion may also inhibit nicotine-induced vesicular release of dopamine.[60] Clinical trial data suggests that bupropion could double the odds of smoking cessation over placebo, and the smoking cessation rate was 12-30% depending on the dose of administered bupropion.[53] Another clinical study revealed that the combination of bupropion and a nicotine patch could achieve higher smoking cessation rate than bupropion or nicotine patch alone.[61] Although bupropion seems to have acceptable efficacy in aiding smoking cessation, it may cause various side effects, such as agitation, insomnia, headache, nausea, stomach pain, dizziness, muscle pain, diarrhea, seizures, weight loss or gain, tremor, and increased urination.[62-65] Due to those potential health risks, FDA requires the manufacturer to put a black box warning on its label.[66]

Varenicline, which was developed by Pfizer, was the latest FDA-approved pharmacological medication for aiding smoking cessation.[67, 68] Varenicline is an $\alpha_4\beta_2$ nicotinic receptor partial agonist. The mechanism of action of varenicline is believed to be attributed to its agonist property at nicotinic receptors.[69] As a partial agonist at the nicotinic receptor, varenicline is able to cause

a moderate and sustained increase of mesolimbic dopamine levels. This can counteract the low dopamine levels resulted from the lack of nicotine during smoking cessation process, which seem to be significant in contributing to craving and withdrawal.[70] Meanwhile, by competitively binding to nicotinic receptor, varenicline is able to shield a smoker from nicotine-induced increases in dopamine levels thereby preventing events of relapse.[71] Clinical trial data suggests that varenicline was more effective than bupropion and placebo after 12 weeks. In addition, it was found that the continuous abstinence rate from 9 to 52 weeks of varenicline (23%) was higher than that of bupropion (15%) and placebo (10%).[70] Moreover, meta-analysis suggests that varenicline is also more effective in aiding smoking cessation than a single form of NRT.[72, 73] It has been noticed that side effects are associated with the use of varenicline. The major side effects are nausea, vomiting, and insomnia.[72] Some neuropsychiatric side effects were reported anecdotally, including psychosis, depression, and suicidal behavior.[74-76] In addition, meta-analysis indicates that varenicline may cause some, although small, cardiovascular side effects.[77]

2.4 The rationale of developing nicotine vaccines for smoking cessation

Smokers need the help of medications to get rid of smoking. Current available pharmacological medications have proven certain extent of success in promoting smoking cessation. However, their success at smoking cessation rate is limited. Also, the adverse side effects associated with them lead to low customer compliance. Therefore, more effective and safe strategies are an urgent need for smoking cessation. In the recent two decades, nicotine vaccines have emerged as a promising immunotherapeutic method for treating nicotine addiction.[78] The mechanism of nicotine vaccines is based on the production of nicotine specific antibodies. In brief, when administered, a nicotine vaccine can stimulate the immune system to induce the production of nicotine specific antibodies. The nicotine specific antibodies are able to bind with nicotine in the blood and

peripheral body fluids to form a nicotine-antibody complex. Because of the large size of the complex, nicotine cannot be transported across the blood-brain barrier. As a result, nicotine will not be accessible to nAChRs and will not cause the release of dopamine.[79, 80] The rationale of developing nicotine vaccines for treating nicotine addiction relies on the fact that the brain nicotine level of a subject could be reduced to an extent to preventing addiction, if a sufficient amount of nicotine specific antibodies could be produced by a nicotine vaccine.[81, 82] Compared to conventional pharmacological medications, nicotine vaccines hold many advantages: 1) unparalleled safety, 2) specific interactions between antibodies and the targeted drug molecule, 3) the limited number of administrations/injections of vaccines for long-lasting effects and hence improved patient compliance, and 4) its complimentary mechanism to pharmacological therapies for potential combination therapies.[83, 84]

2.5 The first-generation nicotine vaccine: nicotine-protein conjugate-based nicotine vaccine

Nicotine is such a small molecule that it cannot be recognized by immune cells on its own. To induce an immune response, nicotine needs to be attached to a support, such as a carrier protein or nanoparticle.[82] The first-generation nicotine vaccine developed for nicotine addiction treatment utilizes a carrier protein as the support to present nicotine haptens. These carrier protein-based nicotine vaccines are commonly referred to as nicotine-protein conjugate nicotine vaccines.[85] Basically, a conjugate nicotine vaccine is constructed by conjugating a nicotine hapten to a carrier protein via a linker. Initially, it was found in preclinical studies that conjugate nicotine vaccines were able to elicit high titers of nicotine specific antibodies and significantly block nicotine from entering the brain. To date, five conjugate nicotine vaccines have tested in human clinical trials, including TA-NIC, NicQb, NicVAX, Niccine, and NIC7.[86] NicVAX and NicQb represent the

most successful conjugate nicotine vaccines so far, and both of them have reached clinical testing levels of at least phase IIb. NIC7 is the only conjugate nicotine vaccine that is still being tested in ongoing clinical trials.

NicVax, another vaccine, is the only conjugate nicotine vaccine that has been tested in phase III clinical trials. Developed by Nabi Pharmaceuticals and GlaxoSmithKline, NicVAX is constructed by linking 3'-aminomethylnicotine (3'-AmNic) to recombinant *Pseudomonas aeruginosa* exoprotein A (rEPA) via a succinyl linker. [87]In phase II and IIb studies, it was found that a subgroup of the top 30% antibody responders achieved a significantly higher smoking cessation rate than the placebo group for up to 34 weeks. In addition, it was found that the target quit day was dependent on the dose regimen, and smokers who were immunized with 5 injections of 400 μg of NicVAX had the highest antibody titers, which resulted in significantly higher abstinence rates than smokers received a placebo. Meanwhile, it was also found that NicVAX could significantly reduce the daily cigarette consumptions in the top 30% antibody responders in weeks 19-52 compared to the placebo group.[88, 89] Two phase III studies were conducted in 1,000 smokers who received 6 injections of 400 μg of NicVAX or placebo. Unfortunately, two phase III studies did not prove the promising efficacy of NicVAX that was shown in the two phase II studies. No significant differences in smoking quit rate were found between the vaccination and placebo groups.[90]

NicQb, another vaccine, is a virus-like particle based nicotine conjugate vaccine that has been tested in phase IIb clinical trials. Developed by Cytos/Novartis in Switzerland, NicQb was constructed by linking O-succinyl-3'-hydroxy-methyl-(±)-nicotine to a virus-like particle self-assembled from the coat protein of the bacteriophage Qb.[91] The phase I study data indicated that all the participants developed an anti-nicotine immune response on day 14. Meanwhile, no obvious

adverse side effects were detected in smokers after being immunized with NicQb.[92] In the phase II study, NicQb was found to be safe, well tolerated, and highly immunogenic. Smokers immunized with NicQb exhibited a significantly higher abstinence rate than the placebo at 2 months, but the continuous abstinence rate between months 2 and 6 was not significantly different. However, subgroup analysis revealed that the top 33% subjects with highest antibody titers showed significantly higher continuous abstinence from month 2 until month 6 compared to the placebo.[93] In the phase IIb study, smokers were immunized with 5 injections of NicQb weekly or bi-weekly. However, unfortunately, no significantly enhanced abstinence rate was observed in the treatment group in comparison to the placebo group.[86]

By summarizing the previous findings in published literature, Pfizer conducted a systematic preclinical optimization and evaluation of a new conjugate vaccine, NIC7. NIC7 was constructed by conjugating (S)-2-(5-(1-methylpyrrolidin-2-yl)pyridin-3-yloxy)ethanamine to cross-reactive material 197 (CRM_{197}). Initially, the vaccine was designed by linking 3'-AmNic that was used in NicVAX to diphtheria toxoid. Preclinical animal trail data indicated that this vaccine with alum adjuvant and CpG oligodeoxynucleotide (CpG ODN) induced high titers of anti-nicotine antibodies with high affinity in mice and non-human primates. However, it only exhibited modest effects in preventing brain nicotine entry.[94, 95] In a later study, Pfizer developed and optimized a series of nicotine haptens. Animal trial data suggested that 5-amino-ethoxy-nicotine resulted in the highest immunological efficacy of NIC7.[96] Subsequently, they optimized other parameters to further improve the immunogenicity of NIC7, such as modulating hapten density, controlling degree of conjugate aggregation, and eliminating adducts.[97] The optimized vaccine formulation can block up to 81% of nicotine from entering the brain in non-human primates.[98] Currently, two formulations of NIC7, NIC7-001 and NIC7-003, are in clinical trials.

Although promising efficacy of conjugate nicotine vaccines has been found in preclinical trails, all the clinically-tested conjugate vaccines have not resulted in an enhanced overall smoking cessation rate. Evidence from the clinical trials of NicVAX and NicQb suggested that the basic concept of using nicotine vaccine to treat nicotine addiction is sound, however, high quantity and quality anti-nicotine antibodies need to be induced by a nicotine vaccine to guarantee the vaccination efficacy.[88, 89] To increase the immunogenicity of conjugate nicotine vaccines, multiple strategies have been investigated, such as hapten screening[96], selection of carrier proteins,[98] modulating hapten density,[97] using modern molecular adjuvants,[95] applying hapten clustering,[99] and designing multivalent vaccines.[100] Meanwhile, it has been proposed that new platforms like nanoparticles can provide a revolutionary strategy to increase the immunogenicity of nicotine vaccines.[82]

2.6 The next-generation nicotine vaccine: nanoparticle-based nicotine vaccine

The first-generation nicotine-protein conjugate-based nicotine vaccines have some innate shortcomings, including poor recognition and internalization by immune cell, low bioavailability, low specificity, difficulty in integrating with molecular adjuvants, short immune persistence, and fast degradation, all of which largely limit their immunological efficacy.[82] As all the clinically-tested conjugate nicotine vaccines have not shown enhanced overall smoking cessation rate than placebo, new technologies and non-protein-based platforms are needed to revolutionize the design of nicotine vaccines. In the era of nanotechnology, nanoparticles have been successfully used as delivery vehicles of drugs, proteins/peptides, and vaccines.[101-107] Considering their numerous advantages, nanoparticles have potential as a new platform for nicotine vaccine development so as to cope with the innate drawbacks of conjugate nicotine vaccines.

The use of nanoparticles as platforms for nicotine vaccine development has many advantages. First, the immune system prefers to recognize particulate antigens (like bacteria and viruses) and is relatively invisible to soluble protein antigens (like nicotine-protein conjugates). The particulate nature of nanoparticles may lead to an enhanced recognition and capture of nicotine vaccine particles by immune cells. Secondly, nanoparticles typically have a high loading capacity of payloads, so nicotine vaccine components can be efficiently loaded to nanoparticles, thereby improving the availability of nicotine vaccine components to the immune system. Thirdly, the physicochemical properties of nanoparticles, such as shape, size, hydrophilicity, and charge, can be tuned to lead to an improved internalization of vaccine particles by immune cells. Fourthly, molecular adjuvants can be easily incorporated to nanoparticles and co-delivered with nicotine antigens to the same immune cells to induce a strong immune response. Last but not least, the load of nicotine vaccine components onto or within nanoparticles may protect them from premature degradation. Meanwhile, nanoparticles can be engineered to have a suitable stability. Therefore, a strong immune response with long persistence can be achieved by nanoparticle-based nicotine vaccines.

To date, several types of nanoparticles have been studied as platforms for nicotine vaccine development, including liposomes,[108, 109] biodegradable polymeric nanoparticles,[110] and DNA scaffolds.[111] Among those nanoparticle-based nicotine vaccines, SEL-068 was the first to enter clinical trials. SEL-068, developed by Selecta Biosciences, was a fully synthetic nicotine vaccine based on self-assembled biodegradable polymeric nanoparticles. SEL-068 is composed of four major components, including a biodegradable and biocompatible polymer matrix, a synthetic toll-like receptor (TLR) agonist, a novel T-cell helper peptide, and nicotine hapten covalently conjugated to nanoparticle surface.[112] According to the developer, SEL-068 was designed to

mimic key recognition features of highly immunogenic microbial pathogens: 1) a particulate form; 2) nano-scale size for unimpeded access to lymph vessels and travel to lymph nodes; 3) pathogen-associated molecular patterns that serve as adjuvant by stimulating antigen presenting cell-expressed receptors, such as TLRs; 4) densely arrayed surface molecules that are capable of cross-linking B-cell receptors on antigen-specific B cells; 5) incorporation of protein sequences that can be processed and presented in diverse major histocompatibility class II complexes for recognition by CD44+ T cells.[113] Preclinical animal trials in mice and non-human primates suggest that SEL-068 could induce high titers of anti-nicotine antibodies with high affinity to nicotine.[112] SEL-068 has entered to phase I clinical trials, but the results have not been reported. However, according to Selecta Biosciences, SEL-068 has been reformulated using a two-nanoparticle strategy to enhance the immune response in humans. The reformulated form, SEL-070, has entered a phase I clinical trial to test the immunological efficacy and safety.

2.7 Conclusion

Tobacco smoking is one of the largest public health concerns the world has ever faced. Tobacco use continues to be the leading cause of preventable diseases and premature deaths, resulting in huge mortality, morbidity, and economic loss. Without the help of medications, smokers may experience huge difficulty in quitting smoking. Current available pharmacological medications, including NRT, bupropion, and varenicline, have shown some extent of success in helping smokers stop smoking, however, their efficacy is far from ideal. Also, the severe adverse effects of pharmacological medications decrease patient compliance. Nicotine vaccines have been developed as a more safe and efficient strategy for smoking cessation. Nicotine vaccines, if successful, may offer an alternative to current pharmacological medications for smoking cessation. Initial efforts on developing the first-generation protein-based conjugate nicotine vaccines have proven that

conjugate nicotine vaccines could induce high titers of anti-nicotine antibodies with high affinity to nicotine in preclinical trials. However, unfortunately, the prominent efficacy of conjugate nicotine vaccines has not been successfully transferred in the clinical setting. As the first-generation conjugate nicotine vaccines have many innate shortcomings, new technologies and platforms are needed to revolutionize the design of nicotine vaccines to lead to the induction of a sufficiently strong immune response. The utilization of various nanoparticle platforms as nicotine vaccine delivery vehicles has the potential to overcome the drawbacks of conjugate nicotine vaccines. Based on those nanoparticles, several nanoparticle-based nicotine vaccines are under development as the next-generation immunotherapeutic strategy for treating nicotine addiction. Future studies may focus on manipulating the versatility of nanoparticle platforms to accurately control every parameter of nanoparticle-based nicotine vaccines, making them more immunogenic so to advance to clinical trials.

References

[1] Samet JM. Tobacco smoking: the leading cause of preventable disease worldwide. Thorac Surg Clin. 2013;23:103-12.

[2] Giovino GA, Mirza SA, Samet JM, Grp GC. Tobacco use in 3 billion individuals from 16 countries: an analysis of nationally representative cross-sectional household surveys (vol 380, pg 668, 2012). Lancet. 2013;382:128-.

[3] Jamal A, King BA, Neff LJ, Whitmill J, Babb SD, Graffunder CM. Current cigarette smoking among adults - United States, 2005-2015. Mmwr-Morbid Mortal W. 2016;65:1205-11.

[4] U.S. Department of Health and Human Services.The health consequences of smoking—50 years of progress: A report of the surgeon general. Atlanta: U.S. Department of Health and Human Services, Centers for Disease Control and Prevention, National Center for Chronic Disease Prevention and Health Promotion, Office on Smoking and Health, 2014.

[5] Screening, PDQ, Prevention Editorial B. Cigarette smoking: health risks and how to quit (PDQ(R)): Health Professional Version. PDQ Cancer Information Summaries. Bethesda (MD)2002.

[6] Alberg AJ. Cigarette smoking: health effects and control strategies. Drugs Today (Barc). 2008;44:895-904.

[7] Benowitz NL. Nicotine addiction. N Engl J Med. 2010;362:2295-303.

[8] Benowitz NL. Pharmacology of nicotine: addiction, smoking-induced disease, and therapeutics. Annu Rev Pharmacol Toxicol. 2009;49:57-71.

[9] Niiranen TJ, Vasan RS. Epidemiology of cardiovascular disease: recent novel outlooks on risk factors and clinical approaches. Expert Rev Cardiovasc Ther. 2016;14:855-69.

[10] Messner B, Bernhard D. Smoking and cardiovascular disease: mechanisms of endothelial dysfunction and early atherogenesis. Arterioscler Thromb Vasc Biol. 2014;34:509-15.

[11] Kelishadi R, Poursafa P. A review on the genetic, environmental, and lifestyle aspects of the early-life origins of cardiovascular disease. Curr Probl Pediatr Adolesc Health Care. 2014;44:54-72.

[12] Maclay JD, MacNee W. Cardiovascular disease in COPD: mechanisms. Chest. 2013;143:798-807.

[13] Ambrose JA, Barua RS. The pathophysiology of cigarette smoking and cardiovascular disease: an update. J Am Coll Cardiol. 2004;43:1731-7.

[14] Benowitz NL. Cigarette smoking and cardiovascular disease: pathophysiology and implications for treatment. Prog Cardiovasc Dis. 2003;46:91-111.

[15] Schane RE, Ling PM, Glantz SA. Health effects of light and intermittent smoking: a review. Circulation. 2010;121:1518-22.

[16] Venn A, Britton J. Exposure to secondhand smoke and biomarkers of cardiovascular disease risk in never-smoking adults. Circulation. 2007;115:990-5.

[17] Pelegrino NR, Tanni SE, Amaral RA, Angeleli AY, Correa C, Godoy I. Effects of active smoking on airway and systemic inflammation profiles in patients with chronic obstructive pulmonary disease. Am J Med Sci. 2013;345:440-5.

[18] Jayes L, Haslam PL, Gratziou CG, Powell P, Britton J, Vardavas C, et al. SmokeHaz: Systematic reviews and meta-analyses of the effects of smoking on respiratory health. Chest. 2016;150:164-79.

[19] Burney P, Jarvis D, Perez-Padilla R. The global burden of chronic respiratory disease in adults. Int J Tuberc Lung Dis. 2015;19:10-20.

[20] Rehan VK, Asotra K, Torday JS. The effects of smoking on the developing lung: insights from a biologic model for lung development, homeostasis, and repair. Lung. 2009;187:281-9.

[21] Lebowitz MD, Sherrill D, Holberg CJ. Effects of passive smoking on lung growth in children. Pediatr Pulmonol. 1992;12:37-42.

[22] Gandini S, Botteri E, Iodice S, Boniol M, Lowenfels AB, Maisonneuve P, et al. Tobacco smoking and cancer: a meta-analysis. Int J Cancer. 2008;122:155-64.

[23] Hecht SS. Cigarette smoking and lung cancer: chemical mechanisms and approaches to prevention. Lancet Oncol. 2002;3:461-9.

[24] Weiderpass E. Lifestyle and cancer risk. J Prev Med Public Health. 2010;43:459-71.

[25] Lee YC, Hashibe M. Tobacco, alcohol, and cancer in low and high income countries. Ann Glob Health. 2014;80:378-83.

[26] Jha P, Ramasundarahettige C, Landsman V, Rostron B, Thun M, Anderson RN, et al. 21st-century hazards of smoking and benefits of cessation in the United States. N Engl J Med. 2013;368:341-50.

[27] Hukkanen J, Jacob P, 3rd, Benowitz NL. Metabolism and disposition kinetics of nicotine. Pharmacol Rev. 2005;57:79-115.

[28] Benowitz NL, Herrera B, Jacob P, 3rd. Mentholated cigarette smoking inhibits nicotine metabolism. J Pharmacol Exp Ther. 2004;310:1208-15.

[29] Dajas-Bailador F, Wonnacott S. Nicotinic acetylcholine receptors and the regulation of neuronal signalling. Trends Pharmacol Sci. 2004;25:317-24.

[30] Paterson D, Nordberg A. Neuronal nicotinic receptors in the human brain. Prog Neurobiol. 2000;61:75-111.

[31] Balfour DJ. The neurobiology of tobacco dependence: a preclinical perspective on the role of the dopamine projections to the nucleus accumbens [corrected]. Nicotine Tob Res. 2004;6:899-912.

[32] Mansvelder HD, McGehee DS. Cellular and synaptic mechanisms of nicotine addiction. J Neurobiol. 2002;53:606-17.

[33] Dani JA, De Biasi M. Cellular mechanisms of nicotine addiction. Pharmacol Biochem Behav. 2001;70:439-46.

[34] Prochaska JJ, Benowitz NL. The past, present, and future of nicotine addiction therapy. Annu Rev Med. 2016;67:467-86.

[35] Herman AI, DeVito EE, Jensen KP, Sofuoglu M. Pharmacogenetics of nicotine addiction: role of dopamine. Pharmacogenomics. 2014;15:221-34.

[36] Benowitz NL. Neurobiology of nicotine addiction: implications for smoking cessation treatment. Am J Med. 2008;121:S3-10.

[37] Babb S, Malarcher A, Schauer G, Asman K, Jamal A. Quitting smoking among adults - United States, 2000-2015. Mmwr-Morbid Mortal W. 2017;65:1457-64.

[38] Kann L, McManus T, Harris WA, Shanklin SL, Flint KH, Hawkins J, et al. Youth risk behavior surveillance - United States, 2015. Mmwr Surveill Summ. 2016;65:1-174.

[39] Jain R, Majumder P, Gupta T. Pharmacological intervention of nicotine dependence. Biomed Res Int. 2013;2013:278392.

[40] Mendelsohn C. Optimising nicotine replacement therapy in clinical practice. Aust Fam Physician. 2013;42:305-9.

[41] Haustein KO. Pharmacotherapy of nicotine dependence. Int J Clin Pharmacol Ther. 2000;38:273-90.

[42] Stead LF, Perera R, Bullen C, Mant D, Hartmann-Boyce J, Cahill K, et al. Nicotine replacement therapy for smoking cessation. Cochrane Database Syst Rev. 2012;11:CD000146.

[43] Molyneux A. Nicotine replacement therapy. BMJ. 2004;328:454-6.

[44] Stead LF, Perera R, Bullen C, Mant D, Lancaster T. Nicotine replacement therapy for smoking cessation. Cochrane Database Syst Rev. 2008:CD000146.

[45] Etter JF, Stapleton JA. Nicotine replacement therapy for long-term smoking cessation: a meta-analysis. Tob Control. 2006;15:280-5.

[46] Moolchan ET, Robinson ML, Ernst M, Cadet JL, Pickworth WB, Heishman SJ, et al. Safety and efficacy of the nicotine patch and gum for the treatment of adolescent tobacco addiction. Pediatrics. 2005;115:e407-14.

[47] Blondal T, Gudmundsson LJ, Olafsdottir I, Gustavsson G, Westin A. Nicotine nasal spray with nicotine patch for smoking cessation: randomised trial with six year follow up. BMJ. 1999;318:285-8.

[48] Rigotti NA, Gonzales D, Dale LC, Lawrence D, Chang Y, Group CS. A randomized controlled trial of adding the nicotine patch to rimonabant for smoking cessation: efficacy, safety and weight gain. Addiction. 2009;104:266-76.

[49] Uyar M, Filiz A, Bayram N, Elbek O, Herken H, Topcu A, et al. A randomized trial of smoking cessation. Medication versus motivation. Saudi Med J. 2007;28:922-6.

[50] Schuurmans MM, Diacon AH, van Biljon X, Bolliger CT. Effect of pre-treatment with nicotine patch on withdrawal symptoms and abstinence rates in smokers subsequently quitting with the nicotine patch: a randomized controlled trial. Addiction. 2004;99:634-40.

[51] Fava M, Rush AJ, Thase ME, Clayton A, Stahl SM, Pradko JF, et al. 15 years of clinical experience with bupropion HCl: from bupropion to bupropion SR to bupropion XL. Prim Care Companion J Clin Psychiatry. 2005;7:106-13.

[52] Tong EK, Carmody TP, Simon JA. Bupropion for smoking cessation: a review. Compr Ther. 2006;32:26-33.

[53] Hurt RD, Sachs DP, Glover ED, Offord KP, Johnston JA, Dale LC, et al. A comparison of sustained-release bupropion and placebo for smoking cessation. N Engl J Med. 1997;337:1195-202.

[54] Richmond R, Zwar N. Review of bupropion for smoking cessation. Drug Alcohol Rev. 2003;22:203-20.

[55] Hughes JR, Stead LF, Hartmann-Boyce J, Cahill K, Lancaster T. Antidepressants for smoking cessation. Cochrane Database Syst Rev. 2014:CD000031.

[56] Warner C, Shoaib M. How does bupropion work as a smoking cessation aid? Addict Biol. 2005;10:219-31.

[57] Nomikos GG, Damsma G, Wenkstern D, Fibiger HC. Effects of chronic bupropion on interstitial concentrations of dopamine in rat nucleus accumbens and striatum. Neuropsychopharmacology. 1992;7:7-14.

[58] Rau KS, Birdsall E, Hanson JE, Johnson-Davis KL, Carroll FI, Wilkins DG, et al. Bupropion increases striatal vesicular monoamine transport. Neuropharmacology. 2005;49:820-30.

[59] Slemmer JE, Martin BR, Damaj MI. Bupropion is a nicotinic antagonist. Journal of Pharmacology and Experimental Therapeutics. 2000;295:321-7.

[60] Miller DK, Sumithran SP, Dwoskin LP. Bupropion inhibits nicotine-evoked [(3)H]overflow from rat striatal slices preloaded with [(3)H]dopamine and from rat hippocampal slices preloaded with [(3)H]norepinephrine. J Pharmacol Exp Ther. 2002;302:1113-22.

[61] Jorenby DE, Leischow SJ, Nides MA, Rennard SI, Johnston JA, Hughes AR, et al. A controlled trial of sustained-release bupropion, a nicotine patch, or both for smoking cessation. New Engl J Med. 1999;340:685-91.

[62] Boshier A, Wilton LV, Shakir SAW. Evaluation of the safety of bupropion (Zyban) for smoking cessation from experience gained in general practice use in England in 2000. Eur J Clin Pharmacol. 2003;59:767-73.

[63] Barrueco M, Otero MJ, Palomo L, Jimenez-Ruiz C, Torrecilla M, Romero P, et al. Adverse effects of pharmacological therapy for nicotine addiction in smokers following a smoking cessation program. Nicotine Tob Res. 2005;7:335-42.

[64] Paluck EC, McCormack JP, Ensom MHH, Levine M, Soon JA, Fielding DW. Outcomes of bupropion therapy for smoking cessation during routine clinical use. Ann Pharmacother. 2006;40:185-90.

[65] Wilkes S, Evans A, Henderson M, Gibson J. Pragmatic, observational study of bupropion treatment for smoking cessation in general practice. Postgrad Med J. 2005;81:719-22.

[66] Moore TJ, Singh S, Furberg CD. The FDA and new safety warnings. Arch Intern Med. 2012;172:78-80.

[67] Niaura R, Jones C, Kirkpatrick P. Varenicline. Nat Rev Drug Discov. 2006;5:537-8.

[68] Nides M, Oncken C, Gonzales D, Rennard S, Watsky EJ, Anziano R, et al. Smoking cessation with varenicline, a selective alpha4beta2 nicotinic receptor partial agonist: results from a 7-week,

randomized, placebo- and bupropion-controlled trial with 1-year follow-up. Arch Intern Med. 2006;166:1561-8.

[69] Mohanasundaram UM, Chitkara R, Krishna G. Smoking cessation therapy with varenicline. Int J Chron Obstruct Pulmon Dis. 2008;3:239-51.

[70] Gonzales D, Rennard SI, Nides M, Oncken C, Azoulay S, Billing CB, et al. Varenicline, an alpha4beta2 nicotinic acetylcholine receptor partial agonist, vs sustained-release bupropion and placebo for smoking cessation: a randomized controlled trial. JAMA. 2006;296:47-55.

[71] Maity N, Chand P, Murthy P. Role of nicotine receptor partial agonists in tobacco cessation. Indian J Psychiatry. 2014;56:17-23.

[72] Fiore MC, Jaen CR. A clinical blueprint to accelerate the elimination of tobacco use. Jama-J Am Med Assoc. 2008;299:2083-5.

[73] Aubin HJ, Bobak A, Britton JR, Oncken C, Billing CB, Jr., Gong J, et al. Varenicline versus transdermal nicotine patch for smoking cessation: results from a randomised open-label trial. Thorax. 2008;63:717-24.

[74] Cinciripini PM, Robinson JD, Karam-Hage M, Minnix JA, Lam C, Versace F, et al. Effects of varenicline and bupropion sustained-release use plus intensive smoking cessation counseling on prolonged abstinence from smoking and on depression, negative affect, and other symptoms of nicotine withdrawal. JAMA Psychiatry. 2013;70:522-33.

[75] Williams JM, Anthenelli RM, Morris CD, Treadow J, Thompson JR, Yunis C, et al. A randomized, double-blind, placebo-controlled study evaluating the safety and efficacy of varenicline for smoking cessation in patients with schizophrenia or schizoaffective disorder. J Clin Psychiatry. 2012;73:654-60.

[76] Anthenelli RM, Morris C, Ramey TS, Dubrava SJ, Tsilkos K, Russ C, et al. Effects of varenicline on smoking cessation in adults with stably treated current or past major depression: a randomized trial. Ann Intern Med. 2013;159:390-400.

[77] Prochaska JJ, Hilton JF. Risk of cardiovascular serious adverse events associated with varenicline use for tobacco cessation: systematic review and meta-analysis. BMJ. 2012;344:e2856.

[78] Murtagh J, Foerster V. Nicotine vaccines for smoking cessation. Issues Emerg Health Technol. 2007:1-4.

[79] Raupach T, Hoogsteder PH, Onno van Schayck CP. Nicotine vaccines to assist with smoking cessation: current status of research. Drugs. 2012;72:e1-16.

[80] Hartmann-Boyce J, Cahill K, Hatsukami D, Cornuz J. Nicotine vaccines for smoking cessation. Cochrane Database Syst Rev. 2012:CD007072.

[81] Lisy K. Nicotine vaccines for smoking cessation. Clin Nurse Spec. 2013;27:71-2.

[82] Pentel PR, LeSage MG. New directions in nicotine vaccine design and use. Adv Pharmacol. 2014;69:553-80.

[83] Orson FM, Kinsey BM, Singh RA, Wu Y, Gardner T, Kosten TR. Substance abuse vaccines. Ann N Y Acad Sci. 2008;1141:257-69.

[84] Shorter D, Kosten TR. Vaccines in the treatment of substance abuse. Focus (Am Psychiatr Publ). 2011;2011:25-30.

[85] Maurer P, Bachmann MF. Therapeutic vaccines for nicotine dependence. Curr Opin Mol Ther. 2006;8:11-6.

[86] Goniewicz ML, Delijewski M. Nicotine vaccines to treat tobacco dependence. Hum Vaccin Immunother. 2013;9:13-25.

[87] Hatsukami DK, Rennard S, Jorenby D, Fiore M, Koopmeiners J, de Vos A, et al. Safety and immunogenicity of a nicotine conjugate vaccine in current smokers. Clin Pharmacol Ther. 2005;78:456-67.

[88] Wagena EJ, de Vos A, Horwith G, van Schayck CP. The immunogenicity and safety of a nicotine vaccine in smokers and nonsmokers: results of a randomized, placebo-controlled phase 1/2 trial. Nicotine Tob Res. 2008;10:213-8.

[89] Hatsukami DK, Jorenby DE, Gonzales D, Rigotti NA, Glover ED, Oncken CA, et al. Immunogenicity and smoking-cessation outcomes for a novel nicotine immunotherapeutic. Clin Pharmacol Ther. 2011;89:392-9.

[90] Hoogsteder PH, Kotz D, van Spiegel PI, Viechtbauer W, Brauer R, Kessler PD, et al. The efficacy and safety of a nicotine conjugate vaccine (NicVAX(R)) or placebo co-administered with varenicline (Champix(R)) for smoking cessation: study protocol of a phase IIb, double blind, randomized, placebo controlled trial. BMC Public Health. 2012;12:1052.

[91] Lockner JW, Janda KD. Immunopharmacotherapy for nicotine addiction. Rsc Drug Discov. 2013:36-67.

[92] Maurer P, Jennings GT, Willers J, Rohner F, Lindman Y, Roubicek K, et al. A therapeutic vaccine for nicotine dependence: preclinical efficacy, and Phase I safety and immunogenicity. Eur J Immunol. 2005;35:2031-40.

[93] Cornuz J, Zwahlen S, Jungi WF, Osterwalder J, Klingler K, van Melle G, et al. A vaccine against nicotine for smoking cessation: a randomized controlled trial. PLoS One. 2008;3:e2547.

[94] Esterlis I, Hannestad JO, Perkins E, Bois F, D'Souza DC, Tyndale RF, et al. Effect of a nicotine vaccine on nicotine binding to beta2*-nicotinic acetylcholine receptors in vivo in human tobacco smokers. Am J Psychiatry. 2013;170:399-407.

[95] McCluskie MJ, Pryde DC, Gervais DP, Stead DR, Zhang N, Benoit M, et al. Enhancing immunogenicity of a 3'aminomethylnicotine-DT-conjugate anti-nicotine vaccine with CpG adjuvant in mice and non-human primates. Int Immunopharmacol. 2013;16:50-6.

[96] Pryde DC, Jones LH, Gervais DP, Stead DR, Blakemore DC, Selby MD, et al. Selection of a novel anti-nicotine vaccine: Influence of antigen design on antibody function in mice. Plos One. 2013;8.

[97] McCluskie MJ, Thorn J, Mehelic PR, Kolhe P, Bhattacharya K, Finneman JI, et al. Molecular attributes of conjugate antigen influence function of antibodies induced by anti-nicotine vaccine in mice and non-human primates. Int Immunopharmacol. 2015;25:518-27.

[98] McCluskie MJ, Thorn J, Gervais DP, Stead DR, Zhang N, Benoit M, et al. Anti-nicotine vaccines: Comparison of adjuvanted CRM197 and Qb-VLP conjugate formulations for immunogenicity and function in non-human primates. Int Immunopharmacol. 2015;29:663-71.

[99] Collins KC, Janda KD. Investigating hapten clustering as a strategy to enhance vaccines against drugs of abuse. Bioconjugate Chem. 2014;25:593-600.

[100] de Villiers SHL, Cornish KE, Troska AJ, Pravetoni M, Pentel PR. Increased efficacy of a trivalent nicotine vaccine compared to a dose-matched monovalent vaccine when formulated with alum. Vaccine. 2013;31:6185-93.

[101] Gregory AE, Titball R, Williamson D. Vaccine delivery using nanoparticles. Front Cell Infect Mi. 2013;3.

[102] Zhao L, Seth A, Wibowo N, Zhao CX, Mitter N, Yu C, et al. Nanoparticle vaccines. Vaccine. 2014;32:327-37.

[103] Akagi T, Baba M, Akashi M. Biodegradable nanoparticles as vaccine adjuvants and delivery systems: Regulation of immune responses by nanoparticle-based vaccine. Adv Polym Sci. 2012;247:31-64.

[104] De Jong WH, Borm PJ. Drug delivery and nanoparticles:applications and hazards. Int J Nanomedicine. 2008;3:133-49.

[105] Wilczewska AZ, Niemirowicz K, Markiewicz KH, Car H. Nanoparticles as drug delivery systems. Pharmacol Rep. 2012;64:1020-37.

[106] Amidi M, Mastrobattista E, Jiskoot W, Hennink WE. Chitosan-based delivery systems for protein therapeutics and antigens. Adv Drug Deliver Rev. 2010;62:59-82.

[107] Solaro R, Chiellini F, Battisti A. Targeted delivery of protein drugs by nanocarriers. Materials. 2010;3:1928-80.

[108] Hu Y, Zheng H, Huang W, Zhang CM. A novel and efficient nicotine vaccine using nano-lipoplex as a delivery vehicle. Hum Vacc Immunother. 2014;10:64-72.

[109] Lockner JW, Ho SO, McCague KC, Chiang SM, Do TQ, Fujii G, et al. Enhancing nicotine vaccine immunogenicity with liposomes. Bioorg Med Chem Lett. 2013;23:975-8.

[110] Desai RI, Bergman J. Effects of the nanoparticle-based vaccine, SEL-068, on nicotine discrimination in squirrel monkeys. Neuropsychopharmacology. 2015;40:2207-16.

[111] Liu X, Hecht SM, Yan H, Pentel PR, Chang Y. Exploration of DNA Nanostructures for rational design of vaccines. 2016:279-93.

[112] Pittet L, Altreuter D, Ilyinskii P, Fraser C, Gao Y, Baldwin S, et al. Development and preclinical evaluation of SEL-068, a novel targeted Synthetic Vaccine Particle (tSVP (TM)) for smoking cessation and relapse prevention that generates high titers of antibodies against nicotine. J Immunol. 2012;188.

[113] Ilyinskii PO, Johnston LPM. Nanoparticle-based nicotine vaccine. 1st ed: Springer; 2016.

Chapter 3: A Nanoparticle-Based Nicotine Vaccine and the Influence of Particle Size on its Immunogenicity and Efficacy

Zongmin Zhao[a*], Yun Hu[a*], Reece Hoerle[a], Meaghan Devine[a], Michael Raleigh[b], Paul Pentel[b], Chenming Zhang[a,†]

[a] Department of Biological Systems Engineering, Virginia Tech University, Blacksburg, VA 24061, United States

[b] Minneapolis Medical Research Foundation, Minneapolis, MN 55404, United States

†Correspondence to: Chenming (Mike) Zhang.

Address: 210 Seitz Hall, Department of Biological Systems Engineering, Virginia Tech University, Blacksburg, VA 24061, USA

Voice: +1-(540)231-7601

Fax: +1-(540)231-3199

Email: chzhang2@vt.edu

* These authors contributed equally to this work.

This manuscript has been published on *Nanomedicine: Nanotechnology, Biology and Medicine* 2017, 13(2): 443-454. Reprinted with permission of the publisher.

Abstract

Traditional hapten-protein conjugate nicotine vaccines have shown less than desired immunological efficacy due to their poor recognition and internalization by immune cells. We developed a novel lipid-polymeric hybrid nanoparticle-based nicotine vaccine to enhance the immunogenicity of the conjugate vaccine, and studied the influence of particle size on its immunogenicity and pharmacokinetic efficacy. The results demonstrated that the nanovaccines, regardless of size, could induce a significantly stronger immune response against nicotine compared to the conjugate vaccine. Particularly, a significantly higher anti-nicotine antibody titer was achieved by the 100 compared to the 500 nm nanovaccine. In addition, both the 100 and 500 nm nanovaccines reduced the distribution of nicotine into the brain significantly. The 100 nm nanovaccine exhibited better ability to reduce brain nicotine concentrations than the 500 nm nanovaccine in the presence of alum adjuvant. These results suggest that a lipid-polymeric nanoparticle-based nicotine vaccine is a promising candidate to treat nicotine dependence.

Key Words

Nicotine addiction; nicotine vaccine; lipid-polymeric hybrid nanoparticle; anti-nicotine antibody; nanovaccine size

3.1 Background

Tobacco addiction has consistently been the top preventable cause of many serious diseases; it continues to result in extensive mortality, morbidity, and economic loss.[1, 2] Currently, nicotine replacement therapies, bupropion, and varenicline, are the major pharmacological interventions available to smokers for quitting smoking.[3] However, even with the help of these medications, the smoking cessation rate is disappointingly low (10-25%) and there are many associated problems, such as various adverse side effects and high cost.[4, 5] Therefore, it is both necessary and urgent to develop new approaches to combat tobacco addiction.

In recent years, nicotine vaccines that can induce the production of nicotine-specific antibodies have emerged as a promising approach to combat smoking addiction.[6, 7] The antibodies elicited by a nicotine vaccine can bind with nicotine molecules in blood to form antibody-nicotine complexes, thereby blocking nicotine from crossing the blood-brain barrier to stimulate the central nervous system.[8] In the past decade, there have been several nicotine vaccine candidates developed and evaluated in human clinical trials.[9] Unfortunately, none of these vaccines are currently available to smokers due to their poor efficacy caused by low antibody titers, high variability, and low antibody affinity for nicotine.[7] The placebo-controlled phase 2 clinical studies of NicVax and NicQβ revealed that, while the overall smoking cessation rate was not enhanced compared to the placebo group, the top 30% of subjects that had the highest antibody titers showed an improved quit rate.[10, 11] This suggests that the basic concept of immunotherapy for smoking cessation is solid but requires more antibodies to be generated to ensure efficacy of the vaccination.

To date, most existing nicotine vaccines are traditional hapten-protein conjugate vaccines in which nicotine analogues are conjugated to a carrier protein to be immunogenic.[11, 12] However, traditional nicotine-protein conjugate vaccines suffer from several shortcomings, including poor recognition

and internalization by immune cells, low bioavailability, fast degradation, difficulty in integration with molecular adjuvants, and short immune persistence, all of which lead to low immunological efficacy.[7]

Nanoparticles (NPs) have been extensively applied for efficient delivery of drugs, antigens, and vaccines,[13-17] making them a promising approach to potentially overcome the limitations of conjugate nicotine vaccines. However, to our knowledge, the use of nanoparticles for the delivery of drug conjugate vaccines has not been widely studied, with only a few studies reporting the utilization of liposomes and negatively charged nanohorn-supported liposomes as nicotine vaccine delivery vehicles.[18-20] Nevertheless, liposomes and nanohorn-supported liposomes have either stability issues or safety concerns, limiting their clinical applications.

Lipid-polymeric hybrid NPs that consist of a poly(lactic-co-glycolic acid) (PLGA) NP core and a lipid shell, both of which have been approved for clinical use, have been used widely as vaccine delivery systems due to their biocompatibility, biodegradability, excellent safety, good stability, ease in fabrication, and ability in controlled antigen release.[21-23] In the current study, we developed a novel NP-based nicotine vaccine in which lipid-polymeric hybrid NPs were utilized as vehicles for the effective delivery of conjugate nicotine vaccines. Particularly, based on the hypothesis that NP size may affect the immunogenicity of NP-based nicotine vaccines, we determined whether the immunogenicity of nanovaccines could be enhanced by modulating NP size. In this study, we selected 100 and 500 nm as representatives of small and large sizes of lipid-polymeric NP-based nicotine vaccines. We compared the physicochemical properties, cellular uptake by dendritic cells, immunogenicity, ability to reduce brain nicotine levels, and safety of the nanovaccines with these two sizes.

3.2 Methods

3.2.1 Synthesis of a Nic-KLH conjugate

O-Succinyl-3'-hydroxymethyl-(±)-nicotine (Nic)-keyhole limpet hemocyanin (KLH) conjugates were synthesized using a carbodiimide-mediated reaction. In brief, 2.4 mg of Nic hapten were mixed with appropriate amounts of 1-ethyl-3-[3-dimethylaminopropyl]carbodiimide hydrochloride (EDC) and *N*-hydroxysulfosuccinimide (Sulfo-NHS) in 0.5 mL of activation buffer (0.1 M 2-(*N*-morpholino)ethanesulfonic acid, 0.5 M NaCl, pH 6.0), and incubated at room temperature for 15 min. The mixture was then added to 5 mg of KLH that was dissolved in 2 mL of coupling buffer (0.1 M sodium phosphate, 0.15 M NaCl, pH 7.2). After reacting overnight, unconjugated Nic hapten and byproducts were eliminated by dialyzing against 0.01 M phosphate-buffered saline (PBS) (pH 7.4) using a dialysis membrane (molecular weight cut-off 6000-8000) at room temperature for 24 h.

3.2.2 Assembly of lipid-polymeric hybrid NP-based nicotine vaccines

Lipid-polymeric hybrid NPs were assembled by attaching Nic-KLH conjugates onto the surface of lipid-PLGA hybrid NPs via a thiol-maleimide-mediated method. In brief, PLGA and lipid-PLGA NPs were fabricated according to the method described in the supplementary materials. An appropriate amount of Traut's reagent was added to 3 mg of Nic-KLH that was dissolved in 0.1 M pH 8.0 bicarbonate buffer, and incubated for 1 h at room temperature to obtain the thiolated Nic-KLH conjugate. Nic-KLH was attached onto lipid-PLGA NPs by reacting the thiolated Nic-KLH with appropriate amounts of lipid-PLGA NPs in 0.1 M, pH 8.0, bicarbonate buffer for 2 h. Nanovaccine NPs were collected by centrifugation at 10,000 *g*, 4°C, for 30 min. Unattached Nic-KLH in the supernatant was quantified by the bicinchoninic acid assay.

3.2.3 Active immunization of mice with nicotine nanovaccines

All animal studies were carried out following the National Institutes of Health guidelines for animal care and use. Animal protocols were approved by the Institutional Animal Care and Use Committee at Virginia Polytechnic Institute and State University. Female Balb/c mice (6-7 weeks of age, 16-20 g) were randomized into vaccine and control groups (8 per group). In the vaccine groups, mice were immunized subcutaneously with conjugate vaccine or nanovaccines containing 25 μg of Nic-KLH immunogen on days 0, 14, and 28. For groups immunized with vaccine and adjuvant, alum (1.5 mg) was pre-mixed with the vaccine solution before injection. Mice were injected with a total volume of 200 μL in all groups. In the blank group, 200 μL of PBS was injected into mice on the same days. Blood samples (~100 μL) were collected from the retro-orbital plexus of mice under isoflurane anesthesia on days 0, 13, 27, 41, 55, and 62 to monitor antibody titers.

3.2.4 Evaluation of the immunogenicity of nicotine vaccines by measuring specific anti-nicotine IgG antibody titers

Anti-nicotine IgG antibody titers in mouse serum samples were analyzed by an enzyme-linked immunosorbent assay (ELISA) according to a method reported previously.[19] Antibody titer was defined as the dilution factor at which absorbance at 450 nm declined to half maximal.

3.2.5 Evaluation of the ability of nicotine vaccines to reduce brain nicotine levels in mice

Female Balb/c mice (6-7 weeks of age, 16-20 g) were immunized with 100 nm nanovaccine, 500 nm nanovaccine, or 6-CMUNic-KLH, and the negative control (KLH protein only), with or without the alum adjuvant using the same procedure described above (4 per group). For 6-CMUNic-KLH, two groups of mice were immunized using either 0.25 or 1.5 mg alum as adjuvant. Two weeks after the second boost injection (day 41), mice were administered 0.06 mg/kg nicotine subcutaneously. Mice were euthanized under anesthesia 4 min post nicotine challenge, and the

blood and brain were collected. Nicotine contents in serum and brain tissues were analyzed by gas chromatography/mass spectrometry according to a method reported previously.[24]

3.2.6 Statistical analyses

Data are expressed as means ± standard deviation. Comparisons among multiple groups were conducted using one-way ANOVA followed by Tukey's HSD test. The analysis of Th1/Th2 index between each vaccine treatment group and the value "1" was carried out by one-sample t-test. Differences were considered significant when the p-values were less than 0.05.

3.3 Results

3.3.1 Synthesis and characterization of lipid-polymeric hybrid NP-based nicotine vaccines with controlled size

Two hybrid NP-based nanovaccines with sizes of 100 and 500 nm were prepared, and their physiochemical properties were studied. As shown in **Table 1**, the sizes of lipid-polymeric hybrid and nanovaccine NPs were dominated by the size of the PLGA NPs. A slight increase of size was observed for the hybrid NPs and the final nanovaccine NPs compared to the initial PLGA NPs. Moreover, the size of the PLGA NPs can be controlled by changing the magnitude and time of sonication in the double emulsion solvent evaporation process. Therefore, hybrid NP-based nanovaccines with different sizes can be prepared reproducibly.

The measured mean diameters of the 100 and 500 nm nanovaccines were 108.7 ± 3.7 and 467.5 ± 10.3 nm, respectively (**Table 1**). This indicated that the fabrication method used in this study allowed accurate size control of the hybrid NP-based nanovaccines. The surface charges of nanovaccine NPs, represented by the zeta potential, were 2.29 ± 0.31 and 2.69 ± 0.07 mV for the 100 and 500 nm vaccines, respectively (**Table 1**). The polydispersity indexes (PDI) were 0.20 ± 0.02 and 0.23 ± 0.03 for the 100 and 500 nm nanovaccines, respectively (**Table 1**). The low PDI

of the two nanovaccines indicated that the size of the NPs was uniform. In this study, 10 mg of KLH was used to associate with 50 mg of hybrid NPs. As shown in **Table 1**, the KLH conjugation efficiency was as high as 88% for both nanovaccines, demonstrating the high conjugation efficiency of the Traut's reagent- and maleimide-mediated reactions, as well as the high antigen loading capacity of hybrid NPs.

The morphology of hybrid NPs with distinct sizes was characterized by transmission electron microscopy (TEM). As shown in **Figure 1A**, hybrid 100 and 500 nm NPs clearly exhibited a core-shell hybrid structure. In the micro-images, the lipid shell is pinpointed by the blue arrows, and the PLGA core is shown by the red arrows. In agreement with the low PDI of NPs (**Table 1**), the particle sizes of both 100 and 500 nm NPs were uniform, suggesting that the NP fabrication method was highly effective and robust.

To confirm the hybridization of PLGA NPs and liposomes, Fourier transform infrared (FTIR) spectra of PLGA NPs, liposomes, and lipid-polymeric hybrid NPs were analyzed. As shown in **Figure 1B**, hybrid NPs shared unique wavelength peaks with either PLGA NPs or liposomes. For example, peaks at 1095 and 1136 cm^{-1} were shared by PLGA and hybrid NPs, while peaks at 2854 and 2925 cm^{-1} were commonly displayed in both liposomes and hybrid NPs. The similarities and differences in the FTIR spectra of hybrid NPs and the other two particles further suggested that a lipid layer was successfully coated onto PLGA NPs.

To verify the successful conjugation of KLH to hybrid NPs, NPs, in which KLH and the lipid layer were fluorescently labeled with rhodamine B and nitro-2-1,3-benzoxadiazol-4-yl (NBD), respectively, were imaged with confocal laser scanning microscopy (CLSM). Co-localization of both red and green color was observed on the majority of NPs, indicating that the maleimide-thiol reaction was highly efficient in conjugating protein to NPs (**Figure 2**). High conjugation efficiency

between Nic-KLH and hybrid NPs is of great value to the vaccine design in this study. Firstly, it allows full utilization of both hybrid NPs and KLH, avoiding laborious purification of unconjugated particles and proteins. Secondly, high quantities of KLH can be loaded onto a single NP, supplying sufficient amount of protein antigen to immune cells once internalized. Finally, high protein loading capacity can deliver more nicotine epitopes on a single NP, increasing the chance of B cell activation.

3.3.2 Uptake of hybrid NPs by dendritic cells

Efficient recognition and capture of antigens by antigen presenting cells largely determines the outcome of the humoral immune response. In this study, the influence of NP size on the uptake of nanovaccines by dendritic cells was investigated. Within 2 h, 99.4%-99.7% of the cells were stained by AF647 fluorescence. There was no marked difference in the percentages of positive dendritic cells for NPs of the two sizes (**Figure 3C**). This suggested that both 500 and 100 nm particles were taken up rapidly by dendritic cells. However, as shown in **Figure 3D** and **3E**, a significantly higher mean intensity of AF647 fluorescence was observed in cells treated with 100 nm particles than in cells treated with 500 nm particles, demonstrating that dendritic cells can more efficiently swallow nanovaccine NPs of smaller size. Moreover, as shown in **Figure 3A** and **3B**, the mean intensity of AF647 fluorescence in the 500 nm nanovaccine group was significantly higher than that in the AF647-KLH group, indicating that the use of hybrid NPs enhanced the bioavailability and internalization of protein antigens.

Cellular uptake of AF647- and NBD-labeled NPs was further studied using CLSM. As shown in **Figure 4**, the fluorescence intensity indicated that the amount of NPs taken up by dendritic cells was time-dependent for both NPs. In agreement with the flow cytometry results, all studied dendritic cells were stained by NPs, supporting the conclusion that both 500 and 100 nm NPs can

be captured effectively by dendritic cells in a short period of time. Moreover, the brighter fluorescence of both AF647 and NBD in the 100 nm group (**Figure 4A**) compared to the 500 nm group (**Figure 4B**) at 2 h showed that more 100 nm NPs were internalized by dendritic cells. The amount of NPs carrying antigens that are internalized by dendritic cells is of great importance to activation of the immune response because the more antigen that is internalized, the more antigen peptides may be presented to naïve T cells, and the more B cells that may be activated.

3.3.3 Immunogenicity of hybrid NP-based nicotine nanovaccines in mice

A steady increase of the anti-nicotine antibody titer was observed for each vaccine after each injection (**Figure 5**). Specially, the anti-nicotine antibody titers increased significantly after the first booster injection (on day 27) for all vaccine groups. In addition, substantially increased antibody titers (>8,500) were detected for all formulations, except for the Nic-KLH conjugate vaccine, on day 41. Compared to the Nic-KLH conjugate vaccine, both the 100 and 500 nm nanovaccines achieved significantly higher anti-nicotine antibody titers on days 27, 41, 55, and 62. This demonstrated that the use of lipid-polymeric NPs as delivery vehicles could improve the immunogenicity of the Nic-KLH conjugate nicotine vaccine. Moreover, at the end of the immunogenicity study on day 62, the 100 nm nanovaccine without alum achieved significantly higher antibody titers over the 500 nm nanovaccine without alum; meanwhile, the 100 nm nanovaccine with alum also induced considerably higher antibody titer than the 500 nm nanovaccine with alum. These results suggest that the 100 nm nanovaccine induced a stronger immunogenic effect.

In this study, 6-CMUNic-KLH, one of the most well-characterized and highly immunogenic conjugate nicotine vaccines[24], was used as a positive control. Among all formulations, the 100 nm nanovaccine with alum generated a much higher anti-nicotine antibody titer over 6-CMUNic-KLH

at all studied time points. To study the long-term persistence of the immune response, antibody titers on days 55 and 62 were measured for all vaccine formulations. The antibody level in the 6-CMUNic-KLH group markedly declined from 11,000 to 8000 between days 41 and 55. Similarly, a pronounced decline of antibody titers was observed for nanovaccines with alum between days 55 and 62. Nevertheless, nanovaccines maintained antibody titers for a longer time compared to 6-CMUNic-KLH. Interestingly, antibody titers of nanovaccines without alum increased between days 55 and 62, especially for the 100 nm nanovaccine. This revealed that, at later times, the antibody titers in groups treated with nanovaccines without alum were higher and longer lasting than nanovaccines with alum. A possible mechanism of this finding is that alum limited the bioavailability of nanovaccines to immune cells, such as dendritic and B cells, due to the over-retention of NPs in alum.[25]

The titers of IgG subclass antibodies, including IgG1, IgG2a, IgG2b, and IgG3 on day 62, were also measured. Nanovaccines, regardless of size, considerably increased the titers of all four IgG subclasses compared to the Nic-KLH conjugate vaccine, especially for IgG1 and IgG2a (**Figure 6**). Interestingly, the 100 nm nanovaccine group had significantly higher titers of IgG1 and IgG2a compared to the 500 nm nanovaccine group. In addition, as shown in **Figure 6** and **Table 2**, IgG1 was dominant among all subclasses for all vaccines.

The Th1/Th2 index, that reflects the relative magnitude of the humoral to the cellular immune response[26], was calculated. Very low Th1/Th2 indexes (significantly less than 1) were found for all vaccine formulations and there were no significant differences among groups (**Table 2**). This indicated that the immune response induced by all tested nicotine vaccines was significantly skewed toward Th2. For nicotine vaccines, a low Th1/Th2 index is desirable because the efficacy

of reducing the rewarding effects of nicotine is dependent on the magnitude of the humoral response.

3.3.4 Effects of nicotine nanovaccines on the distribution of nicotine in serum and brain

The ability of vaccines to prevent nicotine from crossing the blood-brain barrier largely determines the outcomes of smoking cessation efforts.[7] To determine the efficacy of nicotine nanovaccines, mice were challenged with 0.06 mg/kg nicotine two weeks after the second boost immunization (on Day 41) and nicotine contents in serum and brain were analyzed. This dose approximates the mg/kg of nicotine in three smoked cigarettes in humans[27]. The nicotine contents retained in serum are shown **in Figure 7A**. The serum nicotine level increased by 47% in the 500 nm nanovaccine group compared to that of the negative control group. In contrast, serum nicotine levels increased by 119 and 407% in the 100 nm nanovaccine group without or with 1.5 mg of alum, respectively. This suggested that the 100 nm nanovaccine had a better efficacy on retaining nicotine in serum. Remarkably, the serum nicotine level in the 500 nm nanovaccine with alum group was lower than that in the negative controls, although the nicotine antibody titer was fairly high (**Figure 5**).

Figure 7B shows the nicotine contents distributed into brain. Significant reductions of brain nicotine levels were observed in all nanovaccine groups compared to the negative control group. Compared to the negative control group, brain nicotine levels were reduced by 32.0, 56.2, 39.5, and 41.7% in the 100 nm nanovaccine, 100 nm with alum nanovaccine, 500 nm nanovaccine, and 500 nm with alum nanovaccine groups, respectively. Although efficacy was not improved in the 100 nm without alum nanovaccine versus the 500 nm without alum nanovaccine group, the 100 nm with alum nanovaccine group achieved 15% more brain nicotine reduction compared to the 500 nm with alum nanovaccine group. The 100 nm nanovaccine appeared to have a better efficacy

than the 500 nm nanovaccine in the presence of the alum adjuvant, which was reflected by its lower mean nicotine level in the brain of mice.

Due to its poor anti-nicotine antibody producing activity, Nic-KLH was not used in this nicotine challenge study. Instead, we compared the results of nanovaccines to that of a positive control using 6-CMUNic-KLH that blocked up to 80% of nicotine from entering into the brain of rats.[12, 28] The 100 nm without alum and 500 nm without alum nanovaccine groups had comparable average brain nicotine levels compared to the 6-CMUNic-KLH with 0.25 mg of alum group. In addition, the brain nicotine level in the 100 nm with alum group, in which 1.5 mg of alum was used, was also comparable to that in the 6-CMUNic-KLH with 1.5 mg of alum group. In this study, we determined the antibody titer but did not test the specificity of antibodies, because the nicotine challenge study provided the ultimate evaluation of vaccine efficacy.

3.3.5 Evaluation of the safety of hybrid NP-based nicotine nanovaccines in mice

The safety of nanovaccines was investigated histopathologically. There were no lesions in the hearts, lungs, livers, spleens, and kidneys of mice treated with nanovaccines with or without alum (**Figure 8A**). This demonstrated that the hybrid NP-based nicotine nanovaccine did not cause detectable lesions to organs and thus appeared to be safe. In addition, as shown in **Figure 8B**, no changes of body weights were found during the entire study period in all of the mice treated with various nicotine vaccines, nor were the body weights different from the PBS control. These results also suggest that the nanovaccine is safe.

3.4 Discussion

Vaccines are a promising approach to treat nicotine addiction by inducing the production of nicotine-specific antibodies that can bind with nicotine in blood fluid and thus block it from entering the brain where nicotine would stimulate the central nervous system to generate euphoria

and thereby cause nicotine addiction.[8] Unfortunately, to date, all clinically tested hapten-protein conjugate nicotine vaccines have failed due to their poor ability to generate a sufficient anti-nicotine antibody titer. This failure can be attributed to their intrinsic shortfalls including poor recognition and internalization of nicotine by immune cells, low bioavailability, and fast degradation.[7, 29] In this study, for the first time, we report the development of a lipid-polymeric hybrid NP-based nicotine vaccine. We used hybrid NPs as a means for efficient delivery of conjugate nicotine vaccines to address the limitations mentioned above and to improve the immunogenicity of the vaccine. In addition, we studied the influence of particle size on the efficacy of nanovaccines and illustrated the necessity of controlling the particle size in maximizing the immunogenicity of the nanovaccine.

The nanovaccine studied here was designed to have multiple Nic-KLH conjugates attached on the surface of lipid-polymeric hybrid NPs. TEM results indicated that a core-shell hybrid structure was formed for hybrid NPs of both 100 and 500 nm. The hybrid structure was important to the immunological outcome of the nanovaccines. The particulate nature of PLGA NPs offers extra rigidity to liposomes, enhancing their stability and lengthening their circulation time.[30, 31] The lipid membrane surface of hybrid NPs may also improve particle internalization by immune cells through membrane fusion.[32] In addition, the lipid shell may act as a shield between the aqueous surroundings and the PLGA core, providing protection to PLGA NPs from hydrolytic degradation as well as contributing to long-term stability of the hybrid structure.[33]

Due to its many advantages, such as high immunogenicity and clinically proven safety, KLH has been used widely as a carrier protein for vaccine development.[34] In the vaccine design of this study, KLH functioned as a support for the nicotine hapten as well as a potent stimulator of T helper cells. CLSM and protein assay results demonstrated that the Nic-KLH antigen was attached to hybrid

NPs at high conjugation and loading efficiencies. This may not only have supplied sufficient amounts of protein antigen to immune cells to generate enough T helper cells once NPs were internalized, but also provided sufficient nicotine epitopes on a single NP to increase the chance of B cell recognition and activation.

Zeta-potential results revealed that both 100 and 500 nm nanovaccines were positively charged due to the inclusion of a cationic lipid (1,2-dioleoyl-3-trimethylammonium-propane) in the lipid formulation. Because the membranes of immune cells are composed largely of negatively charged phospholipids, the positive surface charge of nanovaccine NPs can enhance their interaction with immune cells, thereby promoting cellular uptake of the nanovaccine.[35] All of these hybrid NP-based nanovaccine properties can potentially enhance the vaccine's immunogenic efficacy.

In vitro cellular uptake data revealed that the internalization of Nic-KLH conjugate antigens was enhanced significantly by the utilization of hybrid NPs as a delivery vehicle. This enhanced internalization may be caused by the increased availability of antigens for uptake following the conjugation of multiple Nic-KLH antigens to one NP. In addition, the optimal physicochemical properties mentioned above may contribute to the improved internalization process. Moreover, 100 nm nanovaccine particles were taken up by dendritic cells more efficiently than 500 nm particles. The enhanced internalization of antigens could lead to a stronger immune response. In agreement with the *in vitro* data, *in vivo* immunization data demonstrated that the use of hybrid NPs, regardless of size, could significantly enhance the immunogenicity of Nic-KLH conjugate vaccines.

As mentioned above, traditional conjugate nicotine vaccines that have been evaluated in clinical trials are ineffective due to their limited immunogenicity.[7] The findings presented here are thus of great value in providing a novel strategy to improve the immunogenicity of conjugate nicotine

vaccines. Both the ELISA and nicotine challenge study results revealed that the 100 nm nanovaccine resulted in better immunological efficacy than the 500 nm nanovaccine, especially in the presence of alum. This finding suggested another potential approach to improve the efficacy of NP-based nicotine vaccines. The 6-CMUNic-KLH conjugate vaccine, which is one of the most well-characterized and highly immunogenic conjugate nicotine vaccines[24], was used as a positive control in this study. 6-CMUNic-KLH exhibited substantial potency in eliciting nicotine antibodies, resulting in excellent pharmacokinetic efficacy in preclinical studies. Previous studies showed that 6-CMUNic-KLH induced an anti-nicotine antibody titer up to 200,000 and blocked up to 80% of nicotine from entering into the brain of rats.[12, 28, 36] In the current study, the 100 nm nanovaccine administered with alum resulted in a considerably higher anti-nicotine antibody titer and a comparable efficacy of reducing brain nicotine levels, compared to 6-CMUNic-KLH. The 6-CMUNic-KLH used in this study was an optimized formulation. However, the lipid-polymeric NP-based nicotine nanovaccines used in this study were not optimized by strategies other than modulating the particle size. It is very possible that the efficacy of hybrid NP-based nicotine vaccines would be further improved after optimization via multiple strategies, such as modulating the hapten density, selection of carrier proteins, and use of molecular adjuvants.

Overall, the hybrid NP-based nicotine nanovaccines used in this study were safe in mice. All data suggest that the lipid-polymeric NP-based nicotine vaccine is a promising candidate to treat nicotine addiction. The immunogenicity of conjugate nicotine vaccine can be improved by the use of lipid-polymeric hybrid NPs, suggesting a new strategy to enhance the efficacy of conjugate nicotine vaccines. The immunological efficacy of the hybrid NP-based nicotine nanovaccine can be enhanced by modulating the particle size. This approach can potentially be applied in the development of other drug abuse and NP-based vaccines.

Acknowledgements

We thank the Morphology Lab at Virginia Tech University for their assistance with the TEM imaging. We also thank the Fralin Confocal Lab for assistance with the CLSM imaging.

References

1. Xue S, Schlosburg JE, Janda KD. A new strategy for smoking cessation: Characterization of a bacterial enzyme for the eegradation of nicotine. *J Am Chem Soc* 2015;**137**:10136-9.

2. Benowitz NL. Nicotine addiction. *N Engl J Med* 2010;**362**:2295-303.

3. Chen LS, Baker TB, Jorenby D, Piper M, Saccone N, Johnson E, et al. Genetic variation (CHRNA5), medication (combination nicotine replacement therapy vs. varenicline), and smoking cessation. *Drug Alcohol Depend* 2015;**154**:278-82.

4. Jain R, Majumder P, Gupta T. Pharmacological intervention of nicotine dependence. *BioMed Res Int* 2013;2013.

5. Carpenter MJ, Jardin BF, Burris JL, Mathew AR, Schnoll RA, Rigotti NA, et al. Clinical strategies to enhance the efficacy of nicotine replacement therapy for smoking cessation: A review of the literature. *Drugs* 2013;**73**:407-26.

6. Raupach T, Hoogsteder PH, Onno van Schayck CP. Nicotine vaccines to assist with smoking cessation: current status of research. *Drugs* 2012;**72**:e1-16.

7. Pentel PR, LeSage MG. New directions in nicotine vaccine design and use. *Adv Pharmacol* 2014;**69**:553-80.

8. LeSage MG, Keyler DE, Pentel PR. Current status of immunologic approaches to treating tobacco dependence: Vaccines and nicotine-specific antibodies. *Aaps J* 2006;**8**:E65-E75.

9. Syed BA, Chaudhari K. Smoking cessation drugs market. *Nat Rev Drug Discov* 2013;**12**:97-8.

10. Hatsukami DK, Jorenby DE, Gonzales D, Rigotti NA, Glover ED, Oncken CA, et al. Immunogenicity and smoking-cessation outcomes for a novel nicotine immunotherapeutic. *Clin Pharmacol Ther* 2011;**89**:392-9.

11. Cornuz J, Zwahlen S, Jungi WF, Osterwalder J, Klingler K, van Melle G, et al. A vaccine against nicotine for smoking cessation: A randomized controlled trial. *Plos One* 2008;**3**:e2547.

12. Keyler DE, Roiko SA, Earley CA, Murtaugh MP, Pentel PR. Enhanced immunogenicity of a bivalent nicotine vaccine. *Int Immunopharmacol* 2008;**8**:1589-94.

13. Song W, Tang Z, Lei T, Wen X, Wang G, Zhang D, et al. Stable loading and delivery of disulfiram with mPEG-PLGA/PCL mixed nanoparticles for tumor therapy. *Nanomedicine* 2016;**12**:377-86.

14. Doll TAPF, Neef T, Duong N, Lanar DE, Ringler P, Muller SA, et al. Optimizing the design of protein nanoparticles as carriers for vaccine applications. *Nanomed-Nanotechnol* 2015;**11**:1705-13.

15. Gebril AM, Lamprou DA, Alsaadi MM, Stimson WH, Mullen AB, Ferro VA. Assessment of the antigen-specific antibody response induced by mucosal administration of a GnRH conjugate entrapped in lipid nanoparticles. *Nanomed-Nanotechnol* 2014;**10**:971-9.

16. Dasgupta Q, Madras G, Chatterjee K. Controlled release kinetics of p-aminosalicylic acid from biodegradable crosslinked polyesters for enhanced anti-mycobacterial activity. *Acta Biomater* 2016;**30**:168-76.

17. Adams JR, Haughney SL, Mallapragada SK. Effective polymer adjuvants for sustained delivery of protein subunit vaccines. *Acta Biomater* 2015;**14**:104-14.

18. Lockner JW, Ho SO, McCague KC, Chiang SM, Do TQ, Fujii G, et al. Enhancing nicotine vaccine immunogenicity with liposomes. *Bioorg Med Chem Lett* 2013;**23**:975-8.

19. Hu Y, Zheng H, Huang W, Zhang CM. A novel and efficient nicotine vaccine using nano-lipoplex as a delivery vehicle. *Hum Vacc Immunother* 2014;**10**:64-72.

20. Zheng H, Hu Y, Huang W, de Villiers S, Pentel P, Zhang JF, et al. Negatively charged carbon nanohorn supported cationic liposome nanoparticles: A novel delivery vehicle for anti-nicotine vaccine. *J Biomed Nanotechnol* 2015;**11**:2197-210.

21. Hu Y, Hoerle R, Ehrich M, Zhang CM. Engineering the lipid layer of lipid-PLGA hybrid nanoparticles for enhanced in vitro cellular uptake and improved stability. *Acta Biomater* 2015;**28**:149-59.

22. Chua BY, Sekiya T, Al Kobaisi M, Short KR, Mainwaring DE, Jackson DC. A single dose biodegradable vaccine depot that induces persistently high levels of antibody over a year. *Biomaterials* 2015;**53**:50-7.

23. Rosalia RA, Cruz LJ, van Duikeren S, Tromp AT, Silva AL, Jiskoot W, et al. CD40-targeted dendritic cell delivery of PLGA-nanoparticle vaccines induce potent anti-tumor responses. *Biomaterials* 2015;**40**:88-97.

24. de Villiers SHL, Cornish KE, Troska AJ, Pravetoni M, Pentel PR. Increased efficacy of a trivalent nicotine vaccine compared to a dose-matched monovalent vaccine when formulated with alum. *Vaccine* 2013;**31**:6185-93.

25. Noe SM, Green MA, HogenEsch H, Hem SL. Mechanism of immunopotentiation by aluminum-containing adjuvants elucidated by the relationship between antigen retention at the inoculation site and the immune response. *Vaccine* 2010;**28**:3588-94.

26. Moser M, Murphy KM. Dendritic cell regulation of TH1-TH2 development. *Nat Immunol* 2000;**1**:199-205.

27. McCluskie MJ, Thorn J, Mehelic PR, Kolhe P, Bhattacharya K, Finneman JI, et al. Molecular attributes of conjugate antigen influence function of antibodies induced by anti-nicotine vaccine in mice and non-human primates. *Int Immunopharmacol* 2015;**25**:518-27.

28. Pravetoni M, Keyler DE, Pidaparthi RR, Carroll FI, Runyon SP, Murtaugh MP, et al. Structurally distinct nicotine immunogens elicit antibodies with non-overlapping specificities. *Biochem Pharmacol* 2012;**83**:543-50.

29. Shen XY, Orson FM, Kosten TR. Vaccines against drug abuse. *Clin Pharmacol Ther*. 2012;**91**:60-70.

30. Hu Y, Ehrich M, Fuhrman K, Zhang CM. In vitro performance of lipid-PLGA hybrid nanoparticles as an antigen delivery system: lipid composition matters. *Nanoscale Res Lett* 2014;**9**:434.

31. Zhang LF, Granick S. How to stabilize phospholipid liposomes (using nanoparticles). *Nano Lett* 2006;**6**:694-8.

32. Le Meins JF, Schatz C, Lecommandoux S, Sandre O. Hybrid polymer/lipid vesicles: state of the art and future perspectives. *Mater Today*. 2014;**17**:92-3.

33. Cheow WS, Hadinoto K. Factors affecting drug encapsulation and stability of lipid-polymer hybrid nanoparticles. *Colloid Surface B* 2011;**85**:214-20.

34. Harris JR, Markl J. Keyhole limpet hemocyanin (KLH): a biomedical review. *Micron* 1999;**30**:597-623.

35. Foged C, Brodin B, Frokjaer S, Sundblad A. Particle size and surface charge affect particle uptake by human dendritic cells in an in vitro model. *Int J Pharm* 2005;**298**:315-22.

36. Hieda Y, Keyler DE, VandeVoort JT, Kane JK, Ross CA, Raphael DE, et al. Active immunization alters the plasma nicotine concentration in rats. *J Pharmacol Exp Ther* 1997;**283**:1076-81.

Table 1. Physicochemical properties of NPs.

NPs	Size (d. nm)	Zeta potential (mV)	PDI	Nic-KLH conjugation efficiency (%)
PLGA NP-100 nm	98.5 ± 7.2	-4.32 ± 0.24	0.23 ± 0.03	--
PLGA NP-500 nm	451.6 ± 14.0	-4.94 ± 0.34	0.24 ± 0.03	--
Liposome	110.7 ± 4.5	10.70 ± 0.78	0.19 ± 0.02	--
Hybrid NP-100 nm	102.1 ± 4.5	9.60 ± 0.47	0.21 ± 0.03	--
Hybrid NP-500 nm	456.9 ± 7.8	10.10 ± 0.58	0.22 ± 0.04	--
Nanovaccine-100 nm	108.7 ± 3.7	2.29 ± 0.31	0.20 ± 0.02	88.28 ± 0.49
Nanovaccine-500 nm	467.5 ± 10.3	2.69 ± 0.07	0.23 ± 0.03	88.53 ± 2.02

Table 2. Th1/Th2 index of nicotine vaccines.

	100 nm	500 nm	6-CMUNic-KLH with Alum	100 nm with Alum	500 nm with Alum	Nic-KLH with Alum
IgG1 (%)	80.9	69.2	73.4	72.1	63.5	73.7
Th1/Th2 index	0.0935 ± 0.0359***	0.1444 ± 0.0214***	0.1090 ± 0.0240***	0.1368 ± 0.0303***	0.1800 ± 0.0457***	0.1098 ± 0.0479***

*** indicates the comparison between the Th1/Th2 indexes from each vaccine treatment group and the value "1", in which p-value is less than 0.001. No significant differences were found among the Th1/Th2 indexes with the different vaccine groups.

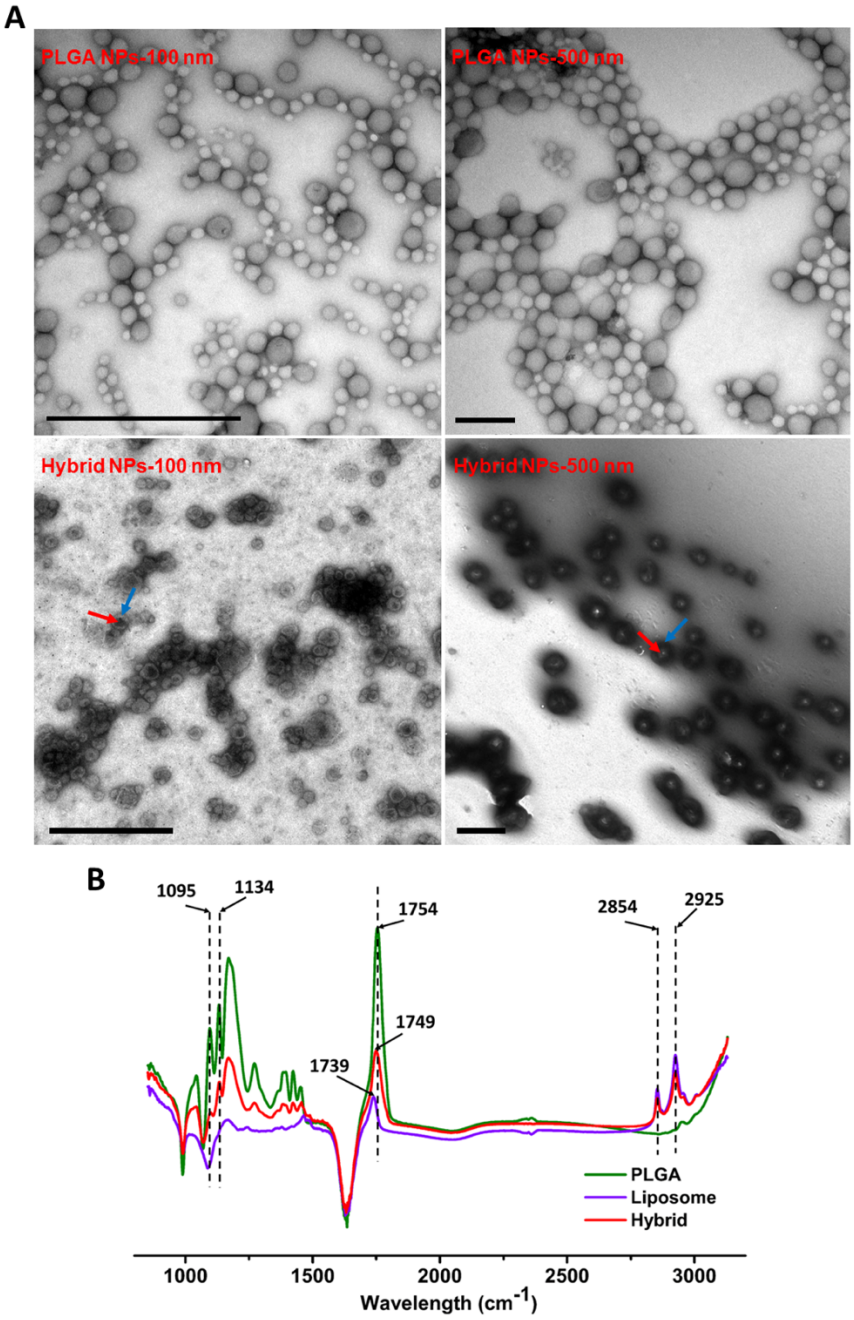

Figure 1. Characterization of lipid-polymeric hybrid NPs with different sizes. (A) Transmission electron microscopic images of poly(lactic-co-glycolic acid) (PLGA) and hybrid NPs with different average sizes. The red and blue arrows denote the PLGA core and lipid shell, respectively. The scale bars represent 1000 nm. (B) Fourier transform infrared spectra of PLGA NPs, liposome NPs, and lipid-polymeric hybrid NPs.

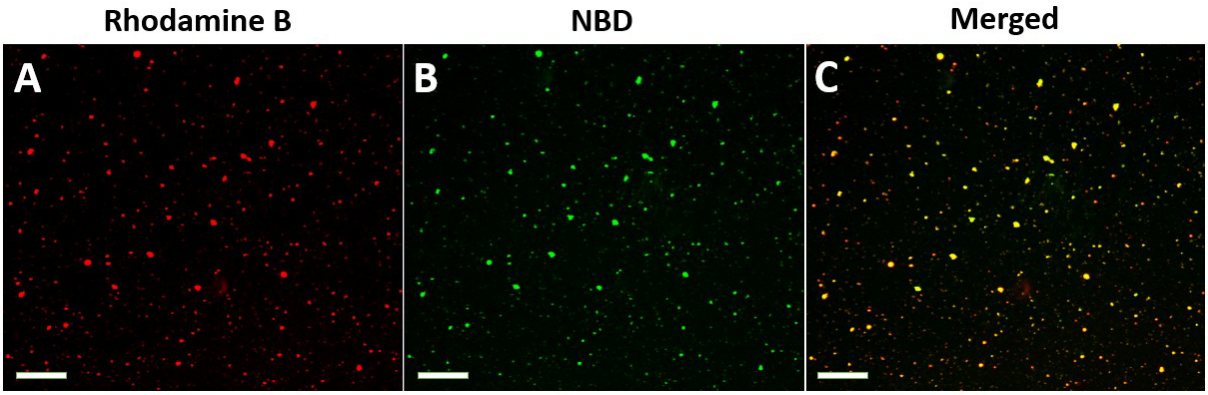

Figure 2. Confocal laser scanning microscopy images of KLH-conjugated lipid-polymeric hybrid NPs. KLH and lipids were labeled by (A) rhodamine B (red) and (B) NBD (green), respectively. (C) Dual labeling is shown in yellow. The scale bars represent 10 μm.

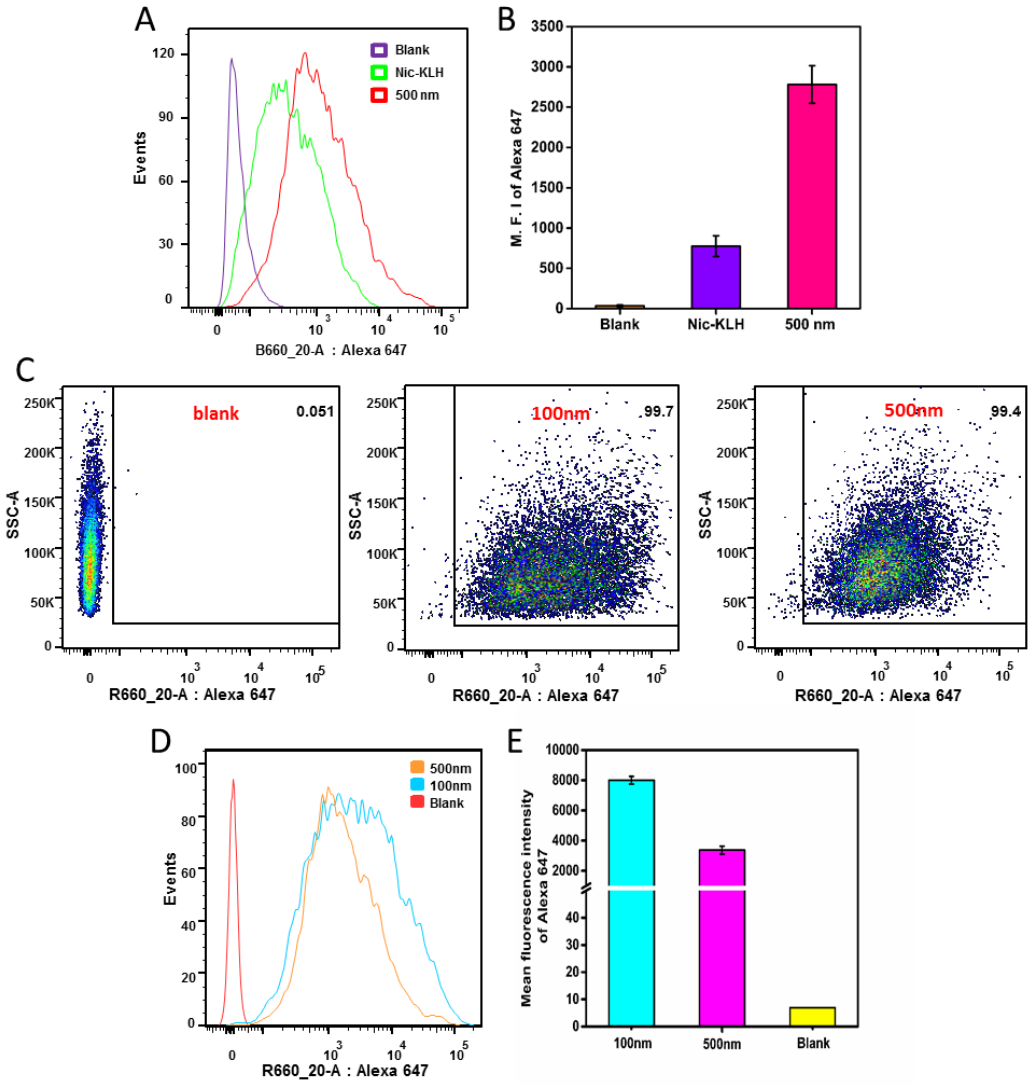

Figure 3. Flow cytometry analysis of JAWSII dendritic cells treated with the AF647-KLH conjugate or AF647-labeled nanovaccine NPs of different sizes for 2 h. (A), (D) and (B), (E) show the intensity distribution and mean intensity of AF647 fluorescence, respectively, in dendritic cells treated with AF647-KLH or AF647-labeled nanovaccines. (C) Recorded events show that more than 99% of cells were labeled for both 100 and 500 nm nanovaccine particles. AF647 was conjugated to KLH to form the AF647-KLH conjugate. AF647-KLH was associated to the surface of hybrid NPs to form fluorescent nanovaccine NPs. The blank group are cells that were not treated with NPs. Quantitative data are expressed as means ± SD.

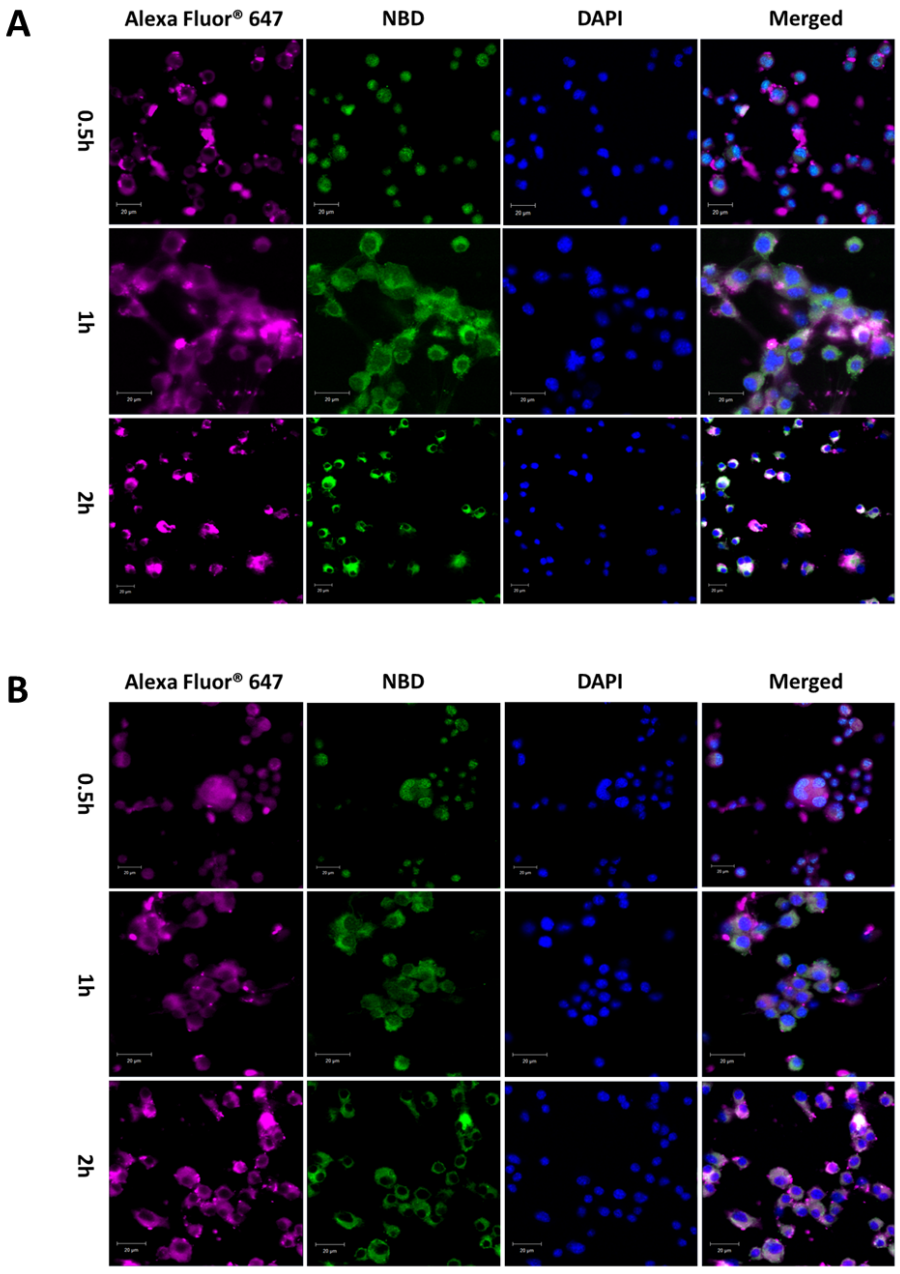

Figure 4. Confocal laser scanning microscopy images of JAWSII dendritic cells treated with (A) 100 nm or (B) 500 nm nanovaccine NPs for 0.5, 1, and 2 h. KLH was labeled with AF647 and the lipid layer of NPs was labeled with NBD. The scale bars represent 20 μm.

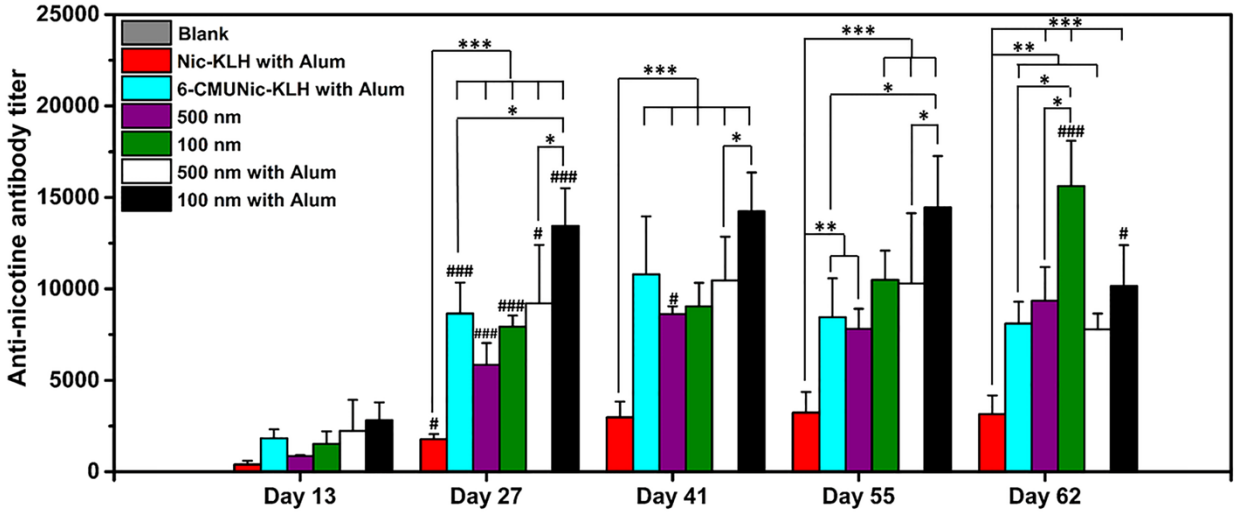

Figure 5. Time course of anti-nicotine-specific antibody formation in mice immunized with various nicotine vaccines. Mice (n = 8 per group) were immunized by subcutaneous injection on days 0, 14, and 28. In the blank group, mice were injected with phosphate-buffered saline as the negative control. Antibody titers were compared among groups using one-way ANOVA followed by Tukey's HSD test. Data are expressed as means ± SD. Significantly different antibody titers: *p < 0.05, **p < 0.01, ***p < 0.001. Antibody titers were significantly different compared to that of the previous study time point: # < 0.05, ### < 0.001.

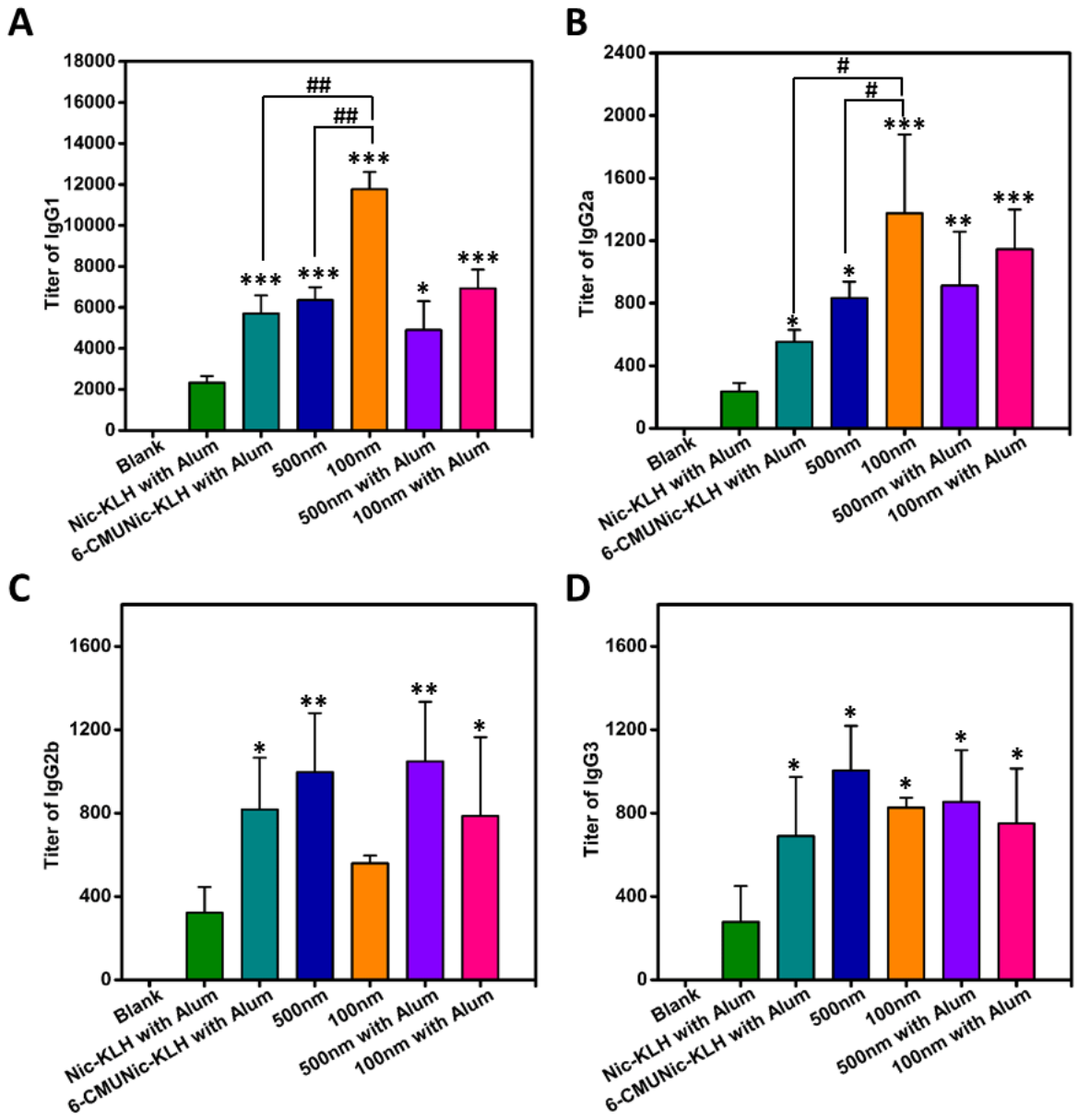

Figure. 6. Distribution of IgG subclasses generated by immunization with nicotine vaccines. (A) IgG1; (B) IgG2a; (C) IgG2b; (D) IgG3. In the blank group, mice were injected with phosphate-buffered saline as the negative control. Comparisons among groups were analyzed by one-way ANOVA followed by Tukey's HSD test. Data are expressed as means ± SD. Significantly different compared to the Nic-KLH with alum groups: *$p < 0.05$, **$p < 0.01$, ***$p < 0.001$. Significantly different: #$p < 0.05$, ##$p < 0.01$.

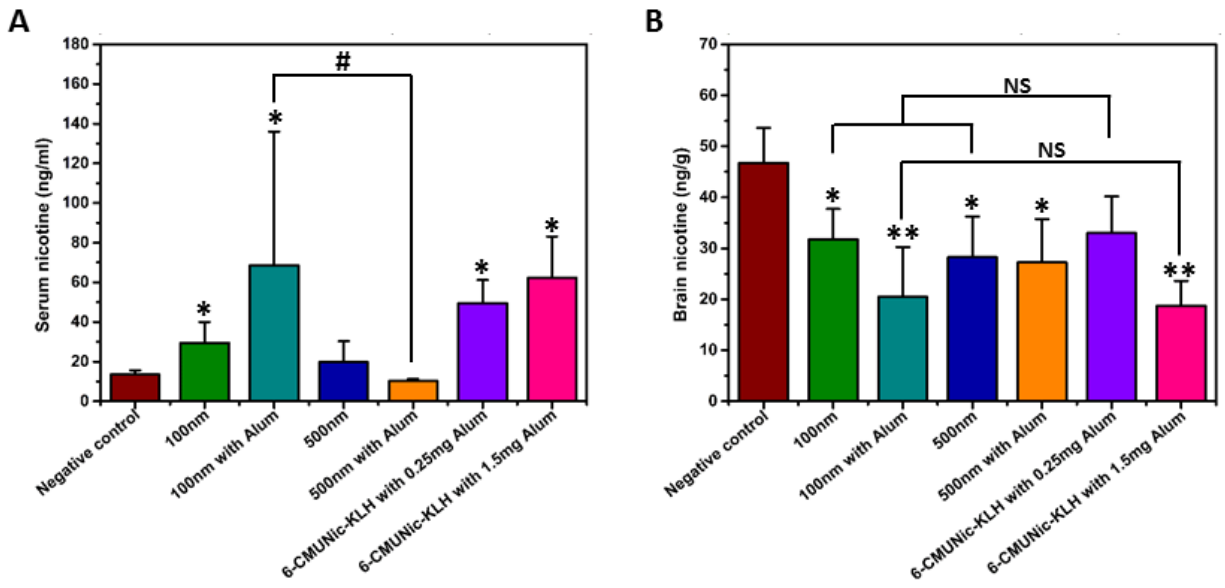

Figure 7. Nicotine distribution in serum and brain in immunized mice. Mice were immunized with vaccines containing immunogens equivalent to 25 μg of Nic-KLH. For groups with alum, 1.5 mg was used as an adjuvant. The 6-CMUNic-KLH positive control used 0.25 or 1.5 mg of alum. Mice in the negative control group were immunized with 25 μg of KLH carrier protein alone. (A) Serum and (B) brain tissues of 4 mice were collected 4 min post administration of 0.06 mg/kg nicotine subcutaneously on Day 41. Data are expressed as means ± SD. Significantly different compared to the negative control group: *$p < 0.05$, **$p < 0.01$. Significantly different: #$p < 0.05$. NS indicates the brain nicotine levels between groups were comparable ($p>0.98$).

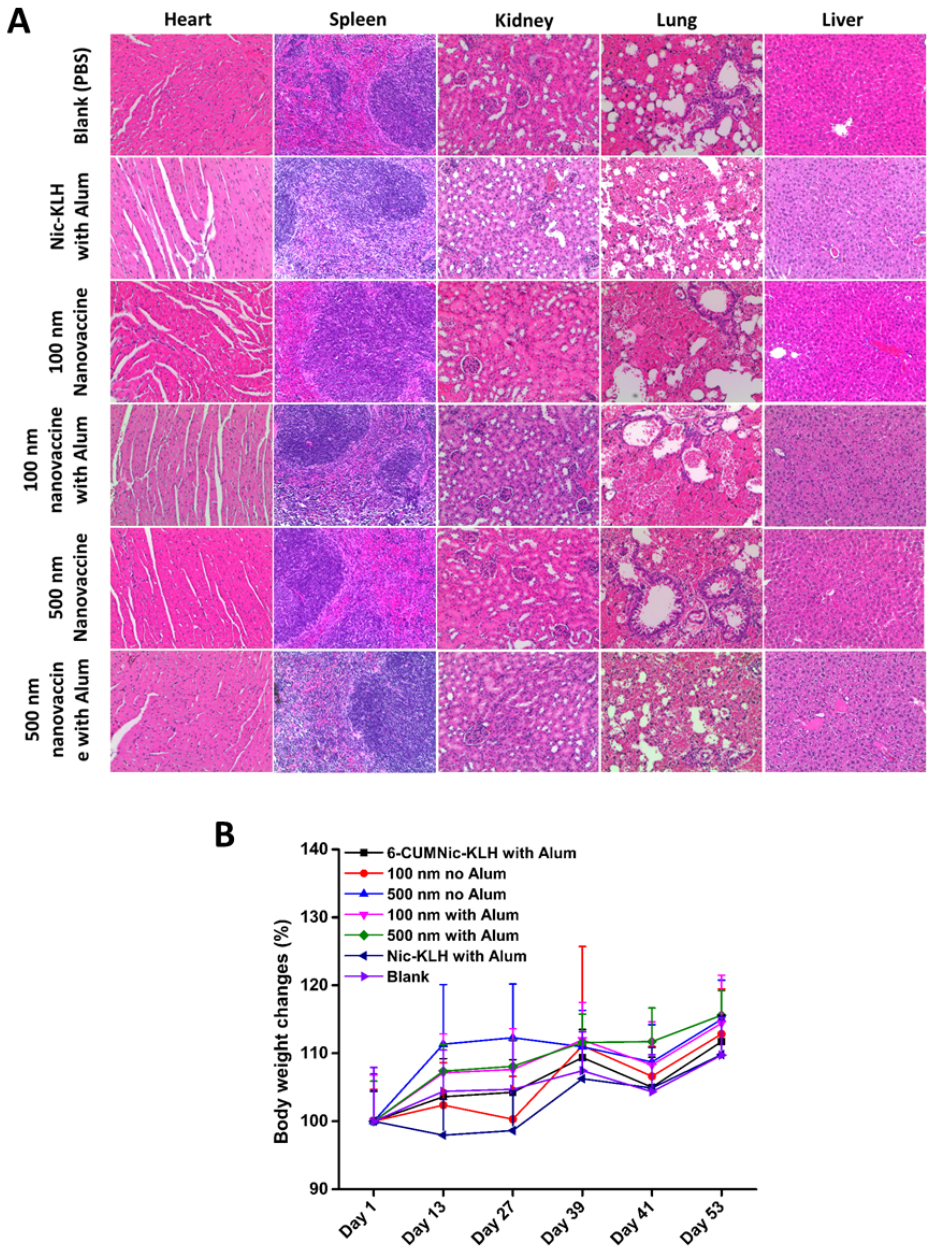

Figure 8. Evaluation of the safety of nicotine vaccines. (A) Representative histopathological images of tissues from mice treated nicotine vaccines. No lesions were observed in heart, kidney, liver, spleen, and lung tissues. (B) Body weight changes of immunized mice. Data are expressed as means ± SD. No significant differences were found between mice treated with different vaccines and those treated with phosphate-buffered saline (blank).

Chapter 4: Engineering of a hybrid nanoparticle-based nicotine nanovaccine as a next-generation immunotherapeutic strategy against nicotine addiction: a focus on hapten density

Zongmin Zhao[†], Kristen Powers[‡], Yun Hu[†], Michael Raleigh[§], Paul Pentel[§], Chenming Zhang[†,*]

[†] Department of Biological Systems Engineering, Virginia Tech, Blacksburg, VA 24061, United States

[‡] Department of Biological Science, Virginia Tech, Blacksburg, VA 24061, United States

[§] Minneapolis Medical Research Foundation, Minneapolis, MN 55404, United States

*Corresponding author.

Address: 210 Seitz Hall, Department of Biological Systems Engineering, Virginia Tech, Blacksburg, VA 24061

Voice: +1-(540)231-7601.

Fax: +1-(540)231-3199.

Email address: chzhang2@vt.edu

This manuscript has been published on *Biomaterials* 2017, 123: 107-117. Reprinted with permission of the publisher.

Abstract

Although a nicotine vaccine is a promising way to combat nicotine addiction, most traditional hapten-protein conjugate nicotine vaccines only show limited efficacy due to their poor recognition and uptake by immune cells. This study aimed to develop a hybrid nanoparticle-based nicotine vaccine to improve the efficacy of the conjugate vaccine. This study also examined the impact of hapten density on the immunological efficacy of the proposed hybrid nanovaccine. In terms of the internalized protein antigens, the nanovaccine nanoparticles were taken up by the dendritic cells more efficiently than the conjugate vaccine particles, regardless of the hapten density of the nanoparticles. At a similar hapten density, the nanovaccine induced a significantly stronger immune response against nicotine than the conjugate vaccine in mice. The high- and medium-density nanovaccines resulted in significantly higher anti-nicotine antibody titers than their low-density counterpart. Specifically, the high-density nanovaccine exhibited better immunogenic efficacy, resulting in higher anti-nicotine antibody titers and lower anti-carrier protein antibody titers than the medium- and low-density versions. The high-density nanovaccine also had the best ability to retain nicotine in serum and to block nicotine from entering the brain. These results suggest that the hybrid nanoparticle-based nicotine vaccine can elicit strong immunogenicity by modulating the hapten density, thereby providing a promising next-generation immunotherapeutic strategy against nicotine addiction.

Key words

Nicotine addiction; nicotine vaccine; hybrid nanoparticle; antibody; hapten density

4.1 Introduction

Tobacco smoking remains the leading cause of preventable diseases and premature deaths; worldwide, it is responsible for nearly 6 million deaths and significant economic losses each year.[1, 2] Despite the use of pharmacological treatments, such as nicotine replacement therapy and nicotine agonists/antagonists, only a small percentage of treated smokers (10-25%) are able to successfully quit.[3-5] Therefore, more efficient approaches are needed to combat tobacco addiction.

Nicotine vaccines induce the production of antibodies that specifically bind to nicotine in serum, thereby blocking its entrance into the brain; they have been presented as an attractive strategy to treat nicotine addiction.[6, 7] Over the past several decades, many nicotine vaccines have been found to achieve high immunogenicity and pharmacokinetic efficacy in preclinical trials.[8-11] However, to date, all human clinical trials of conjugate nicotine vaccines have not achieved the expected efficacies.[12] The phase 2 clinical studies of NicVax and NicQβ revealed that while the overall smoking cessation rate was not enhanced in the study group in comparison to the placebo group, the quit rate improved in the top 30% of the study group subjects that had the highest antibody titers.[13, 14] Together with our previously reported physiologically-based-pharmacokinetic-modeling data,[15] these clinical findings suggest that while the basic concept of using immunotherapy to promote smoking cessation is solid, more antibodies must be generated to ensure the efficacy of vaccinations.

A variety of approaches to strengthen the immunogenicity of traditional conjugate nicotine vaccines have been investigated, including the design of hapten structure,[16, 17] the modulation of the linker position and composition,[8] the selection of carrier proteins,[10] the use of different

adjuvants,[18] the application of multivalent vaccines,[19-22] and the optimization of administration routes[23]. However, as the immune system is relatively poor at recognizing small soluble protein antigens[24, 25], traditional conjugate nicotine vaccines still bear a serious innate shortcoming, poor recognition and internalization by immune cells. Even with the help of alum adjuvants to form particulate antigens, conjugate nicotine vaccines cannot be easily tuned to have optimal physicochemical properties (shape, size, and charge) for uptake. Meanwhile, conjugate nicotine vaccines suffer from several other innate shortfalls, such as fast degradation, difficulty integrating with molecular adjuvants, and short immune persistence, which limit their immunogenic outcomes.[26]

Nanoparticles (NPs) have been widely used for the efficient delivery of drugs, proteins, and vaccines.[27-33] Based on the hypothesis that NPs might provide a new strategy to address the limitations of conjugate nicotine vaccines, this study aimed to develop a lipid-poly(lactic-co-glycolic acid) (lipid-PLGA) hybrid nanoparticle (NP)-based nicotine vaccine to improve the immunogenicity of the conjugate nicotine vaccine. This hybrid NP-based nicotine nanovaccine was designed to enhance the delivery and presentation of B cell epitopes and T cell help proteins, both of which are required to induce an effective humoral immune response, to immune cells. Because hapten density might play an important role in the ability of immune cells to recognize nanovaccine particles, we also investigated its influence on the immunogenicity of the nicotine nanovaccines. Various nanovaccine NPs with different hapten densities were fabricated, and their physicochemical properties and epitope density were characterized. The *in vitro* uptake of the hapten-protein conjugate and nanovaccine particles was studied in immature dendritic cells (DCs). The immunogenicity and pharmacokinetic efficacy of three nanovaccines (low-, medium-, and

high-hapten density) were tested in mice. Finally, histopathological analysis was used to determine the safety of the proposed hybrid NP-based nanovaccine.

4.2 Materials and methods

4.2.1 Materials

Lactel® 50:50 PLGA (acid-terminated) was purchased from Durect Corporation (Cupertino, CA, USA). 2,4,6-trinitrobenzenesulfonic acid (TNBSA), Alexa Fluor 350 (AF350), Alexa Fluor 647 (AF647), and keyhole limpet hemocyanin (KLH) were purchased from Thermo Fisher Scientific Inc. (Rockford, IL, USA). 1,2-Dioleoyl-3-trimethylammonium-propane (DOTAP), cholesterol (CHOL), 1,2-distearoyl-sn-glycero-3-phosphoethanolamine-N-[maleimide(polyethylene glycol)-2000] (ammonium salt) (DSPE-PEG2000-maleimide), and 1,2-diphytanoyl-sn-glycero-3-phosphoethanolamine-N-(7-nitro-2-1,3-benzoxadiazol-4-yl) (ammonium salt) (NBD-PE) were purchased from Avanti Polar Lipids Inc. (Alabaster, AL, USA). O-succinyl-3'-hydroxymethyl-(±)-nicotine (Nic) hapten was purchased from Toronto Research Chemicals (North York, ON, Canada). All other chemicals were of analytical grade.

4.2.2 Preparation of lipid-PLGA NPs

PLGA NPs were prepared using a double emulsion solvent evaporation method. In brief, 50 mg of PLGA was dissolved in 2 mL of dichloromethane (oil phase). Two hundred μL of ultrapure water was added to the oil phase. The mixture was emulsified by sonication for 10 min using a Branson M2800H Ultrasonic Bath sonicator (Danbury, CT, USA). The resultant primary emulsion was added dropwise to 12 mL of 0.5% w/v poly(vinyl alcohol) solution. The suspension was emulsified by sonication using a sonic dismembrator (Model 500; Fisher Scientific, Pittsburg, PA, USA) at an amplitude of 70% for 40 s. The resultant secondary emulsion was stirred overnight to

allow complete dichloromethane evaporation. PLGA NPs were collected by centrifugation at 10,000 *g*, 4 °C for 30 min (Beckman Coulter Avanti J-251, Brea, CA, USA). Pellets were washed three times using ultrapure water.

Lipid-PLGA NPs were assembled using a film-hydration-sonication method as described previously.[34] In brief, 15 mg of lipid mixture dissolved in chloroform consisting of DOTAP, DSPE-PEG2000-maleimide, and CHOL (90:5:5 in moles) was evaporated to form a lipid film. One mL of 0.01 M pH 7.4 phosphate buffer saline (PBS) was added to hydrate the lipid film. The resultant suspension was sonication for 5 min in a Branson M2800H Ultrasonic Bath sonicator. Fifteen mg of PLGA NPs suspended in DI water (10 mg/ml) was added and mixed with the above liposome suspension. Subsequently, the mixture was sonicated in an ice-water bath using a bath sonicator for 5 min. Lipid-PLGA NPs were collected by centrifugation at 10,000 *g*, 4 °C for 30 min.

4.2.3 Assembly of nicotine vaccine NPs with different hapten density

Nic-KLH conjugates were synthesized using a carbodiimide-mediated reaction. In brief, Nic-hapten of various equivalents of KLH was mixed with appropriate amounts of 1-ethyl-3-(3-dimethylaminopropyl)carbodiimide hydrochloride (EDC) and Sulfo-N-hydroxysulfosuccinimide (NHS) in activation buffer (0.1 M MES, 0.5 M NaCl, pH 6.0) and incubated at room temperature for 15 min. The mixture was added to 5 mg of KLH, which was dissolved in coupling buffer (0.1 M sodium phosphate, 0.15 M NaCl, pH 7.2). After the overnight reaction, unconjugated Nic-hapten and byproducts were eliminated by dialyzing against 0.01 M PBS (pH 7.4) at room temperature for 24 h. The number of Nic-haptens on Nic-KLH was determined by measuring the difference in the number of remaining lysine groups on the surface of KLH before and after hapten conjugation using a TNBSA based method. In brief, KLH and Nic-KLH conjugates were prepared

at a concentration of 1 mg/mL. Two hundred μL of the protein solution was taken and mixed with 200 μL of 4% $NaHCO_3$ solution. Two hundred μL of 0.1% TNBSA solution was added to the mixture and incubated at 37 °C for 1 h, and the absorbance was read at 335 nm. Hapten density of KLH was calculated from the differences between the O.D. of the control and the conjugates.

Nanovaccine NPs were assembled by attaching Nic-KLH conjugates onto the surface of lipid-PLGA hybrid NPs via a thiol-maleimide-mediated method. In brief, an appropriate amount of Traut's reagent was added to the Nic-KLH conjugate (containing 3 mg of KLH), which was dissolved in 0.1 M pH 8.0 bicarbonate buffer and incubated for 1 h. Nic-KLH was attached to lipid-PLGA NPs by reacting to the thiolated Nic-KLH with the appropriate amount of lipid-PLGA NPs in 0.1 M pH 8.0 bicarbonate buffer for 2 h. NPs were collected by centrifugation at 10,000 *g*, 4 °C for 30 min. Unattached Nic-KLH in the supernatant was quantified by the BCA assay. The lipid layer of hybrid NPs was labeled by NBD-PE, and the number of lipid-PLGA NPs was counted by flow cytometry. Hapten density (number of haptens per NP) was approximated by the following formula, $D_{nic}=(AF_{Nic\text{-}KLH}*M_{Nic\text{-}KLH}*D_{Nic\text{-}KLH}*N_A)/N_{NPs}$, where D_{nic}, $AF_{Nic\text{-}KLH}$, $M_{Nic\text{-}KLH}$, $D_{Nic\text{-}KLH}$, N_A, and N_{NPs} represent hapten density per NP, Nic-KLH association efficiency, moles of KLH associated on 1 mg of NPs, hapten density of Nic-KLH, Avogadro constant, and NP number per 1 mg of NPs, respectively. Vaccine NPs were lyophilized and stored at 2 °C for later use.

4.2.4 Characterization of NPs

The successful assembly of nanovaccine NPs was validated using confocal laser scanning microscopy (CLSM). Fluorescent vaccine NPs—in which the lipid layer, PLGA layer, and KLH were labeled by NBD, Nile red, and AF350, respectively—were prepared according to a similar method as described above with minor modifications. In brief, PLGA NPs containing Nile red

were fabricated by a double emulsion solvent evaporation method, wherein the appropriate amount of Nile red was dissolved in the oil phase. The lipid layer was labelled by adding 5% w/w of NBD-PE into the lipid mixture. AF350 was conjugated to KLH through an EDC-mediated reaction. NPs were imaged by a Zeiss LSM 510 Laser Scanning Microscope (Carl Zeiss, German). The morphology of NPs was studied using transmission electron microscopy (TEM). In brief, NP suspensions (2 mg/mL) were dropped onto a 300-mesh Formvar-coated copper grid. The remaining suspension was removed with wipes after standing for 10 min. The samples were negatively stained for 20 s using freshly-prepared 1% phosphotungstic acid. The samples were then washed twice using ultrapure water. The dried samples were imaged on a JEOL JEM 1400 transmission electron microscope (JEOL Ltd., Tokyo, Japan). The physicochemical properties of NPs, including particle size and zeta potential, were measured by the Dynamic Light Scattering method and Laser Doppler Micro-electrophoresis method on a Malvern Nano ZS Zetasizer (Malvern Instruments Ltd, Worcestershire, United Kingdom), respectively.

4.2.5 Cellular uptake of vaccine particles by DCs

The uptake of vaccine particles by DCs was quantitatively measured by flow cytometry. JAWSII (ATCC® CRL-11904™) immature DCs were cultured in alpha minimum essential medium (80% v/v) supplemented with ribonucleosides, deoxyribonucleosides, 4 mM L-glutamine, 1 mM sodium pyruvate, 5 ng/mL murine GM-CSF, and fetal bovine serum (20% v/v) at 37 °C, 5% CO_2. Cells were seeded into 24-well plates (2×10^6/well) and cultured overnight. In order to compare the cellular uptake of conjugate vaccine and nanovaccine, AF647, a model of Nic-hapten, was used instead of Nic-hapten to prepare vaccine particles to provide fluorescence. Cells were treated with vaccine particles containing same amounts of KLH protein (10 μg). In order to compare the cellular uptake of nanovaccine particles with different hapten densities, 5% (w/w) NBD-PE was added to

the lipid layer of nanoparticles to provide fluorescence. Cells were treated with nanovaccine particles containing same amounts of hybrid NPs (50 μg). After incubation for 2 h, the medium was immediately removed, and the cells were washed three times with 0.01 M pH 7.4 PBS. Cells were detached from the culture plates using Trypsin/EDTA solution and centrifuged at 200 *g* for 10 min. Cell pellets were re-suspended in 0.01 M pH 7.4 PBS. Samples were immediately analyzed on a flow cytometer (BD FACSAria I, BD, Franklin Lakes, NJ, USA).

The uptake and intracellular distribution of vaccine particles were qualitatively determined by CLSM. Cells were seeded into a 2-well chamber slide (2×10^5/chamber), and cultured overnight. The original medium was replaced with 2 mL of fresh medium containing vaccine particles. After incubation for 2 h, the medium was discarded, and the cells were washed three times using 0.01 M pH 7.4 PBS. One mL of freshly-prepared 4% (w/v) paraformaldehyde was added to each well to fix the cells for 15 min. The fixed cells were washed three times with PBS and were made permeable by adding 0.5 mL of 0.1% (v/v) Triton™ X-100 for 15 min. After washing the cells three times using PBS, the nuclei of cells were stained with DAPI. The intracellular distribution of NPs was visualized on a Zeiss LSM 510 Laser Scanning Microscope.

4.2.6 Immunization of mice with nicotine vaccines

All animal studies were carried out following the National Institutes of Health (NIH) guidelines for animal care and use. Animal protocols were approved by the Institutional Animal Care and Use Committee at Virginia Polytechnic Institute and State University. Female Balb/c mice (6-7 weeks of age, 16-20 g, 8 per group) were immunized subcutaneously on Days 0, 14, and 28 with vaccines of negative control (KLH associated lipid-PLGA NPs), Nic-KLH with alum, low-density nanovaccine, low-density nanovaccine with alum, medium-density nanovaccine, medium-density nanovaccine with alum, high-density nanovaccine, and high-density nanovaccine with alum. For

vaccine groups without alum adjuvant, the mice were injected with vaccine particles (containing 25 μg of protein antigen) that were suspended in 200 μL of 0.01 M pH 7.4 PBS. In the vaccine with alum adjuvant groups, the mice were injected with vaccine particles (containing 25 μg of protein antigen) that were suspended in 100 μL of PBS and mixed with 100 μL of alum (10 mg/mL), and the mixture was used to immunize mice. The alum used was aluminum hydroxide (Alhydrogel® adjuvant 2% from Invivogen). Blood samples were collected on Days 0, 12, 26, 40, and 54.

4.2.7 Measurement of nicotine-specific IgG antibody (NicAb) titer, nicotine-specific IgG subclass antibody titer, and anti-carrier protein antibody titer

The NicAb titers in serum were determined by ELISA as described previously.[35] Anti-KLH antibody titers were measured using a similar ELISA protocol, and KLH was used as the coating material. Antibody titer was defined as the dilution factor at which absorbance at 450 nm declined to half maximal.

4.2.8 Nicotine challenge study in mice

Female Balb/c mice (6-7 weeks of age, 16-20 g, 4-5 per group) were immunized with the same protocol as described in the previous context. On Day 54, mice were administrated with 0.03 mg/Kg nicotine subcutaneously. Mice were euthanized under anesthesia 4 min after nicotine challenge, and the blood and brain were collected. Nicotine contents in serum and brain tissues were analyzed by GC/MS according to a method reported previously. [20]

4.2.9 Preliminary evaluation of the safety of nanovaccines

The safety of the nicotine nanovaccines was preliminarily evaluated in mice by monitoring the body weight change and histopathological analysis. To investigate the body weight change during

the study, mice were weighed before primary immunization and once a week after that. Histopathological analysis of tissues from immunized mice was performed to examine the lesions caused by the administration of nanovaccine NPs. In brief, different mouse organs were fixed with 10% formalin, followed by cutting the organs according to a standard protocol. Tissue blocks were then embedded in paraffin, and the routine sections were stained with hematoxylin and eosin. The stained sections were imaged on a Nikon Eclipse E600 light microscope, and pictures were captured using a Nikon DS-Fi1 camera.

4.2.10 Statistical analysis

Comparisons between two groups were performed by unpaired student's t-test. Comparisons among multiple groups were conducted by one-way ANOVA followed by Tukey's HSD analysis. Differences were considered significant if p-values were less than 0.05.

4.3 Results and discussion

As shown in **Scheme 1**, the NP-based nicotine nanovaccine in this study was formed by conjugating multiple Nic-KLH conjugates to the surface of one hybrid NP. The PLGA core not only serves as a scaffold to support the lipid layer and stabilize the nanovaccine system, but also endows the nanovaccine with a particulate property to achieve improved recognition and internalization by immune cells. The lipid layer was composed of DOTAP, CHOL, and DSPE-PEG2000-maleimide. The DSPE-PEG2000-maleimide component enables the association of hapten-carrier protein conjugates (Nic-KLH) onto the surface of lipid-PLGA NPs. Nic hapten that is a B cell epitope is conjugated to the carrier protein (KLH) to be immunogenic. The KLH carrier protein provides sufficient T cell help peptides to promote the activation and maturation of B cells.

The Nic hapten density of the nicotine nanovaccine was modulated to achieve an optimal immunological efficacy.

4.3.1 Validation of the conjugate chemistry and characterization of the structure of nanovaccine NPs

The nanovaccine NPs assembled in this study are supposed to have a structure composed of a PLGA core, a lipid shell, and multiple Nic-KLH conjugates. Confocal laser scanning microscopy (CLSM) was used to characterize the nanovaccine structure and verify the conjugate chemistry of hapten. The PLGA, lipid, and KLH layers were labeled with Nile Red, NBD, and AF350 fluorescence, respectively. As shown in **Fig. 1**, almost all particles were co-labeled with the three fluorescent colors, indicating that lipids were successfully coated around PLGA NPs to form a hybrid core-shell structure, and KLH was associated to the surface of NPs with very high efficiency. Meanwhile, AF350 was a model of Nic-hapten, having similar size and the same reactive group (NHS ester). In this study, Nic-hapten was attached to KLH by the EDC/NHS-mediated conjugate chemistry, in which the carboxylic groups of Nic were activated by EDC/NHS to form semi-stable Nic-NHS esters that could readily react with the amino groups of KLH. AF350 was conjugated to KLH efficiently, validating the feasibility of the hapten conjugate chemistry.

The structure of the nanovaccine NPs was further investigated using TEM. **Fig. 2A** shows the TEM images exhibiting the morphology of PLGA NPs, liposomes, lipid-PLGA hybrid NPs, and nanovaccine NPs. All four NPs were of spherical shapes. A distinguishing core-shell structure, which was shown as a bright PLGA core and a dark lipid shell, was observed on lipid-PLGA NPs (**Fig. 2A (c)**), indicating the successful coating of lipids onto PLGA NPs. As shown in **Fig. 2A (d)**, multiple black dots, which were Nic-KLH conjugates, were located on the surface of hybrid NPs, confirming the efficient association of Nic-KLH. KLH is a large carrier protein that is composed

of KLH1 and KLH2 subunits, both of which are around 400 kDa.[36] The large size makes it visible in the TEM images. The average size of NPs increased from 90.8 nm to 107.0 nm upon lipid coating and further increased to 121.3 nm after Nic-KLH associating (**Fig. 2B**). Bare PLGA NPs had a negative zeta-potential (-14.3 mV) (**Fig. 2C**), which may be caused by the carboxylic acid terminal groups of the PLGA polymer used in this study. Upon lipid coating and Nic-KLH conjugation, the zeta potential of NPs changed to 12.6 mV of Lipid-PLGA NPs and then to 4.16 mV of nanovaccine NPs (**Fig. 2C**), as the liposome is positively charged (**Fig. 2C**) and Nic-KLH is negatively charged (-17.3 ± 2.3 mV).

4.3.2 Preparation and characterization of nanovaccines with different hapten density

Various molar excess of Nic-hapten to KLH was applied for the conjugating reaction of hapten on KLH. The hapten density of the prepared nanovaccines is shown in **Fig. 3A**. The increased hapten density from NKLP-A to NKLP-I verified the feasibility of modulating the Nic hapten density by changing the molar ratios of hapten to KLH in the preparation process. To date, most reported hapten-protein conjugate nicotine vaccines have hapten density ranging from 2 to 100 per protein particle,[10, 37, 38] depending on the available lysine groups and conjugate chemistry. Noticeably, the design of the hybrid-NP based nicotine nanovaccine significantly increased the epitope numbers per particle over conventional conjugate nicotine vaccines, potentially contributing to an enhanced epitope recognition by B cells. Each NKLP-C, NKLP-F, and NKLP-I nanovaccine NP carried approximately 29×10^3, 146×10^3, and 319×10^3 Nic haptens, respectively (**Table 1**). Statistical analysis revealed that the hapten densities of NKLP-C, NKLP-F, and NKLP-I are significantly different ($p<0.001$). Thus, in this study, NKLP-C, NKLP-F, and NKLP-I were selected as low-, medium-, and high-density nanovaccines for *in vivo* immunogenicity study. The physicochemical properties of different hapten density nanovaccines were characterized and

shown in **Fig. 3B** and **Table 1**. The average zeta potentials of NKLP-C, NKLP-F, and NKLP-I nanovaccine NPs were 4.16 mV, 3.92 mV, and 3.86 mV, respectively. The positively charged surface of nanovaccine NPs will enhance their interaction with the negatively charged surface of immune cells,[39] thereby promoting cellular uptake of the nanovaccines. The average size of NKLP-C, NKLP-F, and NKLP-I was 121.3 nm, 123.8 nm, and 121.2 nm, respectively. According to **Fig. 3C**, all three nanovaccine NPs exhibited narrow size distributions, with most of the NPs less than 200 nm, which were in agreement with the small PDI (0.21-0.24, **Table 1**) and uniform size in the TEM images (**Fig. 2A(d)**). It has been reported that size is a critical parameter influencing the efficacy of nanoparticle vaccines. Particles of 20-200 nm will efficiently enter the lymphatic system, while by contrast, particles that are larger than 200-500 nm do not efficiently enter lymph capillaries in a free form.[40-42] The size of the nanovaccines in this study was relatively optimal and will hopefully result in high immunogenicity.

4.3.3 Cellular uptake of nanovaccine NPs by dendritic cells (DCs)

Efficient capture, internalization, and processing of nicotine containing antigens by DCs largely determine the outcomes of vaccination. Traditional nicotine-protein conjugate vaccines suffer from the disadvantage of poor recognition and internalization by immune cells. Here, we compared the uptake of nanovaccine NPs (AF647-KLP) to nicotine-KLH conjugate vaccine particles (AF647-KLH) by DCs. Nic-hapten was substituted by AF647 to render KLH fluorescent, and the density of AF647 on KLH of either AF647-KLH or AF647-KLP was identical. As shown in **Fig. 4B** and **Fig. 4C**, the M.F.I. of AF647 in the AF647-KLP group was over 500% more than that in the AF647-KLH group, suggesting that more protein antigens were taken up by DCs in the nanovaccine NP group within the same time. The uptake and distribution of particles in DCs were also examined by CLSM. As shown in **Fig. 4A**, in agreement with the flow cytometry results,

brighter AF647 fluorescence was observed in the AF647-KLP group compared to the AF647-KLH group, indicating again that DCs took up antigens more efficiently when treated with AF647-KLP. The conjugation of multiple Nic-KLH to one hybrid nanoparticle may increase the availability of antigens for uptake, thus contributing to an enhanced antigen internalization. Meanwhile, the immune system prefers to recognize and take up particulate pathogens (such as bacteria and virus) and is relatively invisible to small soluble protein antigens.[24, 25] The stable and spherical lipid-PLGA hybrid nanoparticles endowed the nanovaccine with a particulate property. This particulate nature together with the relatively optimal physicochemical properties is beneficial for the improved uptake by DCs. The internalization of more protein antigens by DCs enhanced by the lipid-PLGA NP delivery vehicles will benefit many of the immunogenic outcomes of nicotine nanovaccines. The uptake and processing of protein antigens is a critical prerequisite for T helper cell formation, which is necessary for B cell activation in humoral immunity.[26, 43] Therefore, the more protein antigens internalized by DCs, the more T helper cells may be generated, causing more B cells to be activated, and finally leading to a better immunogenic efficacy of nicotine vaccines.

The uptake of different hapten density nanovaccine NPs by DCs was characterized. As shown in **Fig. 4D**, for all the nanovaccine groups, including KLP (non-hapten-conjugated nanovaccine), NKLP-C, NKLP-F, and NKLP-I, over 96% of the cells were stained by the NBD fluorescence within 2 h. This demonstrated that all the nanovaccine NPs, regardless of hapten density, were rapidly taken up by dendritic cells. Furthermore, as demonstrated in **Fig. 4E**, the M.F.I. of NBD of blank cells was less than 250, while by contrast, the values were around 6000 for all four nanovaccine groups and no marked difference was detected in terms of NBD fluorescence intensity. This indicated that DCs could take up all different hapten density nanovaccine NPs efficiently, and

hapten density would not influence this process discriminately. This similar uptake efficiency can be attributed to the similar physicochemical properties (size and charge) of nanovaccine NPs with different hapten densities. The uptake of nanovaccine NPs was further confirmed by CLSM, shown in **Fig. 4F**, in which the lipid-PLGA NPs and KLH were labeled by NBD and AF647, respectively. Co-localized, bright green and red fluorescence showing simultaneously in all recorded cells verified that the DCs rapidly and efficiently took up the nanovaccine NPs. Despite the similar uptake behavior of different hapten density nanovaccine NPs by DCs, Nic hapten density is expected to impact the recognition and activation of nicotine-specific B cells, and thereby influencing the efficacy of nanovaccines.

4.3.4 Immunogenicity of different hapten density nicotine nanovaccines

A nicotine vaccine aims to induce the production of specific antibodies that bind to nicotine and thereby block its entry into the brain. Previous studies have shown that the pharmacokinetic efficacy of nicotine vaccines closely correlates with the antibody concentration elicited.[11, 44] The phase 2 clinical trials of NicVax revealed that only the top 30% of subjects with the highest antibody titers showed improved smoking cessation rates compared to the placebo.[13] Therefore, the presence of high antibody titers is one of the most critical factors influencing the efficacy of nicotine vaccines, and thus it is necessary to be high enough to ensure the vaccination efficacy.

Fig. 5A shows the time-course results of anti-nicotine antibody titers, demonstrating that administration of all nicotine vaccines resulted in a steady increase of anti-nicotine IgG antibody titers along the study period. Particularly a sharp increase was observed after the first boost injection (on Day 26). In this study, the hapten density on KLH of the Nic-KLH conjugate vaccine and high-density nanovaccine were identical. The antibody titers in the high-density nanovaccine with or without alum groups were much higher (4-10 fold) than that in the Nic-KLH with Alum

group in all the studied days. This enhanced immunogenicity was in agreement with the enhanced internalization of antigens caused by the lipid-PLGA hybrid NP delivery system (**Fig. 4B**). These results were consistent with previous reports. It was reported that a tetrahedral DNA nanostructure delivery system could effectively enhance antigen uptake and induce strong and long-lasting antibody responses against antigens.[45] The ability of different hapten density nanovaccines to induce nicotine-specific antibodies was compared. As shown in **Fig. 5A**, the high-density nanovaccine induced the highest antibody titers compared to the low- and medium-density nanovaccines along the entire study period. Particularly, at the end of the study (on Day 54), the average antibody titer of the low-density without alum group was 5300, and increased by 7%, 159%, 166%, 211%, and 257% to 5700, 13700, 14100, 16500, and 18900, in groups of low-density with alum, medium-density with and without alum, high-density with and without alum, respectively. As shown in **Fig. 5B**, statistical analysis revealed that there were significant differences between the high-/medium-density groups and low-density groups, regardless of the presence of alum or not ($p<0.05$). Although no statistically significant differences were observed between the high- and medium-density groups ($p>0.05$), the high-density nanovaccines resulted in more responders of high antibody titers. Specifically, based on a cutoff of antibody titer >15000, the percentage of high-titer responders was 37.5%, 37.5%, 50%, and 75% in medium-density with and without alum groups, high-density with and without alum groups, respectively. The increased immunogenicity of nanovaccines with higher hapten density could be attributed to the evidence that the nanovaccine NPs with more haptens would have more chances to be recognized by naïve B cells, thereby activating more nicotine-specific B cells and strengthening the immune response. These results are not completely consistent with previous studies reporting the influence of hapten density on the efficacy of nicotine-protein conjugate vaccines. Miller et al. reported that nicotine

6-hexanoic acid-KLH conjugate nicotine vaccine generated higher antibody titers with a density of 100 compared to 22.[10] In another study, McCluskie et al. showed that stronger immune responses were obtained with 5-aminoethoxy-nicotine-CRM conjugate vaccines having hapten density of 11-18, with weaker responses above the range and more variable responses below the range.[37] Pravetoni et al. reported that the antibody titer was highest with a hapten/KLH ratio of 700:1 in a 1-SNic-KLH conjugate vaccine.[22]

The titers of anti-KLH antibody were measured to evaluate the influence of hapten density of nanovaccines on the production of carrier protein specific antibodies. As shown in **Fig. 6**, the anti-KLH antibody titer of the negative control group, in which no hapten was conjugated, was around 90000. Interestingly, in contrast, the anti-KLH antibody titers were reduced by 30.6%, 24.5%, 55.4%, 51.3%, 71.8%, and 68.6% in groups of low-density, low-density with alum, medium-density, medium-density with alum, high-density, and high-density with alum, respectively. This indicated that the anti-carrier protein antibody titers decreased with the increase of hapten density. Statistical analysis revealed significant differences in the anti-KLH antibody titers of different hapten density nanovaccine groups ($p<0.05$). This is probably because hapten conjugation masks the immunogenic epitopes on the carrier protein surface. A low anti-carrier protein antibody titer is considered beneficial for the vaccine design in this study. First, the utilization of nanovaccine to produce antibodies against carrier protein antibody rather than nicotine is a wastage of nanovaccine particles. The low-level production of anti-carrier protein antibody would leave more nanovaccines available to elicit anti-nicotine antibodies. Second, anti-carrier protein antibodies may neutralize the carrier protein on the surface of nanovaccine particles that are injected during the booster immunizations. Therefore, a low anti-carrier protein antibody level might minimally impair the immunological efficacy of nicotine nanovaccines.

4.3.5 Ability of different hapten density nicotine nanovaccines to influence nicotine distribution after nicotine challenge

Nicotine vaccines are designed to retain nicotine in serum and block it from entering the brain. As shown in **Fig. 7A**, the serum nicotine level was 5.75 ng/mL for the low-density nanovaccine group and increased by 160% and 204% to 15.0 ng/mL and 17.5 ng/mL for the medium- and high-density nanovaccine groups, respectively. This suggests the medium- and high-density nanovaccines had better efficacy in retaining nicotine in serum than the low-density nanovaccine, and particularly, the high-density nanovaccine exhibited the best efficacy. **Fig. 7B** shows the results of brain nicotine levels in mice vaccinated with different hapten density nanovaccines. The brain nicotine levels of Nic-KLH with alum group, low-density group, medium-density group, and high-density group, were reduced by 14.0%, 17.2%, 36.7%, and 40.0% compared to that of the negative control group. Statistical analysis revealed that the brain nicotine level for the high-density nanovaccine group was significantly lower than that of the Nic-KLH with alum group, suggesting that the use of lipid-PLGA hybrid NPs as delivery vehicles considerably enhanced the pharmacokinetic efficacy of the conjugate nicotine vaccine. In addition, the medium- and high-density nanovaccines resulted in considerably higher brain nicotine reduction than the low-density nanovaccine, and statistical analysis showed that the high-density nanovaccine had a significantly lower brain nicotine level than the low-density nanovaccine. This indicated that the high-density nanovaccine exhibited the best efficacy in blocking nicotine from entering the brain. These data were in concordance with the results of anti-nicotine antibody titers. Both the results of anti-nicotine antibody titers and brain nicotine reductions revealed that the immunological efficacy of the hybrid NP-based nicotine nanovaccine could be enhanced by modulating the hapten density.

4.3.6 Preliminary safety of nicotine nanovaccines

Mouse organs, including heart, kidney, liver, lung, and spleen, were examined by histopathological analysis after administration of nicotine vaccines. **Fig. 8A** shows the representative histopathological images of the negative control group and nicotine vaccine groups. As for the three different hapten density nanovaccines, mouse organs exhibited similar characteristics. The histopathological review revealed no significant lesions in the five organs of mice of each treatment and control groups. Mouse body weight was monitored as an indicator of vaccine safety along the study period. As shown in **Fig. 8B**, no body weight losses were detected for all the groups, indicating that the administration of nicotine vaccines did not impose apparent adverse impacts on mouse growth. Meanwhile, no short-term effects, including local site reaction, apparent abnormal behavior, and elevation in temperature, were found on mice treated with the nicotine vaccine formulations. The above preliminary safety results prove that the lipid-PLGA NP based nicotine nanovaccines, regardless of hapten density, are of distinguishing safety.

4.4 Conclusion

In this study, lipid-polymeric NP-based nicotine nanovaccines with different hapten density were synthesized and characterized *in vitro* and *in vivo*. The *in vitro* results suggested that all nanovaccine NPs, regardless of hapten density, were taken up by dendritic cells efficiently. Moreover, nanovaccine NPs were internalized by dendritic cells more efficiently compared to the hapten-KLH conjugate particles in terms of internalized antigens. The *in vivo* immunization study in mice indicated that the nanovaccine resulted in a 570% higher antibody titer than the Nic-KLH conjugate vaccine at a similar hapten density. Furthermore, the medium- and high-density nanovaccines exhibited significantly higher immunogenicity compared to the low-density nanovaccine. In addition, although no significant differences in antibody titers were detected between the high- and medium-density nanovaccines, the high-density nanovaccine resulted in

more responders of high antibody titers (>15000). The pharmacokinetic study in mice suggested that the high hapten density nanovaccine had the best efficacy in blocking nicotine from entering the brain. The histopathological study showed that none of the different hapten density nanovaccines caused any apparent toxic effects to mouse organs. All these findings suggest that the immunogenicity of the lipid-polymeric NP based nicotine nanovaccines can be enhanced by modulating hapten density, and therefore providing a promising next-generation immunotherapeutic strategy to treating nicotine addiction.

Acknowledgement

This work was financially supported by National Institute on Drug Abuse (U01DA036850). We thank Ms. Kathy Lowe for her assistance on TEM imaging of NPs. We thank Dr. Tanya LeRoith for providing help on histopathological analysis.

References

[1] N.L. Benowitz, Nicotine addiction, New Engl. J. Med. 362 (2010) 2295-2303.

[2] J.W. Lockner, J.M. Lively, K.C. Collins, J.C.M. Vendruscolo, M.R. Azar, K.D. Janda, A conjugate vaccine using enantiopure hapten imparts superior nicotine-binding capacity, J. Med. Chem. 58 (2015) 1005-1011.

[3] D.E. McCarthy, T.M. Piasecki, D.L. Lawrence, D.E. Jorenby, S. Shiffman, M.C. Fiore, T.B. Baker, A randomized controlled clinical trial of bupropion SR and individual smoking cessation counseling, Nicotine Tob. Res. 10 (2008) 717-729.

[4] J.A. Stapleton, L. Watson, L.I. Spirling, R. Smith, A. Milbrandt, M. Ratcliffe, G. Sutherland, Varenicline in the routine treatment of tobacco dependence: a pre-post comparison with nicotine replacement therapy and an evaluation in those with mental illness, Addiction 103 (2008) 146-154.

[5] M.J. Carpenter, B.F. Jardin, J.L. Burris, A.R. Mathew, R.A. Schnoll, N.A. Rigotti, K.M. Cummings, Clinical strategies to enhance the efficacy of nicotine replacement therapy for smoking cessation: a review of the literature, Drugs 73 (2013) 407-426.

[6] T. Raupach, P.H. Hoogsteder, C.P. Onno van Schayck, Nicotine vaccines to assist with smoking cessation: current status of research, Drugs 72 (2012) e1-16.

[7] X.Y. Shen, F.M. Orson, T.R. Kosten, Vaccines against drug abuse, Clin. Pharmacol. Ther. 91 (2012) 60-70.

[8] D.C. Pryde, L.H. Jones, D.P. Gervais, D.R. Stead, D.C. Blakemore, M.D. Selby, A.D. Brown, J.W. Coe, M. Badland, D.M. Beal, R. Glen, Y. Wharton, G.J. Miller, P. White, N.L. Zhang, M. Benoit, K. Robertson, J.R. Merson, H.L. Davis, M.J. McCluskie, Selection of a novel anti-nicotine vaccine: influence of antigen design on antibody function in mice, Plos One 8 (2013).

[9] Y. Hieda, D.E. Keyler, J.T. VandeVoort, J.K. Kane, C.A. Ross, D.E. Raphael, R.S. Niedbalas, P.R. Pentel, Active immunization alters the plasma nicotine concentration in rats, J. Pharmacol. Exp. Ther. 283 (1997) 1076-1081.

[10] K.D. Miller, R. Roque, C.H. Clegg, Novel anti-nicotine vaccine using a trimeric coiled-coil hapten carrier, Plos One 9 (2014).

[11] M. Pravetoni, D.E. Keyler, M.D. Raleigh, A.C. Harris, M.G. LeSage, C.K. Mattson, S. Pettersson, P.R. Pentel, Vaccination against nicotine alters the distribution of nicotine delivered via cigarette smoke inhalation to rats, Biochem. Pharmacol. 81 (2011) 1164-1170.

[12] M. De Biasi, I. McLaughlin, E.E. Perez, P.A. Crooks, L.P. Dwoskin, M.T. Bardo, P.R. Pentel, D. Hatsukami, Scientific overview: 2013 BBC plenary symposium on tobacco addiction, Drug Alcohol. Depen. 141 (2014) 107-117.

[13] D.K. Hatsukami, D.E. Jorenby, D. Gonzales, N.A. Rigotti, E.D. Glover, C.A. Oncken, D.P. Tashkin, V.I. Reus, R.C. Akhavain, R.E.F. Fahim, P.D. Kessler, M. Niknian, M.W. Kalnik, S.I. Rennard, Immunogenicity and smoking-cessation outcomes for a novel nicotine immunotherapeutic, Clin. Pharmacol. Ther. 89 (2011) 392-399.

[14] J. Cornuz, S. Zwahlen, W.F. Jungi, J. Osterwalder, K. Klingler, G. van Melle, Y. Bangala, I. Guessous, P. Muller, J. Willers, P. Maurer, M.F. Bachmann, T. Cerny, A vaccine against nicotine for smoking cessation: a randomized controlled trial, Plos One 3 (2008).

[15] K. Saylor, C.M. Zhang, A simple physiologically based pharmacokinetic model evaluating the effect of anti-nicotine antibodies on nicotine disposition in the brains of rats and humans, Toxicol. Appl. Pharm. 307 (2016) 150-164.

[16] M.M. Meijler, M. Matsushita, L.J. Altobelli, P. Wirsching, K.D. Janda, A new strategy for improved nicotine vaccines using conformationally constrained haptens, J. Am. Chem. Soc. 125 (2003) 7164-7165.

[17] S.H.L. de Villiers, N. Lindblom, G. Kalayanov, S. Gordon, I. Baraznenok, A. Malmerfelt, M.M. Marcus, A.M. Johansson, T.H. Svensson, Nicotine hapten structure, antibody selectivity and effect relationships: Results from a nicotine vaccine screening procedure, Vaccine 28 (2010) 2161-2168.

[18] J.W. Lockner, S.O. Ho, K.C. McCague, S.M. Chiang, T.Q. Do, G. Fujii, K.D. Janda, Enhancing nicotine vaccine immunogenicity with liposomes, Bioorg. Med. Chem. Lett. 23 (2013) 975-978.

[19] K.E. Cornish, S.H.L. de Villiers, M. Pravetoni, P.R. Pentel, Immunogenicity of individual vaccine components in a bivalent nicotine vaccine differ according to vaccine Formulation and administration conditions, Plos One 8 (2013).

[20] S.H.L. de Villiers, K.E. Cornish, A.J. Troska, M. Pravetoni, P.R. Pentel, Increased efficacy of a trivalent nicotine vaccine compared to a dose-matched monovalent vaccine when formulated with alum, Vaccine 31 (2013) 6185-6193.

[21] D.E. Keyler, S.A. Roiko, C.A. Earley, M.P. Murtaugh, P.R. Pentel, Enhanced immunogenicity of a bivalent nicotine vaccine, Int. Immunopharmacol. 8 (2008) 1589-94.

[22] M. Pravetoni, D.E. Keyler, R.R. Pidaparthi, F.I. Carroll, S.P. Runyon, M.P. Murtaugh, C.A. Earley, P.R. Pentel, Structurally distinct nicotine immunogens elicit antibodies with non-overlapping specificities, Biochem. Pharmacol. 83 (2012) 543-550.

[23] X.Y. Chen, M. Pravetoni, B. Bhayana, P.R. Pentel, M.X. Wu, High immunogenicity of nicotine vaccines obtained by intradermal delivery with safe adjuvants, Vaccine 31 (2012) 159-164.

[24] T. Storni, T.M. Kundig, G. Senti, P. Johansen, Immunity in response to particulate antigen-delivery systems, Adv. Drug. Deliver. Rev. 57 (2005) 333-355.

[25] N. Benne, J. van Duijn, J. Kuiper, W. Jiskoot, B. Slutter, Orchestrating immune responses: How size, shape and rigidity affect the immunogenicity of particulate vaccines, J. Control. Release 234 (2016) 124-134.

[26] P.R. Pentel, M.G. LeSage, New Directions in Nicotine Vaccine Design and Use, Adv. Pharmacol. 69 (2014) 553-580.

[27] S. Thangavel, T. Yoshitomi, M.K. Sakharkar, Y. Nagasaki, Redox nanoparticle increases the chemotherapeutic efficiency of pioglitazone and suppresses its toxic side effects, Biomaterials 99 (2016) 109-123.

[28] J. Liu, T. Wei, J. Zhao, Y.Y. Huang, H. Deng, A. Kumar, C.X. Wang, Z.C. Liang, X.W. Ma, X.J. Liang, Multifunctional aptamer-based nanoparticles for targeted drug delivery to circumvent cancer resistance, Biomaterials 91 (2016) 44-56.

[29] J.H. Yeom, B. Lee, D. Kim, J.K. Lee, S. Kim, J. Bae, Y. Park, K. Lee, Gold nanoparticle-DNA aptamer conjugate-assisted delivery of antimicrobial peptide effectively eliminates intracellular Salmonella enterica serovar Typhimurium, Biomaterials 104 (2016) 43-51.

[30] R.A. Rosalia, L.J. Cruz, S. van Duikeren, A.T. Tromp, A.L. Silva, W. Jiskoot, T. de Gruijl, C. Lowik, J. Oostendorp, S.H. van der Burg, F. Ossendorp, CD40-targeted dendritic cell delivery of PLGA-nanoparticle vaccines induce potent anti-tumor responses, Biomaterials 40 (2015) 88-97.

[31] Y. Qian, H.L. Jin, S. Qiao, Y.F. Dai, C. Huang, L.S. Lu, Q.M. Luo, Z.H. Zhang, Targeting dendritic cells in lymph node with an antigen peptide-based nanovaccine for cancer immunotherapy, Biomaterials 98 (2016) 171-183.

[32] C. Wang, P. Li, L.L. Liu, H. Pan, H.C. Li, L.T. Cai, Y.F. Ma, Self-adjuvanted nanovaccine for cancer immunotherapy: Role of lysosomal rupture-induced ROS in MHC class I antigen presentation, Biomaterials 79 (2016) 88-100.

[33] S. Rahimian, J.W. Kleinovink, M.F. Fransen, L. Mezzanotte, H. Gold, P. Wisse, H. Overkleeft, M. Amidi, W. Jiskoot, C.W. Lowik, F. Ossendorp, W.E. Hennink, Near-infrared labeled, ovalbumin loaded polymeric nanoparticles based on a hydrophilic polyester as model vaccine: In vivo tracking and evaluation of antigen-specific CD8+ T cell immune response, Biomaterials 37 (2015) 469-477.

[34] Y. Hu, M. Ehrich, K. Fuhrman, C.M. Zhang, In vitro performance of lipid-PLGA hybrid nanoparticles as an antigen delivery system: lipid composition matters, Nanoscale Res. Lett. 9 (2014).

[35] H. Zheng, Y. Hu, W. Huang, S. de Villiers, P. Pentel, J.F. Zhang, H. Dorn, M. Ehrich, C.M. Zhang, Negatively charged carbon nanohorn supported cationic liposome nanoparticles: a novel delivery vehicle for anti-nicotine vaccine, J. Biomed. Nanotechnol. 11 (2015) 2197-2210.

[36] J.R. Harris, J. Markl, Keyhole limpet hemocyanin (KLH): a biomedical review, Micron 30 (1999) 597-623.

[37] M.J. McCluskie, J. Thorn, P.R. Mehelic, P. Kolhe, K. Bhattacharya, J.I. Finneman, D.R. Stead, M.B. Piatchek, N.L. Zhang, G. Chikh, J. Cartier, D.M. Evans, J.R. Merson, H.L. Davis, Molecular attributes of conjugate antigen influence function of antibodies induced by anti-nicotine vaccine in mice and non-human primates, Int. Immunopharmacol. 25 (2015) 518-527.

[38] K.C. Collins, K.D. Janda, Investigating hapten clustering as a strategy to enhance vaccines against drugs of abuse, Bioconjugate Chem. 25 (2014) 593-600.

[39] C. Foged, B. Brodin, S. Frokjaer, A. Sundblad, Particle size and surface charge affect particle uptake by human dendritic cells in an in vitro model, Int. J. Pharm. 298 (2005) 315-322.

[40] M.F. Bachmann, G.T. Jennings, Vaccine delivery: A matter of size, geometry, kinetics and molecular patterns, Nat. Rev. Immunol. 10 (2010) 787-796.

[41] S.T. Reddy, A.J. van der Vlies, E. Simeoni, V. Angeli, G.J. Randolph, C.P. O'Neill, L.K. Lee, M.A. Swartz, J.A. Hubbell, Exploiting lymphatic transport and complement activation in nanoparticle vaccines, Nat. Biotechnol. 25 (2007) 1159-1164.

[42] C. Oussoren, J. Zuidema, D.J. Crommelin, G. Storm, Lymphatic uptake and biodistribution of liposomes after subcutaneous injection. II. Influence of liposomal size, lipid compostion and lipid dose, Biochim. Biophys. Acta 1328 (1997) 261-72.

[43] J. Banchereau, R.M. Steinman, Dendritic cells and the control of immunity, Nature 392 (1998) 245-252.

[44] P. Maurer, G.T. Jennings, J. Willers, F. Rohner, Y. Lindman, K. Roubicek, W.A. Renner, P. Muller, M.F. Bachmann, Frontline: A therapeutic vaccine for nicotine dependence: preclinical efficacy, and phase I safety and immunogenicity, Eur. J. Immunol. 35 (2005) 2031-2040.

[45] X.W. Liu, Y. Xu, T. Yu, C. Clifford, Y. Liu, H. Yan, Y. Chang, A DNA nanostructure platform for directed assembly of synthetic vaccines, Nano Lett. 12 (2012) 4254-4259.

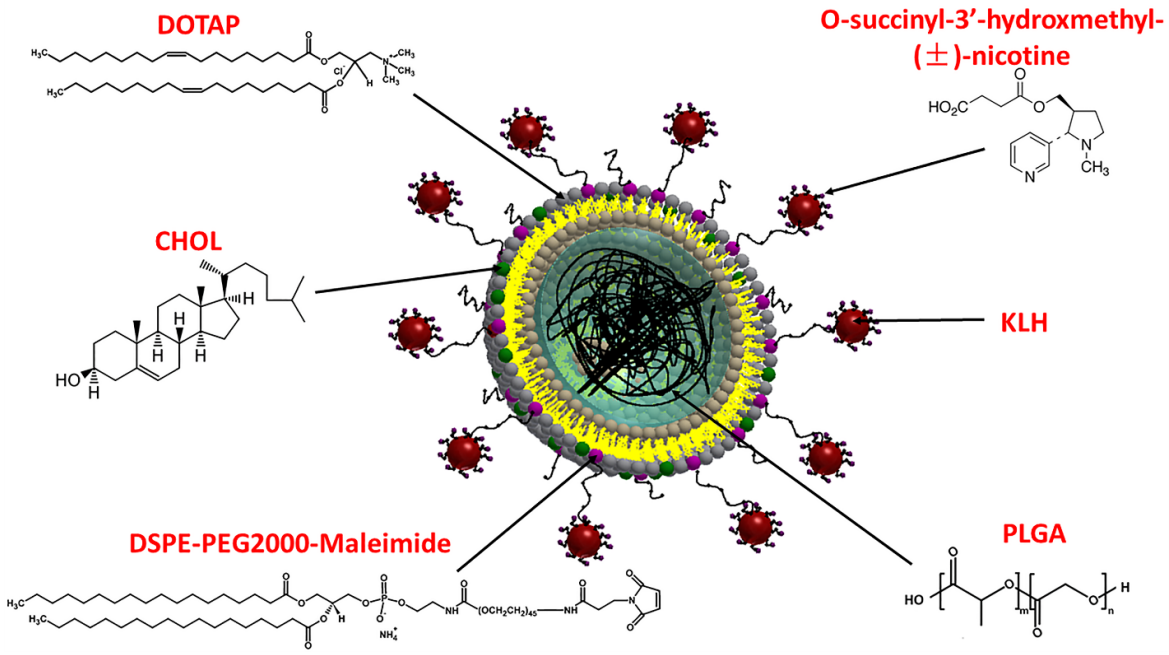

Scheme. 1 Schematic illustration of the structure of hybrid NP-based nicotine nanovaccine NPs.

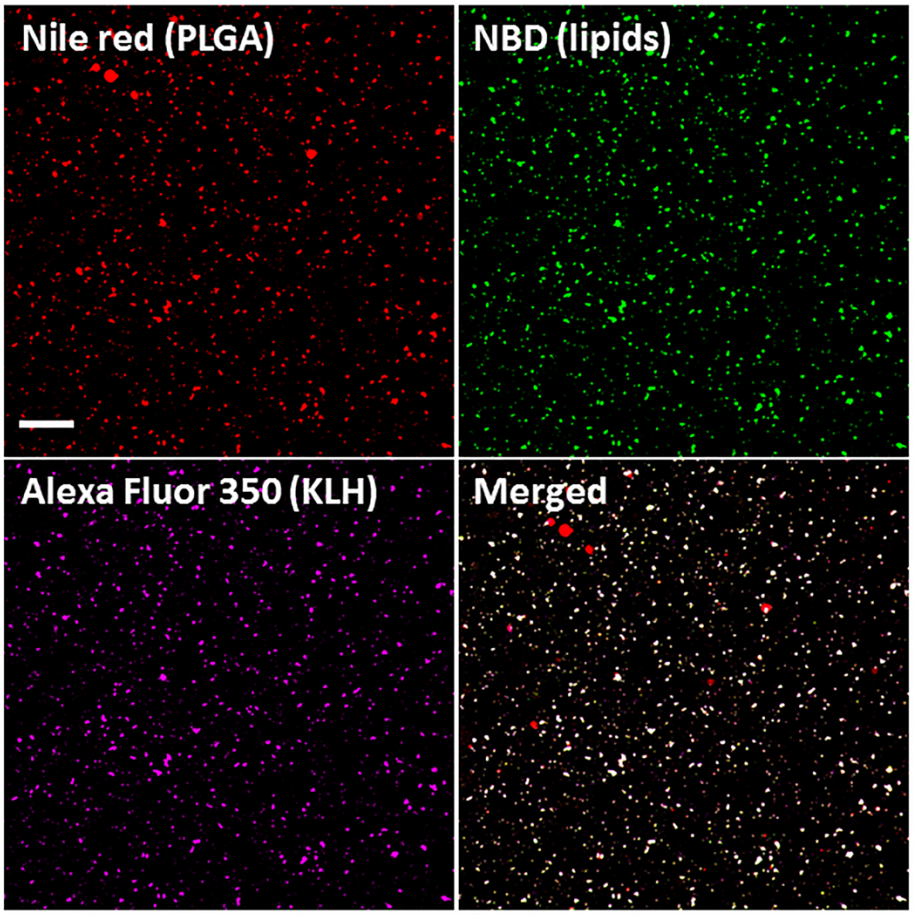

Figure 1. Validation of the successful assembly of nanovaccine NPs by CLSM. The PLGA and lipid layer were labeled by Nile red and NBD, respectively, and AF350 was used as a model of Nic hapten attached on KLH. The scale bar represents 10 μm.

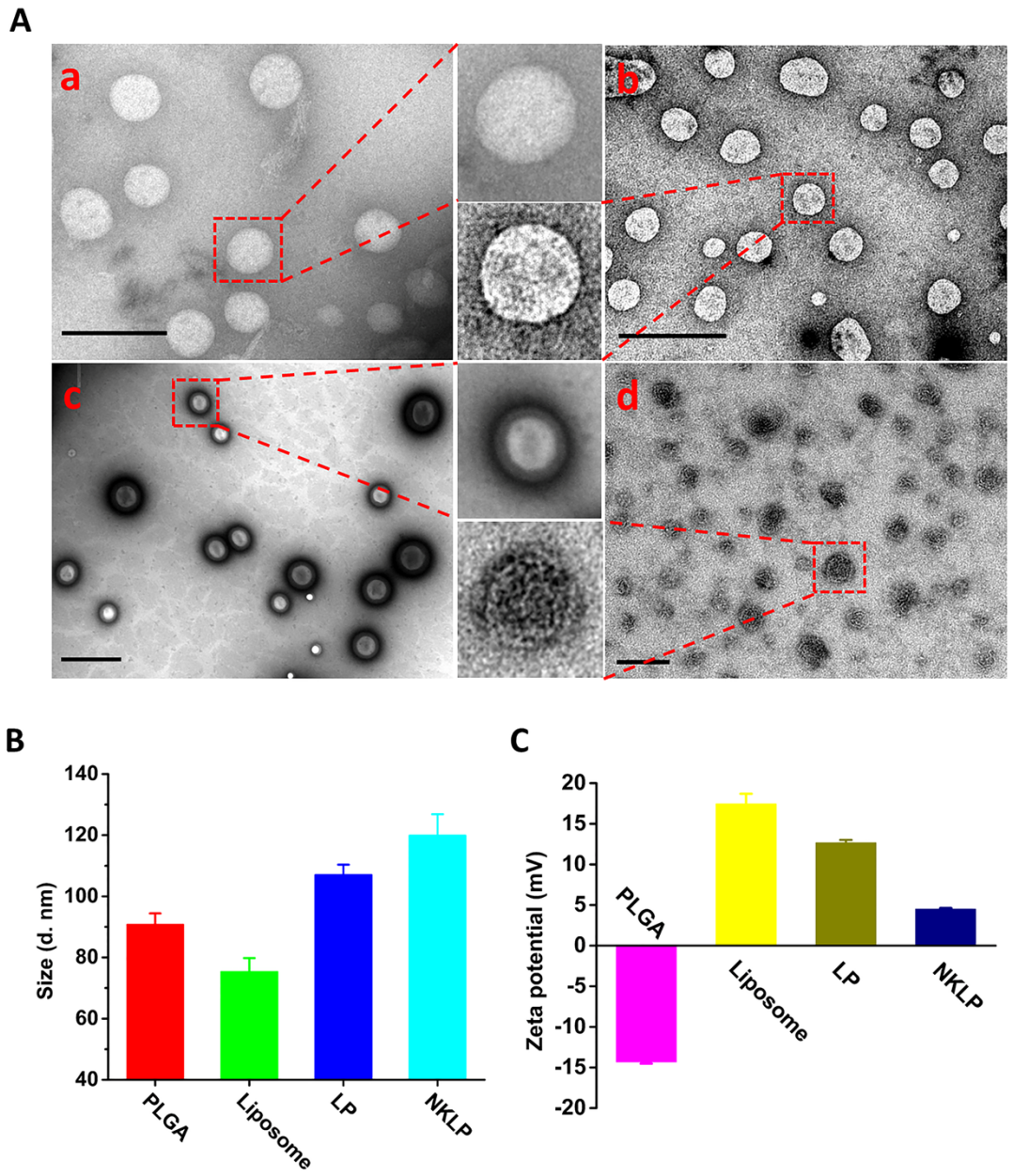

Figure 2. Morphological and physicochemical properties of NPs involved in the preparation of nanovaccine NPs. (A) TEM images of (a) PLGA NPs; (b) liposome NPs; (c) lipid-PLGA hybrid NPs; and (d) nanovaccine NPs. Scale bars in all the TEM images represent 200 nm. (B) Average size of NPs. (C) Zeta potential of NPs.

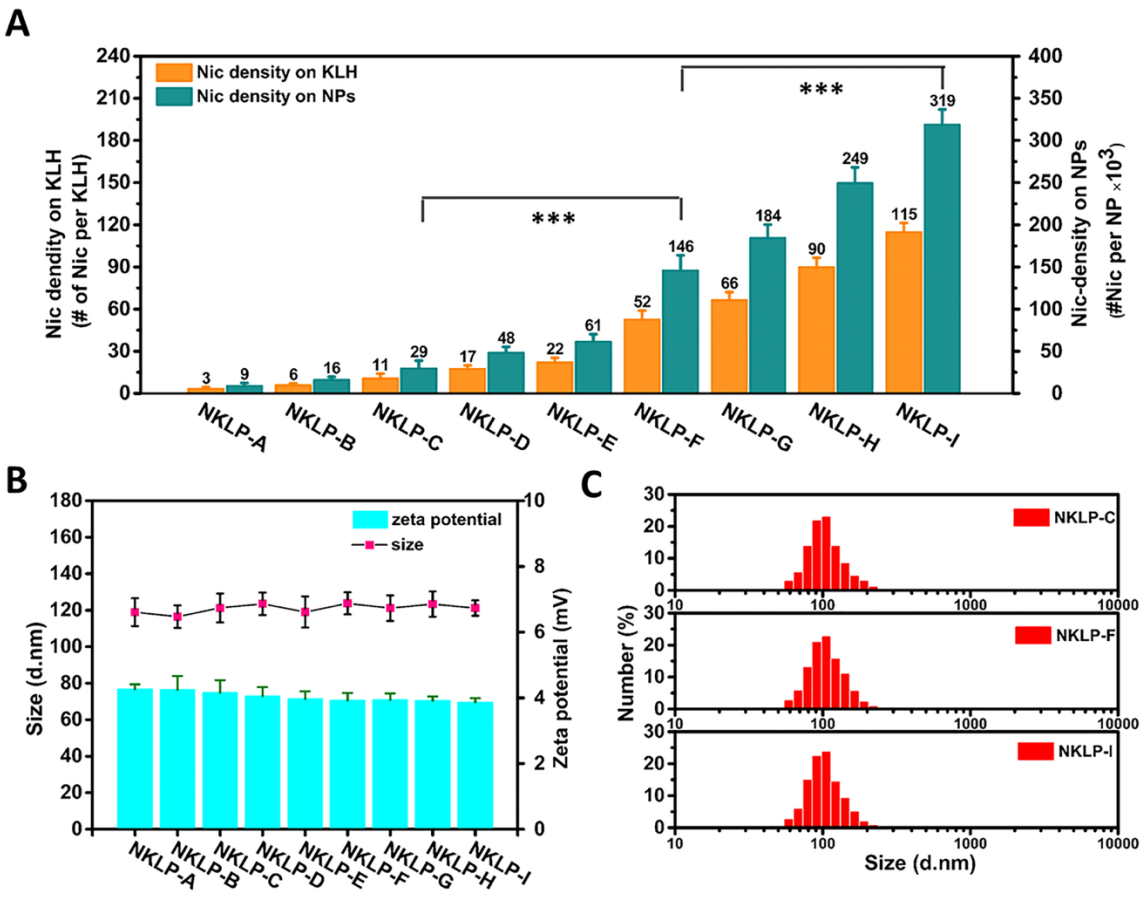

Figure 3. Characterization of the hapten density and physicochemical properties of different hapten density nanovaccine NPs. (A) Hapten density of different nanovaccines, which were prepared using various molar ratios of Nic-hapten to KLH. *** indicates hapten density on NPs are significantly different (p-value < 0.001). (B) Average diameter and zeta potential of various NPs. No significant differences in average size detected for all the nanovaccine NPs with different hapten density. (C) Size distribution of three representative nanovaccine NPs used for immunization of mice. NKLP-A, B, C, D, E, F, G, H, I represent nanovaccines which were prepared using increased Nic/KLH molar ratios.

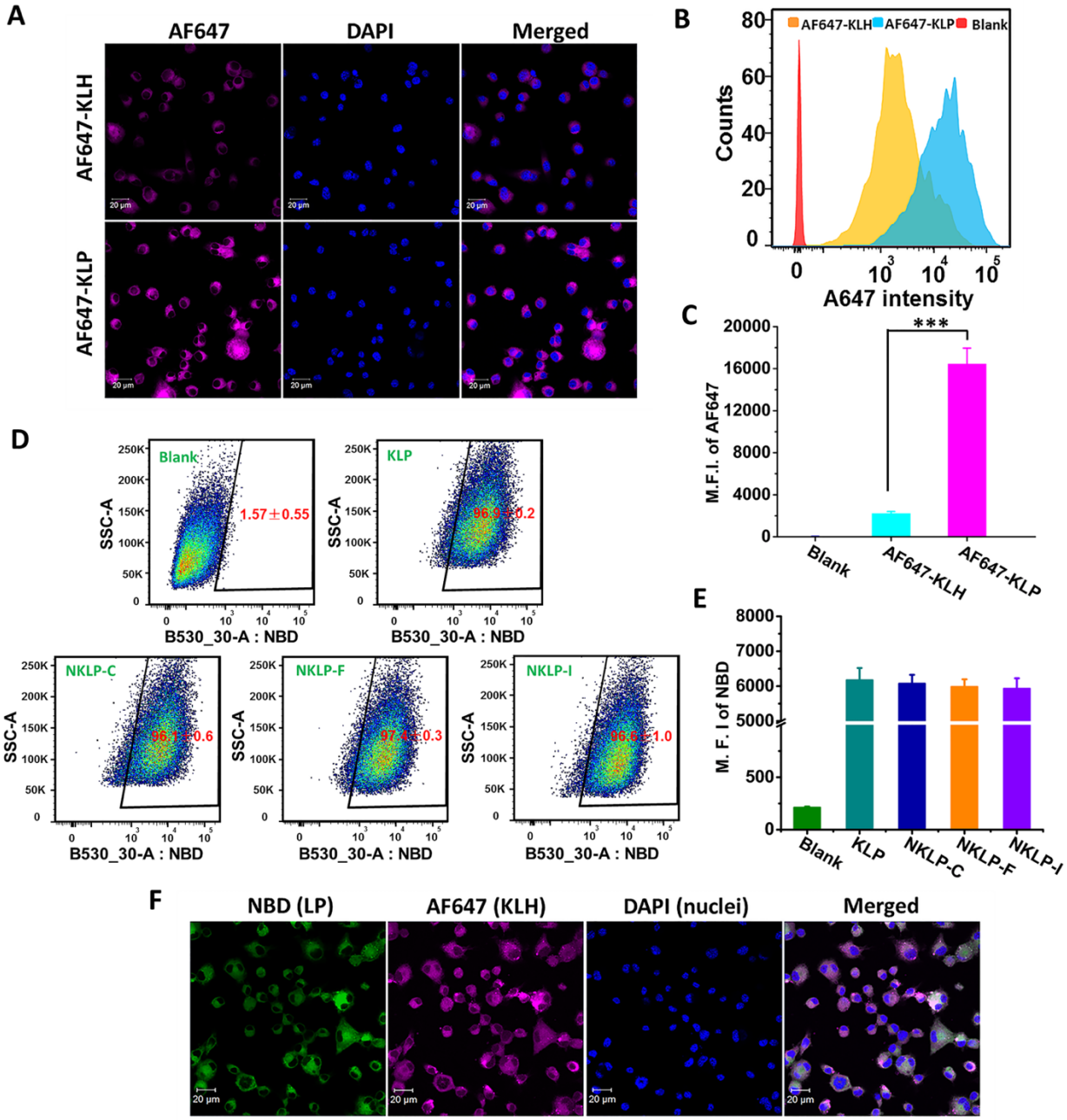

Figure 4. Cellular uptake of the lipid-PLGA NP based nanovaccine and conjugate vaccine particles by dendritic cells. (A) CLSM images showing the uptake of nanovaccine and conjugate vaccine particles. (B) Representative intensity distribution of AF647 fluorescence in dendritic cells. (C) Mean fluorescence intensity (M.F.I) of AF647 in cells corresponding to (B). *** indicates that

AF647 fluorescence intensity was significantly higher in AF647-KLP group than in AF647-KLH group ($p<0.001$). For particles used in (A-C), AF647 was conjugated to KLH as a model of Nic-hapten. For (A-C), Cells were treated with nanovaccine or conjugate vaccine particles containing equal amounts of KLH for 2 h. (D) Recorded events which indicated that most of the studied cells (>95%) had taken up NPs of KLP, NKLP-C, NKLP-F, and NKLP-I, after 2 hours' incubation. The percentages of positive cells were shown in red figures. (E) M.F.I of AF647 in cells after internalizing NPs for 2 h. NPs used in (D) and (E) were labeled by adding NBD to the lipid layer, and cells were treated with equal amounts of different hapten density nanovaccine NPs. (F) CLSM images of cells treated with fluorescent nanovaccine NPs for 2 h, in which the lipid layer was labeled by NBD and AF647 was used as a model of Nic hapten.

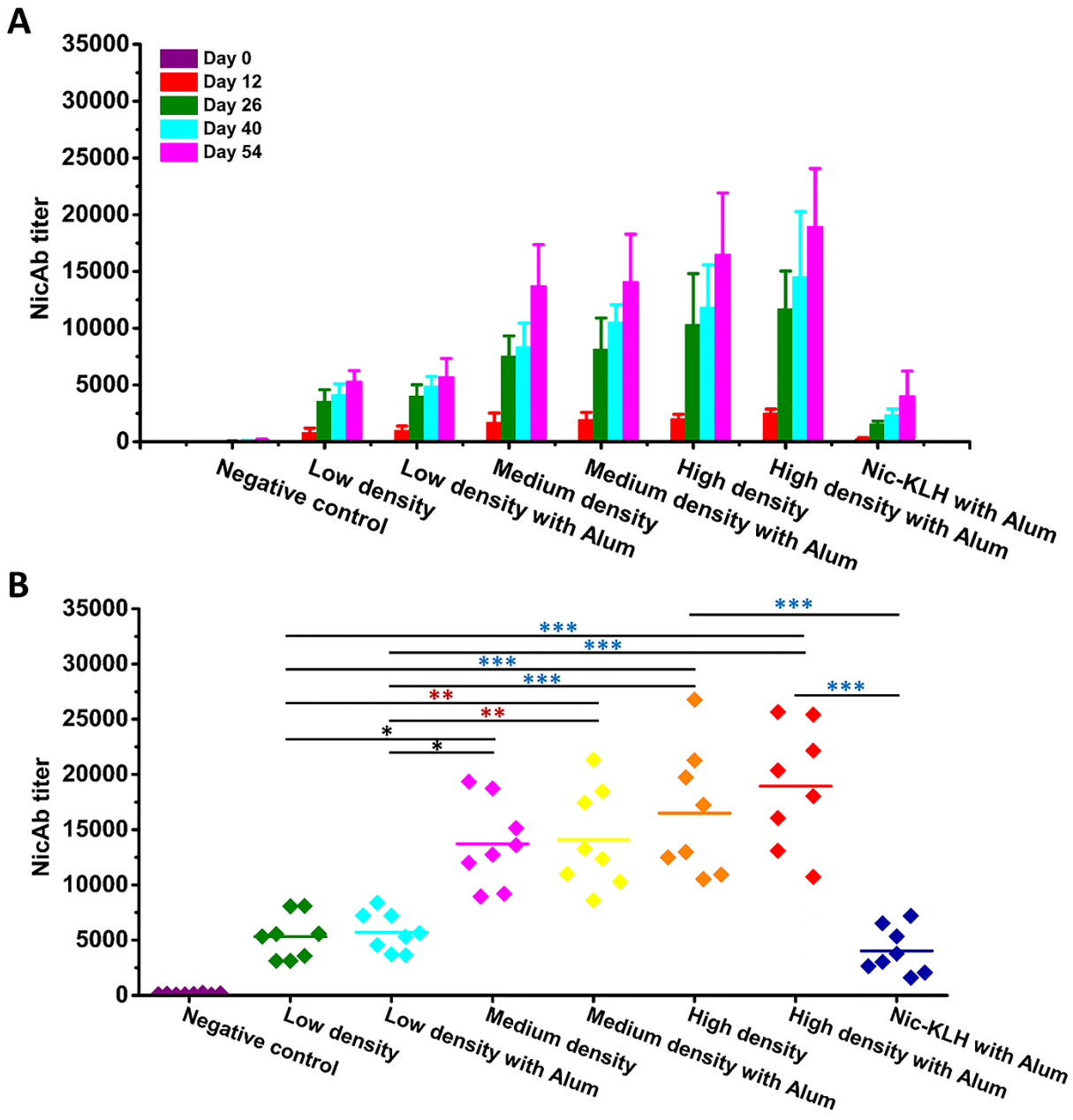

Figure 5. Immunogenicity of nicotine vaccines in mice. (A) Time-course of nicotine-specific antibody (NicAb) titers in response to the Nic-KLH conjugate vaccine and hybrid NP-based nanovaccines. (B) Statistical comparison of the NicAb titers on Day 54. Each diamond represents NicAb titer of each mouse, and the colorful straight lines show the average NicAb titer of each group. Significantly different: * $p<0.05$, ** $p<0.01$, *** $p<0.001$.

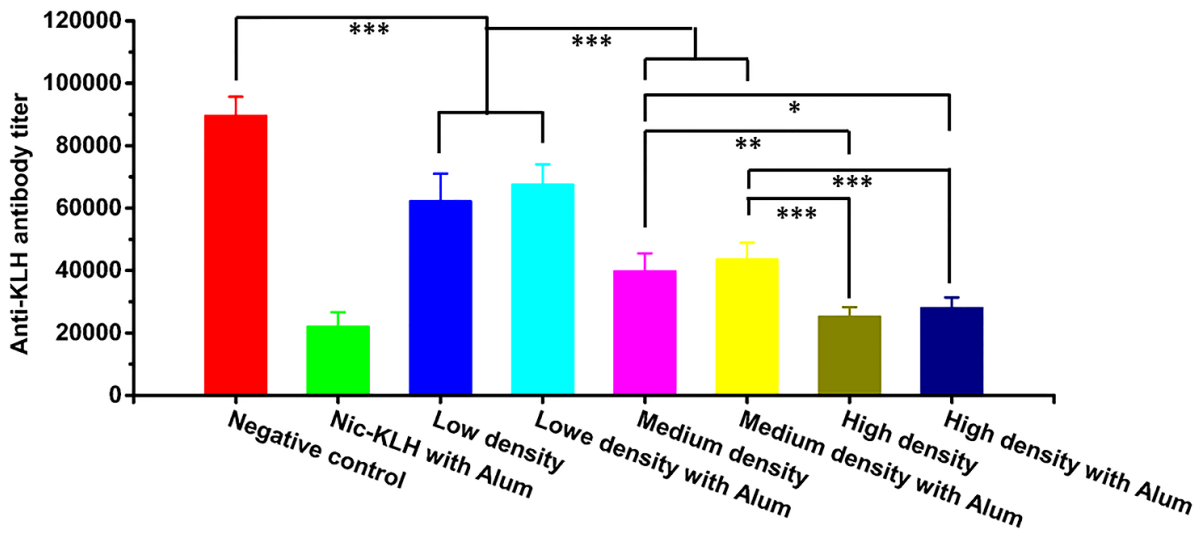

Figure 6. Anti-carrier protein (anti-KLH) antibody titers induced by nicotine vaccines on Day 54. Significantly different: * $p<0.05$, ** $p<0.01$, *** $p<0.001$.

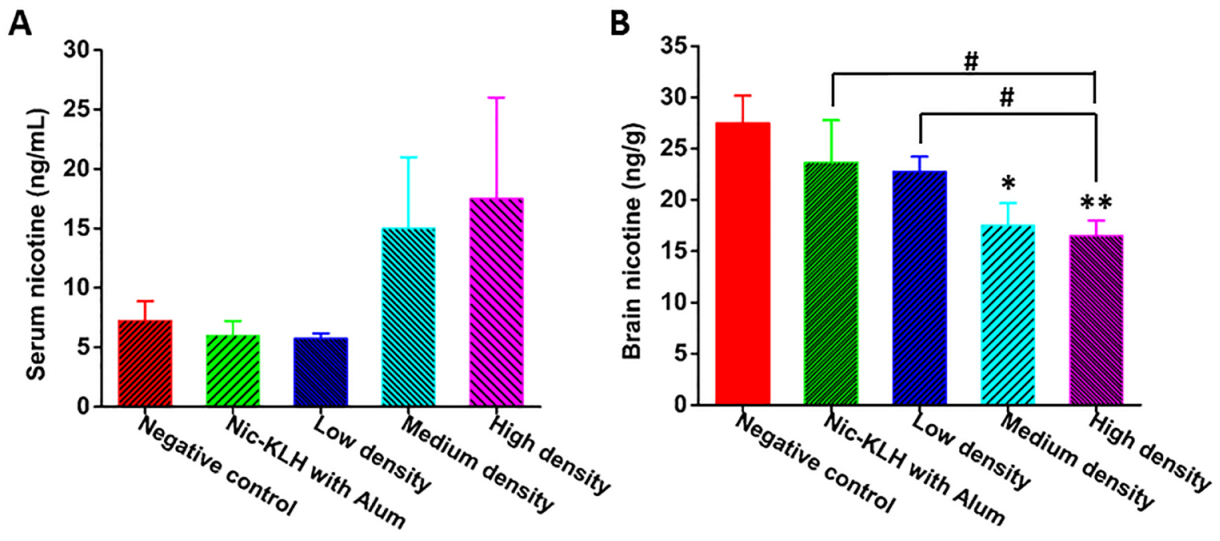

Figure 7. Nicotine distribution in the (A) serum and (B) brain of immunized mice. Serum and brain tissues of mice were collected 4 min after administration of 0.03 mg/kg nicotine subcutaneously on Day 54, and nicotine contents in tissues were analyzed. * and ** indicate significant differences compared to the negative control group, * $p<0.05$, ** $P<0.01$; # $P<0.05$.

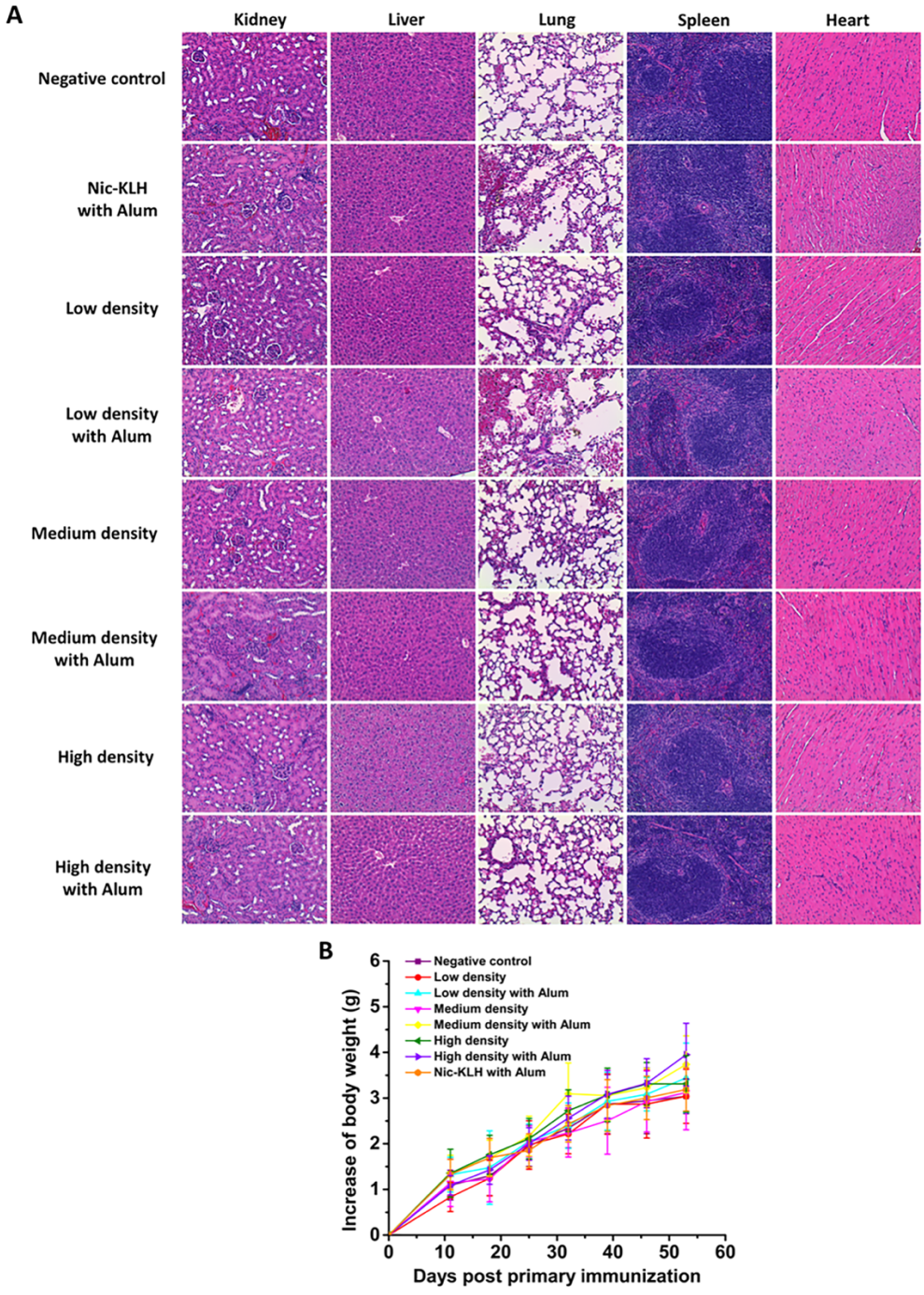

Figure 8. Assessment of the safety of nicotine vaccines. (A) Representative micrographs of mouse tissues after administration of the negative control or nicotine vaccines. No lesions were observed in mouse organs of all the representative groups. (B) The increase of body weight during the immunization study.

Table 1. Physicochemical properties and hapten density of nanovaccine NPs.

NPs	Size (d. nm)	Zeta potential (mv)	PDI	Nic-KLH association efficiency (%)	Hapten density (#×10^3/NP)
NKLP-C (low-density)	121.3±7.9	4.16±0.14	0.22±0.02	86.4±0.97	29.4±9.2
NKLP-F (medium-density)	123.8±6.1	3.92±0.23	0.24±0.03	87.9±1.02	145.6±18.1
NKLP-I (high-density)	121.2±4.2	3.86±0.12	0.21+0.02	86.7±0.45	318.6±18.2

Chapter 5: Rationalization of a nanoparticle-based nicotine nanovaccine as an effective next-generation nicotine vaccine: a focus on hapten localization

Zongmin Zhao[1], Yun Hu[1], Theresa Harmon[2], Paul Pentel[2], Marion Ehrich[3], Chenming Zhang[1,*]

1. Department of Biological Systems Engineering, Virginia Tech, Blacksburg, VA 24061, USA

2. Minneapolis Medical Research Foundation, Minneapolis, MN 55404, USA

3. Department of Biomedical Sciences and Pathobiology, Virginia Tech, Blacksburg, VA 24061, USA

* Correspondence to: Chenming (Mike) Zhang.

Address: 210 Seitz Hall, Department of Biological Systems Engineering, Virginia Tech, Blacksburg, VA 24061, USA.

Voice: +1-(540)231-7601

Fax: +1-(540)231-3199

Email: chzhang2@vt.edu

This manuscript has been published on *Biomaterials* 2017, 138: 46-56. Reprinted with permission from the publisher.

Abstract

A lipid-polymeric hybrid nanoparticle-based next-generation nicotine nanovaccine was developed in this study to combat nicotine addiction. A series of nanovaccines, which had nicotine-haptens localized on carrier protein (LPKN), nanoparticle surface (LPNK), or both (LPNKN), were designed to study the impact of hapten localization on their immunological efficacy. All three nanovaccines were efficiently taken up and processed by dendritic cells. LPNKN induced a significantly higher immunogenicity against nicotine and a significantly lower anti-carrier protein antibody level compared to LPKN and LPNK. Meanwhile, the anti-nicotine antibodies elicited by LPKN and LPNKN bound nicotine stronger than those elicited by LPNK. LPNK and LPNKN resulted in a more balanced Th1-Th2 immunity than LPKN. Moreover, LPNKN exhibited the best ability to block nicotine from entering the brain of mice. Collectively, the results demonstrated that the immunological efficacy of the hybrid nanoparticle-based nicotine vaccine could be enhanced by modulating hapten localization, providing a promising strategy to combatting nicotine addiction.

Key words

Nicotine vaccine; lipid-polymeric hybrid nanoparticle; anti-nicotine antibody; hapten localization; smoking cessation.

5.1 Introduction

Tobacco smoking is one of the most significant public health threats the world has ever faced; approximately, 6 millions of premature deaths are attributed to tobacco use each year in the world.[1-3] Despite strong desires to quit smoking, the majority of unassisted smokers usually relapse within the first month, and only 3-5% of them remain abstinent after 6 months.[4] Even with the help of pharmacological interventions, including nicotine replacement therapy, varenicline, and bupropion, the long-term smoking cessation rate at one year is disappointingly low (10-25%).[5-8]

Nicotine vaccine has been demonstrated to be an attractive approach for smoking cessation.[9, 10] Promisingly, some conjugate nicotine vaccines were successful in inducing strong immunogenicity as well as achieving high pharmacokinetic efficacy in preclinical and early-stage clinical trials.[11-14] However, so far, none of them have increased overall enhanced smoking cessation rate over placebo, mainly due to insufficient and highly-variable antibody titers.[15-17] Although great efforts have been made to improve their immunogenicity by modulating multiple factors,[13, 18-23] conjugate nicotine vaccines bear some intrinsic shortfalls, such as rapid degradation, low nicotine loading capacity, low bioavailability, and poor recognition and uptake by immune cells. These largely limit their immunological efficacy.

To circumvent these disadvantages of conjugate nicotine vaccines, in our previous work, we designed the next-generation nicotine nanovaccines using nanoparticles (NPs) as delivery vehicles for antigen presentation.[24-26] Particularly, lipid-polymeric hybrid nanoparticle (NP)-based nicotine nanovaccines were demonstrated to induce significantly higher immunogenicity over the conjugate vaccines and result in better pharmacokinetic efficacy in mice.[26, 27]

Nicotine hapten is such a small molecule that can only elicit an immune response when attached to a carrier, such as proteins or nanoparticles.[9] In addition, a stimulating protein is always a necessity in NP-based nicotine vaccine, as it will stimulate the T-helper cell formation that is required for B cell maturation.[9, 28] Meanwhile, conjugating protein antigen to the surface of NPs could promote its delivery and presentation.[29, 30] In our previous nanovaccine design, hapten was conjugated to the surface of protein antigens.[26] As the localization of haptens on vaccine NPs may potentially affect the recognition of antigens by immune cells, in this current work, we evaluated the design of a hybrid NP-based nicotine vaccine by studying the impact of hapten localization on its immunogenicity and capability to reduce brain nicotine concentrations. As shown in **Scheme 1**, three nanovaccines, which have haptens localized only on the carrier protein (**LPKN**), only on NP surface (**LPNK**), or on both (**LPNKN**), were synthesized. The immunogenicity and ability to reduce brain nicotine levels of nanovaccines were measured in mice.

5.2 Materials and methods

5.2.1 Materials

Lactel® (50:50 poly(lactic-co-glycolic acid) (PLGA)) was purchased from Durect Corporation (Cupertino, CA, USA). Keyhole limpet hemocyanin (KLH) was purchased from Stellar Biotechnologies (Port Hueneme, CA, USA). Alexa Fluor® 647 NHS ester (AF647), Alexa Fluor® 350 NHS ester (AF350), 1-Ethyl-3-[3-dimethylaminopropyl] carbodiimide hydrochloride (EDC), and N-hydroxysulfosuccinimide (Sulfo-NHS) were purchased from Thermo Fisher Scientific (Rockford, IL, USA). 1,2-Dioleoyl-3-trimethylammonium-propane (DOTAP), cholesterol (CHOL), 1,2-diphytanoyl-sn-glycero-3-phosphoethanolamine-N-(7-nitro-2-1,3-benzoxadiazol-4-yl) (ammonium salt) (NBD-PE), 1,2-distearoyl-sn-glycero-3-phosphoethanolamine-N-[maleimide(polyethylene glycol)-2000] (ammonium salt) (DSPE-PEG2000-maleimide), and 1,2-

distearoyl-sn-glycero-3-phosphoethanolamine-N-[amino(polyethylene glycol)-2000] (ammonium salt) (DSPE-PEG2000-amine) were purchased from Avanti Polar Lipids (Alabaster, AL, USA). O-Succinyl-3'-hydroxymethyl-(±)-nicotine (Nic) was purchased from Toronto Research Chemicals (North York, ON, Canada). All other chemicals were of analytical grade.

5.2.2 Fabrication of PLGA NPs by nanoprecipitation

PLGA NPs were fabricated by a nanoprecipitation method.[31] In brief, 20 mg of PLGA was dissolved in 2 mL of acetone. The PLGA-in-acetone organic solution was injected into 10 mL of 0.5% PVA aqueous phase by a vertically mounted syringe pump with magnetic stir agitation (1200 rpm). The resultant suspension was placed under vacuum for 6 hours to eliminate the organic solvent. PLGA NPs were collected by centrifugation at 10,000 *g*, 4°C for 30 min.

5.2.3 Fabrication of lipid-polymeric hybrid NPs

Lipid-polymeric hybrid NPs were fabricated with a previously reported hydration-sonication method.[26, 32] In brief, 2.5 mg of lipid mixture consisting of different molar ratios of DOTAP, DSPE-PEG2000-maleimide, DSPE-PEG2000-amine, and CHOL, was evaporated to form a lipid film. The lipid film was hydrated with 0.01 M phosphate buffer saline (PBS) and sonicated for 2 min to form a liposome suspension. Lipid-polymeric hybrid NPs were assembled by coating liposomes to PLGA NPs (PLGA: lipids= 10:1 (w/w)) via sonication for 10 min. Lipid-polymeric hybrid NPs were collected by centrifugation at 10,000 *g*, 4°C for 30 min. The PLGA cores were labeled by Nile Red, and the number of NPs per mg was estimated by flow cytometry using an Amnis ImageStream^X Mark 2 imaging flow cytometer.

5.2.4 Synthesis of Nic-KLH conjugates

Nic-KLH conjugates were synthesized by an EDC/NHS-mediated reaction as reported previously.[26] Specifically, the Nic-KLH conjugates used for preparing LPKN or LPNKN

nanovaccines were synthesized by reacting 1.2 mg or 2.4 mg of Nic hapten with 5 mg of KLH. Hapten densities of Nic-KLH conjugates were estimated by a 2,4,6-trinitrobenzene sulfonic acid-based method as reported previously.[33] Nic-BSA conjugate was synthesized using the same method.

5.2.5 Preparation of nanovaccine NPs

LPKN nanovaccine NPs were assembled with the method reported previously.[26] In brief, an appropriate amount of Traut's reagent was added into the Nic-KLH conjugates equivalent to 2 mg of KLH in 0.5 mL of PBS and reacted for 1 h to form thiolated Nic-KLH. The thiolated Nic-KLH equivalent to 1 mg of KLH was conjugated to 30 mg of lipid-polymeric hybrid NPs by reacting the thiolated Nic-KLH with maleimide groups in the lipid layer of NPs for 2 h. Unconjugated Nic-KLH was separated by centrifugation at 10,000 *g*, 4°C for 30 min, and quantified by the bicinchoninic acid assay. Negative control was prepared following a similar procedure, except that KLH, instead of Nic-KLH, was conjugated to NP surface.

For LPNK and LPNKN synthesis, Nic-haptens were conjugated to the surfaces of hybrid NPs via an EDC/NHS-mediated reaction. In brief, an aliquot of Nic-haptens was activated for 30 min in 0.3 mL of activation buffer (0.1 M MES, 0.5 M NaCl, pH 6.0) by adding EDC and NHS (Nic: EDC: NHS=1:10:10). Nic-hapten-conjugated hybrid NPs (LPN) were synthesized by reacting the activated Nic-haptens with 30 mg of hybrid NPs in 2 mL of coupling buffer (0.1 M sodium phosphate, 0.15 M NaCl, pH 7.2) for 10 h. Unconjugated Nic-haptens were eliminated by dialysis and quantified by HPLC using a Luna C18 (2) reverse phased chromatography column and a UV detector (at 254 nm). LPNK and LPNKN NPs were assembled by conjugating KLH or Nic-KLH to LPN NPs with the same method as LPKN nanovaccine. Nanovaccine NPs were collected by centrifugation at 10,000 *g*, 4°C for 30 min, and stored at 2°C for later use.

5.2.6 Characterization of NPs

Size distribution and zeta potential of NPs were measured in 0.01 M pH 7.4 PBS on a Nano ZS Zetasizer (Malvern Instruments, Worcestershire, United Kingdom) at 25°C. The morphology of NPs was characterized by transmission electron microscopy (TEM) on a JEM 1400 transmission electron microscope (JEOL, Tokyo, Japan). Fluorescent nanovaccine NPs, in which the lipid layer was labeled by NBD, and AF647 and AF350 were conjugated to KLH and NP surface, respectively, were imaged on a Zeiss LSM 510 laser scanning microscope (Carl Zeiss, Oberkochen, Germany). The Fourier transform infrared (FT-IR) spectra of NPs were recorded on a Thermo Nicolet 6700 FT-IR spectrometer (Thermo Fisher Scientific, Waltham, MA).

5.2.7 Cellular uptake of nanovaccine NPs in dendritic cells (DCs)

The uptake of nanovaccine NPs by DCs was studied by flow cytometry (FCA). NBD-labelled LPKN, LPNK, and LPNKN NPs were prepared by adding 2.5% of NBD into lipid mixture. JAWSII (ATCC® CRL-11904™) immature DCs (2×10^6/well) were seeded into 24-well plates and cultured overnight. Cells were treated with 20 μg of NBD-labelled nanovaccine NPs for 15 min or 2 h. After washed 3 times with PBS, cells were detached from the culture plates using trypsin/EDTA solution and collected by centrifugation at 200 *g* for 10 min. Cell pellets were re-suspended in PBS. Samples were immediately analyzed on a flow cytometer (FACSAria I, BD Biosciences, Franklin Lakes, NJ, USA).

The cellular uptake and processing of nanovaccine NPs were analyzed by confocal laser scanning microscopy (CLSM). AF647- and NBD-labeled NPs were prepared according to the method described above, except that AF647-KLH was conjugated to KLH and 2.5% of NBD was added into lipids for labeling. Cells (2×10^5/chamber) were seeded into 2-well chamber slides and cultured overnight. Cells were treated with 20 μg of AF647- and NBD-labeled nanovaccine NPs

for 15 min or 2 h. Cells were then washed using PBS and fixed with freshly prepared 4% (w/v) paraformaldehyde for 10 min. The membrane of cells was permeabilized by adding 0.5 mL of 0.1% (v/v) Triton™ X-100 for 10 min. Cell nuclei were stained by 4',6-diamidino-2-phenylindole (DAPI). The intracellular distribution of NPs was visualized on a Zeiss LSM 510 laser scanning microscope.

5.2.8 Immunization of mice with nicotine nanovaccines

All animal studies were carried out following the National Institutes of Health guidelines for animal care and use. Animal protocols were approved by the Institutional Animal Care and Use Committee at Virginia Tech. Female Balb/c mice (6-7 weeks of age, 16-20 g, 6 per group) were immunized subcutaneously with a total volume of 200 μL of nicotine vaccines containing 25 μg of KLH antigen on days 0, 14, and 28. The subcutaneous injection site was over the shoulder of mice (into the loose skin over the neck). For the negative control group, mice were immunized with KLH associated hybrid NPs without Nic-hapten conjugation containing 25 μg of KLH. For the blank group, mice were injected with 200 μL of sterilized PBS. Blood was collected from the retro-orbital plexus under isoflurane anesthesia on days 0, 12, 26, and 40.

5.2.9 Measurement of titers of anti-nicotine IgG antibody, anti-nicotine IgG subclass antibody, and anti-KLH antibody

Anti-nicotine IgG and IgG-subclass antibody titers were measured by an enzyme-linked immunosorbent assay (ELISA) according to a previously reported method.[25] Anti-KLH antibody titers were measured following a similar protocol, except that KLH was used as a coating material. Antibody titer was defined as the dilution factor at which absorbance at 450 nm declined to half maximal.

5.2.10 Measurement of anti-nicotine antibody affinity

The relative affinity of anti-nicotine antibody induced by nicotine nanovaccines was measured by a competition ELISA method.[34] In brief, serum samples were diluted to achieve absorbance values of around 1.0 at 450 nm. Nicotine was serially diluted from 10^{-2} M to 10^{-7} M. One hundred μL of nicotine solutions were added into Nic-BSA coated plates, and 100 μL of serum samples were subsequently added to plates. The other steps were the same as in measuring anti-nicotine antibody titers. Percent inhibition was calculated at each nicotine concentration and plotted against *log* nicotine concentration. The concentration at which 50% inhibition was achieved (IC_{50}) was extrapolated for each sample.

5.2.11 Nicotine challenge study in mice

The nicotine challenge study was conducted using a method reported previously.[26] In brief, mice were administered 0.06 mg/kg nicotine subcutaneously two weeks after the second booster immunization (on day 42). Brain and serum samples were collected 3 min post nicotine dosing. Nicotine concentration in the brain and serum was measured by GC/MS as reported previously.[35]

5.2.12 Histopathological analysis

Histopathological analysis was conducted to detect lesions of mouse organs caused by the immunization with nicotine vaccines following a method reported previously.[26] On day 42, organs of immunized mice, including heart, kidney, liver, lung, and spleen, were harvested and fixed in 10% buffered formalin. Tissue blocks were stained with hematoxylin and eosin (H&E) according to the method described before[25] and imaged on a Nikon Eclipse E600 light microscope.

5.2.13 Statistical analyses

Data are expressed as means ± standard deviation unless otherwise specified. Comparisons among multiple groups were conducted using one-way ANOVA followed by Tukey's HSD test. Differences were considered significant when the p-values were less than 0.05.

5.3 Results

5.3.1 Verification of Nic-hapten conjugate chemistry

CLSM was employed to verify the Nic-hapten conjugate chemistry. AF350-NHS and AF647-NHS, which have the same reactive groups as the Nic-hapten, were used to simulate the hapten and conjugated to NP surface and KLH, respectively. Hybrid NPs were labeled by NBD. The co-localization of AF647 with NBD suggested the successful conjugation of the model hapten to KLH (the upper panel of **Figure 1A**), and thus verified the conjugate chemistry for LPKN synthesis. On the other hand, the overlapping of AF350, AF647, and NBD indicated the efficient conjugation of the model haptens to NP surface and the successful association of the model hapten-KLH conjugate to NPs (the lower panel of **Figure 1A**), and verified the conjugate chemistry for LPNK and LPNKN synthesis.

FT-IR was used to further validate the conjugate chemistry for nanovaccine synthesis. Specific peaks of both Nic-hapten (636 and 708 cm^{-1}) and KLH (1654 cm^{-1}) are evident in the spectrum of Nic-KLH conjugate (**Figure 1B**), suggesting the efficient conjugation of Nic-hapten to KLH. Similarly, characteristic peaks of Nic-hapten (858 and 949 cm^{-1}) appeared in the spectrum of LPN NPs (**Figure 1C**), revealing the successful attachment of Nic-hapten to NP surface. Finally, the spectra of all three nanovaccines included characteristic peaks of both Nic-hapten and KLH/Nic-KLH (**Figure 1D**), indicating the successful synthesis of nanovaccines.

5.3.2 Characterization of nanovaccine NPs

Nanovaccine NPs were characterized morphologically using TEM (**Figure 2A**). A core-shell structure was clearly shown on hybrid NPs, which was displayed as a bright core and dark shell. All three nanovaccine NPs had similar morphological features. Specifically, multiple black dots that were KLH/Nic-KLH showed on the surface of NPs, again suggesting the successful conjugation of protein antigens to hybrid NP surface. The conjugation efficiency of Nic-KLH/KLH was 82.3 ± 5.4%, 85.3 ± 7.4%, and 80.2 ± 6.7%, for LPKN, LPNK, and LPNKN, respectively (**Table 1**). The Nic-hapten densities of LPKN, LPNK, and LPNKN were (6.32 ± 0.39) $\times 10^4$/NP, (5.89 ± 0.67) $\times 10^4$/NP, and (6.02 ± 0.53) $\times 10^4$/NP, respectively (**Table 1**), suggesting that the three nanovaccines with different hapten localizations had similar overall hapten densities. Moreover, the physicochemical properties of NPs were characterized. The three nanovaccines exhibited a similar average diameter, which was 118.1, 122.8, and 115.7 nm for LPKN, LPNK, and LPNKN nanovaccines, respectively (**Table 1**). Dynamic light scattering data revealed that all three nanovaccines had a similar size distribution, with most particles being smaller than 200 nm (**Figure 2B**). The zeta-potentials were 5.46 ± 0.25, 2.85 ± 0.23, and 4.69 ± 0.24 mV, for LPKN, LPNK, and LPNKN, respectively (**Table 1**), revealing that all three nanovaccines were positively charged at pH 7.4.

The stability of nanovaccines, indicated by size change, was tested in PBS and DI water for 7 weeks, a period of time that is sufficient for the entire vaccination regimen and a short period of storage. The size change of all three nanovaccines was less than 20 nm in PBS over the entire study period (**Figure 2C**), suggesting the nanovaccines were highly stable in PBS for at least 7 weeks. The nanovaccines appeared to be less stable in water. However, the size change of nanovaccines was still less than 30 nm for 7 weeks in DI water (**Figure 2D**).

5.3.3 Cellular uptake of nanovaccine NPs

The cellular uptake of nanovaccine NPs was studied in DCs by FCA. The uptake of nanovaccines displayed a time-dependent manner. After 15 min's incubation, except for LPKN, only small portions of cells had taken up NPs (**Figure 3A** and **3B**). The percentages of NBD-positive cells were 43.0 ± 8.3%, 19.2 ± 1.76%, and 24.5 ± 0.8% for LPKN, LPNK, and LPNKN, respectively (**Figure 3B**). The corresponding median NBD intensity was 773 ± 52, 522 ± 30, and 540 ± 6, respectively (**Figure 3C**). After 120 min's incubation, more NPs were internalized for all three nanovaccines. Particularly, the percentages of NBD-positive cells were 93.0 ± 1.4%, 77.3 ± 0.9%, and 84.3 ± 3.0%, for LPKN, LPNK, and LPNKN, respectively (**Figure 3B**); and the median NBD intensity was 1560 ± 44, 1217 ± 28, and 1237 ± 34, respectively (**Figure 3C**). The data of both NBD-positive cells and NBD median intensity revealed that LPKN were taken up by dendritic cells more rapidly than LPNK and LPNKN.

The uptake and processing of nanovaccines were further studied by CLSM. Consistent with the FCA data, the uptake of nanovaccine NPs was time-dependent (**Figure 4**). After 15 min's incubation, weak NBD and AF647 fluorescences were shown in cells. This suggested cells had taken up small amounts of nanovaccine NPs within 15 min. In contrast, the fluorescence of NBD and AF647 was very strong in cells after incubation of 120 min, indicating more NPs were taken up with time. Interestingly, the processing of nanovaccines appeared to be step-wise in cells. After 15 min, NBD fluorescence was widely distributed in cells while AF647 fluorescence was displayed through individual particles. This phenomenon indicates that the lipid-layer was removed from the hybrid NPs to release protein antigens, but the protein antigens had not been efficiently processed. After 120 min, both NBD and AF647 fluorescence were widely distributed in cells, revealing that protein antigens had been effectively processed to small peptides. Moreover, consistent with the FCA data, LPKN was observed to be more efficiently taken up by dendritic

cells than LPNK and LPNKN, as both NBD and AF647 fluorescence were stronger in the LPKN group, especially at 120 min.

5.3.4 Immunogenicity of nanovaccines against nicotine and the carrier protein

The immunogenicity of nanovaccines against nicotine was evaluated in mice, and the results are shown in **Figure 5A**. No anti-nicotine antibody titers were detected in the negative control group on all days in which mice were immunized with KLH associated hybrid NPs without conjugated hapten. After the primary immunization, the anti-nicotine antibody titers of LPKN, LPNK, and LPNKN on day 12 were $(1.3 \pm 0.1) \times 10^3$, $(1.6 \pm 0.2) \times 10^3$, and $(2.3 \pm 0.3) \times 10^3$, respectively. After the first booster immunization, anti-nicotine antibody titers on day 26 significantly increased over that on day 12. The titers were $(9.2 \pm 2.2) \times 10^3$, $(9.8 \pm 6.0) \times 10^3$, and $(21.9 \pm 4.5) \times 10^3$ for LPKN, LPNK, and LPNKN, respectively. After the second booster immunization, anti-nicotine antibody titers considerably increased again on day 40, which were $(15.5 \pm 2.3) \times 10^3$, $(13.1 \pm 4.1) \times 10^3$, and $(31.0 \pm 12.4) \times 10^3$ for LPKN, LPNK, and LPNKN, respectively. Statistical analysis suggested that LPNKN generated significantly higher anti-nicotine antibody titers than LPKN and LPNK ($p < 0.05$), while LPKN and LPNK induced comparable titers ($p > 0.95$), on all studied days.

Titers of anti-KLH antibody were also monitored. The results are shown in **Figure 5B**. Similar to anti-nicotine antibody titers, anti-KLH antibody titers significantly increased after each immunization. On all studied days, the negative control induced the highest level of anti-KLH antibody. For the nanovaccines with different hapten localizations, the anti-KLH antibody titers were in the order of LPKN > LPNK > LPNKN for all studied days. The differences among different nanovaccine groups were significant ($p < 0.05$) on days 26 and 40, except for LPKN and LPNK. Specifically, end-point titers of $(79.1 \pm 14.1) \times 10^3$, $(47.9 \pm 4.3) \times 10^3$, $(44.7 \pm 7.1) \times 10^3$,

and (21.8 ± 2.6) $\times 10^3$ were detected in the negative control, LPKN, LPNK, and LPNKN groups, respectively.

5.3.5 Affinity of anti-nicotine antibody induced by nanovaccines

The binding affinity of nicotine to anti-nicotine antibodies elicited by nanovaccines was estimated by competition ELISA, and the time-course antibody affinity on days 12, 26, and 40 was shown in **Figure 6A**. On day 12, IC_{50} for LPKN, LPNK, and LPNKN was 1085 ± 1103, 1380 ± 460, and 1077 ± 319 μM, respectively. On day 26, IC_{50} decreased to 29 ± 19, 468 ± 302, and 29 ± 31 μM, for LPKN, LPNK, and LPNKN, respectively. Evidently, the first booster immunization significantly promoted the maturation of antibodies. Interestingly, after the second booster immunization (on day 40), the affinity of antibodies induced by the three nanovaccines decreased. The IC_{50} was 115 ± 162, 1004 ± 1276, and 132 ± 51 μM for LPKN, LPNK, and LPNKN, respectively. The affinity of antibodies induced by LPKN and LPNKN was considerably higher over LPNK on all the studied days. Specially, statistical comparison suggested that the end-point affinity of antibodies elicited by LPKN and LPNKN was significantly higher than that induced by LPNK, and no significant differences existed between LPKN and LPNKN (**Figure 6B**).

5.3.6 IgG subclass distribution of anti-nicotine antibodies

The subtype distribution of anti-nicotine IgG antibodies induced by the nanovaccines on day 40 was analyzed. As shown in **Figure 7A-D**, IgG1 was the dominant among all four subtypes for all three nanovaccines. In concordance with the total IgG titers, LPNKN induced higher titers of all four IgG subtypes over LPNK and LPNKN, especially for IgG1 and IgG2a. Interestingly, although the total IgG titers of LPKN and LPNK were very close (**Figure 5A**), LPNK generated significantly higher levels of IgG2a than LPKN. The relative magnitude of Th1 versus Th2 immune response induced by nanovaccines was assessed by the Th1/Th2 index. The Th1/Th2

indexes for LPKN, LPNK, and LPNKN were 0.043 ± 0.042, 0.430 ± 0.288, and 0.191 ± 0.136, respectively, which were all significantly less than 1. The Th1/Th2 index data indicates that the immune responses induced by the nanovaccines, regardless of hapten localizations, was Th2-skewed (humoral response dominated). Interestingly, LPNKN and LPNK resulted in a more balanced Th1-Th2 response than LPKN.

5.3.7 Capability of nanovaccines to influence the distribution of nicotine in the serum and brain

Capability of nanovaccines with different hapten localizations to influence nicotine distribution in the serum and brain was tested in mice. Mice received a dose of 0.06 mg/kg nicotine on day 42, and the nicotine levels in the serum and brain 3 min post-administration were analyzed. Serum nicotine levels are shown in **Figure 8A**. The blank group had a serum nicotine level of 12.5 ng/mL. Compared to the blank group, the nicotine levels in mice injected with LPKN, LPNK or LPNKN increased by 79.2%, 20%, and 192.0%, respectively. These data suggest that LPNKN had the best ability to retain nicotine in serum. Nicotine levels in the brain are shown in **Figure 8B**. The brain nicotine level in the blank group was 98.8 ng/g. The percent reductions in brain nicotine levels were 49.4%, 41.3%, and 66.9% for LPKN, LPNK, and LPNKN vaccinated groups, respectively. Based on the above results, LPNKN would have the best ability of keeping nicotine from entering the brain.

5.3.8 Safety of nanovaccines

The safety of nanovaccines was evaluated by behavioral and histopathological examination (**Figure 9**). Major organs of mice, including heart, kidney, lung, liver, and spleen, were stained with H&E and examined. No significant differences were detected between the blank (PBS) and the three nanovaccine groups, in all examined organs. Moreover, no detectable difference was

observed among the nanovaccines with different hapten localizations. Behavioral and physical conditions of mice during the entire study were monitored. No short-term effects, including local site reaction, elevation in body temperature, abnormal behavior, and abnormal food and water consumption, were detected in treated groups compared to the blank group. Thus, the nanovaccines, regardless of hapten localization, are considered safe.

5.4 Discussion

Nicotine vaccines are a promising strategy for future treatment against nicotine addiction. Currently, conjugate vaccines are the prevalent and most-studied nicotine vaccines. However, their intrinsic shortcomings, such as low nicotine loading capacity, low bioavailability, poor recognition and uptake by immune cells, and difficulty in incorporation of adjuvants, limit their immunological efficacy.[9, 25] Nanoparticles have been widely studied for delivery of drugs and vaccines.[36-40] Nanoparticles are able to maintain the activity of payloads and enhance delivery efficiency. In addition, high payload loading capacity, improved bioavailability, and controlled payload release can be achieved by nanoparticles.[41-44] These advantages inspired us to develop the next-generation nanoparticle-based nicotine vaccines to circumvent the innate shortfalls of conjugate nicotine vaccines. In our previous work, we conceptualized a lipid-polymeric hybrid nanoparticle-based nicotine nanovaccine, and demonstrated that its immunogenicity was significantly higher than that of the conjugate vaccine.[26] In this study, we studied the nanovaccine design by investigating the impact of hapten localization on its immunogenicity and efficacy. The nanovaccines developed in this current study differed in hapten localization, but all had similar overall hapten loading, average size and size distribution, and surface charge.

The nicotine nanovaccines are based on a lipid-polymeric hybrid nanoparticle. TEM images suggested the successful formation of a core-shell hybrid structure. In this study, each component

of the hybrid nanoparticles was adopted for specific purposes. The PLGA core not only supplies extra rigidity to liposomes to stabilize the nanoparticle system,[45] but also controls the size of nanovaccines. We previously demonstrated that nicotine nanovaccines of 100 nm had a significantly higher immunogenicity than those of 500 nm.[26] In this study, the PLGA core was fabricated by a nanoprecipitation method [46] resulting in a precisely controlled particle size. An advantage of the PLGA core is that it provides cargo space for encapsulation and controlled release of molecular adjuvants.[47, 48] The lipid shell was composed of DOTAP, cholesterol, DSPE-PEG2000-maleimide, and DSPE-PEG2000-amine. DOTAP,[49] a cationic lipid, produces a positively-charged nanoparticle surface and may promote the interaction between nanovaccines and negatively-charged immune cells, thus leading to enhanced internalization of vaccine particles. Cholesterol acts as a stabilizer in the lipid layer to improve the stability of nanovaccines.[50] DSPE-PEG2000-maleimide allows conjugation of multiple KLH/Nic-KLH to nanoparticle surface, leading to a high loading efficiency of protein antigen. DSPE-PEG2000-amine enables conjugation of Nic-hapten onto nanoparticle surface. Additionally, PEGylation may prolong the circulation time of nanovaccines and increase the bioavailability of vaccines.[51]

To induce an immune response, vaccine particles need to be efficiently internalized and processed by antigen presenting cells (APCs).[9] Both the FCA and CLSM data suggested that the nanovaccines, regardless of hapten localization, were taken up by DCs efficiently. The positively charged surface of nanovaccines likely contributed to this effect. Specifically, more than 75% of the cells had taken up nanoparticles within 120 min. The efficient internalization of nanovaccines may provide sufficient antigens to induce a quick development of immune response. Moreover, CLSM images indicated the sufficient processing of protein antigens to peptide antigens within 120 min. Efficient processing of protein antigens may ensure effective activation of T-helper cells,

making the immune response fervent and long-lasting. Interestingly, the uptake of LPKN particles is slightly more efficient than that of LPNK and LPNKN particles. This may be caused by the high PEG-grafting in LPNK and LPNKN, as it has been reported that PEG-grafting might decrease the uptake of nanoparticles.[52]

Previous studies suggested that anti-nicotine antibody levels largely determine smoking cessation efficacy.[16, 17] LPNKN induced significantly higher anti-nicotine antibody titers than LPKN and LPNK, while the antibody levels of LPKN and LPNK were comparable. This finding suggests that the immunogenicity of nanovaccines could be improved by conjugating Nic-haptens onto both carrier protein and nanoparticle surface, instead of onto only one. Anti-KLH antibody is considered a non-specific byproduct. Production of anti-KLH antibody would cause wastage of vaccines to generate antibodies against KLH rather than nicotine. Meanwhile, high levels of anti-KLH antibody may neutralize nanovaccines injected during booster immunizations. Interestingly, LPNKN induced the lowest anti-KLH antibody titers among the three nanovaccines with different hapten localizations. This may be explained by the following: First, conjugation of Nic-hapten to KLH masked sufficient amounts of immunogenic epitopes on KLH. Second, the shielding effect of PEG-grafting [53] on LPNKN might decrease the recognition of immunogenic epitopes on KLH by immune cells.

Based on the ELISA results, we found that LPNKN had the highest immunogenicity among the three nanovaccines, eliciting the highest titers of anti-nicotine antibody and the lowest levels of anti-KLH antibody. Although we do not have direct evidences to show the mechanism, the following may explain the immunogenic differences among the nanovaccines that had similar overall hapten densities but different hapten localizations. For examples, generation of an effective humoral immune response against nicotine requires two pivotal processes: the first process is

activation of nicotine-specific B cells; the second process is generation of T-helper cells and the interaction between T-helper cells and B cells, which are required for the maturation of nicotine-specific B cells to antibody-secreting cells.[9] Generation of T-helper cells occurs by specific recognition of T cell epitopes (displayed on APCs) by T cells. Maturation of nicotine-specific B cells is facilitated by specific recognition of T cell epitopes (displayed on B cells) by T helper cells.[9] As for LPKN, the process of B cell activation was sufficient. However, Nic-haptens were localized on KLH at a high density. This could mask some of the T cell epitopes, causing the B cell maturation to be insufficient. For LPNKN, B cell activation was efficient. As less Nic-haptens were localized on KLH, T cell epitopes were minimally masked. Thus, the B cell maturation process was also sufficient. As for LPNK, no Nic-haptens were conjugated to KLH, and thus the immunogenic epitopes of KLH were fully exposed. Therefore, a portion of nanovaccines would be used to generate antibodies against KLH rather than nicotine, leading to a low immunogenicity against nicotine. However, a cellular mechanistic study is not within the scope of this work. The proposed mechanism needs to be verified in future experiments.

Affinity of Anti-nicotine antibodies to nicotine is a critical factor influencing the efficacy of a nicotine vaccine.[9] Interestingly, we found that antibodies induced by LPKN and LPNKN had significantly higher affinity than those induced by LPNK. This indicates that hapten localization appeared to affect affinity of anti-nicotine antibodies. Our analysis of subtype distribution of anti-nicotine IgG antibody revealed that LPNK generated higher percentages of IgG2a, IgG2b, and IgG3 than LPKN, especially IgG2a, although their total IgG titers were close. Hapten localization thus influenced the anti-nicotine IgG subtype distribution, and tended to induce widely-distributed IgG subtypes. Th1/Th2 index is an indicator of the polarization of immune responses.[54] Although LPNK and LPNKN induced more balanced Th1-Th2 immune responses than LPKN, all

three nanovaccines induced Th2-skewed humoral responses (Th1/Th2 significantly less than 1). Th2-skewed immune responses are considered desirable for nicotine vaccine design, as the efficacy of reducing the rewarding effects of nicotine is dependent on the magnitude of the humoral response. Consistent with the immunogenicity and affinity data, we found that LPNKN resulted in a better retention of nicotine in serum and reducing nicotine levels in the brain than LPKN and LPNK. These results suggest the efficacy of nicotine nanovaccines could be improved by conjugating Nic-haptens to both stimulating protein and nanoparticle surface. In our previous study, we found that LPKN induced an anti-nicotine antibody titer of ~ 9,000 on day 41 and resulted in a 32% brain nicotine reduction.[26] However, in this study, we found that LPKN elicited an antibody titer of ~ 15,000 on day 40 and reduced brain nicotine concentrations by 49%. These two studies differed in the two studies differed in Nic-KLH conjugation capacity (the mass ratio of conjugated Nic-KLH to hybrid nanoparticles). Future work is needed to be done to establish an optimal Nic-carrier protein conjugation capacity. In addition, we previously demonstrated that LPKN induced a significantly better pharmacokinetic efficacy than the conjugate vaccine. The finding in this current study may lead to further improvement in the efficacy of hybrid nanoparticle-based nicotine nanovaccines. It should be pointed out that no molecular adjuvants were incorporated to the nanovaccines in this study. A study is undergoing to further improve the immunogenicity of nanovaccines by selecting potent molecular adjuvants.

In summary, a lipid-polymeric hybrid nanoparticle-based next-generation nicotine nanovaccine was successfully fabricated and tested with a focus on studying the impact of hapten localization on its immunogenicity and efficacy. Results from mice trials suggested that vaccines with hapten molecules conjugated on both the carrier protein and nanoparticle surface have better immunogenicity and are more likely to lower brain concentrations of nicotine than vaccines with

haptens only on protein or nanoparticle surface. The findings of this study suggest a novel strategy to improve the immunogenicity and efficacy of the next-generation nanoparticle-based nicotine vaccine, and can be applied to the design of other nanoparticle-based vaccines. Based on all the reported results, hybrid nanoparticle-based next-generation nicotine nanovaccines hold great promise as future clinical vaccines against nicotine addiction.

Conflict of interest

The authors declare no competing financial interests.

Acknowledgment

This work was financially supported by National Institute on Drug Abuse (U01DA036850). We thank Jie Zhu for his help on collecting FT-IR data.

References

[1] Tobacco, Fact Sheet Number 339. World Health Organization; 2015.

[2] Benowitz NL. Nicotine addiction. N Engl J Med. 2010;362:2295-303.

[3] Prochaska JJ, Benowitz NL. The past, present, and future of nicotine addiction therapy. Annu Rev Med. 2016;67:467-86.

[4] Hughes JR, Keely J, Naud S. Shape of the relapse curve and long-term abstinence among untreated smokers. Addiction. 2004;99:29-38.

[5] Paolini M, De Biasi M. Mechanistic insights into nicotine withdrawal. Biochem Pharmacol. 2011;82:996-1007.

[6] Stead LF, Perera R, Bullen C, Mant D, Hartmann-Boyce J, Cahill K, et al. Nicotine replacement therapy for smoking cessation. Cochrane Db Syst Rev. 2012.

[7] Piper ME, Federman EB, McCarthy DE, Bolt DM, Smith SS, Fiore MC, et al. Efficacy of bupropion alone and in combination with nicotine gum. Nicotine Tob Res. 2007;9:947-54.

[8] Koegelenberg CFN, Noor F, Bateman ED, van Zyl-Smit RN, Bruning A, O'Brien JA, et al. Efficacy of varenicline combined with nicotine replacement therapy vs varenicline alone for smoking cessation: A randomized clinical trial. Jama-J Am Med Assoc. 2014;312:155-61.

[9] Pentel PR, LeSage MG. New directions in nicotine vaccine design and use. Adv Pharmacol. 2014;69:553-80.

[10] Raupach T, Hoogsteder PH, Onno van Schayck CP. Nicotine vaccines to assist with smoking cessation: current status of research. Drugs. 2012;72:e1-16.

[11] Goniewicz ML, Delijewski M. Nicotine vaccines to treat tobacco dependence. Hum Vacc Immunother. 2013;9:13-25.

[12] Keyler DE, Roiko SA, Earley CA, Murtaugh MP, Pentel PR. Enhanced immunogenicity of a bivalent nicotine vaccine. Int Immunopharmacol. 2008;8:1589-94.

[13] McCluskie MJ, Thorn J, Mehelic PR, Kolhe P, Bhattacharya K, Finneman JI, et al. Molecular attributes of conjugate antigen influence function of antibodies induced by anti-nicotine vaccine in mice and non-human primates. Int Immunopharmacol. 2015;25:518-27.

[14] Miller KD, Roque R, Clegg CH. Novel anti-nicotine vaccine using a trimeric coiled-coil hapten carrier. Plos One. 2014;9.

[15] De Blasi M, McLaughlin I, Perez EE, Crooks PA, Dwoskin LP, Bardo MT, et al. Scientific overview: 2013 BBC plenary symposium on tobacco addiction (vol 141, pg 107, 2014). Drug Alcohol Depen. 2014;144:290-.

[16] Hatsukami DK, Jorenby DE, Gonzales D, Rigotti NA, Glover ED, Oncken CA, et al. Immunogenicity and smoking-cessation outcomes for a novel nicotine ommunotherapeutic. Clin Pharmacol Ther. 2011;89:392-9.

[17] Cornuz J, Zwahlen S, Jungi WF, Osterwalder J, Klingler K, van Melle G, et al. A Vaccine against Nicotine for Smoking Cessation: A Randomized Controlled Trial. Plos One. 2008;3.

[18] Pryde DC, Jones LH, Gervais DP, Stead DR, Blakemore DC, Selby MD, et al. Selection of a novel anti-nicotine vaccine: Influence of antigen design on antibody function in mice. Plos One. 2013;8.

[19] de Villiers SHL, Lindblom N, Kalayanov G, Gordon S, Baraznenok I, Malmerfelt A, et al. Nicotine hapten structure, antibody selectivity and effect relationships: Results from a nicotine vaccine screening procedure. Vaccine. 2010;28:2161-8.

[20] Chen XY, Pravetoni M, Bhayana B, Pentel PR, Wu MX. High immunogenicity of nicotine vaccines obtained by intradermal delivery with safe adjuvants. Vaccine. 2012;31:159-64.

[21] McCluskie MJ, Pryde DC, Gervais DP, Stead DR, Zhang NL, Benoit M, et al. Enhancing immunogenicity of a 3 ' aminomethylnicotine-DT-conjugate anti-nicotine vaccine with CpG adjuvant in mice and non-human primates. Int Immunopharmacol. 2013;16:50-6.

[22] Lockner JW, Lively JM, Collins KC, Vendruscolo JCM, Azar MR, Janda KD. A Conjugate vaccine using enantiopure hapten imparts superior nicotine-binding capacity. J Med Chem. 2015;58:1005-11.

[23] Collins KC, Janda KD. Investigating hapten clustering as a atrategy to enhance vaccines against drugs of abuse. Bioconjug Chem. 2014;25:593-600.

[24] Hu Y, Zheng H, Huang W, Zhang CM. A novel and efficient nicotine vaccine using nano-lipoplex as a delivery vehicle. Hum Vacc Immunother. 2014;10:64-72.

[25] Zheng H, Hu Y, Huang W, de Villiers S, Pentel P, Zhang JF, et al. Negatively charged carbon nanohorn supported cationic liposome nanoparticles: A novel delivery vehicle for anti-nicotine vaccine. J Biomed Nanotechnol. 2015;11:2197-210.

[26] Zhao Z, Hu Y, Hoerle R, Devine M, Raleigh M, Pentel P, et al. A nanoparticle-based nicotine vaccine and the influence of particle size on its immunogenicity and efficacy. Nanomed-Nanotechnol. 2016.

[27] Zhao Z, Powers K, Hu Y, Raleigh M, Pentel P, Zhang C. Engineering of a hybrid nanoparticle-based nicotine nanovaccine as a next-generation immunotherapeutic strategy against nicotine addiction: A focus on hapten density. Biomaterials. 2017;123:107-17.

[28] Jacob NT, Lockner JW, Schlosburg JE, Ellis BA, Eubanks LM, Janda KD. Investigations of Enantiopure Nicotine Haptens Using an Adjuvanting Carrier in Anti-Nicotine Vaccine Development. J Med Chem. 2016;59:2523-9.

[29] Parra J, Abad-Somovilla A, Mercader JV, Taton TA, Abad-Fuentes A. Carbon nanotube-protein carriers enhance size-dependent self-adjuvant antibody response to haptens. J Control Release. 2013;170:242-51.

[30] Sloat BR, Sandoval MA, Hau AM, He Y, Cui Z. Strong antibody responses induced by protein antigens conjugated onto the surface of lecithin-based nanoparticles. J Control Release. 2010;141:93-100.

[31] Babahosseini H, Srinivasaraghavan V, Zhao ZM, Gillam F, Childress E, Strobl JS, et al. The impact of sphingosine kinase inhibitor-loaded nanoparticles on bioelectrical and biomechanical properties of cancer cells. Lab Chip. 2016;16:188-98.

[32] Hu Y, Zhao ZM, Ehrich M, Fuhrman K, Zhang CM. In vitro controlled release of antigen in dendritic cells using pH-sensitive liposome-polymeric hybrid nanoparticles. Polymer. 2015;80:171-9.

[33] Jalah R, Torres OB, Mayorov AV, Li F, Antoline JF, Jacobson AE, et al. Efficacy, but not antibody titer or affinity, of a heroin hapten conjugate vaccine correlates with increasing hapten densities on tetanus toxoid, but not on CRM197 carriers. Bioconjug Chem. 2015;26:1041-53.

[34] Pravetoni M, Keyler DE, Pidaparthi RR, Carroll FI, Runyon SP, Murtaugh MP, et al. Structurally distinct nicotine immunogens elicit antibodies with non-overlapping specificities. Biochem Pharmacol. 2012;83:543-50.

[35] de Villiers SHL, Cornish KE, Troska AJ, Pravetoni M, Pentel PR. Increased efficacy of a trivalent nicotine vaccine compared to a dose-matched monovalent vaccine when formulated with alum. Vaccine. 2013;31:6185-93.

[36] Thangavel S, Yoshitomi T, Sakharkar MK, Nagasaki Y. Redox nanoparticle increases the chemotherapeutic efficiency of pioglitazone and suppresses its toxic side effects. Biomaterials. 2016;99:109-23.

[37] Liu J, Wei T, Zhao J, Huang YY, Deng H, Kumar A, et al. Multifunctional aptamer-based nanoparticles for targeted drug delivery to circumvent cancer resistance. Biomaterials. 2016;91:44-56.

[38] Qian Y, Jin HL, Qiao S, Dai YF, Huang C, Lu LS, et al. Targeting dendritic cells in lymph node with an antigen peptide-based nanovaccine for cancer immunotherapy. Biomaterials. 2016;98:171-83.

[39] Yan SY, Rolfe BE, Zhang B, Mohammed YH, Gu WY, Xu ZP. Polarized immune responses modulated by layered double hydroxides nanoparticle conjugated with CpG. Biomaterials. 2014;35:9508-16.

[40] Rosalia RA, Cruz LJ, van Duikeren S, Tromp AT, Silva AL, Jiskoot W, et al. CD40-targeted dendritic cell delivery of PLGA-nanoparticle vaccines induce potent anti-tumor responses. Biomaterials. 2015;40:88-97.

[41] Chen MC, Sonaje K, Chen KJ, Sung HW. A review of the prospects for polymeric nanoparticle platforms in oral insulin delivery. Biomaterials. 2011;32:9826-38.

[42] Mandal B, Bhattacharjee H, Mittal N, Sah H, Balabathula P, Thoma LA, et al. Core-shell-type lipid-polymer hybrid nanoparticles as a drug delivery platform. Nanomed-Nanotechnol. 2013;9:474-91.

[43] Grobmyer SR, Zhou GY, Gutwein LG, Iwakuma N, Sharma P, Hochwald SN. Nanoparticle delivery for metastatic breast cancer. Nanomed-Nanotechnol. 2012;8:S21-S30.

[44] Park K. Controlled drug delivery systems: Past forward and future back. J Control Release. 2014;190:3-8.

[45] Zhang LF, Granick S. How to stabilize phospholipid liposomes (using nanoparticles). Nano Lett. 2006;6:694-8.

[46] Zhao PF, Zheng MB, Yue CX, Luo ZY, Gong P, Gao GH, et al. Improving drug accumulation and photothermal efficacy in tumor depending on size of ICG loaded lipid-polymer nanoparticles. Biomaterials. 2014;35:6037-46.

[47] Mueller M, Reichardt W, Koerner J, Groettrup M. Coencapsulation of tumor lysate and CpG-ODN in PLGA-microspheres enables successful immunotherapy of prostate carcinoma in TRAMP mice. J Control Release. 2012;162:159-66.

[48] Wang Q, Tan MT, Keegan BP, Barry MA, Heffernan MJ. Time course study of the antigen-specific immune response to a PLGA microparticle vaccine formulation. Biomaterials. 2014;35:8385-93.

[49] Shen KY, Liu HY, Li HJ, Wu CC, Liou GG, Chang YC, et al. A novel liposomal recombinant lipoimmunogen enhances anti-tumor immunity. J Control Release. 2016;233:57-63.

[50] Nakazawa T, Nagatsuka S, Yukawa O. Effects of membrane stabilizing agents and radiation on liposomal membranes. Drug Exp Clin Res. 1986;12:831-5.

[51] Ibricevic A, Guntsen SP, Zhang K, Shrestha R, Liu YJ, Sun JY, et al. PEGylation of cationic, shell-crosslinked-knedel-like nanoparticles modulates inflammation and enhances cellular uptake in the lung. Nanomed-Nanotechnol. 2013;9:912-22.

[52] Pelaz B, del Pino P, Maffre P, Hartmann R, Gallego M, Rivera-Fernandez S, et al. Surface functionalization of nanoparticles with polyethylene glycol: Effects on protein adsorption and cellular uptake. Acs Nano. 2015;9:6996-7008.

[53] Mickler FM, Vachutinsky Y, Oba M, Miyata K, Nishiyama N, Kataoka K, et al. Effect of integrin targeting and PEG shielding on polyplex micelle internalization studied by live-cell imaging. J Control Release. 2011;156:364-73.

[54] Moser M, Murphy KM. Dendritic cell regulation of TH1-TH2 development. Nat Immunol. 2000;1:199-205.

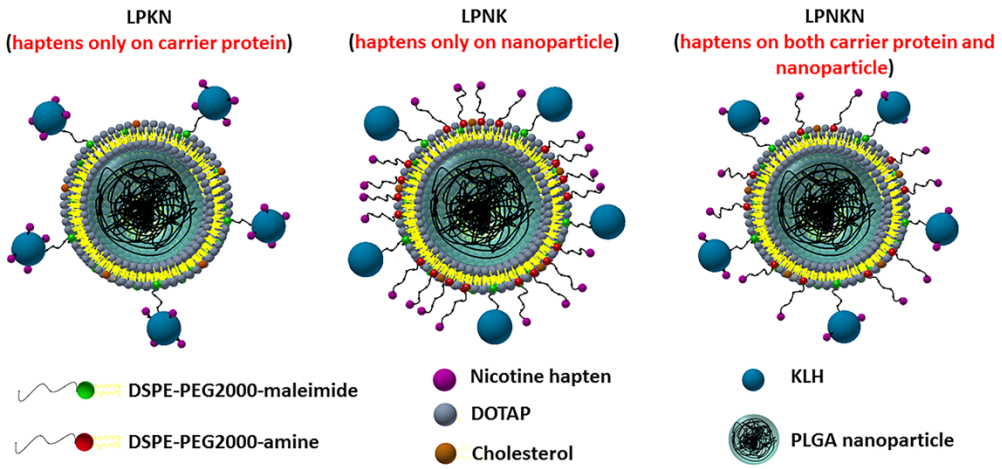

Scheme. Schematic illustration of the structure of hybrid NP-based nicotine nanovaccines with different hapten localizations.

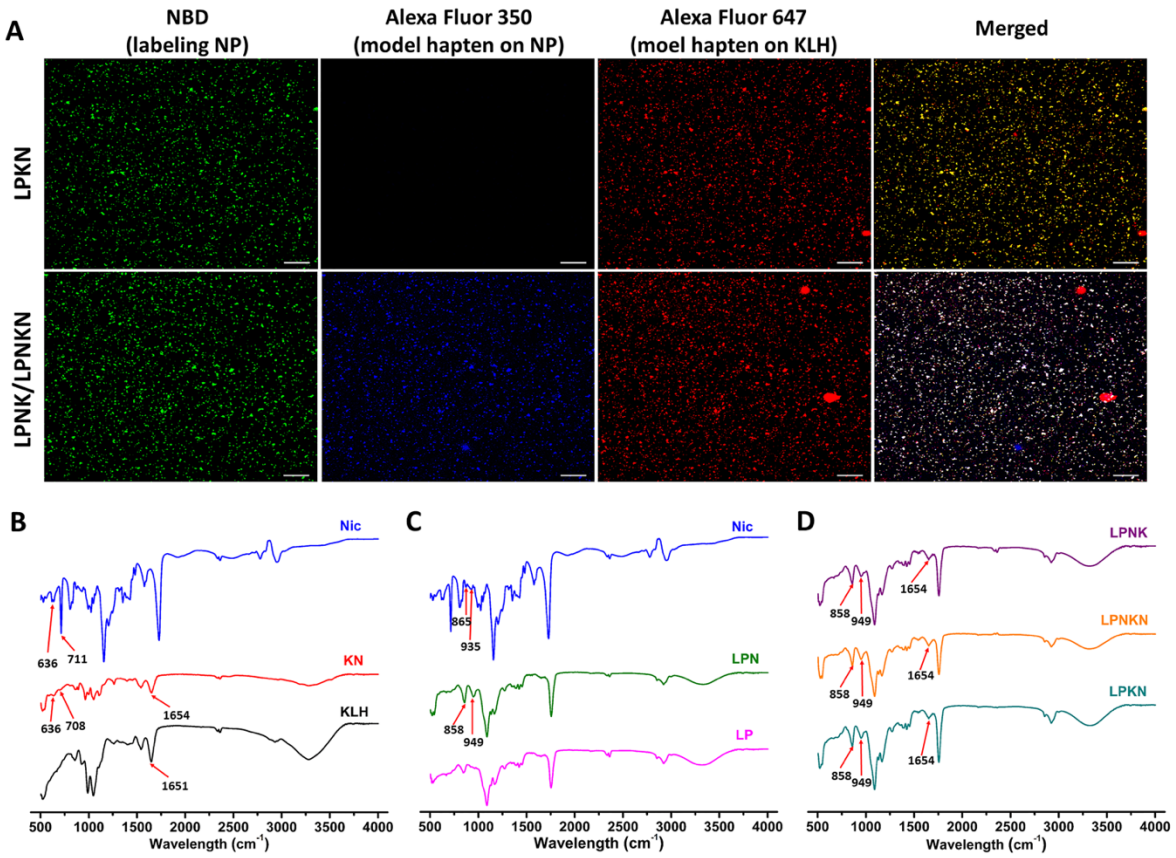

Figure 1. Verification of the hapten conjugate chemistry. (A) CLSM images showing the co-localization of model hapten dyes with hybrid NPs. Scale bars represent 10 μm. FT-IR spectra of Nic-hapten (Nic), Nic-KLH conjugate (KN), and KLH (B); Nic-hapten, hybrid NPs (LP), and Nic-hapten-conjugated LPN NPs (LPN) (C); LPKN, LPNK, and LPNKN (D).

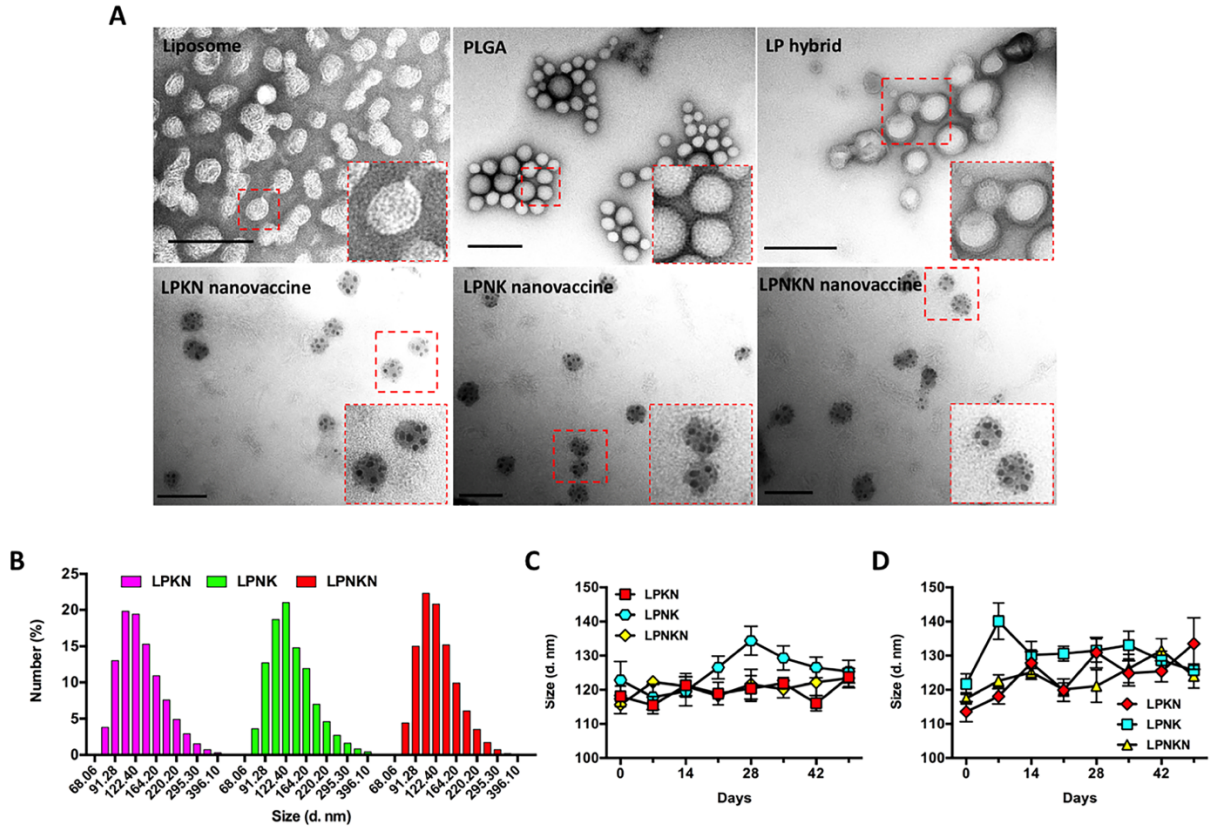

Figure 2. Characterization of nanovaccine NPs. (A) TEM images showing the morphological characteristics of NPs. Scale bars represent 200 nm. (B) Size distribution of LPKN, LPNK, and LPNKN NPs. (C) and (D) show the stability of nanovaccines in PBS and DI water at 4 °C, respectively.

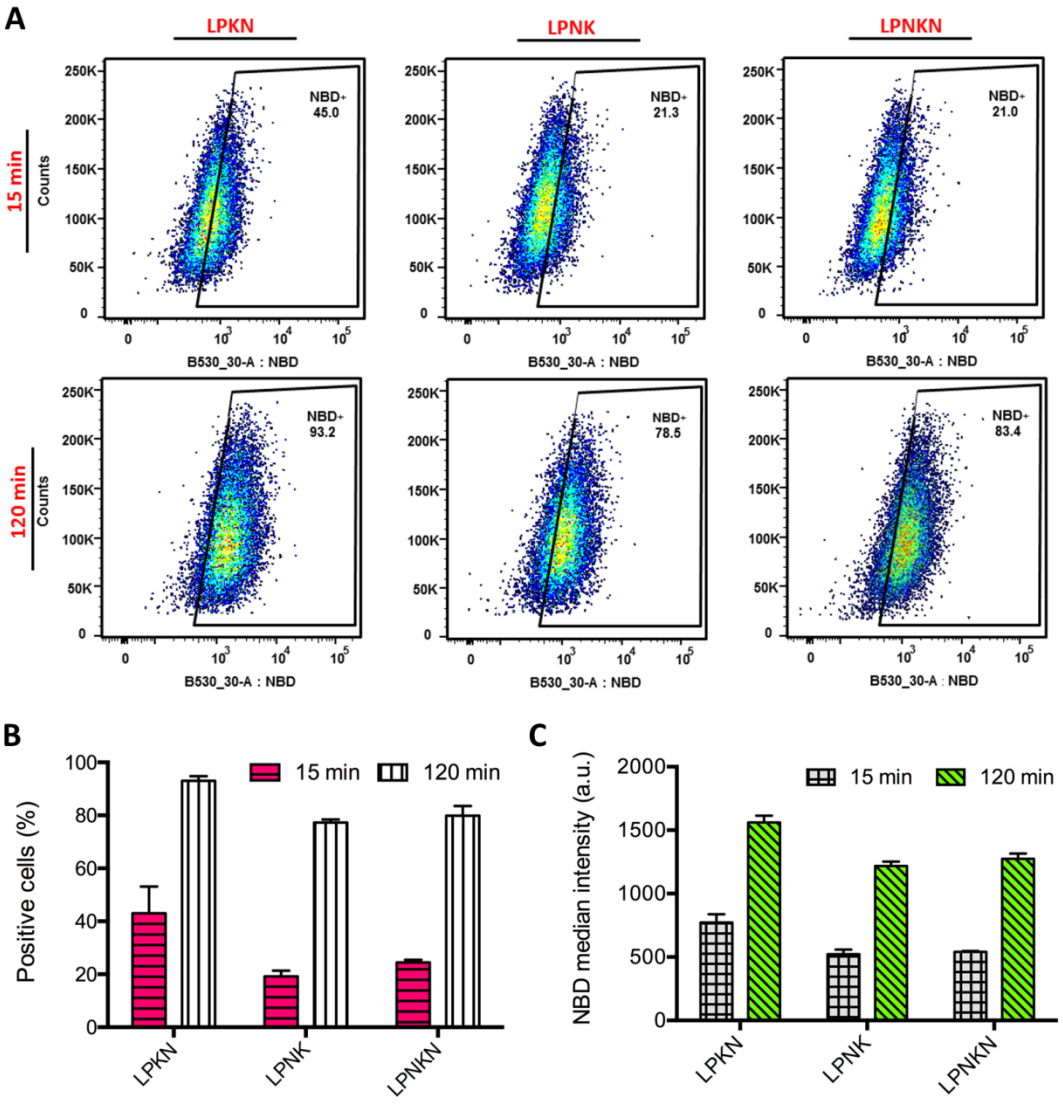

Figure 3. Flow cytometry assay of the uptake of nanovaccine NPs by dendritic cells. (A) Population distribution of cells treated with 20 μg of nanovaccine NPs for 15 min or 120 min. The percentage of NBD-positive cells (B) and NBD median intensity in cells (C) were analyzed.

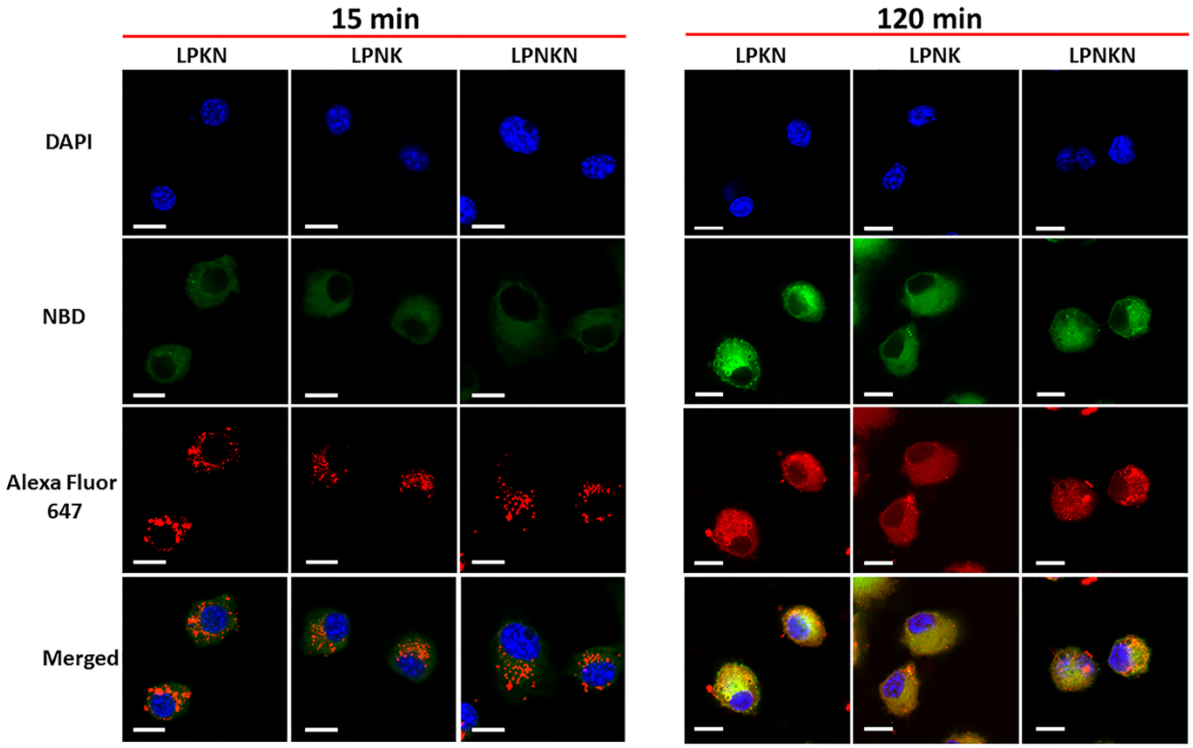

Figure 4. Uptake of nanovaccine NPs by dendritic cells analyzed by CLSM. The lipid-layer of hybrid NPs was labeled by NBD. Nic-hapten on KLH was substituted with AF647 to provide fluorescence. Cells were treated with 20 μg of nanovaccine NPs for 15 min or 120 min. Scale bars represent 10 μm.

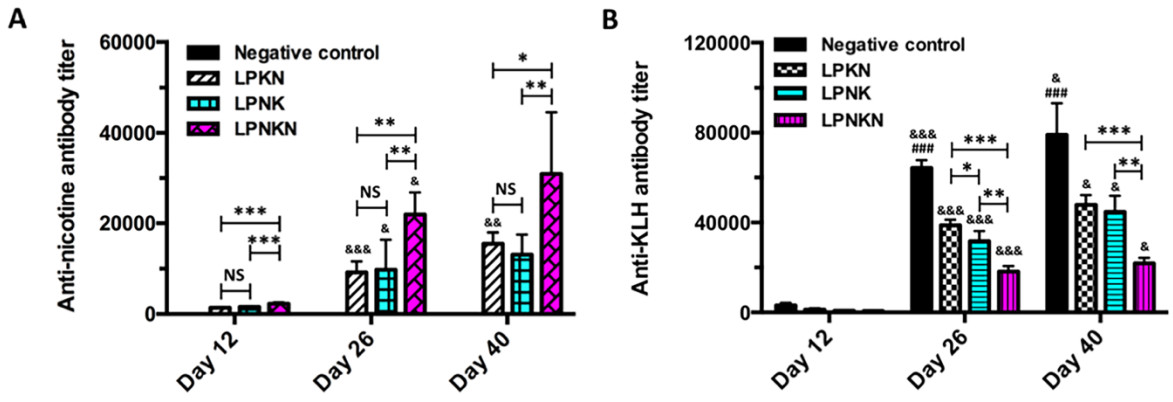

Figure 5. Anti-nicotine antibody titers (A) and anti-KLH antibody titers (B) determined by ELISA. Significantly different compared to the previous studied day: & $p < 0.05$, && $p < 0.01$, &&& $p < 0.001$. Significantly different compared to the other three groups on the same studied day: ## $p < 0.01$, ### $p < 0.001$. Significantly different: * $p < 0.05$, ** $p < 0.01$, *** $p < 0.001$.

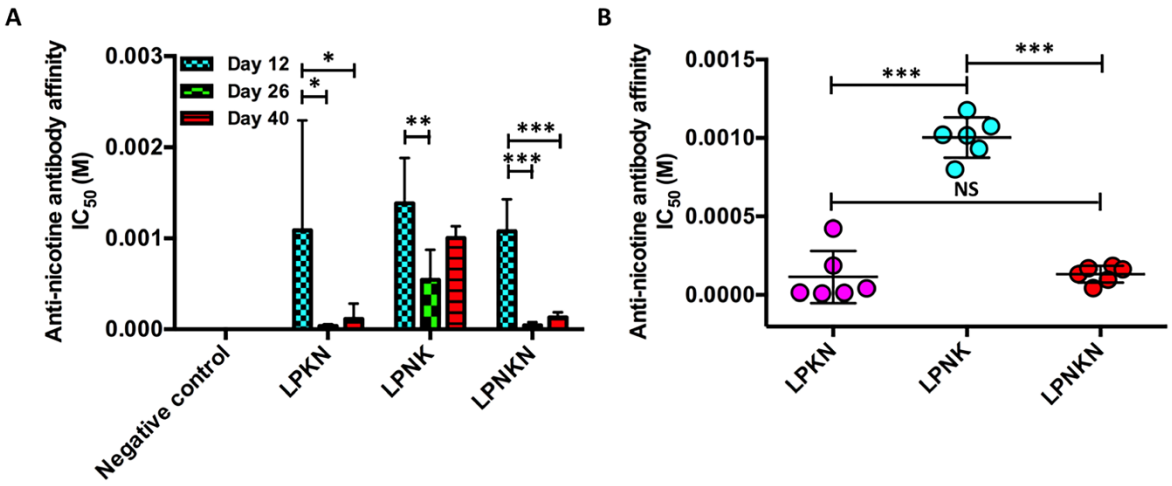

Figure 6. Anti-nicotine antibody affinity estimated by competition ELISA. (A) Time-course affinity of anti-nicotine antibodies induced by various nicotine nanovaccines. (B) Endpoint comparison of antibody's affinity among different hapten localization nanovaccine groups on day 40. Significantly different: * $p < 0.05$, ** $p < 0.01$, *** $p < 0.001$.

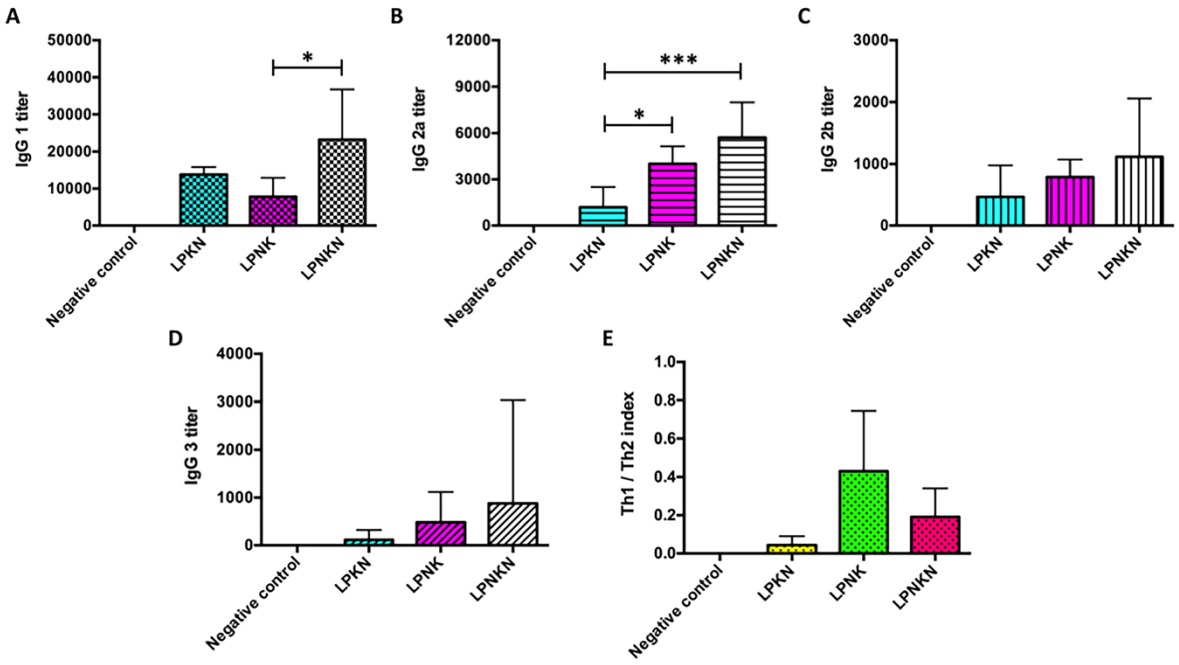

Figure 7. Anti-nicotine subclass antibody titers of (A) IgG 1, (B) IgG 2a, (C) IgG 2b, and (D) IgG 3. (E) Th1/Th2 index induced by immunization with nicotine nanovaccines. Th1/Th2 index= (IgG2a+IgG3)/2/IgG1. Significantly different: * $p < 0.05$, *** $p < 0.001$.

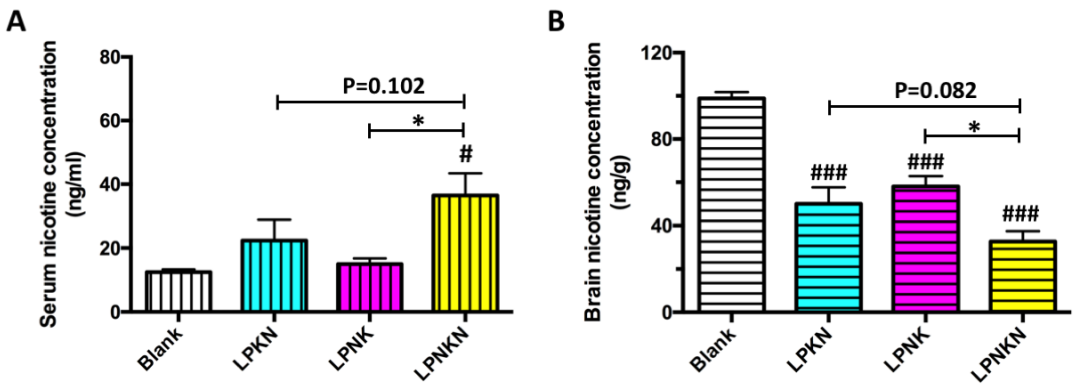

Figure 8. Capability of nanovaccines with different hapten localizations to influence nicotine distribution in the serum and brain after nicotine challenge. Nicotine levels in the serum (A) and brain (B) of mice 3 min after challenged with 0.06 mg/kg nicotine. Data were reported as means ± standard error. Significantly different compared to the blank group: # $p < 0.05$, ### $p < 0.001$. Significantly different: * $p < 0.05$.

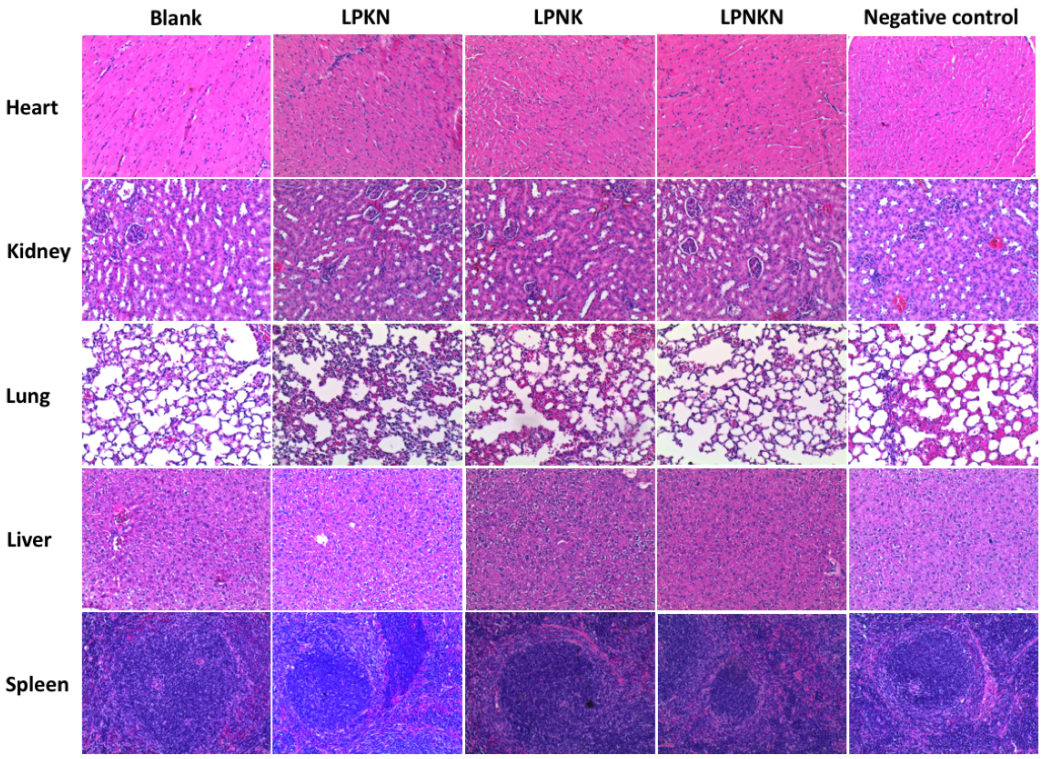

Figure 9. H&E staining of the sections of major organs including heart, kidney, lung, liver, and spleen harvested from the mice immunized with different nicotine vaccines.

Table 1. Characteristics of nanovaccines with different hapten localizations.

Nanovaccines	Size (d. nm)	Zeta-potential (mV)	PDI	KLH/Nic-KLH conjugation efficiency (%)	Nic-hapten density (#/$\times 10^4$/NP)
LPKN	118.1 ± 3.0	5.46 ± 0.25	0.11 ± 0.02	82.3 ± 5.4	6.32 ± 0.39
LPNK	122.8 ± 5.5	2.85 ± 0.23	0.15 ± 0.03	85.3 ± 7.4	5.89 ± 0.67
LPNKN	115.7 ± 2.7	4.69 ± 0.24	0.14 ± 0.03	80.2 ± 6.7	6.02 ± 0.53

Chapter 6: Hybrid nanoparticle-based nicotine nanovaccines (NanoNicVac) as a next-generation immunotherapeutic strategy against nicotine addiction: boosting the immunological efficacy by conjugation of potent stimulating proteins

Zongmin Zhao[1], Theresa Harmon [2], Paul Pentel[2], Marion Ehrich[3], Chenming Zhang[1,*]

1. Department of Biological Systems Engineering, Virginia Tech, Blacksburg, VA 24061, USA

2. Minneapolis Medical Research Foundation, Minneapolis, MN 55404, USA

3. Department of Biomedical Sciences and Pathobiology, Virginia Tech, Blacksburg, VA 24061, USA

* Correspondence to: Chenming (Mike) Zhang.

Address: 210 Seitz Hall, Department of Biological Systems Engineering, Virginia Tech, Blacksburg, VA 24061, USA.

Voice: +1-(540)231-7601

Fax: +1-(540)231-3199

Email: chzhang2@vt.edu

This manuscript is to be submitted to *Nanomedicine: Nanotechnology, Biology and Medicine*.

Abstract

A series of hybrid nanoparticle-based nicotine nanovaccines (NanoNicVac) were engineered in this work by conjugating potent stimulating protein candidates (KLH multimer, KLH subunit, CRM_{197}, or TT) for enhanced immunological efficacy. All four NanoNicVac, regardless of stimulating proteins, were rapidly and efficiently taken up by dendritic cells *in vitro*. NanoNicVac conjugated with CRM_{197} or TT were processed by dendritic cells more efficiently than that conjugated with KLH multimer or KLH subunit. NanoNicVac carrying CRM_{197} or TT exhibited a significantly higher immunogenicity against nicotine and a considerably lower immunogenicity against stimulating proteins than NanoNicVac carrying KLH multimer or KLH subunit in mice. NanoNicVac conjugated with CRM_{197} or TT resulted in lower brain nicotine levels after nicotine challenge. All the findings suggest that an enhanced immunological efficacy of NanoNicVac can be achieved by conjugating potent CRM_{197} or TT stimulating proteins, making NanoNicVac be a promising next-generation immunotherapeutic candidate against nicotine addiction.

Key words

Nicotine addiction; nicotine vaccine; hybrid nanoparticle; stimulating protein; anti-nicotine antibody

6.1 Introduction

Tobacco smoking continues to be the leading preventable cause of disease, disability, and death worldwide.[1] Every year in the United States alone, more than 480,000 people die from tobacco smoking.[2] Current pharmacological medications for smoking cessation are only partially successful and associated with the risk of serious side effects.[3] Nicotine vaccines that can generate nicotine-specific antibodies capable of sequestering nicotine in serum and reducing nicotine entering the brain have shown to be a promising approach to treating nicotine addiction.[4, 5] Several conjugate nicotine vaccines have reached various stages of clinical trials.[6, 7] Despite the prominent results in preclinical and early-stage clinical trials, no conjugate nicotine vaccines have proven overall to enhance smoking cessation rate, mainly due to the insufficient and highly-variable antibody titers.[5, 8, 9]

In our previous work, we devised the next-generation nanoparticle-based nicotine vaccines to achieve improved immunogenicity over conjugate nicotine vaccines.[10-13] These next-generation nanoparticle-based nicotine nanovaccines have many unique properties, such as high bioavailability, enhanced recognition and uptake by immune cells, long immune persistence, high specificity, and ease of incorporation with adjuvants. In particular, a lipid-polymeric hybrid nanoparticle-based nicotine nanovaccine (NanoNicVac) was demonstrated to result in significantly higher immunological efficacy than the conjugate nicotine vaccine.[12] In addition, we previously demonstrated that the immunogenicity of NanoNicVac could be improved by modulating nanoparticle size,[12] hapten density,[14] and hapten localization.[15]

Immunologically, efficient T cell immunity is essential for the generation of an effective humoral immune response against nicotine.[16, 17] The maturation of nicotine-specific B cells to antibody-secreting cells requires two pivotal T cell-dependent processes. The two processes are the

formation of T helper cells and the interaction between T-helper cells and B cells, both of which only occur via presentation of peptidic antigens on the major histocompatibility complex (MHC) of antigen presenting cells.[5, 18] Basically, an effective T cell immunity makes the humoral immune response against nicotine specific, intense, and long-lasting.[19] Therefore, a stimulating protein that provides peptidic antigens is a necessity for a nanoparticle-based nicotine nanovaccine.[20] Incorporation of different stimulating proteins into a nanoparticle-based nicotine nanovaccine may cause differential effectiveness of T cell immunity, thus leading to different immunological efficacy.

In this study, potent stimulating proteins were incorporated into NanoNicVac to boost its immunological efficacy. Specifically, four stimulating protein candidates, including keyhole limpet hemocyanin (KLH) multimer,[21] KLH subunit (KS),[22] cross reactive material 197 (CRM_{197}),[23] and tetanus toxoid (TT),[24] all of which have been reported to be highly-immunogenic and widely used as stimulating proteins, were conjugated to NanoNicVac to study the impact of stimulating proteins on its immunogenicity and capability to reduce brain nicotine levels. NanoNicVac with different stimulating proteins (**Figure 1A**) were prepared and characterized. The cellular uptake and processing of NanoNicVac particles were studied in dendritic cells. The immunogenicity and capability to reduce brain nicotine levels of NanoNicVac were tested in mice.

6.2 Materials and methods

6.2.1 Materials

Lactel® (50:50 poly(lactic-co-glycolic acid) (PLGA)) was purchased from Durect Corporation (Cupertino, CA, USA). 1,2-Dioleoyl-3-trimethylammonium-propane (DOTAP), cholesterol

(CHOL), 1,2-diphytanoyl-sn-glycero-3-phosphoethanolamine-N-(7-nitro-2-1,3-benzoxadiazol-4-yl) (ammonium salt) (NBD-PE), and 1,2-distearoyl-sn-glycero-3-phosphoethanolamine-N-[maleimide(polyethylene glycol)-2000] (ammonium salt) (DSPE-PEG2000-maleimide) were purchased from Avanti Polar Lipids (Alabaster, AL, USA). O-Succinyl-3'-hydroxymethyl-(±)-nicotine (Nic) was purchased from Toronto Research Chemicals (North York, ON, Canada). KLH multimer, KLH subunit, Alexa Fluor® 647 NHS ester (AF647), Fluor® 350 NHS ester (AF350), 1-Ethyl-3-[3-dimethylaminopropyl] carbodiimide hydrochloride (EDC), and N-hydroxysulfosuccinimide (Sulfo-NHS) were purchased from Thermo Fisher Scientific (Rockford, IL, USA). TT was purchased from Statens Serum Institut (Copenhagen, Denmark). CRM_{197} was a gift from Fina Biosolutions (Rockville, MD, USA). All other chemicals were of analytical grade.

6.2.2 Fabrication of lipid-polymeric hybrid nanoparticles

PLGA nanoparticles were fabricated using a nanoprecipitation method.[15] In brief, 60 mg of PLGA were dissolved in 3 mL of acetone to form the organic phase. The PLGA-in-acetone solution was injected perpendicularly into 10 mL of 0.5% (w/v) poly(vinyl alcohol) aqueous solution by a vertically mounted syringe pump with magnetic stir agitation (1200 rpm). The resultant suspension was continuously stirred under vacuum for 6 h to eliminate acetone. PLGA nanoparticles were collected by centrifugation at 10,000 *g*, 4 °C for 45 min.

Liposomes were fabricated with a hydration-sonication method.[12] In brief, 15 mg of lipid mixture, which consisted of DOTAP, DSPE-PEG2000-maleimide, and CHOL at a molar ratio of 90: 5: 5, was placed under vacuum to form a lipid film. The film was hydrated with 1 mL of pre-heated 0.01 M phosphate buffer saline (PBS). The resultant suspension was sonicated for 2 min to form liposomes.

Lipid-polymeric hybrid nanoparticles were assembled by coating liposomes onto PLGA nanoparticles using a sonication method. In brief, 15 mg of liposomes in PBS was mixed with 60 mg of PLGA nanoparticles. The mixture was sonicated using a Branson 1800 Ultrasonic Cleaner for 8 min. The resultant lipid-polymeric hybrid nanoparticles were collected by centrifugation at 10,000 *g*, 4 °C for 30 min.

6.2.3 Synthesis and characterization of Nic-stimulating protein conjugates

Nic-stimulating protein conjugates (Nic-KLH, Nic-KS, Nic-CRM_{197}, and Nic-TT) were synthesized using an EDC/NHS-mediated reaction.[12] In brief, an appropriate amount of Nic-haptens was dissolved in 0.5 mL activation buffer (0.1 M MES, 0.5 M NaCl, pH 6.0). EDC and NHS (EDC: NHS: Nic-hapten = 10: 10: 1) were subsequently added. The mixture was incubated at room temperature for 30 min to activate Nic-haptens. Ten mg of stimulating proteins that were dissolved in 3 mL of a coupling buffer (0.1 M PBS, pH 7.4) were mixed with the activated Nic-haptens. The reaction was allowed to proceed for 10 h, and unconjugated Nic-haptens were eliminated by dialysis. The Nic-hapten loading in Nic-stimulating protein conjugates were estimated by a 2,4,6-trinitrobenzene sulfonic acid (TNBSA)-based method.[11] In brief, stimulating proteins and Nic-stimulating protein conjugates were prepared at a concentration of 1 mg/mL. Two hundred μL of the protein solution was mixed with 200 μL of 4% $NaHCO_3$ solution. Two hundred μL of 0.1% TNBSA solution was added to the mixture and incubated at 37 °C for 1 h, and the absorbance was read at 335 nm. Glycine was used as an amino standard. Unconjugated stimulating proteins were used as a control. Hapten density was calculated from the differences between the O.D. of the control and the conjugates.

6.2.4 Assembly of NanoNicVac particles

NanoNicVac particles were assembled by a thiol-maleimide-mediated reaction.[12] In brief, an appropriate amount of Traut's reagent was added to 6 mg of Nic-stimulating protein conjugates that were dissolved in 2 mL of 0.01 M PBS. The mixture was incubated at room temperature for 1 h to form thiolated Nic-stimulating protein conjugates. The activated conjugates were added to 75 mg of lipid-polymeric hybrid nanoparticles and incubated for 2 h. NanoNicVac nanoparticles were separated by centrifugation at 10,000 *g*, 4 °C for 30 min. Unconjugated Nic-stimulating protein conjugates in the supernatants were quantified by the bicinchoninic acid assay.

6.2.5 Characterization of nanoparticles

The morphology of nanoparticles was characterized by transmission electron microscopy (TEM). Nanoparticles were negatively stained with 1% phosphotungstic acid and imaged on a JEM 1400 transmission electron microscope (JEOL, Tokyo, Japan). The conjugation of protein antigens to the surface of hybrid nanoparticles was verified by confocal laser scanning microscopy (CLSM). Fluorescent NanoNicVac particles, in which the PLGA core, lipid-shell, and stimulating proteins were labeled by Nile red, NBD, and AF350, respectively, were imaged on a Zeiss LSM 510 laser scanning microscope (Carl Zeiss, Germany). The average size and zeta-potential of nanoparticles were measured on a Malvern Nano ZS Zetasizer (Malvern Instruments, Worcestershire, United Kingdom).

6.2.6 *In vitro* study of uptake and processing of NanoNicVac by dendritic cells

JAWSII (ATCC® CRL-11904™) immature dendritic cells were cultured in alpha minimum essential medium supplemented with 5 ng/mL murine GM-CSF and fetal bovine serum (20%) at 37 °C with 5% CO_2. Coumarin-6 (CM-6)-labeled NanoNicVac nanoparticles were prepared by encapsulating 1% (w/w) CM-6 in the PLGA core during the nanoprecipitation process. AF647-

labeled NanoNicVac particles were fabricated by conjugating AF647-stimulating protein conjugates to nanoparticles. The uptake of NanoNicVac particles was quantitatively studied by flow cytometry. In brief, cells (2×10^6/well) were seeded into 6-well plates and cultured overnight. Cells were treated with 50 μg of CM-6-labeled NanoNicVac particles for 10, 90, or 240 min. The medium was removed, and the cells were washed three times using PBS. Cells were detached from plates by trypsinization and re-suspended in PBS. Samples were immediately analyzed on a FACSAria I flow cytometer (BD Biosciences, Franklin Lakes, NJ, USA). The uptake and processing of NanoNicVac particles were qualitatively studied by CLSM. In brief, cells (2×10^5/chamber) were seeded into 2-well chamber slides and cultured overnight. Cells were treated with 50 μg of AF647-labeled NanoNicVac particles for 10 or 90 min. At 90 min, the medium containing NPs were replaced with fresh medium, and the cells were continuously incubated for 240 min. Cells were fixed with 4% (w/v) paraformaldehyde. The nuclei of cells were stained by 4',6-diamidino-2-phenylindole (DAPI). Cells were imaged on a Zeiss LSM 510 laser scanning microscope.

6.2.7 *In vivo* study of the immunogenicity and efficacy of NanoNicVac in mice

Animal studies were carried out following the National Institutes of Health guidelines for animal care and use. Animal protocols were approved by the Institutional Animal Care and Use Committee at Virginia Tech. Female Balb/c mice (6-7 weeks, 5-6 per group) were immunized with nicotine vaccines or PBS on days 0, 14, and 28. For NanoNicVac groups, mice were injected with 200 μL of nanovaccines (Nano-KLH-Nic, Nano-KS-Nic, Nano-CRM_{197}-Nic, or Nano-TT-Nic) containing 25 μg of protein antigens. For the Nic-TT conjugate group, mice were immunized with a mixture of 25 μg Nic-TT and 40 μg Alum that were dissolved in 200 μL of PBS. For the control

group, mice were injected with 200 μL of sterilized PBS. Blood samples were collected on days 0, 12, 26, and 40.

Titers of anti-nicotine antibody, anti-nicotine IgG subclass antibody (IgG1, IgG2a, IgG2b, and IgG3), and anti-stimulating protein antibody in the serum were assayed by an enzyme-linked immunosorbent assay (ELISA) using a method reported previously.[12] Antibody titer was defined as the dilution factor at which absorbance at 450 nm dropped to half maximal.

The affinity and specificity of anti-nicotine antibodies induced by nicotine vaccines were estimated by a competition ELISA method. In brief, serum samples were diluted to a factor at which the absorbance at 450 nm was around 1. Inhibitors (nicotine, cotinine, nornicotine, nicotine-N-oxide, and acetylcholine) with concentrations of 10^{-2} to 10^{-6} M were serially prepared. Inhibitor samples were added to plates that were coated with Nic-BSA, and serum samples were subsequently added. The following steps were the same as in measuring anti-nicotine antibody titers. Percent inhibition was calculated at each inhibitor concentration, and the concentration at which 50% inhibition was achieved (IC_{50}) was determined. Pooled serum samples were used for specificity estimation.

The ability of nicotine nanovaccines to reduce nicotine in the brain of mice was evaluated using a method reported previously.[12] Balb/c female mice (6-7 weeks, 5-6 per group) were immunized as described in the previous context. On day 42, mice were dosed 0.06 mg/kg of nicotine subcutaneously. After 3 min, mice were sacrificed, and the brain and blood samples were collected. The nicotine levels in the brain and serum samples were measured using a GC/MS method as reported previously.[25]

6.2.8 Assessment of the safety of NanoNicVac by Histopathological examination

On day 42, major organs of immunized mice, including heart, liver, spleen, kidney, and lung, were extracted and stored in 10% formalin. The organs were processed by a hematoxylin and eosin staining method. Tissue blocks were imaged on a Nikon Eclipse E600 light microscope (Melville, NY, USA).

6.2.9 Statistical analyses

Data were expressed as means ± standard error of the mean (MSE) unless specified. Comparisons among multiple groups were conducted with one-way ANOVA followed by Tukey's HSD test. Differences were considered significant when p-values were less than 0.05.

6.3 Results

6.3.1 Morphological and physicochemical properties of NanoNicVac conjugated with different stimulating proteins

CLSM was used to characterize the structure of NanoNicVac nanoparticles conjugated with different stimulating proteins. The PLGA core, lipid shell, and stimulating proteins were labeled by Nile Red, NBD, and AF-350, respectively. The co-localization of red, green, and blue fluorescence on most of the particles (**Figure 1B**) suggested the successful and efficient assembly of NanoNicVac particles. The morphology of nanoparticles was characterized by TEM. As shown in **Figure 1C**, a "core-shell" structure was shown on lipid-polymeric (LP) hybrid nanoparticles. Upon conjugation of Nic-stimulating protein conjugates, a dark layer, which was formed by protein antigens, was observed on all four NanoNicVac nanoparticles. This further verified the efficient conjugation of protein antigens to hybrid nanoparticle surface.

The physicochemical properties of NanoNicVac were also characterized. As shown in **Figure 1D**, all four NanoNicVac nanoparticles exhibited narrow size distributions. This narrow size distribution is in concordance with the uniform size shown in the TEM images (**Figure 1C**) and the low PDI indexes (**Table 1**). Specifically, the average size of Nano-KLH-Nic (167.2 nm) and Nano-KS-Nic (153.2 nm) was slightly larger than that of Nano-CRM_{197}-Nic (125.2 nm) and Nano-TT-Nic (136.6 nm) (**Table 1**). The four NanoNicVac nanoparticles, regardless of stimulating proteins, were negatively charged (indicated by the negative zeta-potentials shown in **Table 1**), which was probably caused by the conjugation of negatively-charged Nic-stimulating protein conjugates. The conjugation efficiency of Nic-stimulating protein conjugates was 87.6 ± 7.9%, 83.2 ± 11.3%, 90.0 ± 7.6%, and 84.3 ± 9.4% for Nano-KLH-Nic, Nano-KS-Nic, Nano-CRM_{197}-Nic, and Nano-TT-Nic, respectively (**Table 1**). Meanwhile, the loading contents of Nic-haptens on NanoNicVac particles were 0.88 ± 0.07, 0.93 ± 0.12, 0.84 ± 0.07, and 0.81 ±0.09 μg Nic/mg nanoparticle, respectively. This suggested that the four NanoNicVac nanoparticles had similar hapten loading contents.

6.3.2 Cellular uptake and processing of NanoNicVac by dendritic cells

The uptake efficiency of NanoNicVac nanoparticles by dendritic cells were studied by FCA. As shown in **Figure 2A**, >95.3% of the studied cells had taken up nanoparticles in all four NanoNicVac groups after being incubated with nanoparticles for 10 min. This revealed that NanoNicVac nanoparticles could be internalized by dendritic cells efficiently in a short period of time. As shown in **Figure 2B**, indicated by the significantly increased mean fluorescence intensity (M. F. I.) of CM-6, NanoNicVac nanoparticles were continuously internalized from 10 to 90 min. However, the M. F. I. of CM-6 at 240 min was similar to that at 90 min, suggesting that the uptake of NanoNicVac was saturated after 90 min. Meanwhile, all four NanoNicVac, regardless of

stimulating proteins, had a similar cellular uptake efficiency, as they exhibited comparable M. F. I. of CM-6 at all the studied time points.

The processing of stimulating proteins carried by NanoNicVac was studied using CLSM (**Figure 2C**). The stimulating proteins on NanoNicVac particles were labeled by AF647. At 10 min, the AF647 fluorescence displayed as individual dots in cells, revealing that the stimulating proteins had not been processed. At 90 min, a substantial amount of AF647 fluorescence was found to spread throughout the cells. This suggested that the stimulating proteins began to be processed to small peptidic antigens. At 240 min, a substantial percentage of AF647 fluorescence was still observed to display as individual dots in the Nano-KLH-Nic and Nano-KS-Nic groups, indicating KLH and KS stimulating proteins had not been completely processed. Interestingly, less red individual dots were found in cells treated with Nano-CRM_{197}-Nic and Nano-TT-Nic, suggesting that CRM_{197} and TT stimulating proteins were efficiently processed to small peptidic antigens. NanoNicVac conjugated with CRM_{197} or TT appeared to be processed more efficiently than that conjugated with KLH or KS.

6.3.3 Immunogenicity of NanoNicVac conjugated with different stimulating proteins against nicotine

The immunogenicity of NanoNicVac against nicotine was tested in female Balb/c mice. As shown in **Figure 3A**, comparable anti-nicotine antibody titers were found in all nicotine vaccine groups 12 days after the primary immunization (on day 12). The anti-nicotine antibody levels significantly increased in all vaccine groups 12 days after the first booster immunization (on day 26). Twelve days after the second booster immunization (on day 40), the anti-nicotine antibody titers increased by 7.5×10^3, 5.6×10^3, 26.3×10^3, 17.5×10^3, and 4.8×10^3 in Nano-KLH-Nic, Nano-KS-Nic, Nano-

CRM_{197}-Nic, Nano-TT-Nic, and Nic-TT + alum groups, respectively, compared to that on day 26. The second booster immunization boosted antibody titers in the groups of Nano-CRM_{197}-Nic and Nano-TT-Nic more significantly than in the other groups. The end-point anti-nicotine antibody titers of individual mice on day 40 are shown in **Figure 3B**. Compared to TT-Nic + alum, Nano-TT-Nic induced a significantly higher anti-nicotine antibody titer ($p < 0.05$). This suggested that conjugating hapten-protein conjugates to the hybrid nanoparticle surface would enhance the immunogenicity of the conjugate nicotine vaccine. The titers of Nano-CRM_{197}-Nic and Nano-TT-Nic were comparable ($p > 0.91$), and were significantly higher than that of Nano-KLH-Nic and Nano-KS-Nic ($p < 0.05$). These indicate NanoNicVac conjugated with CRM_{197} or TT had an enhanced immunogenicity against nicotine when compared to NanoNicVac carrying KLH or KS.

6.3.4 Subclass distribution of anti-nicotine IgG antibodies elicited by NanoNicVac

The titers of anti-nicotine IgG subclass antibodies on day 40 were assayed and presented in **Figure 3C**. For all vaccine groups, IgG1 and IgG3 were the most and least dominant subtype, respectively. Compared to Nic-TT conjugate vaccine, Nano-TT-Nic resulted in higher titers of all four IgG subtypes, especially IgG1 and IgG2a, which are consistent with our previous report.[12] Nano-CRM_{197}-Nic and Nano-TT-Nic induced higher levels of IgG1, IgG2a, and IgG3 than Nano-KLH-Nic and Nano-KS-Nic. Specifically, Nano-CRM_{197}-Nic generated the highest IgG1 titer among the four NanoNicVac vaccines. The IgG1 titer of Nano-CRM_{197}-Nic was significantly higher than that of Nano-KLH-Nic and Nano-KS-Nic ($p < 0.01$). Nano-TT-Nic induced the highest IgG2a titer among the four NanoNicVac vaccines, and the IgG2a titer of Nano-TT-Nic was significantly higher than that of Nano-KLH-Nic and Nano-KS-Nic ($p < 0.05$). Interestingly, although the overall IgG titer of Nano-KLH-Nic is slightly higher than that of Nano-KS-Nic (**Figure 3B**), Nano-KLH-Nic had a higher IgG1 titer but lower IgG2a and IgG2b titers compared to Nano-KS-Nic. The

Th1/Th2 indexes were 0.044, 0.192, 0.075, 0.239, and 0.142 for Nano-KLH-Nic, Nano-KS-Nic, Nano-CRM197-Nic, Nano-TT-Nic, and Nic-TT + alum, respectively. All the values were considerably less than 1, indicating that the immune responses induced by all nicotine vaccines were skewed toward Th2 (humoral response). Moreover, the indexes of Nano-TT-Nic and Nano-KS-Nic were considerably larger than that of Nano-KLH-Nic and Nano-CRM_{197}-Nic, indicating that Nano-TT-Nic and Nano-KS-Nic resulted in more balanced Th1/Th2 responses than Nano-KLH-Nic and Nano-CRM_{197}-Nic.

6.3.5 Anti-stimulating protein antibody levels induced by NanoNicVac carrying different stimulating proteins

Anti-stimulating protein antibody titers are shown in **Figure 4**. Similar to anti-nicotine antibody titers, the anti-stimulating protein antibody titers increased after each injection. On day 12, the anti-stimulating protein antibody titers were $(1.8 \pm 0.1) \times 10^3$, $(1.9 \pm 0.2) \times 10^3$, $(0.5 \pm 0.1) \times 10^3$, $(1.9 \pm 0.1) \times 10^3$, and $(3.3 \pm 0.1) \times 10^3$, for Nano-KLH-Nic, Nano-KS-Nic, Nano-CRM_{197}-Nic, Nano-TT-Nic, and Nic-TT + alum, respectively. On day 26, the titers increased to $(35.3 \pm 2.2) \times 10^3$, $(35.2 \pm 2.5) \times 10^3$, $(16.0 \pm 6.0) \times 10^3$, $(23.5 \pm 12.8) \times 10^3$, and $(42.2 \pm 4.2) \times 10^3$, respectively. On day 40, the titers further increased to $(46.2 \pm 1.8) \times 10^3$, $(50.9 \pm 4.6) \times 10^3$, $(27.5 \pm 0.2.9) \times 10^3$, $(36.6 \pm 2.5) \times 10^3$, and $(51.4 \pm 4.0) \times 10^3$, respectively. On all the studied days, Nano-TT-Nic induced significantly lower anti-stimulating protein antibody titers compared to Nic-TT + alum ($p < 0.05$). Among the four NanoNicVac carrying different stimulating proteins, Nano-CRM_{197}-Nic and Nano-TT-Nic elicited considerably lower anti-stimulating protein antibody levels than Nano-KLH-Nic and Nano-KS-Nic, especially on days 26 and 40.

6.3.6 Affinity of anti-nicotine antibodies generated by NanoNicVac

The affinity of anti-nicotine antibodies elicited by NanoNicVac carrying different stimulating proteins was estimated by competition ELISA on days 12, 26, and 40 (**Figure 5**). The affinity of antibodies increased after each immunization in all nicotine vaccine groups, except the Nano-KLH-Nic group, in which the antibody affinity slightly decreased after the second booster immunization. On day 40, the IC_{50} of nicotine was 96 ± 35, 137 ± 92, 167 ± 78, 212 ± 103, and 277 ± 199 μM for Nano-KLH-Nic, Nano-KS-Nic, Nano-CRM_{197}-Nic, Nano-TT-Nic, and Nic-TT + alum, respectively. The antibodies induced by Nano-TT-Nic had a comparable affinity to that elicited by Nic-TT + alum ($p > 0.99$). Nano-KLH-Nic resulted in the highest average antibody affinity, but the differences among the four NanoNicVac were not significant ($p > 0.92$). Interestingly, the maturation of anti-nicotine antibody affinity exhibited different patterns in the four NanoNicVac groups. Specifically, the maturation of antibody affinity in the Nano-KLH-Nic and Nano-KS-Nic groups was significantly completed after the first booster immunization, and the second booster immunization did not remarkably enhance the antibody affinity. In contrast, the anti-nicotine antibody affinity gradually increased in the Nano-CRM_{197}-Nic and Nano-TT-Nic groups. Both the first and second booster immunizations remarkably promoted the affinity maturation.

6.3.7 Specificity of anti-nicotine antibodies elicited by NanoNicVac

The specificity of anti-nicotine antibodies on day 40 was assayed by competition ELISA. The dose-dependent inhibitions of nicotine binding by nicotine metabolites (cotinine, nornicotine, and nicotine-N-oxide) and endogenous nicotine receptor ligand (acetylcholine) are shown in **Figure 6**. As shown in **Figure 6A-E**, in all nicotine vaccine groups, anti-nicotine antibodies had the highest relative affinity to nicotine. A somewhat lower affinity was detected to the inactive nicotine metabolite (cotinine) and active but minor nicotine metabolite (nornicotine) in all nicotine vaccine

groups. Specifically, the cross-reactivity between nicotine and cotinine was less than 2%, and that between nicotine and nornicotine was less than 7%, in all groups (**Figure 6F**). Meanwhile, antibodies elicited by all nicotine vaccines had little affinity for the inactive nicotine metabolite (nicotine-N-oxide) and endogenous nicotine receptor ligand (acetylcholine). The cross-reactivity between nicotine and nicotine-N-oxide/acetylcholine was less than 1% in all groups (**Figure 6F**). The anti-nicotine antibodies generated by NanoNicVac, regardless of stimulating protein, exhibited high specificity for nicotine.

6.3.8 Effect of NanoNicVac conjugated with different stimulating proteins on reducing brain concentrations of nicotine

The ability of NanoNicVac to retain nicotine in serum and reduce nicotine in the brain of mice was evaluated. **Figure 7A** shows the serum nicotine levels of mice 3 min after being challenged with 0.06 mg/kg nicotine subcutaneously. More nicotine was retained in serum after immunization with NanoNicVac, regardless of the stimulating proteins used. Compared to that of the unvaccinated, PBS-treated group, the serum nicotine levels of Nano-KLH-Nic, Nano-KS-Nic, Nano-CRM_{197}-Nic, and Nano-TT-Nic increased by 79.2%, 21.6%, 403.7%, and 370.7%, respectively. Nano-CRM_{197}-Nic and Nano-TT-Nic exhibited considerably better abilities for sequestering nicotine in the serum of mice than Nano-KLH-Nic and Nano-KS-Nic. The brain nicotine levels of mice after being challenged with nicotine are shown in **Figure 7B**. All NanoNicVac groups, regardless of the stimulating proteins used, had significantly lower brain nicotine concentrations than the PBS-treated group ($p < 0.001$). Specifically, the brain nicotine levels were lowered by 48.5%, 45.9%, 65.2%, and 63.1% after treatment with Nano-KLH-Nic, Nano-KS-Nic, Nano-CRM_{197}-Nic, and Nano-TT-Nic groups, compared to nicotine levels in PBS-treated mice. Nano-CRM_{197}-Nic and Nano-TT-Nic had a significantly better capability for reducing nicotine in the brain of mice than

Nano-KS-Nic ($p < 0.05$). Meanwhile, Nano-CRM_{197}-Nic and Nano-TT-Nic also exhibited a considerably better ability in reducing the brain nicotine concentrations than Nano-KLH-Nic. Overall, NanoNicVac conjugated with CRM_{197} or TT had an enhanced efficacy in sequestering nicotine in serum and reducing nicotine levels in brain than NanoNicVac conjugated with KLH or KS.

6.3.9 Safety of NanoNicVac carrying different stimulating proteins

The safety of NanoNicVac was evaluated by histopathological analysis. **Figure 8** shows the images of major organs of mice after being treated with PBS or NanoNicVac conjugated with different stimulating proteins. No significant differences on all the studied organs were found between the PBS group and all NanoNicVac groups. None of the four NanoNicVac conjugated with different stimulating proteins caused detectable lesions to mouse organs, suggesting they would be safe.

6.4 Discussion

Conventional hapten-protein conjugate nicotine vaccines tested in human clinical trials have not proven to enhance overall smoking cessation rate so far.[5-7] In our previous work, we suggested a novel strategy to improve the immunological efficacy of conjugate nicotine vaccines by using biodegradable lipid-polymeric hybrid nanoparticles as delivery vehicles.[12, 13] The hybrid nanoparticle-based nicotine nanovaccine (NanoNicVac) was demonstrated to have a significantly higher immunogenicity than the conjugate nicotine vaccine. In addition, we proved that the immunogenicity of NanoNicVac could be enhanced by modulating the particle size [12], hapten density [14], and hapten localization [15]. In this study, we developed a series of NanoNicVac in which various potent stimulating proteins were conjugated with, and systemically studied their

physicochemical properties, cellular uptake and processing by immune cells, immunogenicity, and ability to lower brain nicotine concentrations. We demonstrated in this current work that enhanced immunological efficacy could be achieved by conjugating CRM_{197} or TT to NanoNicVac, making NanoNicVac be a promising next-generation nanoparticle-based immunotherapeutic against nicotine addiction.

The ELISA results demonstrated that NanoNicVac conjugated with TT (Nano-TT-Nic) exhibited a significantly higher immunogenicity against nicotine over Nic-TT + alum even in the absence of alum adjuvant. This result is in agreement with our previous report that Nano-KLH-Nic was more immunogenic against nicotine than the Nic-KLH conjugate.[12] Also, the result strengthened our hypothesis that the use of hybrid nanoparticles as delivery vehicles improves the immunogenicity of conjugate nicotine vaccines. The higher immunogenicity of Nano-TT-Nic over Nic-TT may be attributed to the better recognition and internalization by immune cells. The conjugation of multiple TT-Nic to one hybrid nanoparticle may increase the availability of antigens for uptake, thus contributing to an enhanced antigen internalization. Meanwhile, the immune system prefers to recognize and take up particulate pathogens (such as bacteria and virus) and is relatively invisible to small soluble protein antigens.[26-28] The stable and spherical lipid-polymeric hybrid nanoparticles[29-33] endowed Nano-TT-Nic with a particulate property that mimics that of particulate pathogens. This particulate nature together with the optimal particle size (~100 nm) is beneficial for improved recognition and uptake by immune cells.[12, 34]

Efficient uptake and processing of NanoNicVac by antigen presenting cells (such as dendritic cells and macrophages) are prerequisites for the generation of a potent immune response.[5, 35, 36] The *in vitro* data demonstrated that NanoNicVac conjugated with different stimulating proteins were similarly taken up but differently processed by dendritic cells. All NanoNicVac developed in this

study, regardless of stimulating proteins, were found to be internalized rapidly and efficiently. The rapid and efficient internalization of vaccine particles may provide sufficient amounts of antigens for processing, and thus contributes to the generation of a quick immune response. The CLSM data suggested that Nano-CRM_{197}-Nic and Nano-TT-Nic, especially Nano-CRM_{197}-Nic, were processed more efficiently than Nano-KLH-Nic and Nano-KS-Nic. This higher effectiveness of antigen processing may be attributed to the smaller size and lower structural complexity of CRM_{197} and TT as stimulating proteins. KS has a molecular weight of ~400 kDa, and KLH multimer is an assembled form of multiple KS.[37] Both of them have a relatively high structural complexity due to the large size. In contrast, CRM_{197} and TT have a molecular weight of ~150 kDa and ~59 kDa, respectively. The relatively small size makes them have a relatively low structural complexity.[38, 39] Immunologically, the generation of an effective humoral immune response requires two T cell-dependent processes, the formation of T helper cells and the interaction between B cells and T-helper cells, both of which only occur via the presentation of peptidic antigens on MHC of antigen presenting cells.[18, 40] Thus, the efficient processing of protein antigens to peptidic antigens may enhance the T cell-dependent processes, subsequently leading to a potent humoral immune response.

The immunogenicity data demonstrated that Nano-CRM_{197}-Nic and Nano-TT-Nic could induce significantly higher anti-nicotine antibody titers and considerably lower anti-stimulating protein antibody titers than Nano-KLH-Nic and Nano-KS-Nic. The lower antibody titers against stimulating proteins induced by Nano-CRM_{197}-Nic and Nano-TT-Nic may be caused by the relatively smaller size of CRM_{197} and TT. Compared with larger KS and KLH multimer, smaller CRM_{197} and TT had fewer immunogenic epitopes available for B cells, thus producing fewer anti-stimulating protein antibodies. A lower anti-stimulating protein antibody level is desirable in

nicotine vaccine design, as the anti-stimulating protein antibodies may neutralize the vaccine particles that are injected during booster immunizations. This neutralization may impair the efficacy of nicotine vaccines.[13, 41] Noticeably, the levels of anti-nicotine antibodies induced by NanoNicVac were in concordance with the effectiveness of antigen processing by dendritic cells. As discussed in the previous context, the efficient processing of protein antigens that were carried by Nano-CRM_{197}-Nic and Nano-TT-Nic would result in a potent T-cell immunity and contribute to an enhanced immunogenicity against nicotine. Interestingly, the second booster immunization boosted the anti-nicotine antibody titers in Nano-CRM_{197}-TT and Nano-TT-Nic groups more remarkably than in Nano-KLH-Nic and Nano-KS-Nic groups. Although we do not have direct evidences to show the mechanism, the following may explain the finding. On one hand, the higher effectiveness of Nano-CRM_{197}-Nic and Nano-TT-Nic in generating a T-cell immunity may enhance the humoral immune response, resulting in more anti-nicotine antibodies to be generated. On the other hand, Nano-CRM_{197}-Nic and Nano-TT-Nic had lower anti-stimulating protein antibody titers than Nano-KLH-Nic and Nano-KS-Nic after the first booster immunization. The lower anti-stimulating protein antibody levels may neutralize less vaccine particles administered in the second booster immunization, and thus leave more vaccine particles available for inducing the production of anti-nicotine antibodies. In agreement with the data of anti-nicotine antibody titer, affinity, and specificity, the pharmacokinetic data showed that NanoNicVac conjugated with CRM_{197} or TT exhibited better capability to sequester nicotine in serum and reduce nicotine entering the brain than NanoNicVac conjugated with KLH or KS.

In summary, a series of hybrid nanoparticle based nicotine nanovaccines (NanoNicVac) were developed in this study by conjugating potent stimulating proteins (KLH, KS, CRM_{197}, and TT) to the nanoparticle surface. Although all four NanoNicVac were taken up by dendritic cells

efficiently, NanoNicVac conjugated with CRM_{197} or TT were processed more efficiently than that conjugated with KLH or KS. In addition, compared to NanoNicVac carrying KLH or KS, NanoNicVac conjugated with CRM_{197} or TT induced remarkably higher anti-nicotine antibody titers and considerably lower anti-stimulating protein antibody levels. Meanwhile, the anti-nicotine antibodies induced by all four NanoNicVac, regardless of stimulating proteins, exhibited high affinity and specificity to nicotine. Also, NanoNicVac conjugated with CRM_{197} or TT had better capability to reduce nicotine in the brain of mice than NanoNicVac conjugated with KLH or KS. This study illustrated the necessity of selecting potent stimulating proteins in maximizing the immunological efficacy of nicotine nanovaccine. The findings can potentially be applied in the development of other drug abuse and nanoparticle-based vaccines. Furthermore, NanoNicVac with boosted immunological efficacy could be a promising candidate for treating nicotine addiction.

Conflict of interest

The authors declare no competing financial interests.

Acknowledgment

This work was financially supported by National Institute on Drug Abuse (U01DA036850). We thank Andrew Lees from Fina Biosolutions for providing us with CRM_{197}.

References

[1] Benowitz NL. Nicotine addiction. N Engl J Med. 2010;362:2295-303.

[2] Prochaska JJ, Benowitz NL. The past, present, and future of nicotine addiction therapy. Annual Review of Medicine, Vol 67. 2016;67:467-86.

[3] Polosa R, Benowitz NL. Treatment of nicotine addiction: present therapeutic options and pipeline developments. Trends Pharmacol Sci. 2011;32:281-9.

[4] Moreno AY, Janda KD. Immunopharmacotherapy: Vaccination strategies as a treatment for drug abuse and dependence. Pharmacology Biochemistry and Behavior. 2009;92:199-205.

[5] Pentel PR, LeSage MG. New directions in nicotine vaccine design and use. Emerging Targets & Therapeutics in the Treatment of Psychostimulant Abuse. 2014;69:553-80.

[6] Cornuz J, Zwahlen S, Jungi WF, Osterwalder J, Klingler K, van Melle G, et al. A Vaccine against nicotine for smoking cessation: A randomized controlled trial. Plos One. 2008;3.

[7] Hatsukami DK, Jorenby DE, Gonzales D, Rigotti NA, Glover ED, Oncken CA, et al. Immunogenicity and smoking-cessation outcomes for a novel nicotine immunotherapeutic. Clinical Pharmacology & Therapeutics. 2011;89:392-9.

[8] Goniewicz ML, Delijewski M. Nicotine vaccines to treat tobacco dependence. Hum Vaccin Immunother. 2013;9:13-25.

[9] Raupach T, Hoogsteder PH, Onno van Schayck CP. Nicotine vaccines to assist with smoking cessation: current status of research. Drugs. 2012;72:e1-16.

[10] Hu Y, Zheng H, Huang W, Zhang CM. A novel and efficient nicotine vaccine using nano-lipoplex as a delivery vehicle. Hum Vacc Immunother. 2014;10:64-72.

[11] Zheng H, Hu Y, Huang W, de Villiers S, Pentel P, Zhang JF, et al. Negatively charged carbon nanohorn supported cationic liposome nanoparticles: A novel delivery vehicle for anti-nicotine vaccine. Journal of Biomedical Nanotechnology. 2015;11:2197-210.

[12] Zhao Z, Hu Y, Hoerle R, Devine M, Raleigh M, Pentel P, et al. A nanoparticle-based nicotine vaccine and the influence of particle size on its immunogenicity and efficacy. Nanomedicine. 2016.

[13] Hu Y, Smith D, Frazier E, Hoerle R, Ehrich M, Zhang C. The next-generation nicotine vaccine: a novel and potent hybrid nanoparticle-based nicotine vaccine. Biomaterials. 2016;106:228-39.

[14] Zhao Z, Powers K, Hu Y, Raleigh M, Pentel P, Zhang CM. Engineering of a hybrid nanoparticle-based nicotine nanovaccine as a next-generation immunotherapeutic strategy against nicotine addiction: A focus on hapten density. Biomaterials. 2017;123:107-17.

[15] Zhao Z, Hu Y, Harmon T, Pentel P, Ehrich M, Zhang C. Rationalization of a nanoparticle-based nicotine nanovaccine as an effective next-generation nicotine vaccine: A focus on hapten localization. Biomaterials. 2017;138:46-56.

[16] Crotty S. A brief history of T cell help to B cells. Nat Rev Immunol. 2015;15:185-9.

[17] Abbas AK, Murphy KM, Sher A. Functional diversity of helper T lymphocytes. Nature. 1996;383:787-93.

[18] Collins KC, Janda KD. Investigating hapten clustering as a strategy to enhance vaccines against drugs of abuse. Bioconjugate Chemistry. 2014;25:593-600.

[19] Jacob NT, Lockner JW, Schlosburg JE, Ellis BA, Eubanks LM, Janda KD. Investigations of enantiopure nicotine haptens using an adjuvanting carrier in anti-nicotine vaccine development. Journal of Medicinal Chemistry. 2016;59:2523-9.

[20] Fraser CC, Altreuter DH, Ilyinskii P, Pittet L, LaMothe RA, Keegan M, et al. Generation of a universal CD4 memory T cell recall peptide effective in humans, mice and non-human primates. Vaccine. 2014;32:2896-903.

[21] Bi SG, Bailey W, Brisson C. Performance of keyhole limpet hemocyanin (KLH) as an antigen carrier for protein antigens depends on KLH property and conjugation route. Journal of Immunology. 2016;196.

[22] Zhong TY, Arancibia S, Born R, Tampe R, Villar J, Del Campo M, et al. Hemocyanins stimulate innate immunity by inducing different temporal patterns of proinflammatory Cytokine Expression in Macrophages. Journal of Immunology. 2016;196:4650-62.

[23] McCluskie MJ, Thorn J, Gervais DP, Stead DR, Zhang NL, Benoit M, et al. Anti-nicotine vaccines: Comparison of adjuvanted CRM197 and Qb-VLP conjugate formulations for immunogenicity and function in non-human primates. International Immunopharmacology. 2015;29:663-71.

[24] Haile CN, Kosten TA, Shen XY, O'Malley PW, Winoske KJ, Kinsey BM, et al. Altered methamphetamine place conditioning in mice vaccinated with a succinyl-methamphetamine-tetanus-toxoid vaccine. American Journal on Addictions. 2015;24:748-55.

[25] de Villiers SHL, Cornish KE, Troska AJ, Pravetoni M, Pentel PR. Increased efficacy of a trivalent nicotine vaccine compared to a dose-matched monovalent vaccine when formulated with alum. Vaccine. 2013;31:6185-93.

[26] Storni T, Kundig TM, Senti G, Johansen P. Immunity in response to particulate antigen-delivery systems. Adv Drug Deliver Rev. 2005;57:333-55.

[27] Benne N, van Duijn J, Kuiper J, Jiskoot W, Slutter B. Orchestrating immune responses: How size, shape and rigidity affect the immunogenicity of particulate vaccines. J Control Release. 2016;234:124-34.

[28] De Temmerman ML, Rejman J, Demeester J, Irvine DJ, Gander B, De Smedt SC. Particulate vaccines: on the quest for optimal delivery and immune response. Drug Discov Today. 2011;16:569-82.

[29] Zheng MB, Yue CX, Ma YF, Gong P, Zhao PF, Zheng CF, et al. Single-step assembly of DOX/ICG loaded lipid-polymer nanoparticles for highly effective chemo-photothermal combination therapy. Acs Nano. 2013;7:2056-67.

[30] Zhang LF, Chan JM, Gu FX, Rhee JW, Wang AZ, Radovic-Moreno AF, et al. Self-assembled lipid-polymer hybrid nanoparticles: A robust drug delivery platform. Acs Nano. 2008;2:1696-702.

[31] Hu Y, Hoerle R, Ehrich M, Zhang CM. Engineering the lipid layer of lipid-PLGA hybrid nanoparticles for enhanced in vitro cellular uptake and improved stability. Acta Biomater. 2015;28:149-59.

[32] Hu Y, Zhao ZM, Ehrich M, Fuhrman K, Zhang CM. In vitro controlled release of antigen in dendritic cells using pH-sensitive liposome-polymeric hybrid nanoparticles. Polymer. 2015;80:171-9.

[33] Hadinoto K, Sundaresan A, Cheow WS. Lipid-polymer hybrid nanoparticles as a new generation therapeutic delivery platform: A review. Eur J Pharm Biopharm. 2013;85:427-43.

[34] Bachmann MF, Jennings GT. Vaccine delivery: a matter of size, geometry, kinetics and molecular patterns. Nat Rev Immunol. 2010;10:787-96.

[35] Metlay JP, Pure E, Steinman RM. Control of the immune-response at the level of antigen-presenting cells - a comparison of the function of dendritic cells and lymphocytes-B. Adv Immunol. 1989;47:45-116.

[36] Banchereau J, Steinman RM. Dendritic cells and the control of immunity. Nature. 1998;392:245-52.

[37] Harris JR, Markl J. Keyhole limpet hemocyanin (KLH): a biomedical review. Micron. 1999;30:597-623.

[38] Broker M, Costantino P, DeTora L, McIntosh ED, Rappuoli R. Biochemical and biological characteristics of cross-reacting material 197 (CRM197), a non-toxic mutant of diphtheria toxin: Use as a conjugation protein in vaccines and other potential clinical applications. Biologicals. 2011;39:195-204.

[39] Pichichero ME. Protein carriers of conjugate vaccines: Characteristics, development, and clinical trials. Hum Vacc Immunother. 2013;9:2505-23.

[40] Liu XW, Xu Y, Yu T, Clifford C, Liu Y, Yan H, et al. A DNA nanostructure platform for directed assembly of synthetic vaccines. Nano Lett. 2012;12:4254-9.

[41] Skolnick P. Biologic approaches to treat substance-use disorders. Trends Pharmacol Sci. 2015;36:628-35.

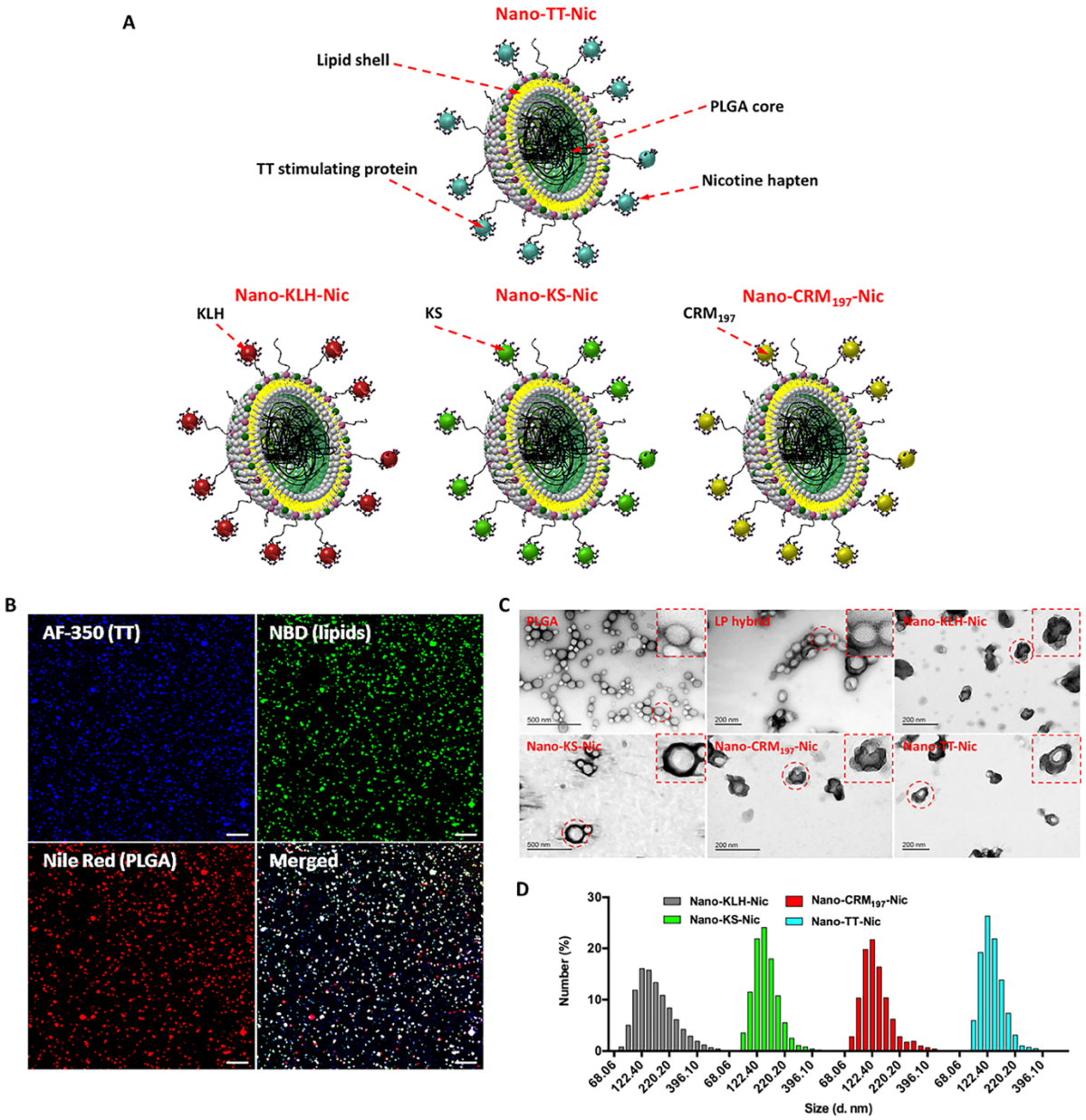

Figure 1. Synthesis and characterization of NanoNicVac. (A) Schematic illustration of NanoNicVac carrying different stimulating proteins. (B) CLSM images showing the co-localization of TT stimulating protein, lipid shell, and PLGA core, which were labeled by AF-350, NBD, and Nile Red, respectively. Scale bars represent 10 μm. (C) TEM images showing the morphological characteristics of NanoNicVac nanoparticles. (D) Dynamic size distribution of NanoNicVac nanoparticles.

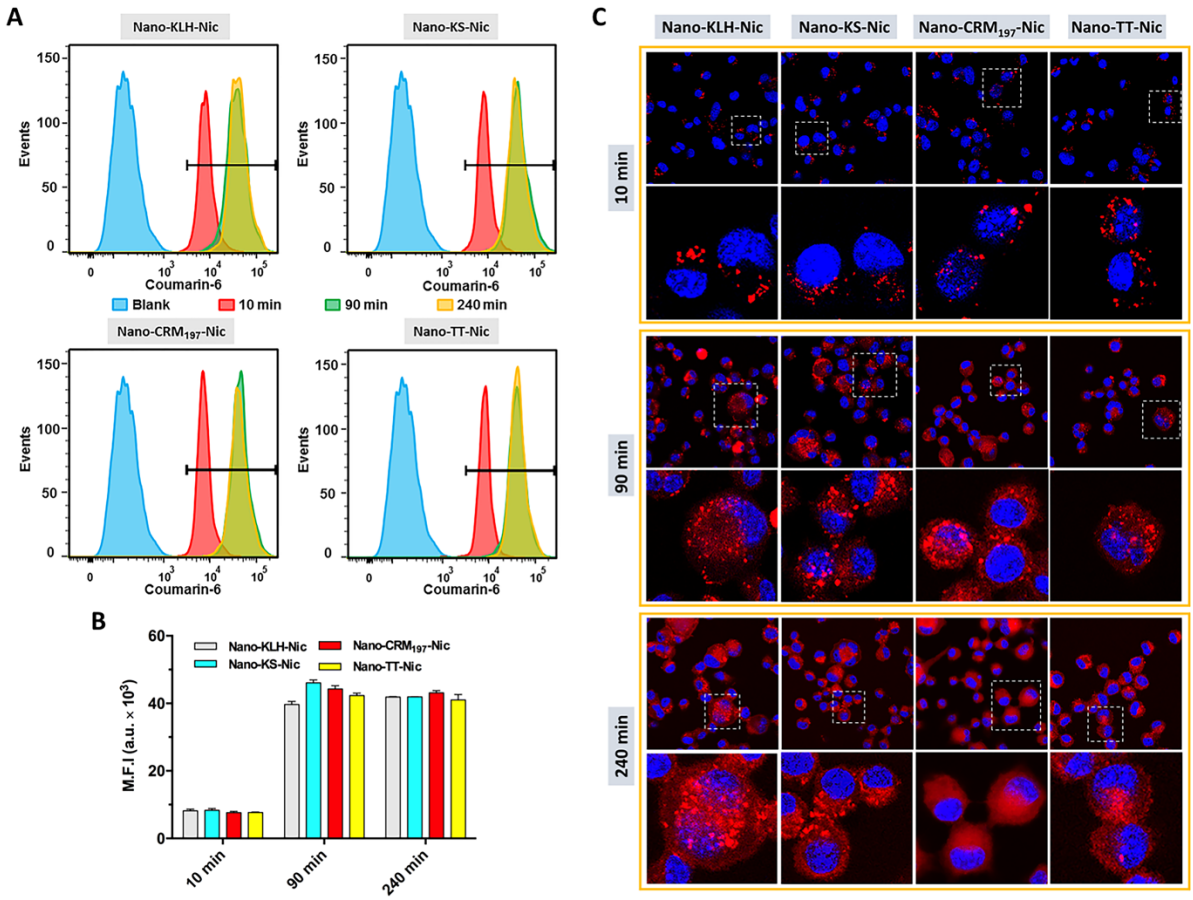

Figure 2. Cellular uptake and processing of NanoNicVac conjugated with different stimulating proteins. (A) Intensity distribution and (B) M.F.I. of CM-6 fluorescence in cells treated with CM-6 labeled NanoNicVac nanoparticles for 10, 90, or 240 min. Blank represents non-treated cells. (C) Processing of protein antigens carried by NanoNicVac particles. Protein antigens on NanoNicVac particles were labeled by AF647. Cells were treated with NanoNicVac particles for 10 or 90 min. The medium containing particles were replaced with fresh medium at 90 min, and cells were continuously incubated until 240 min.

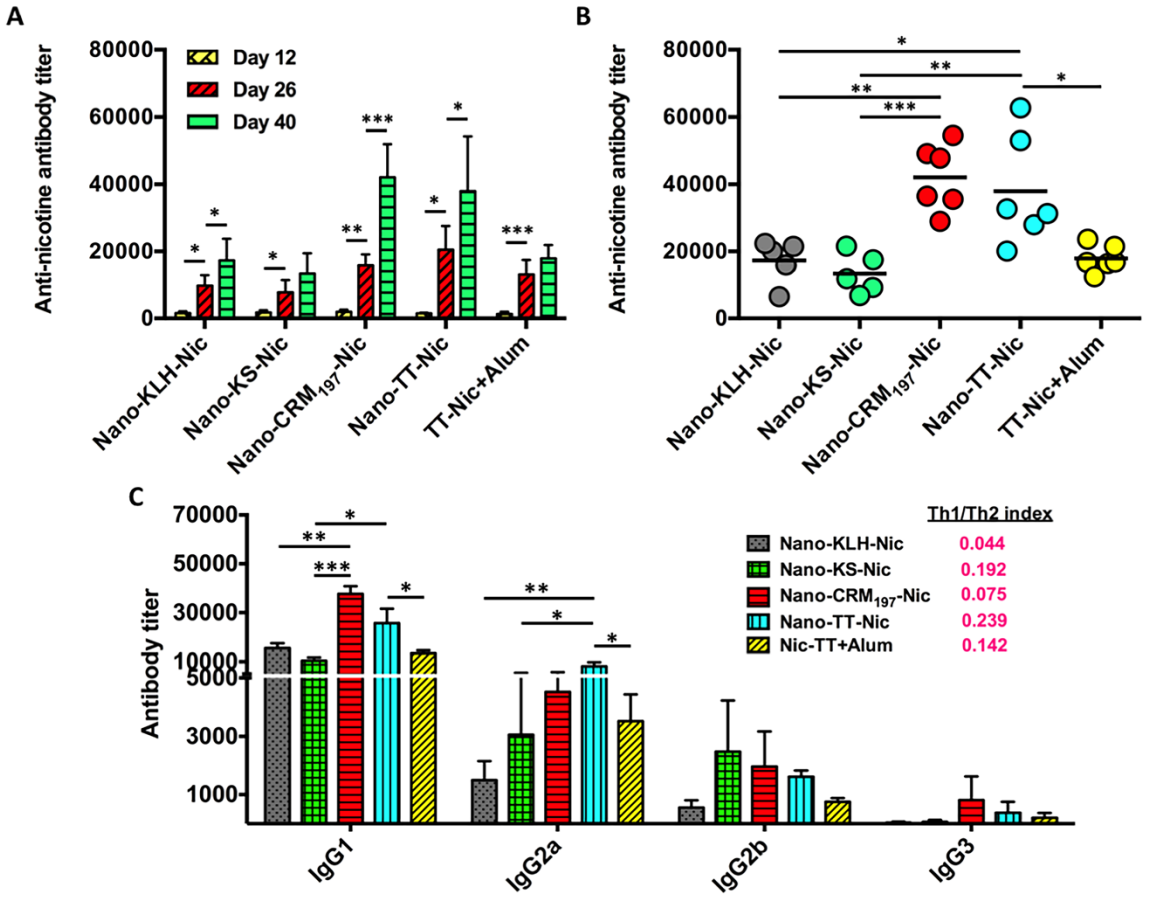

Figure 3. Immunogenicity of NanoNicVac conjugated with different stimulating proteins against nicotine. (A) Time-course of the anti-nicotine antibody titers induced by NanoNicVac. Bars are shown as means ± standard deviation. (B) End-point anti-nicotine antibody titers of individual mice on day 40. (C) Titers of anti-nicotine IgG subclass antibodies and Th1/Th2 indexes induced by NanoNicVac on day 40. Significantly different: * $p < 0.05$, ** $p < 0.01$, *** $p < 0.001$.

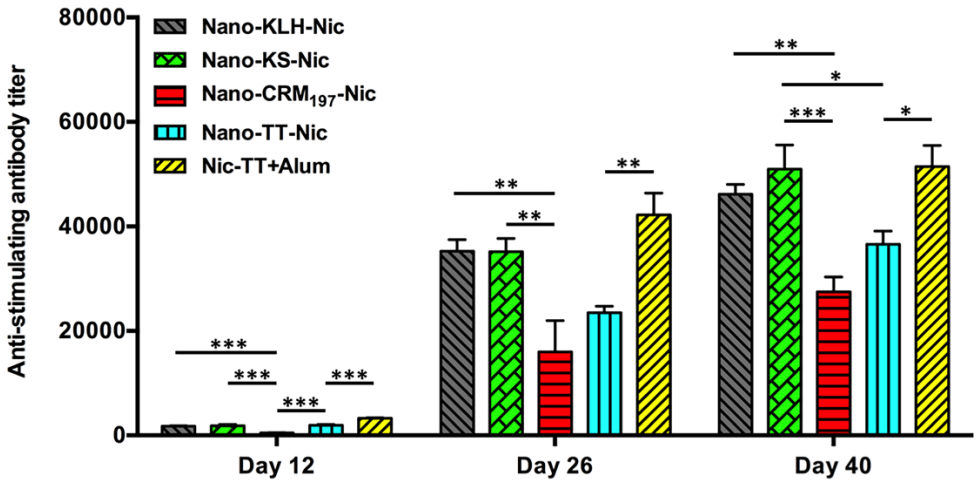

Figure 4. Time-course of anti-stimulating protein antibody titers induced by NanoNicVac with different stimulating proteins. Significantly different: * $p < 0.05$, ** $p < 0.01$, *** $p < 0.001$.

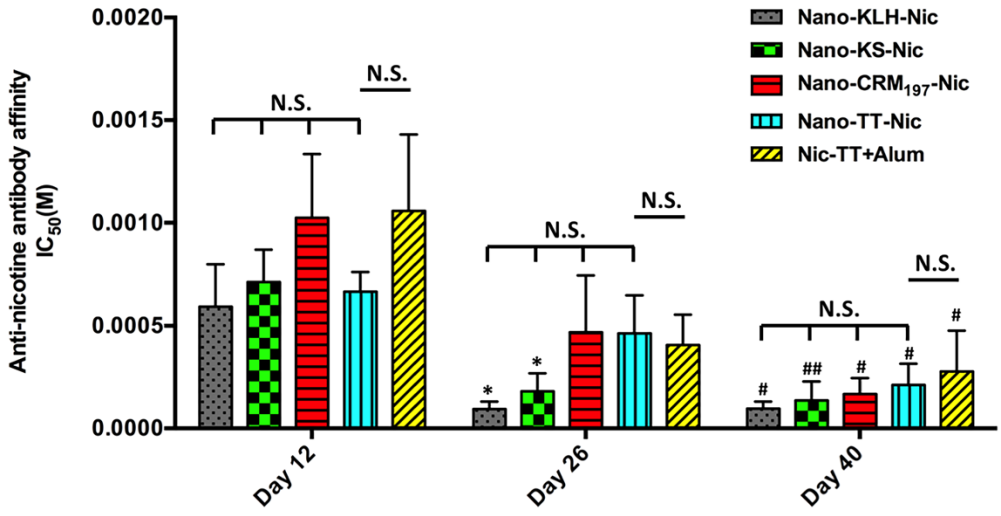

Figure 5. Affinity of anti-nicotine antibodies induced by nicotine vaccines estimated by competition ELISA. N.S. indicates no significant differences were found among groups ($p > 0.55$). Significantly different compared to the previous studied day: * $p < 0.05$. Significantly different compared to day 12: # $p < 0.05$, ## $p < 0.01$.

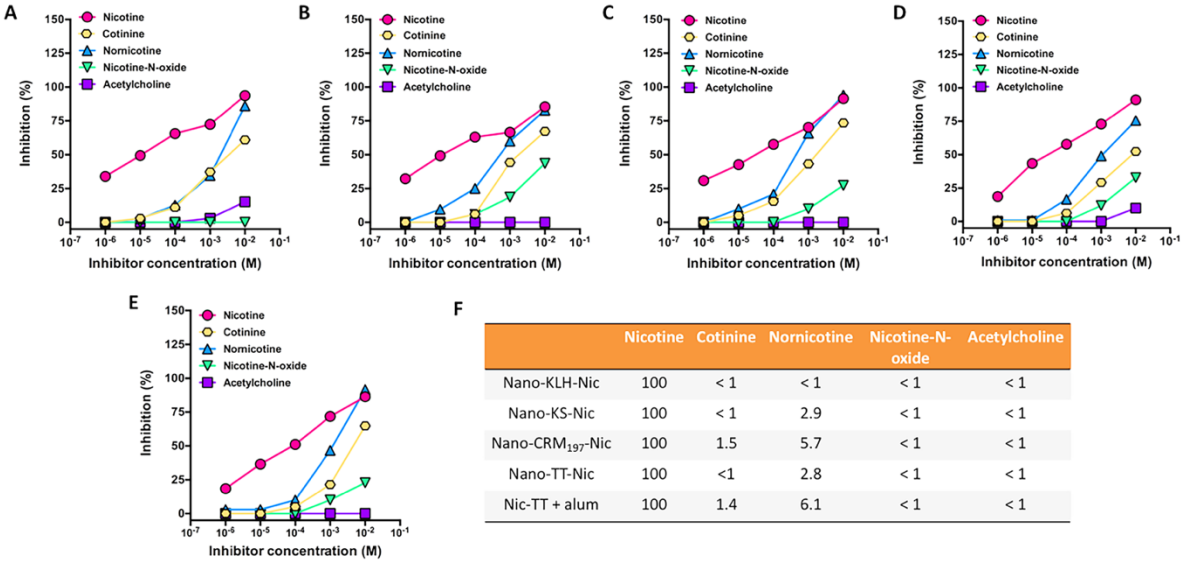

F

	Nicotine	Cotinine	Nornicotine	Nicotine-N-oxide	Acetylcholine
Nano-KLH-Nic	100	< 1	< 1	< 1	< 1
Nano-KS-Nic	100	< 1	2.9	< 1	< 1
Nano-CRM_{197}-Nic	100	1.5	5.7	< 1	< 1
Nano-TT-Nic	100	<1	2.8	< 1	< 1
Nic-TT + alum	100	1.4	6.1	< 1	< 1

Figure 6. Specificity of anti-nicotine antibodies induced by NanoNicVac conjugated with different stimulating proteins. Dose-dependent inhibitions of nicotine binding by various inhibitors in groups of (A) Nano-KLH-Nic, (B) Nano-KS-Nic, (C) Nano-CRM197-Nic, (D) Nano-TT-Nic, and (E) Nic-TT + alum were estimated by competition ELISA. (F) Percent ligand cross-reactivity defined as (IC_{50} of nicotine/IC_{50} of inhibitors).

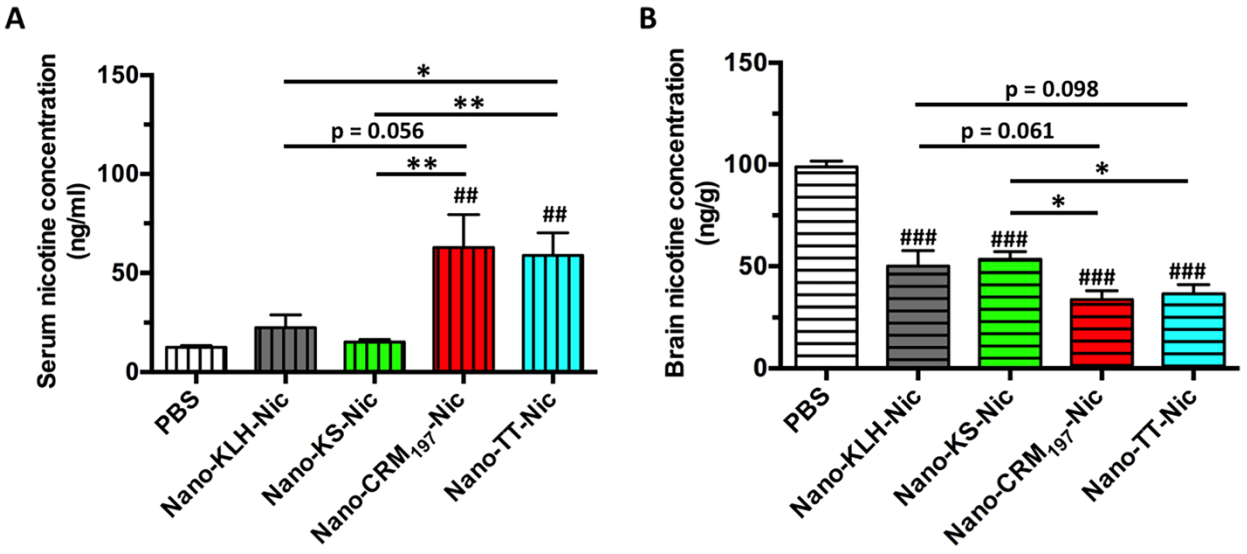

Figure 7. Effect of NanoNicVac conjugated with different stimulating proteins on influencing nicotine distribution in the serum and brain after nicotine challenge. The nicotine levels in the serum and brain of mice were analyzed 3 min after challenging the mice with 0.06 mg/kg nicotine subcutaneously. Significantly different compared to the PBS-treated group: ## $p < 0.01$, ### $p < 0.001$. Significantly different: * $p < 0.05$, ** $p < 0.01$.

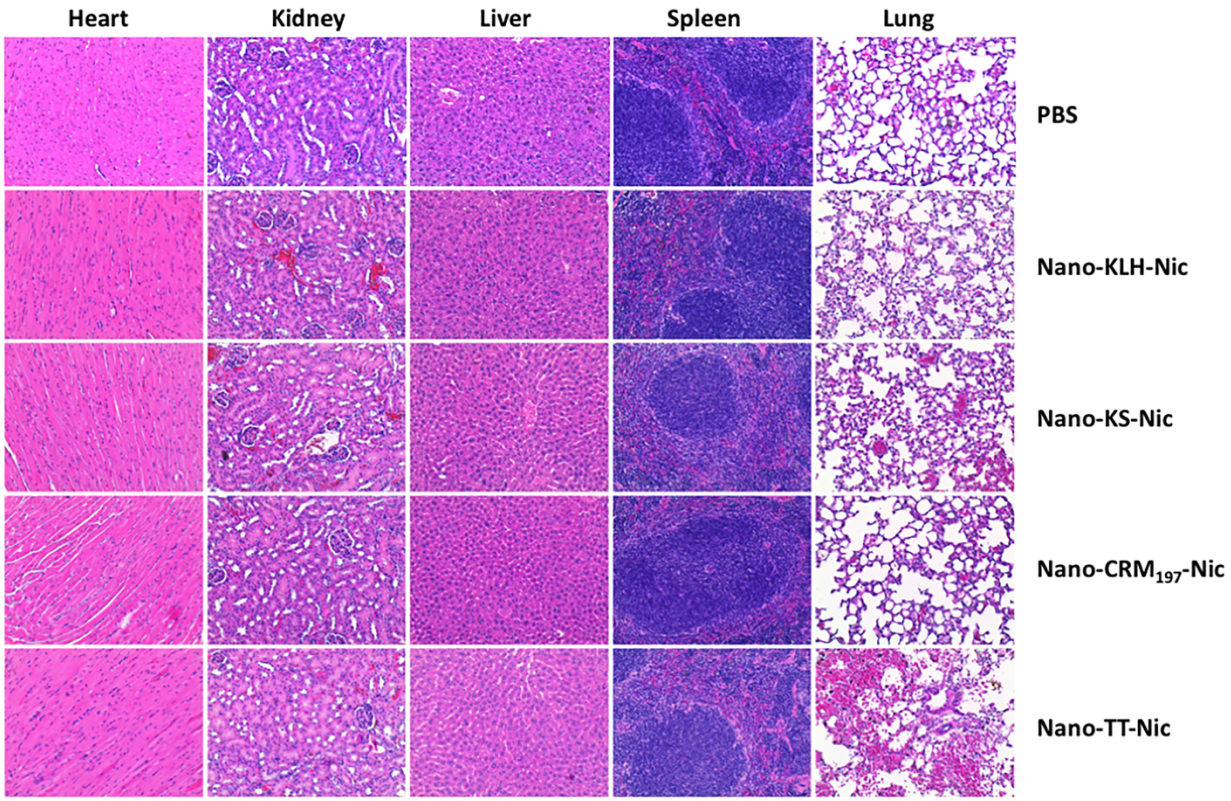

Figure 8. Safety of NanoNicVac conjugated with different stimulating proteins evaluated by histopathology. Organs of mice from groups of PBS blank group, Nano-KLH-Nic, Nano-KS-Nic, Nano-CRM197-Nic, and Nano-TT-Nic were processed by H&E staining and imaged.

Table 1. Physicochemical properties of NanoNicVac nanoparticles conjugated with different stimulating proteins

NanoNicVac	Size (d. nm)	Zeta-potential (mV)	PDI	Conjugation efficiency (%)	Hapten loading (µg Nic/mg NP)
Nano-KLH-Nic	167.2 ± 9.7	-11.00 ± 0.98	0.256 ± 0.067	87.6 ± 7.9	0.88 ± 0.07
Nano-KS-Nic	153.2 ± 10.2	-11.80 ± 0.93	0.271 ± 0.076	83.2 ± 11.3	0.91 ± 0.12
Nano-CRM$_{197}$-Nic	125.2 ± 13.5	-12.50 ± 0.75	0.230 ± 0.066	90.0 ± 7.6	0.86 ± 0.07
Nano-TT-Nic	136.6 ± 7.4	-11.20 ± 2.07	0.218 ± 0.045	84.3 ± 9.4	0.81 ± 0.09

Data were expressed as means ± standard deviation (n=3).

Chapter 7: Rational incorporation of molecular adjuvants into a hybrid nanoparticle-based nicotine nanovaccine for immunotherapy against nicotine addiction

Zongmin Zhao[1], Brian Harris[1], Yun Hu[1], Theresa Harmon[2], Paul R. Pentel[2], Marion Ehrich[3], Chenming Zhang[1,*]

1. Department of Biological Systems Engineering, Virginia Tech, Blacksburg, VA 24061, USA

2. Minneapolis Medical Research Foundation, Minneapolis, MN 55404, USA

3. Department of Biomedical Sciences and Pathobiology, Virginia Tech, Blacksburg, VA 24061, USA

* Correspondence to: Chenming (Mike) Zhang.

Address: 210 Seitz Hall, Department of Biological Systems Engineering, Virginia Tech, Blacksburg, VA 24061, USA.

Voice: +1-(540)231-7601

Fax: +1-(540)231-3199

Email: chzhang2@vt.edu

This manuscript is to be submitted to *Biomaterials*.

Abstract

Nanoparticle-based nicotine vaccines represent a promising next-generation immunotherapeutic strategy against nicotine addiction. This study aims to facilitate the immunogenicity of a hybrid nanoparticle-based nicotine nanovaccine by rationally incorporating toll-like receptor (TLR)-based adjuvants, including monophosphoryl lipid A (MPLA), Resiquimod (R848), CpG oligodeoxynucleotide 1826 (CpG ODN 1826), and their combinations. The nanoparticle-delivered model adjuvant was found to be taken up more efficiently by dendritic cells than the free counterpart. Nanovaccine nanoparticles were transported to endosomal compartments upon cellular internalization. The incorporation of single or dual TLR adjuvants not only considerably increased total anti-nicotine IgG titers but also significantly affected IgG subtype distribution in mice. Particularly, the nanovaccines carrying MPLA+R848 or MPLA+ODN 1826 generated a much higher anti-nicotine antibody titer than those carrying none or one adjuvant. Meanwhile, the anti-nicotine antibody elicited by the nanovaccine adjuvanted with MPLA+R848 had a significantly higher affinity than that elicited by the nanovaccine carrying MPLA+ODN 1826. Moreover, the incorporation of all the selected TLR adjuvants (except MPLA) reduced the brain nicotine levels in mice after nicotine challenge. Particularly, the nanovaccine with the adjuvant MPLA+R848 exhibited the best ability to reduce levels of nicotine entering the brain. Collectively, rational incorporation of TLR adjuvants could enhance the immunological efficacy of the hybrid nanoparticle-based nicotine nanovaccine, making it a promising next-generation immunotherapeutic candidate for treating nicotine addiction.

Key words

Nicotine addiction; nicotine vaccine; hybrid nanoparticle; toll-like receptors; molecular adjuvant; anti-nicotine antibody

7.1 Introduction

Tobacco smoking has constantly been one of the largest public health concerns worldwide for decades. It is the leading cause of preventable diseases and premature deaths, and results in huge socioeconomic burdens.[1, 2] In recent decades, nicotine vaccines have been studied as a promising immunotherapeutic strategy to combating nicotine addiction.[3, 4] In principle, nicotine vaccines can induce the production of nicotine-specific antibodies that can bind with nicotine in serum and thus keep nicotine from entering the brain.[5] To date, numerous conjugate nicotine vaccines (CNVs) have been reported to achieve high immunological efficacy in preclinical trials, and some of them have entered various stages of clinical trials.[6-9] However, none of these clinically tested CNVs have shown improved overall smoking cessation rate compared to placebo, mainly due to the insufficient antibody titers and low binding capacity.[5, 10]

Immunologically, the immune system prefers to recognize particulate antigens and is relatively invisible to soluble protein antigens.[11, 12] Therefore, the insufficient immunogenicity of conventional CNVs can be partially attributed to their intrinsic shortfalls, such as poor recognition and internalization by immune cells and low bioavailability. In addition, even with the help of alum to form particulate particles, CNVs cannot be easily tuned to have optimal physicochemical properties (such as size, shape, and charge) for cellular uptake.[13, 14] Moreover, molecular adjuvants cannot be easily incorporated into CNVs, and they are typically co-administered with CNVs via physical mixing. In this way, molecular adjuvants are not specifically available to immune cells and their release cannot be controlled in immune cells, thus leading to low adjuvant efficacy and systemic toxicity.[13, 15, 16]

In our previous study, by taking advantage of the superiorities of nanoparticles (NPs), such as particulate nature, tunable physicochemical properties, and controlled payload release, we

developed a lipid-polymeric hybrid nanoparticle (NP)-based nicotine nanovaccine (NanoNicVac) as a next-generation immunotherapeutic strategy against nicotine addiction.[17, 18] We demonstrated that NanoNicVac had a significantly higher immunogenicity than the conjugate vaccine, and its immunological efficacy could be enhanced by modulating NP size,[17] hapten localization,[19] hapten density,[20] and stimulating proteins.

From the immunological point of view, adjuvants are an important component of a vaccine formulation, and they are necessary for the induction of a strong immune response, especially for poorly-immunogenic antigens.[15, 21] Currently, alum is the most-widely used adjuvant for vaccine development. However, alum has shown to be a relatively weak adjuvant and sometimes may cause lesions at injection sites.[22, 23] Especially, for NP-based vaccines, alum may absorb vaccine NPs to form very large particles, resulting in sizes that are not optimal for cellular uptake.[14] Also, due to the high viscosity, alum may disrupt the structure of vaccine NPs. In addition, alum can limit the release of vaccine NPs from injection sites and impair their availability to antigen presenting cells (APCs).[16, 24] Our previous studies suggested that the use of alum would not significantly improve the immunogenicity of NanoNicVac.[20] As alternatives, molecular adjuvants, such as toll-like receptor (TLR) agonists, have been studied as a promising class of potent adjuvants.[25-27] TLR agonists are capable of enhancing the secretion of cytokines, promoting the activation of antigen presenting cells, and enhancing the production of antibodies.[28-30]

Based on the hypothesis that incorporation of appropriate molecular adjuvants may enhance the immunological efficacy of NanoNicVac, this study aims to further rationalize the design of NanoNicVac by developing a NanoNicVac NP capable of co-delivering nicotine antigens and TLR agonists. As shown in **Figure 1A**, the nicotine-protein conjugate was conjugated to the surface of

lipid-polymeric hybrid NPs for presentation. The lipid-shell and PLGA-core served as harbors for cell-surface-TLR and endosomal-TLR agonists, respectively. Monophosphoryl lipid A (MPLA),[31, 32] Resiquimod (R848),[13, 33] and CpG oligodeoxynucleotide 1826 (CpG ODN 1826),[34, 35] all of which have been reported to significantly enhance immune responses, were selected as three adjuvant candidates. In this study, NanoNicVac NPs carrying different TLR adjuvants or combinations were fabricated, and their physicochemical properties were characterized. The cellular uptake of NanoNicVac NPs was studied in dendritic cells. The immunogenicity and capability to reduce brain nicotine levels of NanoNicVac were investigated in mice.

7.2 Materials and methods

7.2.1 Materials

1,2-Dioleoyl-3-trimethylammonium-propane (DOTAP), cholesterol (CHOL), 1,2-diphytanoyl-sn-glycero-3-phosphoethanolamine-N-(7-nitro-2-1,3-benzoxadiazol-4-yl) (ammonium salt) (NBD-PE), 1,2-distearoyl-sn-glycero-3-phosphoethanolamine-N-[maleimide(polyethylene glycol)-2000] (ammonium salt) (DSPE-PEG2000-maleimide), and MPLA were purchased from Avanti Polar Lipids (Alabaster, AL, USA). Lactel® 50:50 poly(lactic-co-glycolic acid) (PLGA) was purchased from Durect Corporation (Cupertino, CA, USA). O-Succinyl-3'-hydroxymethyl-(±)-nicotine (Nic) was purchased from Toronto Research Chemicals (North York, ON, Canada). Keyhole limpet hemocyanin (KLH), Alexa Fluor® 647 NHS ester (AF647), coumarin-6 (CM-6), 1-Ethyl-3-[3-dimethylaminopropyl] carbodiimide hydrochloride (EDC), and N-hydroxysulfosuccinimide (Sulfo-NHS) were purchased from Thermo Fisher Scientific (Rockford, IL, USA). CpG ODN 1826 and R848 were purchased from InvivoGen (San Diego, CA, USA). All other chemicals were of analytical grade.

7.2.2 Fabrication of adjuvant-loaded PLGA NPs

Adjuvant-loaded PLGA NPs were fabricated using a w/o/w double-emulsion-solvent-evaporation method.[17] In brief, 40 mg of PLGA was dissolved in 2 mL of dichloromethane (DCM) to form an organic phase. For CpG ODN 1826- or R848-encapsulated PLGA NP preparation, 1.20 mg of CpG ODN 1826 in 200 μL of DI water or 1.50 mg of R848 in 200 μL of DI water-DMSO (9:1) was added into the organic phase. For CpG ODN 1826 and R848 co-encapsulated PLGA NP preparation, 1.20 mg of CpG ODN 1826 in 100 μL of DI water and 1.50 mg of R848 in 100 μL of DI water-DMSO (9:1) were added into the organic phase. The water-in-oil solution was mixed and emulsified by sonication for 10 min using a Branson M2800H Ultrasonic Bath Sonicator (Danbury, CT, USA). The resultant primary emulsion was added dropwise to 12 mL of 0.5% w/v poly(vinyl alcohol) solution under continuous stirring. The suspension was emulsified again by sonication using a sonic dismembrator (Model 500; Fisher Scientific, Pittsburg, PA, USA) at an amplitude of 70% for 40 s. The resultant secondary emulsion was stirred overnight to allow complete DCM evaporation. Blank PLGA NPs were prepared using a similar method, except that 200 μL of DI water was used as the first aqueous phase. Blank and adjuvant-loaded PLGA NPs were collected by centrifugation at 10,000 *g*, 4 °C for 30 min (Beckman Coulter Avanti J-251, Brea, CA, USA), washed three times, and stored at 4 °C for later use. To quantify the loading efficiency of R848 and ODN 1826, 20 mg of NPs were disrupted by incubating with 0.2 N NaOH for 14 h. After particles were completely dissolved, the solution was neutralized using 1 N HCl. The concentration of ODN 1826 was measured using a Quant-iT^{TM} OliGreen^{TM} ssDNA Assay kit (Thermo Fisher Scientific, Rockford, IL). The concentration of R848 was quantified by reverse-phase HPLC using a Luna C18 (2) reverse phase column. The loading efficiency of adjuvants is shown in **Table 1**.

7.2.3 Preparation of lipid-PLGA hybrid NPs

Blank and MPLA-carrying liposomes were prepared using a lipid-film-hydration-sonication method as reported previously.[17] The lipid mixtures used for preparing blank and MPLA-carrying liposomes were composed of DOTAP, DSPE-PEG2000-maleimide, CHOL, and MPLA at molar ratios of 90:5:5:0 and 80:5:5:10, respectively. Lipid-PLGA hybrid NPs were fabricated using a sonication method as reported previously.[17] Particularly, 2.5 mg of liposomes were mixed with 25 mg of PLGA NPs for hybrid NP fabrication. Lipid-PLGA hybrid NPs were collected by centrifugation at 10,000 *g*, 4 °C for 30 min, washed three times, and stored at 4 °C for later use.

7.2.4 Assembly of NanoNicVac NPs

Nic-KLH conjugates were synthesized using an EDC/NHS mediated reaction as reported previously.[20] NanoNicVac NPs were assembled by conjugating an appropriate amount of Nic-KLH conjugates to the surface of lipid-PLGA hybrid NPs according to a previously reported method.[20]. NanoNicVac NPs were collected by centrifugation at 10,000 *g*, 4 °C for 30 min. Unconjugated Nic-KLH in the supernatant was quantified by the bicinchoninic acid assay. NanoNicVac NPs were stored at 4 °C for later use.

7.2.5 Characterization of NPs

The morphology of NPs was characterized by transmission electron microscopy (TEM) on a JEM 1400 transmission electron microscope (JEOL, Tokyo, Japan). Size distribution and zeta potential of NPs were measured on a Nano ZS Zetasizer (Malvern Instruments, Worcestershire, United Kingdom) at 25°C.

7.2.6 Testing the uptake of NanoNicVac NPs in dendritic cells (DCs)

The uptake of NanoNicVac NPs carrying different adjuvants by DCs was studied by flow cytometry. NBD-labelled NPs were prepared by adding 2.5% of NBD-PE into a lipid mixture. JAWSII (ATCC® CRL-11904™) immature DCs (2×10^6/well) were seeded into 35-mm petri dish and cultured overnight. Cells were treated with 20 μg of NBD-labelled NanoNicVac NPs for 1, 2, or 4 h. Cells were washed 3 times using phosphate buffer saline (PBS) and detached from the petri dish using 0.25% trypsin/EDTA solution. Cells were collected by centrifugation at 200 *g* for 10 min and re-suspended in PBS. Samples were immediately analyzed on a flow cytometer (FACSAria I, BD Biosciences, Franklin Lakes, NJ, USA).

The intracellular distribution of NanoNicVac NPs was analyzed by confocal laser scanning microscopy (CLSM). AF647- and CM-6-labeled NPs were prepared according to the method described above, except that AF647-KLH conjugated to hybrid NPs and CM-6 was encapsulated in the PLGA core for labeling. Cells (2×10^5/chamber) were seeded into 2-well chamber slides and cultured overnight. Cells were treated with 20 μg of AF647- and CM-6-labeled nanovaccine NPs for 1, 2, or 4 h. Cells were then washed using PBS and fixed with freshly prepared 4% (w/v) paraformaldehyde for 10 min. The membrane of cells was permeabilized by adding 0.5 mL of 0.1% (v/v) Triton™ X-100 for 10 min. Cell nuclei were stained by 4',6-diamidino-2-phenylindole (DAPI). The intracellular distribution of NPs was visualized on a Zeiss LSM 510 laser scanning microscope.

7.2.7 Testing the immunogenicity of NanoNicVac in mice

All animal studies were carried out following the National Institutes of Health guidelines for animal care and use. Animal protocols were approved by the Institutional Animal Care and Use Committee at Virginia Tech. Female Balb/c mice (6-7 weeks of age, 16-20 g, 5-6 per group) were immunized subcutaneously with a total volume of 200 μL of nicotine vaccines equivalent to 25 μg

of KLH on days 0, 14, and 28. For the control group, mice were injected with 200 μL of sterilized PBS. Blood was collected from the retro-orbital plexus under isoflurane anesthesia on days 12, 26, and 40.

Anti-nicotine antibody titers in the serum were measured by an enzyme-linked immunosorbent assay (ELISA) as reported previously.[17] Antibody titer was defined as the dilution factor at which the absorbance at 450 nm dropped to half maximal. The relative affinity of anti-nicotine antibodies elicited by NanoNicVac carrying different adjuvants was measured using a competition ELISA method as reported previously.[19] The nicotine concentration at which 50% inhibition was achieved (IC_{50}) was extrapolated and used as an indicator of the affinity of anti-nicotine antibodies.

7.2.8 Testing the ability of NanoNicVac to reduce brain concentrations of nicotine in mice

The capability of NanoNicVac to decrease brain nicotine concentrations of nicotine was assayed using a method reported previously.[17] In brief, female Balb/c mice (6-7 weeks of age, 16-20 g, 5-6 per group) were immunized according to the same protocol as described in the above context. Mice were administered 0.06 mg/kg nicotine subcutaneously two weeks after the second booster immunization (on day 42). Brain and serum samples were collected 3 min post nicotine challenge. Nicotine levels in the brain and serum were measured by GC/MS as reported previously.[36]

7.2.9 Evaluating the safety of NanoNicVac by histopathological analysis

The behavioral and physical conditions of mice during the entire study were monitored. The lesions of mouse organs caused by the immunization with NanoNicVac were determined by histopathological review. In brief, on day 42, mice were euthanized, and their organs, including liver, kidney, heart, spleen, and lung, were extracted and immerged in 10% formalin. Tissue blocks

were stained with hematoxylin and eosin (H&E) and imaged on a Nikon Eclipse E600 light microscope.

7.2.10 Statistical analyzes

Data are expressed as means ± standard error unless specified. Comparisons among multiple groups were conducted using one-way ANOVA followed by Tukey's HSD test. Differences were considered significant when p-values were less than 0.05.

7.3 Results

7.3.1 Characterization of adjuvant-loaded NanoNicVac NPs

The structure of NPs involved in the fabrication of NanoNicVac was characterized morphologically by TEM (**Figure 1A**). A "core-shell" structure was observed on lipid-PLGA hybrid NPs, suggesting the successful hybridization of PLGA NPs and liposomes. The various adjuvant-loaded NanoNicVac NPs shared similar morphological characteristics with non-adjuvant-loaded NPs. Interestingly, a distinct black "cloud" was found on the surface of NanoNicVac NPs, which was most likely caused by the efficient conjugation of Nic-KLH conjugates.

The size of NanoNicVac NPs was characterized by dynamic light scattering (**Figure 1B**). NanoNicVac NPs loaded with no adjuvant, MPLA, R848, ODN 1826, MPLA+R848, MPLA+ODN 1826, and R848+ODN 1826 have average diameters of 140.9, 126.3, 194.7, 188.4, 176.3, 177.4, and 204.7 nm, respectively. Interestingly, the incorporation of MPLA into the lipid-layer did not increase the particle size. However, the inclusion of R848 and/or ODN 1826 into the PLGA-core led to considerable particle size increases. The surface charge of NanoNicVac NPs was measured by electrophoretic light scattering (**Figure 1C**). The zeta-potential of NanoNicVac

NPs loaded with no adjuvant, MPLA, R848, ODN 1826, MPLA+R848, MPLA+ODN 1826, and R848+ODN 1826 was -8.43, -8.77, -7.07, -13.00, -7.74, -13.20, and -10.32 mV, respectively, indicating that all NanoNicVac NPs were negatively charged, which might be caused by the conjugation of negatively charged Nic-KLH conjugates.

7.3.2 Cellular uptake of adjuvant-loaded NanoNicVac NPs

The impact of NanoNicVac NPs on the cellular uptake efficiency of nicotine-protein antigens and adjuvants was studied using flow cytometry (**Figure 2A-2C**). AF647 was used as a model of hapten to be conjugated to KLH for fluorescent labelling. CM-6, a model of TLR adjuvant, was loaded into the PLGA core. DCs were treated with free AF647-KLH+CM-6 ("In free form") or NanoNicVac NPs ("In nanoparticles") carrying the same amounts of AF647-KLH and CM-6 for 1 or 4 h. Interestingly, at both 1 h and 4 h, the mean influence intensity (M.F.I.) of CM-6 and AF647 in the group of "In free form" was significantly higher than that in the group of "In nanoparticles" (**Figure 2B** and **2C**). This data reveals that the use of hybrid NPs as delivery vehicles would significantly improve the internalization of both nicotine-protein antigens and molecular adjuvants.

The cellular uptake of adjuvant-loaded NanoNicVac NPs in DCs was investigated using flow cytometry (**Figure 2D**). DCs were treated with same amounts of NanoNicVac NPs loaded with different TLR adjuvants for 1, 2, or 4 h. NanoNicVac NPs were fluorescently labeled by adding NBD-PE to the lipid-layer. Consistent with the data shown in **Figure 2A**, the uptake of NanoNicVac NPs was time-dependent. Particularly, NanoNicVac NPs were rapidly taken up at 2 h, and the uptake process appeared to be saturated after that. NanoNicVac NPs loaded with R848, ODN 1826, MPLA+R848, MPLA+ODN 1826, and R848+ODN 1826 exhibited similar cellular uptake efficiency at all the studied time points, which may be attributed to their similar size

(**Figure 1B**). In addition, DCs took up non-adjuvant-loaded and MPLA-loaded NPs more efficiently than the other NPs, especially at 1 h and 2 h. This higher cellular uptake efficiency may be due to the fact that non-adjuvant-loaded and MPLA-loaded NPs had a smaller size than the other adjuvant-loaded NPs (**Figure 1B**).

The cellular internalization of NanoNicVac NPs was visualized using CLSM (**Figure 2E**). DCs were treated with NanoNicVac NPs in which KLH was labeled by AF647 and CM-6 (a model adjuvant) was loaded to the PLGA core. The endosomes and lysosomes of cells were labeled by Lysotracker Red. Both bright AF647 and CM-6 fluorescence were found within DCs, especially at 2 h and 4 h, revealing that both protein antigens and adjuvants could be efficiently co-delivered into DCs. At 1 h, a substantial portion of CM-6 was co-localized with Lysotracker Red, suggesting NanoNicVac NPs were transported to endosomes/lysosomes after being internalized by DCs. At 2 h and 4 h, most CM-6 fluorescence was distributed widely in cells and did not overlap with Lysotracker Red. This suggested that the model adjuvant CM-6 was efficiently released from NPs. As TLR 7/8 and 9 are primarily localized in the endosomal compartments of cells, the endosomal localization of NanoNicVac NPs and the efficient release of adjuvant from NPs would be beneficial for promoting an effective interaction between TLRs and TLR adjuvants.

7.3.3 Anti-nicotine antibody response induced by adjuvant-loaded NanoNicVac

The immunogenicity of adjuvant-loaded NanoNicVac was tested in mice (**Figure 3**). As shown in **Figure 3A**, after the primary immunization, anti-nicotine antibody titers were detected in all vaccine groups on day 12. All adjuvant-loaded NanoNicVac generated comparable anti-nicotine antibody titers as NanoNicVac with no adjuvant. As shown in **Figure 3B**, the first booster immunization significantly increased the antibody response in all vaccine groups. On day 26, NanoNicVac loaded with MPLA or R848+ODN 1826 did not increase the antibody titers

compared to NanoNicVac with no adjuvant. However, the antibody titers elicited by NanoNicVac loaded with R848, ODN 1826, MPLA+R848, or MPLA+ODN 1826 increased by 69%, 127%, 305%, and 180%, respectively, compared to that induced by NanoNicVac with no adjuvant. The co-delivery of MPLA and R848 or ODN 1826 generated a higher anti-nicotine antibody response than the delivery of only one adjuvant. As shown in **Figure 3C**, the second booster injection significantly enhanced antibody titers in all vaccine groups. On day 40, NanoNicVac loaded with MPLA, R848, ODN 1826, MPLA+R848, MPLA+ODN 1826, or R848+ODN 1826 induced 1.44-, 1.84-,1.89-, 3.06-, 2.64-, and 1.26-fold higher antibody titers than NanoNicVac with no adjuvant. Interestingly, the co-delivery of R848 and ODN 1826 did not result in a higher antibody titer than the delivery of only one adjuvant. However, the co-delivery of MPLA and R848 or ODN 1826 resulted in a considerably stronger antibody response than the delivery of only one adjuvant.

7.3.4 Subtype distribution of anti-nicotine IgG induced by adjuvant-loaded NanoNicVac

The titers of anti-nicotine subtype IgGs on day 40 were assayed (**Figure 4A-D**). The incorporation of different single TLR adjuvant to NanoNicVac resulted in different patterns of increasing titers of specific subtype IgGs. Specifically, the incorporation of MPLA or ODN 1826 mainly increased the levels of IgG2a and IgG2b, while the inclusion of R848 also considerably increased the titers of IgG1 as well as IgG2a and IgG2b. The effects of co-incorporating different TLR adjuvant combinations to NanoNicVac on enhancing the levels of subtype IgGs also appeared to be different. Specifically, the incorporation of R848+ODN 1826 considerably increased the titers of IgG2a, IgG2b, and IgG3 but decreased the levels of IgG1. The incorporation of MPLA+ODN 1826 significantly increased the titers of all subtype IgGs except IgG1. The incorporation of MPLA+R848 considerably increased the titers of all four subtype IgGs, especially IgG1 and IgG2b. The relative percentage of subtype IgGs induced by adjuvant-loaded NanoNicVac was analyzed

(**Figure 4E**). Interestingly, the distribution of subtype IgGs was significantly changed by the incorporation of different TLR adjuvants. IgG1 is the only major subtype detected when no adjuvant was used. The incorporation of MPLA+R848 did not significantly alter the subtype distribution. The incorporation of MPLA or R848 increased the percentage of IgG2a but IgG1 is still the major subtype. In contrast, the inclusion of ODN 1826, MPLA+ODN 1826, or R848+ODN 1826 significantly increased the percentage of IgG2a and IgG2a became the major IgG subtype.

7.3.5 Relative affinity of anti-nicotine antibodies induced by adjuvant-loaded NanoNicVac

The affinity of anti-nicotine antibodies was estimated by competition ELISA (**Figure 5**). As shown in **Figure 5A**, 12 days after the primary immunization (on day 12), the IC_{50} values of all vaccine groups were high (>540 μM), suggesting the antibodies had not matured sufficiently to have a high affinity to nicotine. As shown in **Figure 5B**, the IC_{50} values of groups of NanoNicVac loaded with no adjuvant, MPLA, R848, MPLA+R848, or R848+ODN 1826 were significantly lower on day 26 than on day 12. In addition, although no significant differences were detected, the IC_{50} values of NanoNicVac loaded with ODN 1826 or MPLA+ODN 1826 were considerably lower on day 26 compared to the values on day 12. These data may suggest that the first booster immunization promoted the affinity maturation of anti-nicotine antibodies. Interestingly, as shown in **Figure 5C**, the second booster immunization exhibited different effects on the affinity maturation of anti-nicotine antibodies among NanoNicVac loaded with different TLR adjuvants. Specifically, the average IC_{50} values of antibodies induced by NanoNicVac loaded with no adjuvant, MPLA, or MPLA+ODN 1826 were higher on day 40 than those on day 26. However, for samples of NanoNicVac loaded with R848, ODN 1826, or MPLA+R848, the IC_{50} values were slightly lower on day 40 than those on day 26. In terms of the end-point affinity, compared to NanoNicVac loaded

with no adjuvant, NanoNicVac loaded with R848 or MPLA+R848 resulted in a slightly lower average IC_{50} while NanoNicVac loaded with the other adjuvants caused a higher average IC_{50}.

7.3.6 Effect of adjuvant-loaded NanoNicVac on reducing brain nicotine concentrations in mice

The ability of adjuvant-loaded NanoNicVac to reduce nicotine levels in the brain was studied in mice (**Figure 6**). Mice received subcutaneous administration of 0.06 mg/kg nicotine on day 42. The serum and brain nicotine levels after nicotine challenge were analyzed. As shown in **Figure 6A**, the serum nicotine levels in all NanoNicVac groups were much higher than that in the PBS (control) group, suggesting that the immunization with NanoNicVac led to enhanced serum nicotine sequestration. In addition, compared to that of NanoNicVac loaded with no adjuvant, the serum nicotine levels increased by 15.3%, 38.4%, 62.9%, 295.5%, and 44.3% in the groups of NanoNicVac loaded with MPLA, R848, ODN 1826, MPLA+R848, and MPLA+ODN 1826, respectively. Particularly, NanoNicVac loaded with MPLA+R848 resulted in a considerably higher serum nicotine sequestration than NanoNicVac loaded with MPLA or R848 alone. As shown in **Figure 6B**, the incorporation of MPLA to NanoNicVac did not reduce brain nicotine levels. In contrast, the brain nicotine levels of NanoNicVac loaded with R848, ODN 1826, MPLA+R848, MPLA+ODN 1826, and R848+ODN 1826 were 19.6%, 21.0%, 54.0%, 32.0%, 16.7% lower than that of NanoNicVac with no adjuvant, respectively, suggesting the incorporation of these adjuvants facilitated the ability of NanoNicVac to keep nicotine from entering the brain. Particularly, NanoNicVac loaded with MPLA+R848 exhibited the best ability to reduce nicotine levels in the brain of mice, which was much better than that of NanoNicVac loaded with MPLA or R848.

7.3.7 Preliminary safety of adjuvant-loaded NanoNicVac

The behavioral and physical conditions of immunized mice during the entire study period were monitored. In all mouse groups immunized with NanoNicVac loaded with various adjuvants, no abnormal behavioral changes were observed compared to the mice injected with PBS. In addition, no short-term reactions, such as local reaction near the injection sites, apparent body temperature increase, and abnormal food and water consumption, were detected in any group. The body weight of mice was also monitored (**Figure 7A**). No weight loss was observed in any group of mice. In addition, there were no significant differences of body weight change between the PBS and all NanoNicVac groups. NanoNicVac had no effect on major organs of mice, including spleen, liver, lung, kidney, and heart, as determined by histopathological examination (**Figure 7B**). In all mouse groups injected with various NanoNicVac, no detectable lesions were found in any of the studied organs. All the above data suggest that NanoNicVac, regardless of the adjuvants, was safe for mice.

7.4 Discussion

The clinical trials of NicVAX and NicQb revealed that the top 30% subjects with the highest antibody levels showed enhanced smoking cessation rate than placebo.[6, 7] On one hand, this information suggests that the basic concept of using nicotine vaccines for treating nicotine addiction is sound. However, on the other hand, this information also indicates that more powerful nicotine vaccines that have sufficiently high immunogenicity are required so as to achieve an enhanced overall smoking cessation rate. The failure of the first-generation nicotine-protein conjugate nicotine vaccines (CNVs) inspired researchers to develop completely new nicotine vaccine platforms that can circumvent the innate shortfalls of conjugate vaccines. Because of their excellent properties, such as particulate nature, tunable physicochemical property, and high payload loading capacity,[37-40] NPs can be a basis for the development of the next-generation nicotine vaccines that can induce a stronger immune response. In our previous study, we developed

a lipid-polymeric hybrid NP-based nicotine nanovaccine (NanoNicVac) and demonstrated that NanoNicVac could induce a significantly higher anti-nicotine antibody titer than CNVs.[17] In other studies, we demonstrated that the immunogenicity of NanoNicVac could be facilitated by modulating multiple factors, such as particle size,[17] hapten density,[20] hapten localization,[19] and stimulating protein. Adjuvants are a critical component of a nicotine vaccine to induce a strong and long-lasting immune response. In this current study, we rationally incorporated potent TLR-based molecular adjuvants to NanoNicVac NPs and studied the impact of different TLR adjuvants on its immunological efficacy, finding the improved immunogenicity of NanoNicVac.

Efficient and specific delivery of nicotine vaccine components (hapten, T help protein, and adjuvant) to APCs is a prerequisite to initiate an effective immune response.[5] In our experiments, flow cytometry suggested that the design of NanoNicVac NPs significantly enhanced the delivery efficiency of both nicotine antigens and adjuvants. These data are in agreement with previous report showing that the use of NPs as delivery vehicles could improve the cellular internalization of soluble proteins and small molecules.[41] APCs have a relatively poor ability in recognizing and taking up soluble protein antigens,[11, 12] and thus CNVs cannot be internalized by APCs efficiently. Meanwhile, molecular adjuvants cannot be easily integrated with CNVs and are typically added to vaccine formulations by physical mixing. As a result, adjuvants cannot be targeted to APCs specifically and thus are poorly available to APCs.[13] The design of NanoNicVac NPs can overcome the abovementioned drawbacks of CNVs. On one hand, NanoNicVac NPs provide a harbor for the loading of protein antigens and molecular adjuvants. On the other hand, the particulate nature of NanoNicVac can achieve an enhanced recognition and internalization by APCs, increasing the availability of nicotine antigens and adjuvants to APCs.

It has been reported that co-localization of antigens and adjuvants within the same APCs can augment antigen presentation and T help cell activation, which are required for B cell activation and maturation. Our CLSM results suggest that nicotine antigen and model adjuvant were efficiently co-delivered to the same DCs by NanoNicVac NPs. Therefore, NanoNicVac may induce enhanced antigen presentation and T cell activation, thus helping to elicit a strong immune response. Moreover, our CLSM results also revealed that NanoNicVac NPs were transported to endosomes/lysosomes upon cellular internalization, and model adjuvant was efficiently released from NPs. In the design of NanoNicVac, MPLA, an agonist to TLR4, which is primarily localized on cell surface, was loaded to the outer lipid-layer. R848 and ODN 1826 that are agonists to TLR7/8 and TLR9, respectively, which are localized in endosomal compartments, were loaded to the inner PLGA-core. The specified localization of adjuvants based on their relevant TLRs, the endosomal transportation of NPs, and the efficient release of adjuvants would promote effective interactions between TLRs and TLR adjuvants.

Our antibody titer results demonstrated that the incorporation of single TLR adjuvants (MPLA, R848, or OND 1826) increased the antibody titers but the enhancement was not significant. This suggests that the use of single TLR adjuvant may not be sufficient to significantly improve the immunogenicity of NanoNicVac. Also, the incorporation of different TLR adjuvant combinations exhibited dramatically different impacts on the antibody titers. Specifically, the combination of R848 and ODN 1826 exhibited an antagonistic effect on the antibody titers compared to R848 or ODN 1826 alone. However, the combination of MPLA and R848 or ODN 1826 synergistically induced a much higher antibody titer than the corresponding single adjuvant. The difference in the adjuvant effects of different TLR adjuvant combinations may be attributed to the fact that MPLA, R848, and ODN 1826 act through different signaling pathways. MPLA, a TLR4 agonist, was

reported to act in a TRIF pathway biased manner.[42] R848 and ODN 1826, which are TLR7/8 and TLR 9 agonists, respectively, are predominantly acting through MyD88-dependent signaling pathways.[43] It has been reported that the co-activation of these different pathways has the potential to induce complementary or synergistic effects, while antagonism more commonly occurs with agonists that act through the same pathway.[43, 44] The combination of MPLA and R848 or ODN 1826 may co-activate both TRIF and MyD88 pathways. The cross-talk between MyD88 and TRIF may lead to enhanced cytokine production, reciprocal upregulation of each receptor,[45] and enhanced activation of T-helper cell responses,[46, 47], thus promoting antibody production.[48, 49] In contrast, as TLR7/8 and TLR9 signal via the same pathway, the combination of R848 and ODN 1826 may only stimulate the MyD88 pathway. As a result, the induction of immune responses cannot be enhanced due to the lack of MyD88-TRIF cross-talk.

Our antibody affinity results reveal that compared to non-adjuvant-loaded NanoNicVac, NanoNicVac adjuvanted with MPLA, ODN 1826, MPLA+ODN 1826, or R848+ODN 1826 resulted in a comparable or lower antibody affinity while NanoNicVac adjuvanted with R848 or MPLA+R848 led to a higher antibody affinity. Surprisingly, the antibodies elicited by NanoNicVac adjuvanted with MPLA+R848 or MPLA+ODN 1826 had comparable quantity but significantly different affinity. This phenomenon indicates that the incorporation of different TLR adjuvants to NanoNicVac not only significantly influences the production of anti-nicotine antibodies but also significantly affects the quality of the produced anti-nicotine antibodies. The reductions of brain nicotine levels seen in our experiments were in agreement with the antibody titer data and antibody affinity data. Noticeably, NanoNicVac with MPLA+R848 adjuvant had a significantly better ability to reduce brain nicotine levels compared to non-adjuvant-loaded NanoNicVac. However, NanoNicVac adjuvanted with MPLA+ODN 1826 or R848+ODN 1826

did not result in significantly different brain nicotine concentrations than non-adjuvant-loaded NanoNicVac. These results were as expected. NanoNicVac with MPLA+R848 adjuvant induced both significantly higher titer and much higher affinity of anti-nicotine antibodies, so more nicotine could be prevented from entering the brain. However, the anti-nicotine antibodies elicited by NanoNicVac with MPLA+ODN 1826 or R848+ODN 1826 adjuvants had either lower affinity or comparable titer compared to that induced by non-adjuvant-loaded NanoNicVac. Therefore, the ability of NanoNicVac to reduce brain nicotine concentrations could not be significantly improved by the incorporation of MPLA+ODN 1826 or R848+ODN 1826.

In conclusion, a series of lipid-polymeric hybrid NP-based nicotine nanovaccines, in which various TLR adjuvants or their combinations were incorporated, were successfully fabricated and tested. The impacts of TLR adjuvants on the immunogenicity and ability to reduce brain nicotine concentrations of the nicotine nanovaccines were examined. Mouse trial results suggested that the use of single TLR adjuvants (MPLA, R848, or ODN 1826) was not sufficient to significantly enhance the immunogenicity of NanoNicVac. The co-incorporation of appropriate TLR adjuvant combinations (MPLA+R848 or MPLA+ODN 1826) exhibited a complementary effect and thus significantly improved the immunogenicity of NanoNicVac. Especially, the incorporation of MPLA+R848 induced the highest titers of anti-nicotine antibody that had a high affinity to nicotine, and thus exhibited the best capability to block nicotine from entering the brain of mice. The findings of this work demonstrated that incorporating appropriate TLR adjuvants could be a novel strategy to improve the immunological efficacy of the next-generation NP-based nicotine vaccines. Based on all the reported results, hybrid NP-based nicotine nanovaccines can be a promising next-generation immunotherapeutic candidate for treating nicotine addiction.

Conflict of interest

The authors declare no competing financial interests.

Acknowledgements

This work was financially supported by National Institute on Drug Abuse (U01DA036850).

References

[1] Prochaska JJ, Benowitz NL. The past, present, and future of nicotine addiction therapy. Annu Rev Med. 2016;67:467-86.

[2] Benowitz NL. Nicotine addiction. N Engl J Med. 2010;362:2295-303.

[3] Lisy K. Nicotine vaccines for smoking cessation. Clin Nurse Spec. 2013;27:71-2.

[4] Kitchens CM, Foster SL. Nicotine conjugate vaccines: A novel approach in smoking cessation. J Am Pharm Assoc (2003). 2012;52:116-8.

[5] Pentel PR, LeSage MG. New directions in nicotine vaccine design and use. Adv Pharmacol. 2014;69:553-80.

[6] Hatsukami DK, Jorenby DE, Gonzales D, Rigotti NA, Glover ED, Oncken CA, et al. Immunogenicity and smoking-cessation outcomes for a novel nicotine immunotherapeutic. Clin Pharmacol Ther. 2011;89:392-9.

[7] Cornuz J, Zwahlen S, Jungi WF, Osterwalder J, Klingler K, van Melle G, et al. A vaccine against nicotine for smoking cessation: a randomized controlled trial. PLoS One. 2008;3:e2547.

[8] Tonstad S, Heggen E, Giljam H, Lagerback PA, Tonnesen P, Wikingsson LD, et al. Niccine(R), a nicotine vaccine, for relapse prevention: a phase II, randomized, placebo-controlled, multicenter clinical trial. Nicotine Tob Res. 2013;15:1492-501.

[9] McCluskie MJ, Thorn J, Gervais DP, Stead DR, Zhang N, Benoit M, et al. Anti-nicotine vaccines: Comparison of adjuvanted CRM197 and Qb-VLP conjugate formulations for immunogenicity and function in non-human primates. Int Immunopharmacol. 2015;29:663-71.

[10] Raupach T, Hoogsteder PH, Onno van Schayck CP. Nicotine vaccines to assist with smoking cessation: current status of research. Drugs. 2012;72:e1-16.

[11] Storni T, Kundig TM, Senti G, Johansen P. Immunity in response to particulate antigen-delivery systems. Adv Drug Deliv Rev. 2005;57:333-55.

[12] Benne N, van Duijn J, Kuiper J, Jiskoot W, Slutter B. Orchestrating immune responses: How size, shape and rigidity affect the immunogenicity of particulate vaccines. J Control Release. 2016;234:124-34.

[13] Ilyinskii PO, Johnston LPM. Nanoparticle-based nicotine vaccine. 1st ed: Springer; 2016.

[14] Li XR, Aldayel AM, Cui ZR. Aluminum hydroxide nanoparticles show a stronger vaccine adjuvant activity than traditional aluminum hydroxide microparticles. J Control Release. 2014;173:148-57.

[15] Coffman RL, Sher A, Seder RA. Vaccine adjuvants: putting innate immunity to work. Immunity. 2010;33:492-503.

[16] Gregory AE, Titball R, Williamson D. Vaccine delivery using nanoparticles. Front Cell Infect Mi. 2013;3.

[17] Zhao Z, Hu Y, Hoerle R, Devine M, Raleigh M, Pentel P, et al. A nanoparticle-based nicotine vaccine and the influence of particle size on its immunogenicity and efficacy. Nanomedicine. 2017;13:443-54.

[18] Hu Y, Smith D, Frazier E, Hoerle R, Ehrich M, Zhang C. The next-generation nicotine vaccine: a novel and potent hybrid nanoparticle-based nicotine vaccine. Biomaterials. 2016;106:228-39.

[19] Zhao ZM, Hu Y, Harmon T, Pentel P, Ehrich M, Zhang CM. Rationalization of a nanoparticle-based nicotine nanovaccine as an effective next-generation nicotine vaccine: A focus on hapten localization. Biomaterials. 2017;138:46-56.

[20] Zhao Z, Powers K, Hu Y, Raleigh M, Pentel P, Zhang CM. Engineering of a hybrid nanoparticle-based nicotine nanovaccine as a next-generation immunotherapeutic strategy against nicotine addiction: A focus on hapten density. Biomaterials. 2017;123:107-17.

[21] Bonam SR, Partidos CD, Halmuthur SKM, Muller S. An overview of novel adjuvants designed for improving vaccine efficacy. Trends Pharmacol Sci. 2017.

[22] Petrovsky N. Comparative Safety of Vaccine Adjuvants: A summary of current evidence and future needs. Drug Saf. 2015;38:1059-74.

[23] Tomljenovic L, Shaw CA. Aluminum vaccine adjuvants: Are they safe? Curr Med Chem. 2011;18:2630-7.

[24] Ghimire TR. The mechanisms of action of vaccines containing aluminum adjuvants: an in vitro vs in vivo paradigm. Springerplus. 2015;4:181.

[25] Steinhagen F, Kinjo T, Bode C, Klinman DM. TLR-based immune adjuvants. Vaccine. 2011;29:3341-55.

[26] Kaisho T, Akira S. Toll-like receptors as adjuvant receptors. Bba-Mol Cell Res. 2002;1589:1-13.

[27] Mbow ML, De Gregorio E, Valiante NM, Rappuoli R. New adjuvants for human vaccines. Curr Opin Immunol. 2010;22:411-6.

[28] Toussi DN, Massari P. Immune adjuvant effect of molecularly-defined toll-like receptor ligands. Vaccines (Basel). 2014;2:323-53.

[29] Maisonneuve C, Bertholet S, Philpott DJ, De Gregorio E. Unleashing the potential of NOD- and Toll-like agonists as vaccine adjuvants. P Natl Acad Sci USA. 2014;111:12294-9.

[30] Seya T, Akazawa T, Tsujita T, Matsumoto M. Role of Toll-like receptors in adjuvant-augmented immune therapies. Evid Based Complement Alternat Med. 2006;3:31-8; discussion 133-7.

[31] Lockner JW, Ho SO, McCague KC, Chiang SM, Do TQ, Fujii G, et al. Enhancing nicotine vaccine immunogenicity with liposomes. Bioorg Med Chem Lett. 2013;23:975-8.

[32] Alving CR, Matyas GR, Torres O, Jalah R, Beck Z. Adjuvants for vaccines to drugs of abuse and addiction. Vaccine. 2014;32:5382-9.

[33] Ilyinskii PO, Roy CJ, O'Neil CP, Browning EA, Pittet LA, Altreuter DH, et al. Adjuvant-carrying synthetic vaccine particles augment the immune response to encapsulated antigen and exhibit strong local immune activation without inducing systemic cytokine release. Vaccine. 2014;32:2882-95.

[34] Bremer PT, Schlosburg JE, Lively JM, Janda KD. Injection route and TLR9 agonist addition significantly impact heroin vaccine efficacy. Mol Pharmaceut. 2014;11:1075-80.

[35] Kimishima A, Wenthur CJ, Eubanks LM, Sato S, Janda KD. Cocaine vaccine development: Evaluation of carrier and adjuvant combinations that activate multiple Toll-like receptors. Mol Pharmaceut. 2016;13:3884-90

[36] de Villiers SHL, Cornish KE, Troska AJ, Pravetoni M, Pentel PR. Increased efficacy of a trivalent nicotine vaccine compared to a dose-matched monovalent vaccine when formulated with alum. Vaccine. 2013;31:6185-93.

[37] Courant T, Bayon E, Reynaud-Dougier HL, Villiers C, Menneteau M, Marche PN, et al. Tailoring nanostructured lipid carriers for the delivery of protein antigens: Physicochemical properties versus immunogenicity studies. Biomaterials. 2017;136:29-42.

[38] Rincon-Restrepo M, Mayer A, Hauert S, Bonner DK, Phelps EA, Hubbell JA, et al. Vaccine nanocarriers: Coupling intracellular pathways and cellular biodistribution to control CD4 vs CD8 T cell responses. Biomaterials. 2017;132:48-58.

[39] Pavot V, Climent N, Rochereau N, Garcia F, Genin C, Tiraby G, et al. Directing vaccine immune responses to mucosa by nanosized particulate carriers encapsulating NOD ligands. Biomaterials. 2016;75:327-39.

[40] Chavez-Santoscoy AV, Roychoudhury R, Pohl NLB, Wannemuehler MJ, Narasimhan B, Ramer-Tait AE. Tailoring the immune response by targeting C-type lectin receptors on alveolar macrophages using "pathogen-like" amphiphilic polyanhydride nanoparticles. Biomaterials. 2012;33:4762-72.

[41] Liu X, Xu Y, Yu T, Clifford C, Liu Y, Yan H, et al. A DNA nanostructure platform for directed assembly of synthetic vaccines. Nano Lett. 2012;12:4254-9.

[42] Mata-Haro V, Cekic C, Martin M, Chilton PM, Casella CR, Mitchell TC. The vaccine adjuvant monophosphoryl lipid A as a TRIF-biased agonist of TLR4. Science. 2007;316:1628-32.

[43] Tan RS, Ho B, Leung BP, Ding JL. TLR cross-talk confers specificity to innate immunity. Int Rev Immunol. 2014;33:443-53.

[44] McKay PF, King DF, Mann JF, Barinaga G, Carter D, Shattock RJ. TLR4 and TLR7/8 adjuvant combinations generate different vaccine antigen-specific immune outcomes in minipigs when administered via the ID or IN routes. PLoS One. 2016;11:e0148984.

[45] Makela SM, Strengell M, Pietila TE, Osterlund P, Julkunen I. Multiple signaling pathways contribute to synergistic TLR ligand-dependent cytokine gene expression in human monocyte-derived macrophages and dendritic cells. J Leukocyte Biol. 2009;85:664-72.

[46] Napolitani G, Rinaldi A, Bertoni F, Sallusto F, Lanzavecchia A. Selected Toll-like receptor agonist combinations synergistically trigger a T helper type 1-polarizing program in dendritic cells. Nat Immunol. 2005;6:769-76.

[47] Bohnenkamp HR, Papazisis KT, Burchell JM, Taylor-Papadimitriou J. Synergism of Toll-like receptor-induced interleukin-12p70 secretion by monocyte-derived dendritic cells is mediated through p38 MAPK and lowers the threshold of T-helper cell type 1 responses. Cell Immunol. 2007;247:72-84.

[48] Mitsdoerffer M, Lee Y, Jager A, Kim HJ, Korn T, Kolls JK, et al. Proinflammatory T helper type 17 cells are effective B-cell helpers. Proc Natl Acad Sci U S A. 2010;107:14292-7.

[49] Milpied PJ, McHeyzer-Williams MG. High-affinity IgA needs TH17 cell functional plasticity. Nat Immunol. 2013;14:313-5.

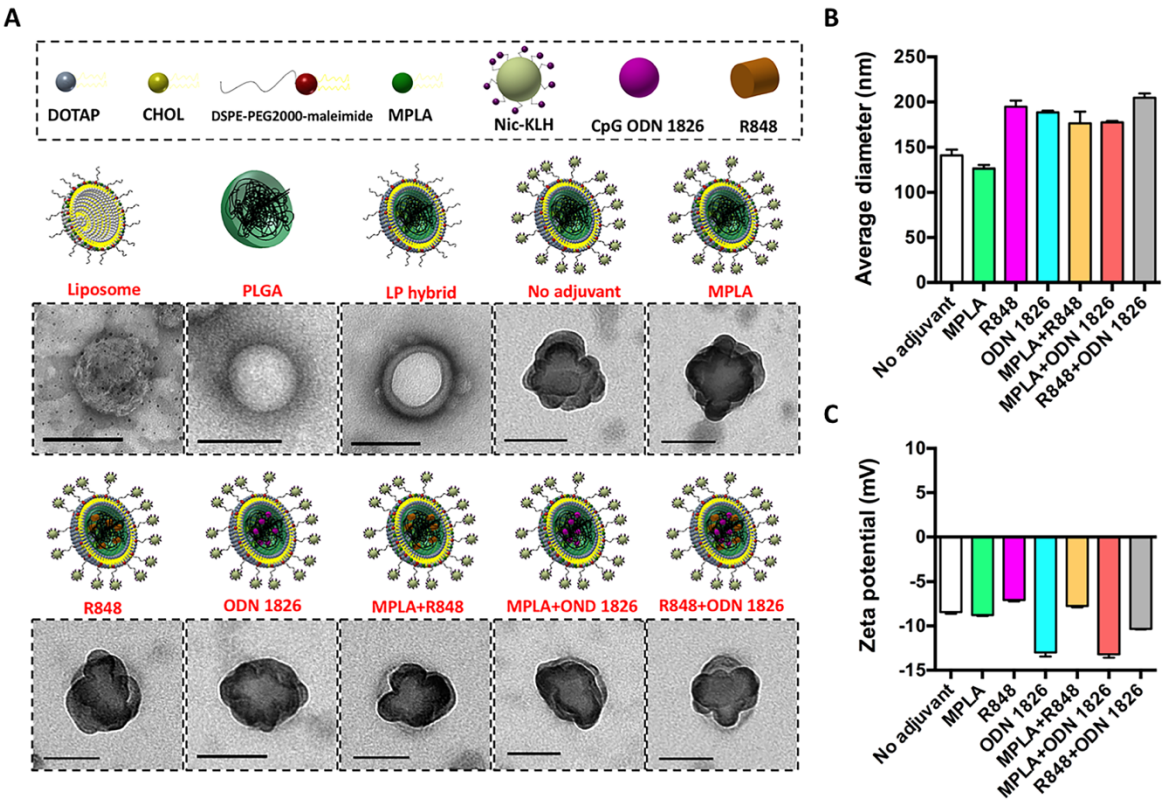

Figure 1. Characterization of NPs. (A) Schematic illustration and TEM images of liposomes, PLGA NPs, lipid-PLGA hybrid NPs, and adjuvant-loaded NanoNicVac NPs. Scale bars represent 100 nm. (B) Average diameters of NanoNicVac NPs. (C) Zeta-potential of NanoNicVac NPs.

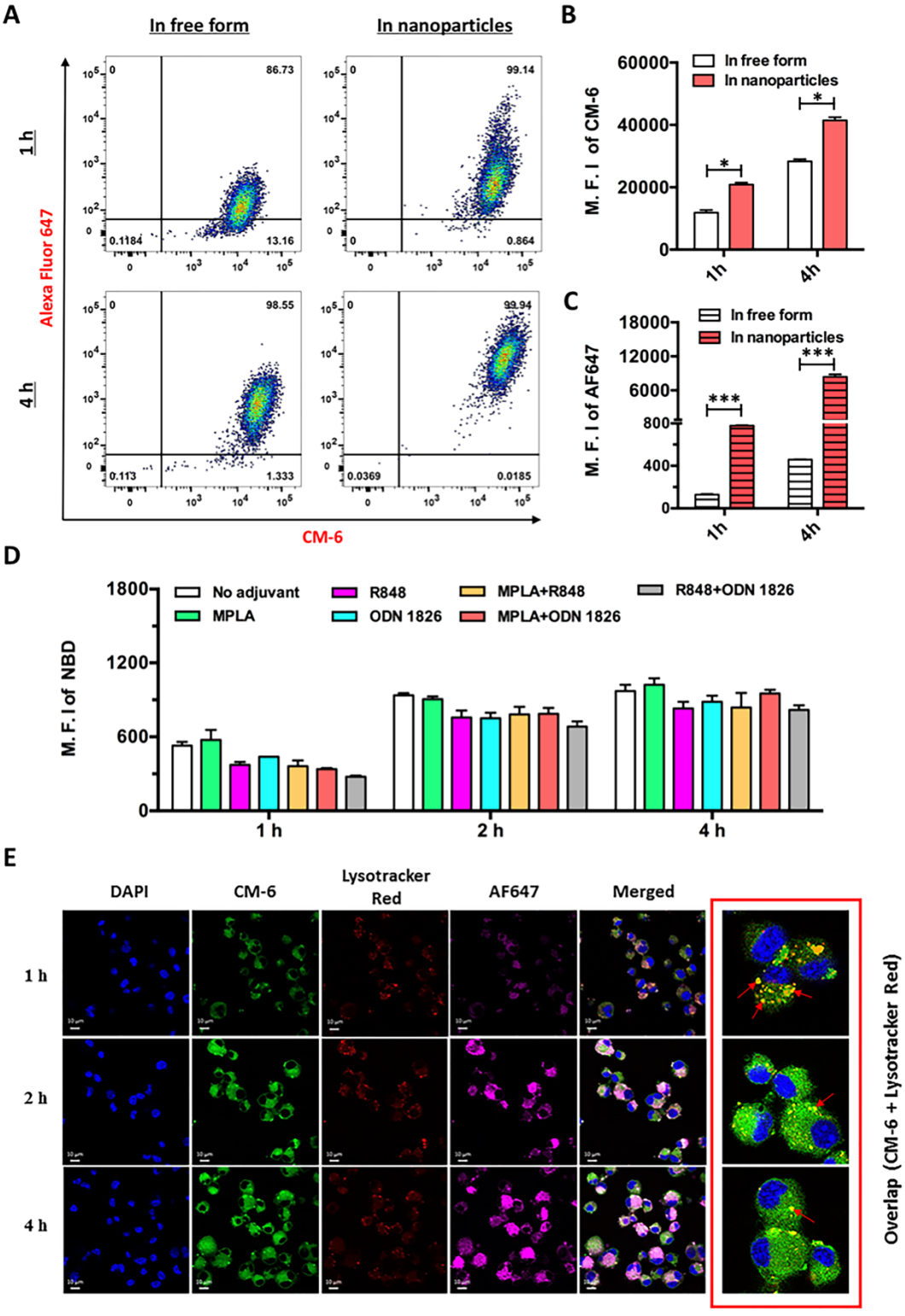
A
In free form
In nanoparticles
1 h
4 h
Alexa Fluor 647
CM-6
86.73
99.14
0.1184
13.16
0.864
98.55
99.94
0.113
1.333
0.0369
0.0185
B
M. F. I of CM-6
In free form
In nanoparticles
C
M. F. I of AF647
D
M. F. I of NBD
No adjuvant
MPLA
R848
ODN 1826
MPLA+R848
MPLA+ODN 1826
R848+ODN 1826
1 h
2 h
4 h
E
DAPI
CM-6
Lysotracker Red
AF647
Merged
Overlap (CM-6 + Lysotracker Red)

Figure 2. Cellular Uptake of NanoNicVac NPs by dendritic cells. (A) Flow cytometry recorded events, (B) M.F.I. of CM-6, and (C) M.F.I. of AF647 of dendritic cells after being treated with free AF467-KLH+CM-6 (In free form) or NanoNicVac NPs carrying AF647-KLH and CM-6 (In nanoparticles). AF647 was used to label KLH, and CM-6 was used as a model adjuvant to load into the PLGA core. Significantly different: * $p < 0.05$, *** $p < 0.001$. (D) M.F.I. of NBD in dendritic cells after being treated with NanoNicVac NPs loaded with different adjuvants. NBD was added to the lipid-layer to label NPs. (E) CLSM images of dendritic cells after being treated with NanoNicVac NPs for 1, 2, or 4 h. AF647 was used as a model hapten to provide fluorescence and CM-6 was used as a model adjuvant to load into the PLGA core. Scale bars represent 10 μm.

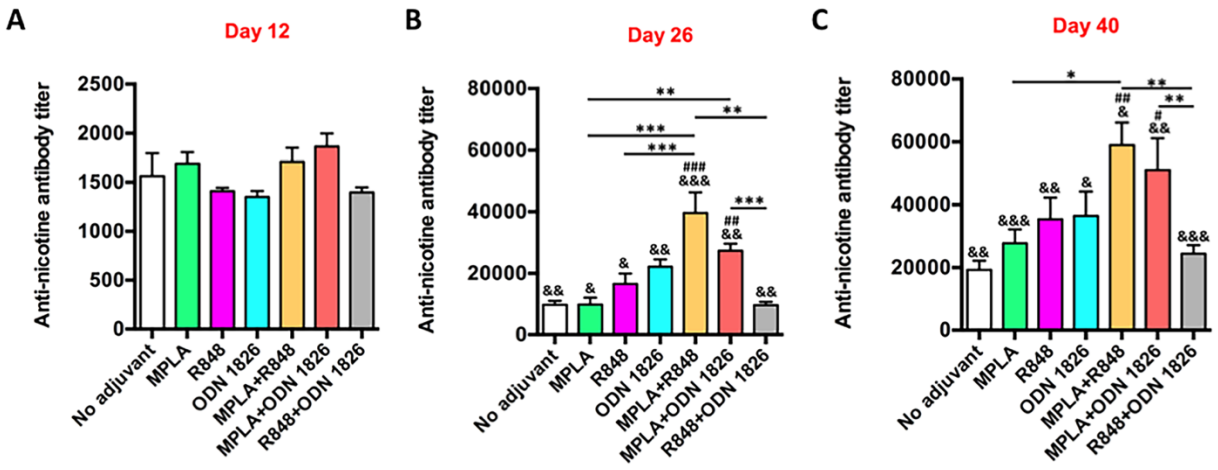

Figure 3. Immunogenicity of adjuvant-loaded NanoNicVac. The titers of anti-nicotine IgG antibodies elicited by NanoNicVac on (A) day 12, (B) day 26, and (C) day 40 were measured by ELISA. Significantly different compared to the previous studied day: & $p < 0.05$, && $p < 0.01$, and &&& $p < 0.001$. Significantly different compared to NanoNicVac group with no adjuvant: # $p < 0.05$, ## $p < 0.01$, and ### $p < 0.001$. Significantly different: * $p < 0.05$, ** $p < 0.01$, and *** $p < 0.001$.

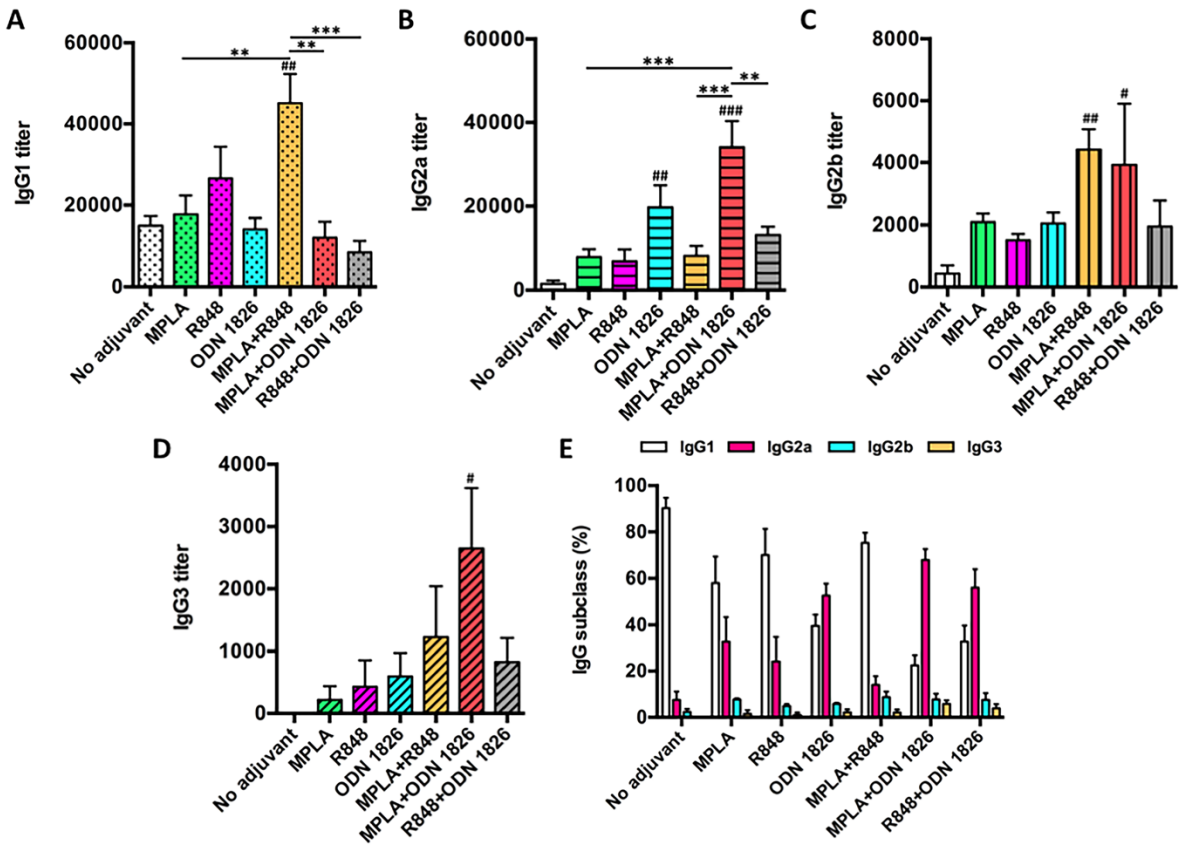

Figure 4. Subtype distribution of anti-nicotine IgGs. The titers of anti-nicotine IgG subtypes on day 40, including (A) IgG1, (B) IgG2a, (C) IgG2b, and (D) IgG3, were assayed. (E) shows the relative percentages of subtype anti-nicotine IgGs. Significantly different compared to NanoNicVac with no adjuvant: # $p < 0.05$, ## $p < 0.01$, and ### $p < 0.001$. Significantly different: ** $p < 0.01$, *** $p < 0.001$.

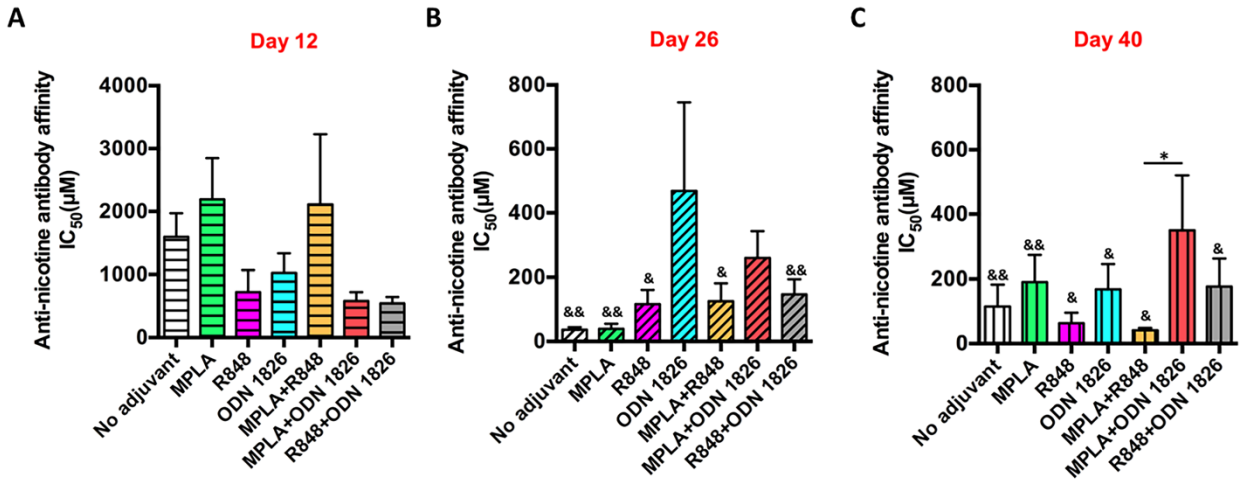

Figure 5. Affinity of anti-nicotine antibodies elicited by NanoNicVac on (A) day 12, (B) day 26, and (C) day 40. The antibody affinity was estimated by competition ELISA. Significantly different compared to the IC_{50} on day 12: & $p < 0.05$, && $p < 0.01$. Significantly different: * $p < 0.05$.

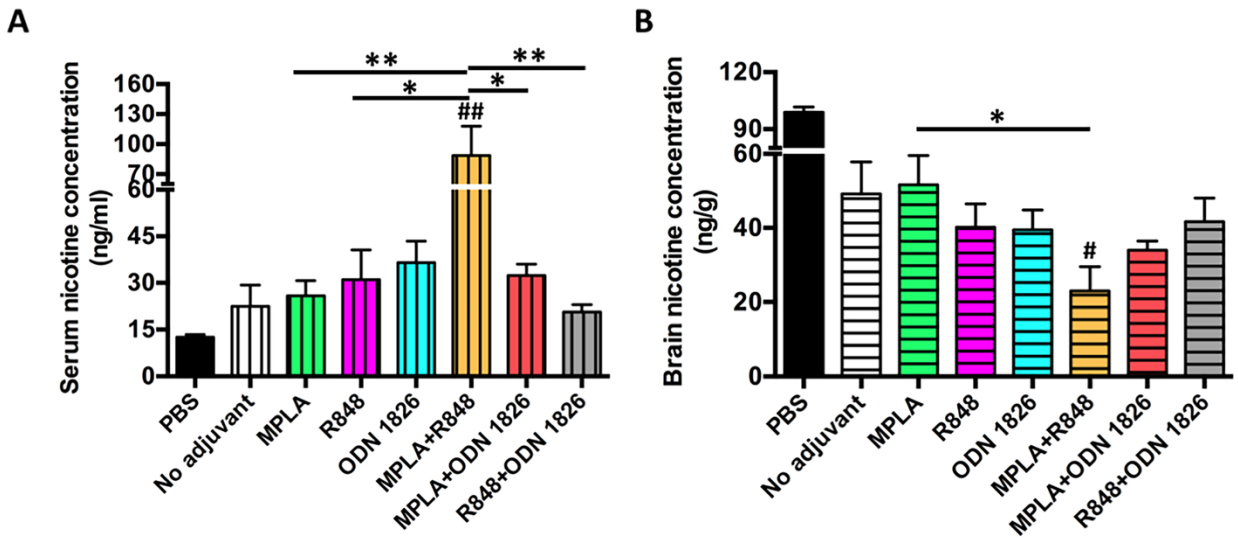

Figure 6. Effect of adjuvant-loaded NanoNicVac on the distribution of nicotine in the serum and brain after nicotine challenge in mice. (A) Serum nicotine concentration. (B) Brain nicotine concentration. Mice were administered 0.06 mg/kg nicotine on day 42, and the brain and serum samples were collected 3 min after nicotine administration. Significantly different compared to NanoNicVac with no adjuvant: # $p < 0.05$, ## $p < 0.01$. Significantly different: * $p < 0.05$, ** $p < 0.01$.

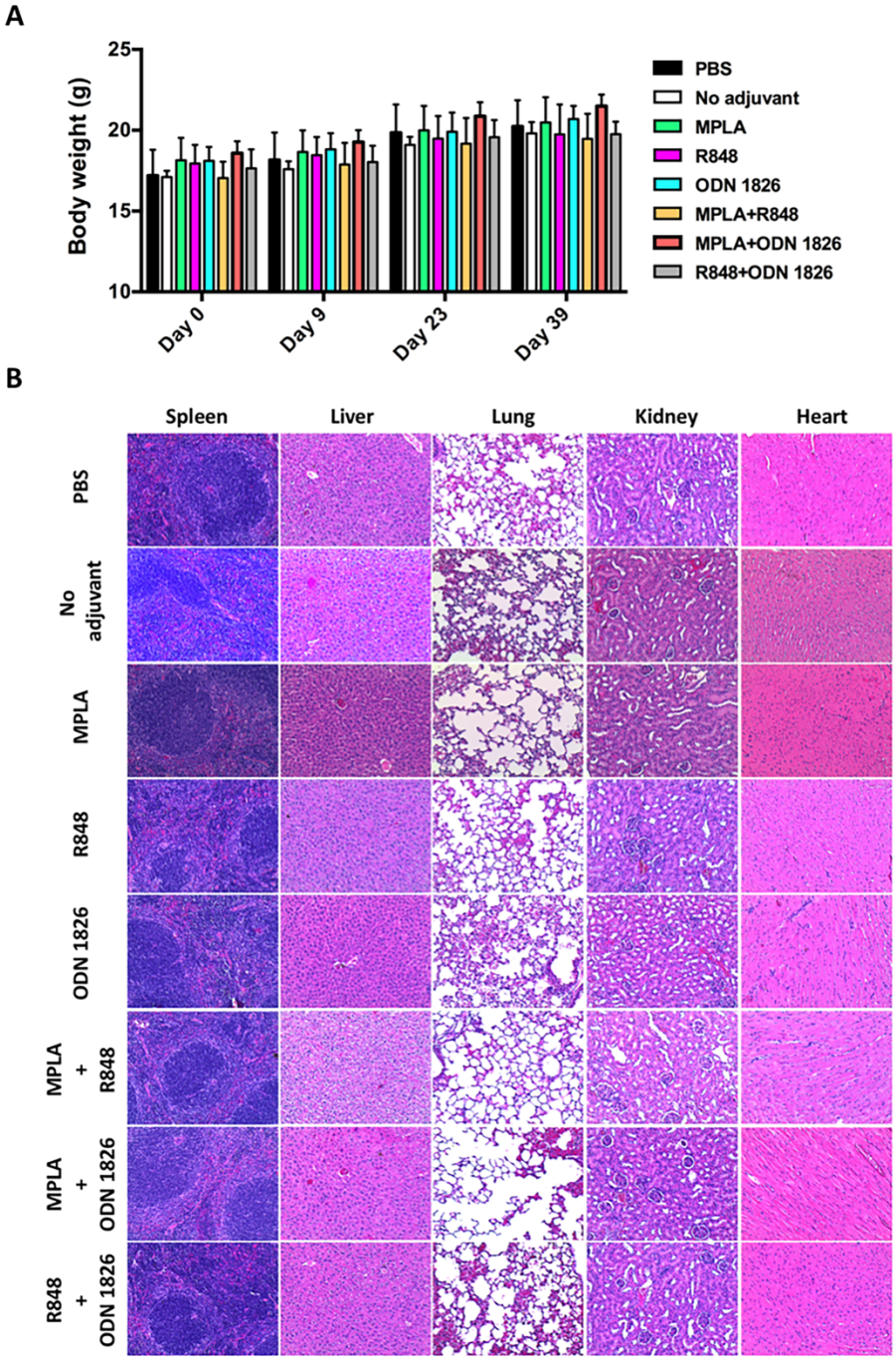

Figure 7. Preliminary safety of adjuvant-loaded NanoNicVac NPs. (A) Body weight of immunized mice. (B) Representative H&E staining images of major organs of mice immunized with NanoNicVac carrying different adjuvants.

Table 1. The loading efficiency of adjuvants in NanoNicVac

NPs	MPLA loading (μg/mg NP)	R848 loading (μg/mg NP)	ODN 1826 loading (μg/mg NP)
NanoNicVac (No adjuvant)	/	/	/
NanoNicVac (MPLA)	17.85[#]	/	/
NanoNicVac (R848)	/	38.72 ± 4.47	/
NanoNicVac (ODN 1826)	/	/	34.01 ± 2.10
NanoNicVac (MPLA+R848)	17.85[#]	37.35 ± 4.33	/
NanoNicVac (MPLA+ODN 1826)	17.85[#]	/	34.52 ± 0.75
NanoNicVac (R848+ODN 1826)	/	32.82 ± 3.42	33.72 ± 1.21

[#] It is assumed that 100% of MPLA in the lipid mixture was incorporated into the lipid-layer of NanoNicVac.

Chapter 8: General Conclusions

Tobacco smoking remains a leading cause of preventable diseases and premature deaths in the world. Because of the severe addictiveness of nicotine, smokers need the help of medications to quit smoking. The ineffectiveness of currently available pharmacological medications necessitates the development of new strategies for smoking cessation. Nicotine vaccines have been proposed as a promising immunotherapeutic strategy to treat nicotine addiction. Many conjugate nicotine vaccines have been developed in the past two decades and several of them have entered various stages of clinical trials. The clinical studies of conjugate nicotine vaccines provided the following information: 1) the basic concept of nicotine vaccine is sound; 2) more effective nicotine vaccines that can induce much stronger immune responses are required to achieve an enhanced overall smoking cessation rate. Since all the clinically tested conjugate nicotine vaccines have failed, it has been convincingly argued that it is necessary to utilize completely new paradigms to develop novel nicotine vaccines. The use of nanoparticles rather than proteins as carriers is such a new paradigm.

The immune system has evolved to better recognize and capture particulate antigens and is relatively invisible to soluble protein antigens. One major innate drawback of conjugate nicotine vaccines is their poor recognition and internalization by immune cells. To overcome this shortfall, a nicotine nanovaccine based on lipid-polymeric hybrid nanoparticles that have a particulate nature was developed in this study. The cellular uptake assay revealed that the hybrid nanoparticle-based nicotine nanovaccine particles were taken up by dendritic cells more efficiently than the conjugate nicotine vaccine particles. In concordance with these data, the mouse trial results suggested that the hybrid nanoparticle-based nicotine vaccine could induce a significantly higher anti-nicotine

antibody titer and result in a significantly lower brain nicotine level than the conjugate nicotine vaccine.

Although the hybrid nanoparticle-based nicotine nanovaccine exhibited promising immunological efficacy, it is still necessary to better understand the influence of multiple factors on its immunogenicity and thus to further improve its efficacy by tuning these factors. Efficient uptake of vaccine particles by antigen presenting cells is a necessity in inducing a strong immune response. Particle size is one of the most important physicochemical properties of a nanoparticle-based nanomedicine that largely impact the cellular uptake process. In this study, we fabricated nanovaccine nanoparticles with different sizes (100 and 500 nm) and studied the impact of particle size on their immunogenicity. The smaller sized nanovaccine (100 nm) was found to elicit a significantly higher anti-nicotine antibody titer than the larger sized nanovaccine (500 nm) in the presence of alum. The findings provided useful guidance on how to enhance the efficacy of nanoparticle-based nicotine vaccines by modulating particle size.

The activation of hapten-specific B cells requires the recognition and interaction between haptens and hapten-specific B cells. The density of hapten on nanovaccine surface is an important factor potentially influencing this recognition and interaction process. In this study, we fabricated nanovaccine nanoparticles with tunable hapten densities (high-, medium-, and low-density) and studied the impact of hapten density on the immunogenicity of the hybrid nanoparticle-based nicotine vaccine. Mouse trial results indicated that hapten density not only impacted anti-nicotine antibody titers but also influenced anti-carrier protein antibody levels. With the increase of hapten density, the nanovaccine elicited higher titers of anti-nicotine antibodies and lower levels of anti-carrier protein antibodies. The findings showcase the necessity of tuning hapten density in improving the immunogenicity and specificity of nanoparticle-based nicotine vaccines.

The generation of a strong immune response requires the activation of both B cells and T helper cells. The conjugation of high-density haptens to carrier protein does facilitate the activation of B cells but may mask T cell epitopes that are necessary for T helper cell activation. A balanced B cell immunity and T cell immunity may be beneficial for inducing a strong immune response. The localization of haptens on nanovaccine nanoparticles is such a factor that affects both B cell activation and T helper cell activation. In this study, we fabricated nanovaccine nanoparticles with haptens localized on carrier protein alone, on nanoparticle surface alone, or on both, to study the impact of hapten localization on the immunogenicity of the hybrid nanoparticle-based nicotine nanovaccine. Mouse trial results suggested that the nanovaccine with hapten localized on both carrier protein and nanoparticle surface resulted in a significantly higher anti-nicotine antibody titer and capability to reduce brain nicotine levels than the nanovaccine with haptens localized on carrier protein or nanoparticle surface alone. The findings suggested a novel strategy to facilitate the efficacy of nanoparticle-based nicotine vaccines by engineering hapten localization.

The maturation of B cells to antibody-secreting plasma cells needs the help of T helper cells. The generation of T helper cells is achieved by the processing and presentation of T help proteins/peptides. Thus, the selection of T help proteins potentially influences the generation of T helper cells. In this study, we fabricated nanovaccine nanoparticles, on which different T help protein candidates were conjugated, to study the impact of selection of T help proteins on the immunogenicity of the hybrid nanoparticle-based nicotine nanovaccine. *In vivo* results indicated that the use of tetanus toxoid (TT) and cross reactive material 197 (CRM_{197}) induced significantly higher anti-nicotine antibody titers and considerably lower anti-protein antibody titers than the use of keyhole limpet hemocyanin (KLH) or KLH subunit. The findings demonstrated that the

immunogenicity of nanoparticle-based nicotine vaccines can be enhanced by rational selection of T help proteins.

An adjuvant is an essential component of a vaccine formulation as it may facilitate cytokine secretion, enhance antigen presenting cell activation, and increase antibody generation. Incorporating appropriate adjuvants to a vaccine formulation may significantly improve its immunogenicity. In this study, we incorporated various toll-like receptor (TLR) agonists to the hybrid nanoparticle-based nicotine nanovaccine and investigated the impact of molecular adjuvants on its immunogenicity. *In vivo* results suggested that the incorporation of single TLR adjuvant was not sufficient to significantly increase the titers of anti-nicotine antibodies. In contrast, the incorporation of appropriate TLR adjuvant combinations significantly enhanced the immunological efficacy of the hybrid nanoparticle-based nicotine nanovaccine. The findings showcase the necessity of incorporating appropriate molecular adjuvants in enhancing the immunogenicity of nanoparticle-based nicotine vaccines.

In conclusion, the use of lipid-polymeric hybrid nanoparticle as a particulate platform for developing nicotine vaccines can achieve a significantly better immunological efficacy than conventional conjugate nicotine vaccines. The immunogenicity of the lipid-polymeric hybrid nanoparticle-based nicotine nanovaccine is affected by multiple factors that potentially influence one or multiple processes involved in the induction of an immune response against nicotine. By modulating these factors, including nanoparticle size, hapten density, hapten localization, carrier protein, and molecular adjuvant, the immunological efficacy of the hybrid nanoparticle-based nicotine nanovaccine can be significantly enhanced. The hybrid nanoparticle-based nicotine nanovaccine can be a promising next-generation immunotherapeutic candidate for treating nicotine addiction.

Future studies can focus on tuning other factors to further improve the immunogenicity of the hybrid nanoparticle-based nicotine nanovaccine. First, the loading quantity of molecular adjuvants in nanovaccine nanoparticles can be optimized to achieve a better adjuvant efficacy. Secondly, enantiopure nicotine haptens can be conjugated to nanovaccine nanoparticles to improve the specificity and affinity of anti-nicotine antibodies. Thirdly, bivalent or trivalent nicotine nanovaccines can be fabricated to co-activate B cell subclasses and thus to increase the overall anti-nicotine antibody titers. Last but not least, the immunization regimen, such as vaccine doses and injection intervals, can be optimized to achieve a strong and long-lasting immune response.

Appendix A: Supplementary Information for Chapter 3

Materials

Lactel® (50:50 poly(lactic-co-glycolic acid) (PLGA)) was purchased from Durect Corporation (Cupertino, CA, USA). Fetal bovine serum, GM-CSF recombinant mouse protein, minimum essential medium, keyhole limpet hemocyanin (KLH), and Alexa Fluor® 647 hydrazide (AF647) were purchased from Life Technologies Corporation (Grand Island, NY, USA). Poly(vinyl alcohol) (MW 89,000-98,000), dichloromethane (DCM), rhodamine B, paraformaldehyde, and Triton™X-100 were purchased from Sigma-Aldrich (Saint Louis, MO, USA). 1-Ethyl-3-[3-dimethylaminopropyl] carbodiimide hydrochloride (EDC) and N-hydroxysulfosuccinimide (Sulfo-NHS) were purchased from Thermo Fisher Scientific (Rockford, IL, USA). 1,2-Dioleoyl-3-trimethylammonium-propane, cholesterol, 1,2-diphytanoyl-sn-glycero-3-phosphoethanolamine-N-(7-nitro-2-1,3-benzoxadiazol-4-yl) (ammonium salt) (NBD PE), and 1,2-distearoyl-sn-glycero-3-phosphoethanolamine-N-[maleimide(polyethylene glycol)-2000] (ammonium salt) (DSPE-PEG2000-maleimide) were purchased from Avanti Polar Lipids (Alabaster, AL, USA). JAWSII (ATCC® CRL-11904™) immature dendritic cells and trypsin/EDTA were purchased from American Type Culture Collection (Manassas, VA, USA). O-Succinyl-3'-hydroxymethyl-(±)-nicotine (Nic) was purchased from Toronto Research Chemicals (North York, ON, Canada). All other chemicals were of analytical grade.

Preparation of PLGA nanoparticles (NPs)

PLGA NPs were prepared using a double emulsion solvent evaporation method with minor modifications. In brief, 50 mg of PLGA were dissolved in 2 mL of DCM (oil phase). Two hundred microliters of ultrapure water were then added into the oil phase. The resultant mixture was emulsified by sonication for 10 min using a Branson M2800H Ultrasonic Bath (Danbury, CT,

USA). This primary emulsion was added drop-wise into 15 mL of poly(vinyl alcohol) solution (0.5%, w/v) under continuous stirring. The suspension was then emulsified by sonication at 70% amplitude for 20 s (for 100 nm PLGA NP preparation) or at 20% amplitude for 10 s (for 500 nm PLGA NP preparation) using a sonic dismembrator (Model 500; Fisher Scientific, Pittsburg, PA, USA). The secondary emulsion was stirred overnight to allow complete DCM evaporation. PLGA NPs were collected by centrifugation at 10,000 *g*, 4°C, for 30 min (Beckman Coulter Avanti J-251, Brea, CA, USA). Pellets were washed three times using ultrapure water. The final suspension was freeze-dried (Labconco Freezone 4.5, Kansas City, MO, USA), and NPs were stored at 2°C for later use.

Fabrication of lipid-polymeric hybrid NPs

Lipid-polymeric NPs were assembled using a hydration-sonication method. Briefly, 25 mg of lipid mixture, which was dissolved in chloroform containing 1,2-dioleoyl-3-trimethylammonium-propane, DSPE-PEG2000-maleimide, and cholesterol, was evaporated to form a lipid film. The lipid film was then hydrated with 2 mL of pre-warmed hydration buffer (0.9% saline, 5% dextrose, and 10% sucrose). The resultant suspension was cooled to room temperature. An appropriate amount of PLGA NPs, suspended in ultrapure water, was added into the liposome suspension and mixed thoroughly, followed by sonication for 10 min in an ice-water bath using a Branson M2800H Ultrasonic Bath sonicator. Lipid-polymeric NPs were collected by centrifugation at 10,000 *g*, 4°C, for 30 min, freeze-dried, and stored at 2°C for later use.

Characterization of NPs

The morphology of lipid-polymeric hybrid NPs of different sizes was analyzed by transmission electron microscopy. NP samples were negatively stained using 1% phosphotungstic acid, and imaged on a JEM 1400 transmission electron microscope (JEOL, Tokyo, Japan). Fluorescent

nanovaccine NPs, in which KLH and the lipid layer were labeled by rhodamine B and NBD, respectively, were imaged on a Zeiss LSM 510 laser scanning microscope (Carl Zeiss, Oberkochen, Germany). The Fourier transform infrared spectra of NPs were recorded on a Thermo Nicolet 6700 FT-IR spectrometer (Thermo Fisher Scientific, Waltham, MA). Particle size (diameter, nm) and surface charge (zeta-potential, mV) of NPs were analyzed on a Nano ZS Zetasizer (Malvern Instruments, Worcestershire, United Kingdom) at 25°C.

Cell culture

JAWSII (ATCC® CRL-11904™) immature dendritic cells were cultured in alpha minimum essential medium supplemented with ribonucleosides, deoxyribonucleosides, 4 mM L-glutamine, 1 mM sodium pyruvate, 5 ng/mL murine GM-CSF, and fetal bovine serum (20%) at 37°C with 5% CO_2.

Confocal laser scanning microscopy analysis of the uptake of NPs by dendritic cells

AF647 and NBD fluorescently labeled NPs were prepared according to the method described above, except that AF647-KLH was conjugated to hybrid NPs and 0.25 mg of NBD was added into lipids for labeling. Cells (2×10^5/chamber) were seeded into 2-well chamber slides (Thermo Fisher Scientific) in 2 mL of medium, and cultured overnight. The original medium was then replaced with 2 mL of fresh medium containing 100 μg of AF647- and NBD-labeled nanovaccine NPs. At predetermined time points (0.5, 1, and 2 h) the medium was discarded and cells were washed 3 times using 0.01 M, pH 7.4, phosphate-buffered saline (PBS). One mL of freshly prepared 4% (w/v) paraformaldehyde was added into each well to fix cells for 15 min. The fixed cells were washed 3 times against PBS and permeabilized by adding 0.5 mL of 0.1% (v/v) Triton™ X-100 for 15 min at room temperature. After again washing cells 3 times using PBS, cell nuclei were stained by 4',6-diamidino-2-phenylindole (DAPI) according to the standard protocol

provided by the supplier. The coverslips were finally placed onto the glass microscope slides. The intracellular distribution of NPs was visualized on a Zeiss LSM 510 laser scanning microscope.

Flow cytometry analysis of NP uptake by dendritic cells

AF647-KLH was synthesized using a EDC/NHS-mediated reaction and was conjugated to hybrid NPs. Dendritic cells (2×10^6/well) were seeded into 24-well plates (Corning, Tewksbury, MA, USA) and cultured for 24 h. The original medium was replaced with fresh medium containing 100 μg of AF647-labeled NPs or the same amount of AF647-KLH conjugate contained in AF647 labeled NPs. The medium was removed after 2 h and cells were washed 3 times with PBS. Cells were detached from the culture plates using trypsin/EDTA solution and collected by centrifugation at 200 *g* for 10 min. Cell pellets were re-suspended in PBS. Samples were immediately analyzed on a flow cytometer (FACSAria I, BD Biosciences, Franklin Lakes, NJ, USA).

Measurement of anti-nicotine IgG subclasses

Similar enzyme-linked immunosorbent assay protocols as that were applied to measure IgG antibody titers, were used to determine titers of the four IgG antibody isotypes, except that horseradish peroxidase-conjugated goat anti-mouse IgG1, IgG2a, IgG2b, and IgG3 (Alpha Diagnostic, San Antonio, TX, USA) were used as the secondary antibodies. The Th1/Th2 index was calculated using the following formula:

Th1/Th2 index = ((IgG2a + IgG3)/2)/IgG1

Histopathological analyses

Histopathological analyses of tissues from mice vaccinated with the nicotine vaccines, including heart, kidney, liver, spleen, and lung, were performed to identify any lesions caused by the administration of vaccine NPs. In brief, different mouse organs were first fixed with 10% formalin, followed by cutting the organs according to a standard protocol. Tissue blocks were then embedded

in paraffin and sections were stained by hematoxylin and eosin. The stained sections were imaged on a Nikon Eclipse E600 light microscope and pictures were captured using a Nikon DS-Fi1 camera.

Appendix B: Permission for reproduction of materials from Elsevier for Chapter 3

This Agreement between Mr. Zongmin Zhao ("You") and Elsevier ("Elsevier") consists of your license details and the terms and conditions provided by Elsevier and Copyright Clearance Center.

License Number	4134911183032
License date	Jun 23, 2017
Licensed Content Publisher	Elsevier
Licensed Content Publication	Nanomedicine: Nanotechnology, Biology and Medicine
Licensed Content Title	A nanoparticle-based nicotine vaccine and the influence of particle size on its immunogenicity and efficacy
Licensed Content Author	Zongmin Zhao,Yun Hu,Reece Hoerle,Meaghan Devine,Michael Raleigh,Paul Pentel,Chenming Zhang
Licensed Content Date	Feb 1, 2017
Licensed Content Volume	13
Licensed Content Issue	2
Licensed Content Pages	12
Start Page	443
End Page	454
Type of Use	reuse in a thesis/dissertation
Portion	full article
Format	electronic
Are you the author of this Elsevier article?	Yes
Will you be translating?	No
Order reference number	
Title of your thesis/dissertation	Factors that affect the immunogenicity of lipid-PLGA nanoparticle-based nanovaccines against nicotine addiction
Expected completion date	Aug 2017
Estimated size (number of pages)	28
Elsevier VAT number	GB 494 6272 12
Requestor Location	Mr. Zongmin Zhao 1000H Progress St BLACKSBURG, VA 24060 United States Attn: Mr. Zongmin Zhao
Publisher Tax ID	98-0397604
Total	0.00 USD

Terms and Conditions

INTRODUCTION

1. The publisher for this copyrighted material is Elsevier. By clicking "accept" in connection with completing this licensing transaction, you agree that the following terms and conditions apply to this transaction (along with the Billing and Payment terms and conditions established by Copyright Clearance Center, Inc. ("CCC"), at the time that you opened your Rightslink account and that are available at any time at http://myaccount.copyright.com).

GENERAL TERMS

2. Elsevier hereby grants you permission to reproduce the aforementioned material subject to the terms and conditions indicated.
3. Acknowledgement: If any part of the material to be used (for example, figures) has appeared in our publication with credit or acknowledgement to another source, permission must also be sought from that source. If such permission is not obtained then that material may not be included in your publication/copies. Suitable acknowledgement to the source must be made, either as a footnote or in a reference list at the end of your publication, as follows:
"Reprinted from Publication title, Vol /edition number, Author(s), Title of article / title of chapter, Pages No., Copyright (Year), with permission from Elsevier [OR APPLICABLE SOCIETY COPYRIGHT OWNER]." Also Lancet special credit - "Reprinted from The Lancet, Vol. number, Author(s), Title of article, Pages No., Copyright (Year), with permission from Elsevier."
4. Reproduction of this material is confined to the purpose and/or media for which permission is hereby given.
5. Altering/Modifying Material: Not Permitted. However figures and illustrations may be altered/adapted minimally to serve your work. Any other abbreviations, additions, deletions and/or any other alterations shall be made only with prior written authorization of Elsevier Ltd. (Please contact Elsevier at permissions@elsevier.com). No modifications can be made to any Lancet figures/tables and they must be reproduced in full.
6. If the permission fee for the requested use of our material is waived in this instance, please be advised that your future requests for Elsevier materials may attract a fee.
7. Reservation of Rights: Publisher reserves all rights not specifically granted in the combination of (i) the license details provided by you and accepted in the course of this licensing transaction, (ii) these terms and conditions and (iii) CCC's Billing and Payment terms and conditions.
8. License Contingent Upon Payment: While you may exercise the rights licensed immediately upon issuance of the license at the end of the licensing process for the transaction, provided that you have disclosed complete and accurate details of your proposed use, no license is finally effective unless and until full payment is received from you (either by publisher or by CCC) as provided in CCC's Billing and Payment terms and conditions. If full payment is not received on a timely basis, then any license preliminarily granted shall be deemed automatically revoked and shall be void as if never granted. Further, in the event that you breach any of these terms and conditions or any of CCC's Billing and Payment terms and conditions, the license is automatically revoked and shall be void as if never granted. Use of materials as described in a revoked license, as well as any use of the materials beyond the scope of an unrevoked license, may constitute copyright infringement and publisher reserves the right to take any and all action to protect its copyright in the materials.
9. Warranties: Publisher makes no representations or warranties with respect to the licensed material.
10. Indemnity: You hereby indemnify and agree to hold harmless publisher and CCC, and their respective officers, directors, employees and agents, from and against any and all claims arising out of your use of the licensed material other than as specifically authorized pursuant to this license.
11. No Transfer of License: This license is personal to you and may not be sublicensed, assigned, or transferred by you to any other person without publisher's written permission.
12. No Amendment Except in Writing: This license may not be amended except in a writing signed by both parties (or, in the case of publisher, by CCC on publisher's behalf).
13. Objection to Contrary Terms: Publisher hereby objects to any terms contained in any purchase order, acknowledgment, check endorsement or other writing prepared by you, which terms are inconsistent with these terms and conditions or CCC's Billing and Payment terms and conditions. These terms and conditions, together with CCC's Billing

and Payment terms and conditions (which are incorporated herein), comprise the entire agreement between you and publisher (and CCC) concerning this licensing transaction. In the event of any conflict between your obligations established by these terms and conditions and those established by CCC's Billing and Payment terms and conditions, these terms and conditions shall control.
14. Revocation: Elsevier or Copyright Clearance Center may deny the permissions described in this License at their sole discretion, for any reason or no reason, with a full refund payable to you. Notice of such denial will be made using the contact information provided by you. Failure to receive such notice will not alter or invalidate the denial. In no event will Elsevier or Copyright Clearance Center be responsible or liable for any costs, expenses or damage incurred by you as a result of a denial of your permission request, other than a refund of the amount(s) paid by you to Elsevier and/or Copyright Clearance Center for denied permissions.

LIMITED LICENSE

The following terms and conditions apply only to specific license types:
15. **Translation**: This permission is granted for non-exclusive world **English** rights only unless your license was granted for translation rights. If you licensed translation rights you may only translate this content into the languages you requested. A professional translator must perform all translations and reproduce the content word for word preserving the integrity of the article.
16. **Posting licensed content on any Website**: The following terms and conditions apply as follows: Licensing material from an Elsevier journal: All content posted to the web site must maintain the copyright information line on the bottom of each image; A hyper-text must be included to the Homepage of the journal from which you are licensing at http://www.sciencedirect.com/science/journal/xxxxx or the Elsevier homepage for books at http://www.elsevier.com; Central Storage: This license does not include permission for a scanned version of the material to be stored in a central repository such as that provided by Heron/XanEdu.
Licensing material from an Elsevier book: A hyper-text link must be included to the Elsevier homepage at http://www.elsevier.com . All content posted to the web site must maintain the copyright information line on the bottom of each image.

Posting licensed content on Electronic reserve: In addition to the above the following clauses are applicable: The web site must be password-protected and made available only to bona fide students registered on a relevant course. This permission is granted for 1 year only. You may obtain a new license for future website posting.
17. **For journal authors:** the following clauses are applicable in addition to the above:
Preprints:
A preprint is an author's own write-up of research results and analysis, it has not been peer-reviewed, nor has it had any other value added to it by a publisher (such as formatting, copyright, technical enhancement etc.).
Authors can share their preprints anywhere at any time. Preprints should not be added to or enhanced in any way in order to appear more like, or to substitute for, the final versions of articles however authors can update their preprints on arXiv or RePEc with their Accepted Author Manuscript (see below).
If accepted for publication, we encourage authors to link from the preprint to their formal publication via its DOI. Millions of researchers have access to the formal publications on ScienceDirect, and so links will help users to find, access, cite and use the best available version. Please note that Cell Press, The Lancet and some society-owned have different preprint policies. Information on these policies is available on the journal homepage.
Accepted Author Manuscripts: An accepted author manuscript is the manuscript of an article that has been accepted for publication and which typically includes author-incorporated changes suggested during submission, peer review and editor-author communications.
Authors can share their accepted author manuscript:

- immediately

- via their non-commercial person homepage or blog
- by updating a preprint in arXiv or RePEc with the accepted manuscript
- via their research institute or institutional repository for internal institutional uses or as part of an invitation-only research collaboration work-group
- directly by providing copies to their students or to research collaborators for their personal use
- for private scholarly sharing as part of an invitation-only work group on commercial sites with which Elsevier has an agreement

- After the embargo period
  - via non-commercial hosting platforms such as their institutional repository
  - via commercial sites with which Elsevier has an agreement

In all cases accepted manuscripts should:

- link to the formal publication via its DOI
- bear a CC-BY-NC-ND license - this is easy to do
- if aggregated with other manuscripts, for example in a repository or other site, be shared in alignment with our hosting policy not be added to or enhanced in any way to appear more like, or to substitute for, the published journal article.

Published journal article (JPA): A published journal article (PJA) is the definitive final record of published research that appears or will appear in the journal and embodies all value-adding publishing activities including peer review co-ordination, copy-editing, formatting, (if relevant) pagination and online enrichment.
Policies for sharing publishing journal articles differ for subscription and gold open access articles:
Subscription Articles: If you are an author, please share a link to your article rather than the full-text. Millions of researchers have access to the formal publications on ScienceDirect, and so links will help your users to find, access, cite, and use the best available version.
Theses and dissertations which contain embedded PJAs as part of the formal submission can be posted publicly by the awarding institution with DOI links back to the formal publications on ScienceDirect.
If you are affiliated with a library that subscribes to ScienceDirect you have additional private sharing rights for others' research accessed under that agreement. This includes use for classroom teaching and internal training at the institution (including use in course packs and courseware programs), and inclusion of the article for grant funding purposes.
Gold Open Access Articles: May be shared according to the author-selected end-user license and should contain a CrossMark logo, the end user license, and a DOI link to the formal publication on ScienceDirect.
Please refer to Elsevier's posting policy for further information.
18. **For book authors** the following clauses are applicable in addition to the above: Authors are permitted to place a brief summary of their work online only. You are not allowed to download and post the published electronic version of your chapter, nor may you scan the printed edition to create an electronic version. **Posting to a repository:** Authors are permitted to post a summary of their chapter only in their institution's repository.
19. **Thesis/Dissertation**: If your license is for use in a thesis/dissertation your thesis may be submitted to your institution in either print or electronic form. Should your thesis be published commercially, please reapply for permission. These requirements include permission for the Library and Archives of Canada to supply single copies, on demand, of the complete thesis and include permission for Proquest/UMI to supply single copies, on demand, of the complete thesis. Should your thesis be published commercially, please reapply for permission. Theses and dissertations which contain embedded PJAs as part of the formal submission can be posted publicly by the awarding institution with DOI links back to the formal publications on ScienceDirect.

Appendix C: Permission for reproduction of materials from Elsevier for Chapter 4

This Agreement between Mr. Zongmin Zhao ("You") and Elsevier ("Elsevier") consists of your license details and the terms and conditions provided by Elsevier and Copyright Clearance Center.

License Number	4134911417381
License date	Jun 23, 2017
Licensed Content Publisher	Elsevier
Licensed Content Publication	Biomaterials
Licensed Content Title	Engineering of a hybrid nanoparticle-based nicotine nanovaccine as a next-generation immunotherapeutic strategy against nicotine addiction: A focus on hapten density
Licensed Content Author	Zongmin Zhao,Kristen Powers,Yun Hu,Michael Raleigh,Paul Pentel,Chenming Zhang
Licensed Content Date	Apr 1, 2017
Licensed Content Volume	123
Licensed Content Issue	n/a
Licensed Content Pages	11
Start Page	107
End Page	117
Type of Use	reuse in a thesis/dissertation
Intended publisher of new work	other
Portion	full article
Format	both print and electronic
Are you the author of this Elsevier article?	Yes
Will you be translating?	No
Order reference number	
Title of your thesis/dissertation	Factors that affect the immunogenicity of lipid-PLGA nanoparticle-based nanovaccines against nicotine addiction
Expected completion date	Aug 2017
Estimated size (number of pages)	28
Elsevier VAT number	GB 494 6272 12
Requestor Location	Mr. Zongmin Zhao 1000H Progress St BLACKSBURG, VA 24060 United States Attn: Mr. Zongmin Zhao
Publisher Tax ID	98-0397604
Total	0.00 USD
Terms and Conditions	

INTRODUCTION

1. The publisher for this copyrighted material is Elsevier. By clicking "accept" in connection with completing this licensing transaction, you agree that the following terms and conditions apply to this transaction (along with the Billing and Payment terms and conditions established by Copyright Clearance Center, Inc. ("CCC"), at the time that you opened your Rightslink account and that are available at any time at http://myaccount.copyright.com).

GENERAL TERMS

2. Elsevier hereby grants you permission to reproduce the aforementioned material subject to the terms and conditions indicated.
3. Acknowledgement: If any part of the material to be used (for example, figures) has appeared in our publication with credit or acknowledgement to another source, permission must also be sought from that source. If such permission is not obtained then that material may not be included in your publication/copies. Suitable acknowledgement to the source must be made, either as a footnote or in a reference list at the end of your publication, as follows:
"Reprinted from Publication title, Vol /edition number, Author(s), Title of article / title of chapter, Pages No., Copyright (Year), with permission from Elsevier [OR APPLICABLE SOCIETY COPYRIGHT OWNER]." Also Lancet special credit - "Reprinted from The Lancet, Vol. number, Author(s), Title of article, Pages No., Copyright (Year), with permission from Elsevier."
4. Reproduction of this material is confined to the purpose and/or media for which permission is hereby given.
5. Altering/Modifying Material: Not Permitted. However figures and illustrations may be altered/adapted minimally to serve your work. Any other abbreviations, additions, deletions and/or any other alterations shall be made only with prior written authorization of Elsevier Ltd. (Please contact Elsevier at permissions@elsevier.com). No modifications can be made to any Lancet figures/tables and they must be reproduced in full.
6. If the permission fee for the requested use of our material is waived in this instance, please be advised that your future requests for Elsevier materials may attract a fee.
7. Reservation of Rights: Publisher reserves all rights not specifically granted in the combination of (i) the license details provided by you and accepted in the course of this licensing transaction, (ii) these terms and conditions and (iii) CCC's Billing and Payment terms and conditions.
8. License Contingent Upon Payment: While you may exercise the rights licensed immediately upon issuance of the license at the end of the licensing process for the transaction, provided that you have disclosed complete and accurate details of your proposed use, no license is finally effective unless and until full payment is received from you (either by publisher or by CCC) as provided in CCC's Billing and Payment terms and conditions. If full payment is not received on a timely basis, then any license preliminarily granted shall be deemed automatically revoked and shall be void as if never granted. Further, in the event that you breach any of these terms and conditions or any of CCC's Billing and Payment terms and conditions, the license is automatically revoked and shall be void as if never granted. Use of materials as described in a revoked license, as well as any use of the materials beyond the scope of an unrevoked license, may constitute copyright infringement and publisher reserves the right to take any and all action to protect its copyright in the materials.
9. Warranties: Publisher makes no representations or warranties with respect to the licensed material.
10. Indemnity: You hereby indemnify and agree to hold harmless publisher and CCC, and their respective officers, directors, employees and agents, from and against any and all claims arising out of your use of the licensed material other than as specifically authorized pursuant to this license.
11. No Transfer of License: This license is personal to you and may not be sublicensed, assigned, or transferred by you to any other person without publisher's written permission.
12. No Amendment Except in Writing: This license may not be amended except in a writing signed by both parties (or, in the case of publisher, by CCC on publisher's behalf).
13. Objection to Contrary Terms: Publisher hereby objects to any terms contained in any purchase order, acknowledgment, check endorsement or other writing prepared by you, which terms are inconsistent with these terms and

conditions or CCC's Billing and Payment terms and conditions. These terms and conditions, together with CCC's Billing and Payment terms and conditions (which are incorporated herein), comprise the entire agreement between you and publisher (and CCC) concerning this licensing transaction. In the event of any conflict between your obligations established by these terms and conditions and those established by CCC's Billing and Payment terms and conditions, these terms and conditions shall control.
14. Revocation: Elsevier or Copyright Clearance Center may deny the permissions described in this License at their sole discretion, for any reason or no reason, with a full refund payable to you. Notice of such denial will be made using the contact information provided by you. Failure to receive such notice will not alter or invalidate the denial. In no event will Elsevier or Copyright Clearance Center be responsible or liable for any costs, expenses or damage incurred by you as a result of a denial of your permission request, other than a refund of the amount(s) paid by you to Elsevier and/or Copyright Clearance Center for denied permissions.

LIMITED LICENSE

The following terms and conditions apply only to specific license types:
15. **Translation**: This permission is granted for non-exclusive world **English** rights only unless your license was granted for translation rights. If you licensed translation rights you may only translate this content into the languages you requested. A professional translator must perform all translations and reproduce the content word for word preserving the integrity of the article.
16. **Posting licensed content on any Website**: The following terms and conditions apply as follows: Licensing material from an Elsevier journal: All content posted to the web site must maintain the copyright information line on the bottom of each image; A hyper-text must be included to the Homepage of the journal from which you are licensing at http://www.sciencedirect.com/science/journal/xxxxx or the Elsevier homepage for books at http://www.elsevier.com; Central Storage: This license does not include permission for a scanned version of the material to be stored in a central repository such as that provided by Heron/XanEdu.
Licensing material from an Elsevier book: A hyper-text link must be included to the Elsevier homepage at http://www.elsevier.com . All content posted to the web site must maintain the copyright information line on the bottom of each image.

Posting licensed content on Electronic reserve: In addition to the above the following clauses are applicable: The web site must be password-protected and made available only to bona fide students registered on a relevant course. This permission is granted for 1 year only. You may obtain a new license for future website posting.
17. **For journal authors:** the following clauses are applicable in addition to the above:
Preprints:
A preprint is an author's own write-up of research results and analysis, it has not been peer-reviewed, nor has it had any other value added to it by a publisher (such as formatting, copyright, technical enhancement etc.).
Authors can share their preprints anywhere at any time. Preprints should not be added to or enhanced in any way in order to appear more like, or to substitute for, the final versions of articles however authors can update their preprints on arXiv or RePEc with their Accepted Author Manuscript (see below).
If accepted for publication, we encourage authors to link from the preprint to their formal publication via its DOI. Millions of researchers have access to the formal publications on ScienceDirect, and so links will help users to find, access, cite and use the best available version. Please note that Cell Press, The Lancet and some society-owned have different preprint policies. Information on these policies is available on the journal homepage.
Accepted Author Manuscripts: An accepted author manuscript is the manuscript of an article that has been accepted for publication and which typically includes author-incorporated changes suggested during submission, peer review and editor-author communications.
Authors can share their accepted author manuscript:

- immediately
    - via their non-commercial person homepage or blog
    - by updating a preprint in arXiv or RePEc with the accepted manuscript
    - via their research institute or institutional repository for internal institutional uses or as part of an invitation-only research collaboration work-group
    - directly by providing copies to their students or to research collaborators for their personal use
    - for private scholarly sharing as part of an invitation-only work group on commercial sites with which Elsevier has an agreement
- After the embargo period
    - via non-commercial hosting platforms such as their institutional repository
    - via commercial sites with which Elsevier has an agreement

In all cases accepted manuscripts should:

- link to the formal publication via its DOI
- bear a CC-BY-NC-ND license - this is easy to do
- if aggregated with other manuscripts, for example in a repository or other site, be shared in alignment with our hosting policy not be added to or enhanced in any way to appear more like, or to substitute for, the published journal article.

Published journal article (JPA): A published journal article (PJA) is the definitive final record of published research that appears or will appear in the journal and embodies all value-adding publishing activities including peer review co-ordination, copy-editing, formatting, (if relevant) pagination and online enrichment.
Policies for sharing publishing journal articles differ for subscription and gold open access articles:
Subscription Articles: If you are an author, please share a link to your article rather than the full-text. Millions of researchers have access to the formal publications on ScienceDirect, and so links will help your users to find, access, cite, and use the best available version.
Theses and dissertations which contain embedded PJAs as part of the formal submission can be posted publicly by the awarding institution with DOI links back to the formal publications on ScienceDirect.
If you are affiliated with a library that subscribes to ScienceDirect you have additional private sharing rights for others' research accessed under that agreement. This includes use for classroom teaching and internal training at the institution (including use in course packs and courseware programs), and inclusion of the article for grant funding purposes.
Gold Open Access Articles: May be shared according to the author-selected end-user license and should contain a CrossMark logo, the end user license, and a DOI link to the formal publication on ScienceDirect.
Please refer to Elsevier's posting policy for further information.
18. **For book authors** the following clauses are applicable in addition to the above: Authors are permitted to place a brief summary of their work online only. You are not allowed to download and post the published electronic version of your chapter, nor may you scan the printed edition to create an electronic version. **Posting to a repository:** Authors are permitted to post a summary of their chapter only in their institution's repository.
19. **Thesis/Dissertation**: If your license is for use in a thesis/dissertation your thesis may be submitted to your institution in either print or electronic form. Should your thesis be published commercially, please reapply for permission. These requirements include permission for the Library and Archives of Canada to supply single copies, on demand, of the complete thesis and include permission for Proquest/UMI to supply single copies, on demand, of the complete thesis. Should your thesis be published commercially, please reapply for permission. Theses and dissertations which contain

embedded PJAs as part of the formal submission can be posted publicly by the awarding institution with DOI links back to the formal publications on ScienceDirect.

Elsevier Open Access Terms and Conditions

You can publish open access with Elsevier in hundreds of open access journals or in nearly 2000 established subscription journals that support open access publishing. Permitted third party re-use of these open access articles is defined by the author's choice of Creative Commons user license. See our open access license policy for more information.

Terms & Conditions applicable to all Open Access articles published with Elsevier:

Any reuse of the article must not represent the author as endorsing the adaptation of the article nor should the article be modified in such a way as to damage the author's honour or reputation. If any changes have been made, such changes must be clearly indicated.

The author(s) must be appropriately credited and we ask that you include the end user license and a DOI link to the formal publication on ScienceDirect.

If any part of the material to be used (for example, figures) has appeared in our publication with credit or acknowledgement to another source it is the responsibility of the user to ensure their reuse complies with the terms and conditions determined by the rights holder.

Additional Terms & Conditions applicable to each Creative Commons user license:

CC BY: The CC-BY license allows users to copy, to create extracts, abstracts and new works from the Article, to alter and revise the Article and to make commercial use of the Article (including reuse and/or resale of the Article by commercial entities), provided the user gives appropriate credit (with a link to the formal publication through the relevant DOI), provides a link to the license, indicates if changes were made and the licensor is not represented as endorsing the use made of the work. The full details of the license are available at http://creativecommons.org/licenses/by/4.0.

CC BY NC SA: The CC BY-NC-SA license allows users to copy, to create extracts, abstracts and new works from the Article, to alter and revise the Article, provided this is not done for commercial purposes, and that the user gives appropriate credit (with a link to the formal publication through the relevant DOI), provides a link to the license, indicates if changes were made and the licensor is not represented as endorsing the use made of the work. Further, any new works must be made available on the same conditions. The full details of the license are available at http://creativecommons.org/licenses/by-nc-sa/4.0.

CC BY NC ND: The CC BY-NC-ND license allows users to copy and distribute the Article, provided this is not done for commercial purposes and further does not permit distribution of the Article if it is changed or edited in any way, and provided the user gives appropriate credit (with a link to the formal publication through the relevant DOI), provides a link to the license, and that the licensor is not represented as endorsing the use made of the work. The full details of the license are available at http://creativecommons.org/licenses/by-nc-nd/4.0. Any commercial reuse of Open Access articles published with a CC BY NC SA or CC BY NC ND license requires permission from Elsevier and will be subject to a fee. Commercial reuse includes:

- Associating advertising with the full text of the Article
- Charging fees for document delivery or access
- Article aggregation
- Systematic distribution via e-mail lists or share buttons

Posting or linking by commercial companies for use by customers of those companies.

20. **Other Conditions**:

v1.9

Appendix D: Permission for reproduction of materials from Elsevier for Chapter 5

This Agreement between Mr. Zongmin Zhao ("You") and Elsevier ("Elsevier") consists of your license details and the terms and conditions provided by Elsevier and Copyright Clearance Center.

License Number	4134911508028
License date	Jun 23, 2017
Licensed Content Publisher	Elsevier
Licensed Content Publication	Biomaterials
Licensed Content Title	Rationalization of a nanoparticle-based nicotine nanovaccine as an effective next-generation nicotine vaccine: A focus on hapten localization
Licensed Content Author	Zongmin Zhao,Yun Hu,Theresa Harmon,Paul Pentel,Marion Ehrich,Chenming Zhang
Licensed Content Date	Sep 1, 2017
Licensed Content Volume	138
Licensed Content Issue	n/a
Licensed Content Pages	11
Start Page	46
End Page	56
Type of Use	reuse in a thesis/dissertation
Intended publisher of new work	other
Portion	full article
Format	both print and electronic
Are you the author of this Elsevier article?	Yes
Will you be translating?	No
Order reference number	
Title of your thesis/dissertation	Factors that affect the immunogenicity of lipid-PLGA nanoparticle-based nanovaccines against nicotine addiction
Expected completion date	Aug 2017
Estimated size (number of pages)	28
Elsevier VAT number	GB 494 6272 12
Requestor Location	Mr. Zongmin Zhao 1000H Progress St BLACKSBURG, VA 24060 United States Attn: Mr. Zongmin Zhao
Publisher Tax ID	98-0397604
Total	0.00 USD

Terms and Conditions

INTRODUCTION

1. The publisher for this copyrighted material is Elsevier. By clicking "accept" in connection with completing this licensing transaction, you agree that the following terms and conditions apply to this transaction (along with the Billing and Payment terms and conditions established by Copyright Clearance Center, Inc. ("CCC"), at the time that you opened your Rightslink account and that are available at any time at http://myaccount.copyright.com).

GENERAL TERMS

2. Elsevier hereby grants you permission to reproduce the aforementioned material subject to the terms and conditions indicated.
3. Acknowledgement: If any part of the material to be used (for example, figures) has appeared in our publication with credit or acknowledgement to another source, permission must also be sought from that source. If such permission is not obtained then that material may not be included in your publication/copies. Suitable acknowledgement to the source must be made, either as a footnote or in a reference list at the end of your publication, as follows:
"Reprinted from Publication title, Vol /edition number, Author(s), Title of article / title of chapter, Pages No., Copyright (Year), with permission from Elsevier [OR APPLICABLE SOCIETY COPYRIGHT OWNER]." Also Lancet special credit - "Reprinted from The Lancet, Vol. number, Author(s), Title of article, Pages No., Copyright (Year), with permission from Elsevier."
4. Reproduction of this material is confined to the purpose and/or media for which permission is hereby given.
5. Altering/Modifying Material: Not Permitted. However figures and illustrations may be altered/adapted minimally to serve your work. Any other abbreviations, additions, deletions and/or any other alterations shall be made only with prior written authorization of Elsevier Ltd. (Please contact Elsevier at permissions@elsevier.com). No modifications can be made to any Lancet figures/tables and they must be reproduced in full.
6. If the permission fee for the requested use of our material is waived in this instance, please be advised that your future requests for Elsevier materials may attract a fee.
7. Reservation of Rights: Publisher reserves all rights not specifically granted in the combination of (i) the license details provided by you and accepted in the course of this licensing transaction, (ii) these terms and conditions and (iii) CCC's Billing and Payment terms and conditions.
8. License Contingent Upon Payment: While you may exercise the rights licensed immediately upon issuance of the license at the end of the licensing process for the transaction, provided that you have disclosed complete and accurate details of your proposed use, no license is finally effective unless and until full payment is received from you (either by publisher or by CCC) as provided in CCC's Billing and Payment terms and conditions. If full payment is not received on a timely basis, then any license preliminarily granted shall be deemed automatically revoked and shall be void as if never granted. Further, in the event that you breach any of these terms and conditions or any of CCC's Billing and Payment terms and conditions, the license is automatically revoked and shall be void as if never granted. Use of materials as described in a revoked license, as well as any use of the materials beyond the scope of an unrevoked license, may constitute copyright infringement and publisher reserves the right to take any and all action to protect its copyright in the materials.
9. Warranties: Publisher makes no representations or warranties with respect to the licensed material.
10. Indemnity: You hereby indemnify and agree to hold harmless publisher and CCC, and their respective officers, directors, employees and agents, from and against any and all claims arising out of your use of the licensed material other than as specifically authorized pursuant to this license.
11. No Transfer of License: This license is personal to you and may not be sublicensed, assigned, or transferred by you to any other person without publisher's written permission.
12. No Amendment Except in Writing: This license may not be amended except in a writing signed by both parties (or, in the case of publisher, by CCC on publisher's behalf).
13. Objection to Contrary Terms: Publisher hereby objects to any terms contained in any purchase order, acknowledgment, check endorsement or other writing prepared by you, which terms are inconsistent with these terms and conditions or CCC's Billing and Payment terms and conditions. These terms and conditions, together with CCC's Billing

and Payment terms and conditions (which are incorporated herein), comprise the entire agreement between you and publisher (and CCC) concerning this licensing transaction. In the event of any conflict between your obligations established by these terms and conditions and those established by CCC's Billing and Payment terms and conditions, these terms and conditions shall control.
14. Revocation: Elsevier or Copyright Clearance Center may deny the permissions described in this License at their sole discretion, for any reason or no reason, with a full refund payable to you. Notice of such denial will be made using the contact information provided by you. Failure to receive such notice will not alter or invalidate the denial. In no event will Elsevier or Copyright Clearance Center be responsible or liable for any costs, expenses or damage incurred by you as a result of a denial of your permission request, other than a refund of the amount(s) paid by you to Elsevier and/or Copyright Clearance Center for denied permissions.

LIMITED LICENSE

The following terms and conditions apply only to specific license types:
15. **Translation**: This permission is granted for non-exclusive world **English** rights only unless your license was granted for translation rights. If you licensed translation rights you may only translate this content into the languages you requested. A professional translator must perform all translations and reproduce the content word for word preserving the integrity of the article.
16. **Posting licensed content on any Website**: The following terms and conditions apply as follows: Licensing material from an Elsevier journal: All content posted to the web site must maintain the copyright information line on the bottom of each image; A hyper-text must be included to the Homepage of the journal from which you are licensing at http://www.sciencedirect.com/science/journal/xxxxx or the Elsevier homepage for books at http://www.elsevier.com; Central Storage: This license does not include permission for a scanned version of the material to be stored in a central repository such as that provided by Heron/XanEdu.
Licensing material from an Elsevier book: A hyper-text link must be included to the Elsevier homepage at http://www.elsevier.com . All content posted to the web site must maintain the copyright information line on the bottom of each image.

Posting licensed content on Electronic reserve: In addition to the above the following clauses are applicable: The web site must be password-protected and made available only to bona fide students registered on a relevant course. This permission is granted for 1 year only. You may obtain a new license for future website posting.
17. **For journal authors:** the following clauses are applicable in addition to the above:
Preprints:
A preprint is an author's own write-up of research results and analysis, it has not been peer-reviewed, nor has it had any other value added to it by a publisher (such as formatting, copyright, technical enhancement etc.).
Authors can share their preprints anywhere at any time. Preprints should not be added to or enhanced in any way in order to appear more like, or to substitute for, the final versions of articles however authors can update their preprints on arXiv or RePEc with their Accepted Author Manuscript (see below).
If accepted for publication, we encourage authors to link from the preprint to their formal publication via its DOI. Millions of researchers have access to the formal publications on ScienceDirect, and so links will help users to find, access, cite and use the best available version. Please note that Cell Press, The Lancet and some society-owned have different preprint policies. Information on these policies is available on the journal homepage.
Accepted Author Manuscripts: An accepted author manuscript is the manuscript of an article that has been accepted for publication and which typically includes author-incorporated changes suggested during submission, peer review and editor-author communications.
Authors can share their accepted author manuscript:

- immediately

- via their non-commercial person homepage or blog
- by updating a preprint in arXiv or RePEc with the accepted manuscript
- via their research institute or institutional repository for internal institutional uses or as part of an invitation-only research collaboration work-group
- directly by providing copies to their students or to research collaborators for their personal use
- for private scholarly sharing as part of an invitation-only work group on commercial sites with which Elsevier has an agreement

- After the embargo period
  - via non-commercial hosting platforms such as their institutional repository
  - via commercial sites with which Elsevier has an agreement

In all cases accepted manuscripts should:

- link to the formal publication via its DOI
- bear a CC-BY-NC-ND license - this is easy to do
- if aggregated with other manuscripts, for example in a repository or other site, be shared in alignment with our hosting policy not be added to or enhanced in any way to appear more like, or to substitute for, the published journal article.

Published journal article (JPA): A published journal article (PJA) is the definitive final record of published research that appears or will appear in the journal and embodies all value-adding publishing activities including peer review co-ordination, copy-editing, formatting, (if relevant) pagination and online enrichment.
Policies for sharing publishing journal articles differ for subscription and gold open access articles:
Subscription Articles: If you are an author, please share a link to your article rather than the full-text. Millions of researchers have access to the formal publications on ScienceDirect, and so links will help your users to find, access, cite, and use the best available version.
Theses and dissertations which contain embedded PJAs as part of the formal submission can be posted publicly by the awarding institution with DOI links back to the formal publications on ScienceDirect.
If you are affiliated with a library that subscribes to ScienceDirect you have additional private sharing rights for others' research accessed under that agreement. This includes use for classroom teaching and internal training at the institution (including use in course packs and courseware programs), and inclusion of the article for grant funding purposes.
Gold Open Access Articles: May be shared according to the author-selected end-user license and should contain a CrossMark logo, the end user license, and a DOI link to the formal publication on ScienceDirect.
Please refer to Elsevier's posting policy for further information.
18. **For book authors** the following clauses are applicable in addition to the above: Authors are permitted to place a brief summary of their work online only. You are not allowed to download and post the published electronic version of your chapter, nor may you scan the printed edition to create an electronic version. **Posting to a repository:** Authors are permitted to post a summary of their chapter only in their institution's repository.
19. **Thesis/Dissertation**: If your license is for use in a thesis/dissertation your thesis may be submitted to your institution in either print or electronic form. Should your thesis be published commercially, please reapply for permission. These requirements include permission for the Library and Archives of Canada to supply single copies, on demand, of the complete thesis and include permission for Proquest/UMI to supply single copies, on demand, of the complete thesis. Should your thesis be published commercially, please reapply for permission. Theses and dissertations which contain embedded PJAs as part of the formal submission can be posted publicly by the awarding institution with DOI links back to the formal publications on ScienceDirect.